On Efficient A Posteriori Error Analysis for Variational Inequalities

Dissertation

zur Erlangung des akademischen Grades
doctor rerum naturalium (Dr. rer. nat.)
im Fach Mathematik

eingereicht an der
Mathematisch-Naturwissenschaftlichen Fakultät
der Humboldt-Universität zu Berlin

von

Dipl.-Math. Karoline Sophie Köhler

Präsidentin der Humboldt-Universität zu Berlin
Prof. Dr. Dr. Sabine Kunst

Dekan der Mathematisch-Naturwissenschaftlichen Fakultät
Prof. Dr. Elmar Kulke

Gutachter:
1. Prof. Dr. Carsten Carstensen
2. Prof. Dr. Andreas Schröder
3. Prof. Dr. Neela Nataraj

Tag der Verteidigung: 26.09.2016

Zusammenfassung

Effiziente und zuverlässige a posteriori Fehlerabschätzungen sind eine Hauptzutat für die effiziente numerische Berechnung von Lösungen zu Variationsungleichungen durch die Finite-Elemente-Methode. Die vorliegende Arbeit untersucht solche zuverlässigen und effizienten Fehlerabschätzungen für beliebige Finite-Elemente-Methoden und drei repräsentativen Variationsungleichungen, nämlich dem Hindernisproblem, dem Signorini Modelproblem und dem Bingham Strömungsproblem in zwei Raumdimensionen.

Die Fehlerabschätzungen hängen vom zum Problem gehörenden Lagrange Multiplikator ab, der eine Verbindung zwischen der Variationsungleichung und dem zugehörigen linearen Problem darstellt. Effizienz und Zuverlässigkeit werden bezüglich eines totalen Fehlers gezeigt. Dieser Fehler beinhaltet den Fehler der primalen Variablen in der Energienorm, den Fehler in den Lagrange Multiplikatoren in der dualen Norm, und zwei Terme, die die Komplementaritätsbedingungen widerzpiegeln. Die Fehleranschätzungen fordern minimale Regularität. Sie setzen nur eine H^1 Approximation der exakten Lösung und eine Approximation des Lagrange Multiplikators voraus. Die Approximation der exakten Lösung erfüllt die Dirichlet Randbedingungen und die Approximation des Lagrange Multiplikators ist nicht-positiv im Falle des Hindernis- und Signoriniproblems, und hat Betrag kleiner gleich 1 für das Bingham Problem. Durch dieses allgemeine Vorgehen wird das Einbinden nicht-exakter diskreter Lösungen ermöglicht, die auf natürliche Weise im Kontext von nicht-linearen Problemen, wie Variationsungleichungen, auftreten.

Aus dem Blickwinkel der Anwendungen ist Effizienz und Zuverlässigkeit im Bezug auf den Fehler der primalen Variablen in der Energienorm von großem Interesse. Solche Abschätzungen hängen von der Wahl eines effizienten diskreten Lagrange Multiplikators ab. Im Falle des Hindernis- und Signorini Problems werden postive Beispiele für drei Finite-Elemente Methoden, der P_1 konformen Courant Methode (CFEM), der P_1 nicht-konformen Crouzeix-Raviart Methode (NCFEM) und der gemischten Raviart-Thomas Methode (MFEM) niedrigster Ordnung hergeleitet. Partielle Resultate liegen im Fall des Bingham Strömungsproblems vor.

Eine große Anzahl numerischer Experimente heben die theoretischen Ergebnisse hervor und zeigen Effizienz und Zuverlässigkeit bezüglich des total Fehlers und auch im Bezug auf den Fehler der primalen Variablen in der Energienorm. Die numerischen Tests legen nahe, dass der aus den Abschätzungen resultierende adaptive Algorithmus mit optimaler Konvergenzrate konvergiert.

Abstract

Efficient and reliable a posteriori error estimates are a key ingredient for the efficient numerical computation of solutions for variational inequalities by the finite element method. This thesis studies such reliable and efficient error estimates for arbitrary finite element methods and three representative variational inequalities, namely the obstacle problem, the Signorini model problem, and the Bingham flow problem in two space dimensions.

The error estimates strongly rely on a problem connected Lagrange multiplier, which presents a connection between the variational inequality and the corresponding linear problem. Reliability and efficiency are shown with respect to some total error, which consists of the error of the primal variable in the energy norm, the dual norm of the error of the Lagrange multiplier, and two terms which represent errors of the complementary conditions. Reliability and efficiency are shown under minimal regularity assumptions and only demand an H^1 approximation to the exact solution, which satisfies the Dirichlet boundary conditions, and an approximation of the Lagrange multiplier which is non-positive in the case of the obstacle and Signorini problem and has an absolute value smaller than 1 for the Bingham flow problem. These general assumptions allow for reliable and efficient a posteriori error analysis even in the presence of inexact solve, which naturally occurs in the context of non-linear problems such as variational inequalities.

From the point of view of the applications, reliability and efficiency with respect to the error of the primal variable in the energy norm is of great interest. Such estimates depend on the efficient design of a discrete Lagrange multiplier. Affirmative examples of discrete Lagrange multipliers are presented for the obstacle and Signorini problem and three different first-order finite element methods (FEMs), namely the P_1 conforming Courant (CFEM), the P_1 non-conforming Crouzeix-Raviart (NCFEM), and the mixed Raviart-Thomas (MFEM) FEM. Partial results exist for the Bingham flow problem.

A large number of numerical experiments highlight the theoretical results, and show efficiency and reliability with respect to the total error and also with respect to the error of the primal variable in the energy norm. The numerical tests suggest that the resulting adaptive algorithms converge with optimal convergence rates.

Contents

1. Introduction

The approximation of solutions to variational inequalities with finite element methods (FEMs) is a fundamental task of computational science and engineering with applications in many different areas. The long list of examples includes minimal surfaces, the capacity of a set in potential theory, option pricing in financial mathematics, problems of fluid filtration in porous media, contact problems, or constraint heating. Many of those problems come from the natural sciences, geophysics, or computational mechanics and engineering.
This thesis studies three representative variational inequalities, namely the obstacle problem, the Signorini model problem, and the two dimensional Bingham flow problem (or Mosolov's problem) and three finite element methods (FEMs), namely the conforming Courant FEM (CFEM), the non-conforming Crouzeix-Raviart FEM (NCFEM), and the mixed Raviart-Thomas FEM (MFEM), with respect to three aspects of reliable and efficient error estimators with guaranteed upper and lower error bounds.

Given a real Hilbert space V and a convex, closed, and non-empty subset K, a variational inequality of the first kind seeks $u \in K$ such that

$$F(v-u) \leq a(u, v-u) \quad \text{for all } v \in K$$

for a bilinear form $a : V \times V \to \mathbb{R}$ and a linear form $F \in V^*$. In the case of the obstacle problem with homogeneous Dirichlet boundary conditions, an obstacle $\chi \in H^2(\Omega)$, $V := H_0^1(\Omega)$, and $K := \{v \in V \mid \chi \leq v \text{ a.e. in } \Omega\}$, the variational inequality is associated to a Lagrange multiplier $\Lambda \in V_-^* := \{G \in V^* \mid G(\varphi) \leq 0 \text{ for all } \varphi \in V \text{ with } \varphi \geq 0 \text{ a.e.}\}$. Lagrange multipliers presenta connection between variational inequalities and variational equalities. For a general approximation $v \in V$ to the exact solution $u \in K$ to the obstacle problem, and an approximation $M \in V_-^*$ to the Lagrange multiplier Λ, known error estimates (cf. Bartels and Carstensen (2004); Braess (2005); Braess et al. (2007, 2008); Nochetto et al. (2003, 2005); Veeser (2001)) concern the total error $|||u - v||| + |||\Lambda - M|||_*$ of the error of the primal variable in the energy norm $|||\bullet||| := a(\bullet, \bullet)^{1/2}$, and the error of the Lagrange multipliers in the dual norm $|||\bullet|||_*$. The authors provide reliable bounds, but leave the question of efficiency open. The approaches in the above references focus on conforming finite element methods. This thesis contributes reliable and efficient error estimates for three variational inequalities, which are independent of the finite element method at hand. Given an arbitrary approximation $v \in V$ to the exact solution $u \in K$ and an approximation $M \in V_-^*$ to the exact Lagrange multiplier Λ, the appropriate definitions of an error Err and a guaranteed upper bound GUB lead to a version of the first main result for each variational inequality.

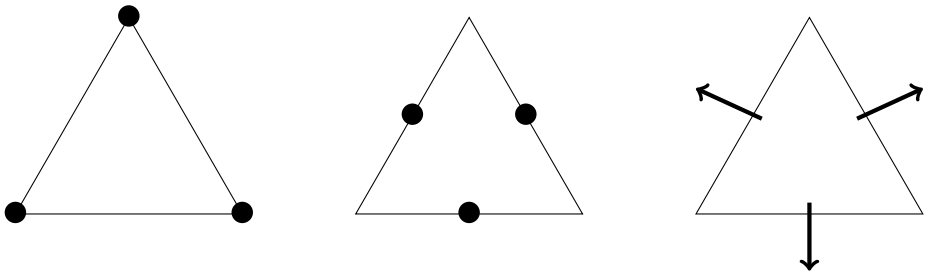

Figure 1.1.: Schematic representation of lowest-order conforming, non-conforming, and mixed finite element method.

Theorem A. *Let* Err *be an appropriate error and* GUB *the corresponding guaranteed upper bound, then the error* Err *and the guaranteed upper bound* GUB *satisfy*

$$\mathrm{Err} \leq \mathrm{GUB} \leq C_{\mathrm{eff}}\mathrm{Err}.$$

For the obstacle problem with pure Dirichlet boundary conditions and an obstacle $\chi \in H^2(\Omega)$, the exact solution $u \in K := \{v \in H^1_0(\Omega) \mid \chi \leq v \text{ a.e. in } \Omega\}$ is approximated by any $v \in V$ and the exact Lagrange multiplier Λ, with L^2 representation $\lambda := \Delta u + f \in L^2(\Omega; (-\infty, 0])$ is approximated by the functional $M \in V^*$, given by $M(\varphi) := \int_\Omega \mu\varphi \,\mathrm{d}x$ for any $\mu \in L^2(\Omega; (-\infty, 0])$ and all $\varphi \in V$. The error reads

$$\begin{aligned}\mathrm{Err}^2 :=& \|\!| u - v |\!|\!|^2 + |\!|\!| u - v + \min\{0, v - \chi\} |\!|\!|^2 \\ &+ |\!|\!| \lambda - \mu |\!|\!|_*^2 + \int_\Omega (-\lambda)(v - \chi)_+ \,\mathrm{d}x + \int_\Omega (-\mu)(u - \chi) \,\mathrm{d}x \end{aligned} \tag{1.1}$$

with the positive part $(v - \chi)_+ := \max\{v - \chi, 0\}$ of $v - \chi$. The guaranteed upper bound is

$$\mathrm{GUB}^2 := 30 \left(|\!|\!| \operatorname{Res} |\!|\!|_*^2 + \int_\Omega (-\mu)(v - \chi)_+ \,\mathrm{d}x + |\!|\!| \min\{0, v - \chi\} |\!|\!|^2 \right) \tag{1.2}$$

for the residual $\operatorname{Res} \in V^*$,

$$\operatorname{Res}(\varphi) := F(\varphi) - \int_\Omega \mu\varphi \,\mathrm{d}x - a(v, \varphi) \quad \text{for all } \varphi \in V.$$

It is remarkable that the estimate in Theorem A requires only very general approximations to the exact solution $u \in K$ and the exact Lagrange multiplier Λ. From a computational point of view, this opens the door to an analysis with inexact solve, obligatory for the iterative solution of non-linear problems, such as are given by variational inequalities.

Such an approach immediately shows reliability with respect to the error $|\!|\!| u - v |\!|\!|$ in the energy norm of the primal variable $u \in K$ and any approximation $v \in V$ to $u \in K$. For the three finite element methods depicted in Figure 1.1, namely the conforming Courant FEM (CFEM), the non-conforming Crouzeix-Raviart FEM (NCFEM), and the mixed Raviart-Thomas FEM (MFEM), this thesis also analyzes efficiency for this reduced error term. Let $\Lambda \in V^*_-$ be the exact Lagrange multiplier

and $M \in V_{\preceq}^*$ any approximation. In the setting of the obstacle problem, M is efficient if the following theorem can be proven.

Theorem B. *Let $\Lambda \in V^*$ be the exact Lagrange multiplier. Then the approximation $M \in V^*$ is efficient in the sense that*

$$\|\!|\Lambda - M|\!|_* \lesssim |\!|\!|u - v|\!|\!| + \textit{higher-order terms}.$$

In the case of the obstacle problem for CFEM and NCFEM and Signorini's problem for CFEM, the higher-order terms in Theorem B include oscillations of the exact Lagrange multiplier Λ. Realizations of Theorem B for the obstacle problem with MFEM and the Signorini problem for NCFEM and MFEM avoid such terms and only include data approximation terms.

The algebraic arguments in the proof of Theorem A suggest, that, for the obstacle problem, the two integrals in (1.1) and the one in (1.2) are connected. They measure the non-fulfilment of the complementary condition and seem to be reasonable terms in the error and the guaranteed upper bound. Nonetheless, it is unclear whether they are at all small or dominate the error. To obtain the desired reduced efficiency, the approximation $M \in V^*$ to the exact Lagrange multiplier $\Lambda \in V^*$ has to allow for a proof of the following theorem.

Theorem C. $\int_\Omega (-\mu) \max\{v - \chi, 0\} \,\mathrm{d}x \lesssim |\!|\!|u - v|\!|\!| + \mathrm{apx}.$

The results of Theorems B and C can be reformulated also in the context of the Signorini model problem and Mosolov's problem, although the natural discrete Lagrange multiplier for NCFEM in Mosolov's problem does not allow for a proof of Theorem C. For each variational inequality and each finite element method the term apx will be studied in more detail in this thesis. With these results at hand, reliability and efficiency can be shown, only with respect to the error in the energy norm of the primal variable and leads to

Conclusion.

$$|\!|\!|u - v|\!|\!|^2 \leq \mathrm{Err}^2 \leq \mathrm{GUB}^2 \leq C'_{\mathrm{eff}} |\!|\!|u - v|\!|\!|^2 + \textit{higher-order terms}^2 + \mathrm{apx}^2.$$

Contrary to the results in Theorem A, Theorems B and C depend strongly on the finite element method at hand. The analysis in this thesis suggests, that the proof of Theorem B for each problem and each finite element method depends on an appropriate interpolation operator $I : V \to V_h$, where V_h is the employed finite element space in each case. The discrete Lagrange multiplier M and the interpolation operator I, together with the discrete solution $u_h \in V_h$, have the following connection

$$M(\varphi) = F(I\varphi) - a(u_h, I\varphi) \quad \text{for all } \varphi \in V.$$

This is a fundamental observation for all three problems and the three finite element methods considered in this thesis. For the obstacle problem, the conforming Courant finite element method is well studied and the Lagrange multipliers suggested by Bartels and Carstensen (2004) and Veeser (2001) satisfy the connection with the

Problem	FEM	Theorem A	Theorem B	Theorem C
Obstacle	CFEM	Theorem 3.18	Theorem 3.26	Theorem 3.29
	NCFEM	Theorem 3.18	Theorem 3.38	Theorem 3.40
	MFEM	Theorem 3.18	Theorem 3.47	Theorem 3.49
Signorini	CFEM	Theorem 4.14	Theorem 4.20	Theorem 4.24
	NCFEM	Theorem 4.14	Theorem 4.35	Theorem 4.38
	MFEM	Theorem 4.14	Theorem 4.48	Theorem 4.49
Bingham	CFEM	Theorem 5.12	unclear, cf. P. 103	0 by design
	NCFEM	Theorem 5.12	Theorem 5.21	unclear, cf. P. 107

Table 1.1.: Realizations of Theorems A, B, and C.

interpolation operators from Carstensen (1999) and Carstensen and Verfürth (1999). For the remaining problems, the thesis designs such interpolation operators and proves that in the case of the conforming FEM for Mosolov's problem, such an interpolation operator cannot exist. Table 1.1 lists the realizations of Theorems A, B, and C for each problem and each finite element method.

Historic overview

The error analysis for conforming finite element methods for variational inequalities began in the 1970s with Falk (1974). First error estimates for mixed formulations of variational inequalities are presented in Brezzi et al. (1978) and complement the results for finite element methods used to discretize the primal formulations contained in Brezzi et al. (1977). The three articles focus mainly on the obstacle problem and the unilateral problem, both of which are important model problems in the analysis of variational inequalities. The a priori error analysis for non-conforming FEMs for the obstacle problem is relatively new. First results, under unreasonably high regularity assumptions, are presented in Wang (2003). These results are improved in Carstensen and Köhler (2016b), where an a priori error estimate is presented under minimal regularity assumptions. The survey article of Wohlmuth (2011) gives a large overview over a priori and a posteriori error estimates in the analysis of variational inequalities.

The a posteriori error analysis, including the reliability and efficiency of error estimators, for variational equalities is well established in the books of Ainsworth and Oden (2000) and Verfürth (2013). A posteriori error results for variational inequalities of the first kind are for example obtained in Braess (2005); Bartels and Carstensen (2004); Carstensen and Köhler (2016b); Veeser (2001) for the obstacle problem and in Hild and Nicaise (2005) for the Signorini problem. Repin (2007) presents general a posteriori error estimates for variational inequalities of the first and second kind. For mixed finite element methods Gatica and Maischak (2005) derive a posteriori error estimates which employ Lagrange multipliers to include further physically interesting unknowns. Mixed finite element methods, and

also higher-order *hp* methods, are analyzed in Banz and Schröder (2015) for non-symmetric obstacle problems. The a posteriori error analysis for obstacle problems also plays an important part in the study of optimal control problems, for example in Gaevskaya et al. (2014) and Dond et al. (2016). For a posteriori error estimates for variational inequalities of the second kind see for example Bostan et al. (2005); Bostan and Han (2006); Schröder (2012). They present a posteriori error estimates mainly for the frictional contact problem. For a reliable and efficient a posteriori error analysis for elastoplasticity and elastoviscoplasticity with hardening see Carstensen et al. (2006).

The work of Braess (2005) presents a connection between the variational inequality and the corresponding linear problem with the help of a Lagrange multiplier to obtain reliable a posteriori results for variational inequalities. This approach is taken up in Carstensen and Merdon (2013b) for the obstacle problem where the authors also present efficiency of such estimators for the obstacle problem for lowest order conforming finite element methods. The results in Bürg and Schröder (2015) employ this approach for the reliable a posteriori error analysis of *hp* finite element methods of general variational inequalities of first and second kind, but leave the question of efficiency untouched. The general approach of Braess (2005) for variational inequalities of the first kind, namely the obstacle problem, is taken up by Wang and Han (2013) who adapt this approach to variational inequalities of the second kind to derive reliable a posteriori error estimates in a general setting.

Main results

The thesis develops the result of Braess (2005) to obtain reliable and efficient a posteriori error estimates for three different representative variational inequalities of first and second kind. The problems discussed in this thesis are the obstacle problem, Signorini's problem, and the Bingham flow problem in two space-dimensions (or Mosolov's problem). In the case of the obstacle problem and Signorini's problem, this result is obtained for mixed boundary conditions. The extended analysis leads to a general framework, which is independent of the concrete finite element method at hand, and so even allows estimates for inexact discrete solutions, which occur naturally, since the considered problems are non-linear and hence require iterative solvers. The choice of three prototypical examples suggests the possibility to extend the results of this thesis to general variational inequalities in a fashion similiar to the results in Bürg and Schröder (2015).

The general framework is transferred to three different finite element methods, the lowest-order conforming Courant, non-conforming Crouzeix-Raviart, and mixed Raviart-Thomas FEM. In each case a discrete Lagrange multiplier is designed, which is efficient in the sense of Theorem B (with the exception of CFEM for the Bingham problem) and allows for a novel efficient and reliable error estimate only with respect to the error of the primal variable in the energy norm for the obstacle problem and Signorini's problem and with partial results also for the Bingham flow problem. The

specific analysis for each problem and each finite element method brings to light a strong connection between the design of the discrete Lagrange multiplier and an appropriate interpolation operator. It seems reasonable, that such an approach can be carried over to other finite element methods and variational inequalities.

For each of the analyzed problems, there is a connection between the non-conforming FEM and the mixed FEM in the spirit of Marini (1985). An important tool for these methods is the design of appropriate conforming companions as in Carstensen et al. (2015a), which is extended here also to variational inequalities.

Numerical experiments highlight the reliable and efficient a posteriori error results and suggest quasi-optimal convergence of the resulting adaptive scheme.

Structure of the thesis

Chapter 2 provides the theoretical background for this thesis. Functional analytical concepts employed in this thesis are defined here, as well as the finite element spaces, the triangulation, and the finite element methods for the three variational inequalities analyzed in this thesis. Some preliminary general results for variational inequalities of first and second kind are explained in this chapter.

In Chapter 3 the obstacle problem is studied. It begins with the definition of the problem, as well as regularity results and some properties of the exact solution. Several equivalent formulations are stated and their equivalence is shown. Section 3.2 gives a proof of Theorem A in the case of the obstacle problem. Sections 3.3–3.5 prove Theorems B and C for the conforming Courant, the non-conforming Crouzeix-Raviart, and the mixed Raviart-Thomas FEM.

The 4th chapter discusses the Signorini model problem and begins with a general introduction to this problem, where the problem is defined, the regularity results are clarified, and several equivalent formulations are studied. In Section 4.2, Theorem A is proven for this problem, followed by the analysis which corresponds to Theorems B and C in this introduction, for the conforming Courant, the non-conforming Crouzeix-Raviart, and the mixed Raviart-Thomas FEM in Sections 4.3–4.5. These results hinge on novel interpolation operators defined in those sections. Furthermore, Section 4.5.1 includes the equivalences of the Crouzeix-Raviart and the Raviart-Thomas finite element methods for this specific problem.

Chapter 5 begins with the formulation of the Bingham flow problem in Section 5.1. It clarifies the equivalence between the physical energy minimization formulation, the corresponding variational inequality of second kind, and the mixed three-field formulation from Carstensen et al. (2015b). This section also states regularity results and the existence (and partial uniqueness) of solutions. Section 5.2 provides Theorem A for the Bingham problem. Section 5.3 discusses the conforming FEM for the Bingham problem. The role of the interpolation operator is discussed and arguments are given, why such an interpolation operator cannot exist. Section 5.4 discusses the non-conforming and the mixed finite element method, which are equivalent for this problem. The non-conforming and mixed finite element method for the

Bingham problem allow for the definition of an efficient discrete Lagrange multiplier in the sense of Theorem B which is proven in Section 5.4.

Chapter 6 presents the numerical experiments which highlight the theoretical findings in the previous three chapters, and presents numerical evidence for the optimal convergence of the resulting adaptive algorithms. Section 6.1 presents five benchmark examples for the obstacle problem. Section 6.2 displays the results of four benchmark examples for Signorini's problem. Section 6.3 gives numerical evidence for the reliability and efficiency of the finite element methods considered for the Bingham problem. A conclusion in Section 6.4 completes the chapter.

Appendix A provides a table of the notation used within this thesis.

Appendix B shows the main parts of the `MATLAB` implementation employed for the numerical experiments and lists the programs contained on the data medium attached to this thesis in Appendix C.

Conclusion and outlook

This thesis proves reliability and efficiency with respect to the total error for three representative variational inequalities (i.e., the obstacle problem, the Signorini model problem in any space dimension, and the Bingham flow problem in two space dimensions) and general finite element methods. In two dimensions, these results are improved to reliable and efficient estimates with respect to the error of the primal variables in the energy norm for three finite element methods, with the exception of the lowest-order conforming FEM for the Bingham flow problem. The numerical experiments suggest reliability and efficiency also in this case, as well as quasi-optimal convergence for the resulting adaptive algorithms for the considered variational inequalities and the three finite element methods.

The results of this thesis hinge on the choice of suitable discrete Lagrange multipliers for each variational inequality and each finite element method. The analysis in this thesis leads to the conjecture, that the efficiency of the discrete Lagrange multiplier as in Theorem B is connected to the existence of a suitable interpolation operator. This may be the first step to cover a wide range of variational inequalities and characterize the conditions for which a finite element method provides reliable and efficient error estimates. Generalizations of the results presented within this thesis, to higher dimensions is possible but very technical and therefore out of the scope of this thesis.

The thorough study of the discrete Lagrange multipliers and the corresponding interpolation operators gives a connection between the variational inequality and the corresponding linear problem. This may offer a possibility to study the resulting adaptive algorithms with respect to optimal convergence rates, employing results from the well studied linear problems. This analysis is out of the scope of this thesis and is the objective of future research.

Acknowledgements

I would like to thank Professor C. Carstensen for the supervision of this thesis and Professor D. Peterseim for the collaboration in the project C33 “Modeling and simulation of composite materials” within the DFG Research Center MATHEON. The support of the Berlin Mathematical School “BMS”, and the Deutsche Forschungsgemeinschaft “DFG” is gratefully acknowledged.
Many thanks go to my family and friends for fruitful discussions on more or less work-related topics, day-to-day politics, the Eurovision Songcontest, and the greater good. Especially Alex and Mira are thanked for many distracting coffee breaks. Loving thoughts go to Moritz, who was always there and on many long days, in the process of this thesis, made sure that dinner was ready. Leander’s helping kicks will not be forgotten.

2. Preliminaries

This chapter gives an overview of the notation for the function spaces and operators (Section 2.1) and introduces the finite element spaces (Section 2.2) which are analyzed in this thesis. The chapter concludes with a collection of important results (Section 2.3), the definition of conforming companions (Section 2.4), results for the treatment of inhomogeneous Dirichlet boundary conditions (Section 2.5), the definition of variational inequalities (Section 2.6), and commonly used scalar products and norms (Section 2.7). Throughout the thesis $A \lesssim B$ abbreviates $A \leq CB$ for a generic constant $C < \infty$ which is independent of the mesh-size.

2.1. Function spaces and operators

Lebesgue and Sobolev spaces

This thesis applies standard notation for Lebesgue and Sobolev spaces (Evans, 2010). Let (ω, Σ, μ) with $\omega \subset \mathbb{R}^n$, $n \geq 1$ be a measure space. Given some μ-measurable function $f : \omega \to \mathbb{R}$, then $\int_\omega f \,\mathrm{d}\mu$ denotes the Lebesgue integral, and for $\mu(\omega) < \infty$, $\fint_\omega f \,\mathrm{d}\mu := \mu(\omega)^{-1} \int_\omega f \,\mathrm{d}\mu$ denotes the integral mean. A measurable function f is called integrable, if $\int_\omega f \,\mathrm{d}\mu < \infty$. For $f : \omega \to X \subseteq \mathbb{R}^{k\times\ell}$ with $k, \ell \in \mathbb{N}$ and μ measurable components, $\int_\omega f \,\mathrm{d}\mu$ denotes the component-wise Lebesgue integral. For $1 \leq p < \infty$ the L^p semi norm is given by

$$||f||_{L^p(\omega)} := \Big(\int_\omega |f|^p \,\mathrm{d}\mu \Big)^{1/p},$$

where $|\bullet|$ denotes the Frobenius norm. If $p = \infty$, the L^∞ semi norm is defined with the essential supremum

$$||f||_{L^\infty(\omega)} := \inf\{C > 0 \;\big|\; |f(x)| \leq C \text{ for almost every } x \in \omega\}$$

where $|\bullet|$ denotes the Euclidean norm.

Definition 2.1 (Lebesgue space)**.** *For $1 \leq p \leq \infty$, the Lebesgue space $L^p(\omega, X)$ is given by the space of equivalence classes of p-integrable function (up to equality almost everywhere)*

$$L^p(\omega; X) := \big\{ f : \omega \to X \;\big|\; f \text{ is measurable and } ||f||_{L^p(\omega)} < \infty \big\} / \big\{ ||\bullet||_{L^p(\omega)} = 0 \big\}.$$

For a Lebesgue measurable set $\omega \subset \mathbb{R}^n$ and a Lebesgue measurable function $f : \omega \to X$, the integral with respect to the n-dimensional Lebesgue measure is denoted by $\int_\omega f \,\mathrm{d}x$, while the integral over an $(n-1)$-dimensional hyper-surface $\gamma \subset \omega$ with respect to the $(n-1)$-dimensional Hausdorff measure is denoted by $\int_\gamma f \,\mathrm{d}s$. The n-dimensional Lebesgue measure of ω is denoted by $\mathrm{meas}(\omega)$ and the

$(n-1)$-dimensional Hausdorff measure of γ reads $\mathrm{meas}_{n-1}(\gamma)$.
Given $\omega \subset \mathbb{R}^n$, $C^m(\omega; X)$ denotes the set of $m \in \mathbb{N}_0 \cup \{\infty\}$ times continuously differentiable functions $f : \omega \to X$. The set of m times continuously differentiable functions with compact support is abbreviated by $C_0^m(\omega; X)$. The set of m times continuously differentiable functions that are zero on a subset $\gamma \subseteq \partial\omega$, with $\mathrm{meas}_{n-1}(\gamma) > 0$ are denoted by $C_\gamma^m(\omega; X)$. If $X = \mathbb{R}$, X is omitted, i.e., $C^m(\omega; \mathbb{R}) =: C^m(\omega)$; $C_0^m(\omega; \mathbb{R}) =: C_0^m(\omega)$, etc.
Let $\alpha \in \mathbb{N}_0^n$ be a multi-index with $|\alpha| := \sum_{j=1}^n \alpha_j$. Then the partial derivative of $f \in C^\infty(\omega; X)$ reads

$$D^\alpha f := \partial^{|\alpha|} f / \partial x^\alpha := \partial^{|\alpha|} f / (\partial x_1^{\alpha_1} \dots x_n^{\alpha_n}).$$

For open and bounded Lipschitz domains $\omega \subset \mathbb{R}^n$, a function $f \in L^p(\omega)$ is called m times weakly differentiable with respect to α with $|\alpha| = m$, if there exists some $g \in L^p(\omega; X)$ such that

$$\int_\omega f D^\alpha \varphi \,\mathrm{d}x = (-1)^m \int_\omega g\varphi \,\mathrm{d}x \quad \text{for all } \varphi \in C_0^\infty(\omega).$$

The function $D^\alpha f := g$ is called the mth weak derivative of f with respect to α. For $\alpha_k = 1$ and $\alpha_j = 0$ for all $j \in \{1, \dots, n\} \setminus \{k\}$, $\partial^{|\alpha|} f / \partial x^\alpha$ is abbreviated by $\partial f / \partial x_k$.

For $\omega \subseteq \mathbb{R}^n$, $n \in \mathbb{N}$, define the Sobolev space by

$$H^k(\omega) := \{f \in L^2(\omega) \mid \text{for all } \alpha \in \mathbb{N}_0^n \text{ with } |\alpha| \le k \text{ there exists } D^\alpha f \in L^2(\omega; X)\}.$$

For a vector space $X \subseteq \mathbb{R}^{M \times N}$, $M, N \in \mathbb{N}$, define

$$H^k(\omega; X) := \{f \in L^2(\omega; X) \mid f_{j,\ell} \in H^k(\omega) \text{ for all } j \in \{1, \dots, M\} \text{ and } \ell \in \{1, \dots, N\}\}.$$

Define the Sobolev norm of $f \in H^k(\omega; X)$ by

$$||f||_{H^k(\omega)} := \Big(\sum_{j=1}^M \sum_{\ell=1}^N \sum_{|\alpha| \le k} ||D^\alpha f_{j\ell}||_{L^2(\omega)}^2 \Big)^{1/2}.$$

Let $\gamma \subseteq \partial\omega$ with $\mathrm{meas}_{n-1}(\gamma) > 0$. Then the closure of $C_\gamma^\infty(\omega; X)$ with respect to the norm $||\bullet||_{H^k(\omega)}$ is denoted by $H_\gamma^k(\omega; X)$. If $\gamma = \partial\omega$, $H_0^k(\omega; X) = H_\gamma^k(\omega; X)$. The dual of $H_\gamma^1(\omega)$ is denotes by $H_\gamma^{-1}(\omega)$ and $\langle \bullet, \bullet \rangle$ denotes the dual pairing of $H_\gamma^1(\omega)$ and $H_\gamma^{-1}(\omega)$. If $\gamma = \partial\omega$, $H_{\partial\omega}^{-1}(\omega)$ is abbreviated by $H^{-1}(\omega)$.
Let

$$H^{1/2}(\partial\omega) := \{v \in L^2(\partial\omega) \mid \exists w \in H^1(\omega) \text{ with } w|_{\partial\omega} = v\}.$$

For a union of closed arcs $\gamma \subset \partial\omega$, with $\mathrm{meas}_{n-1}(\gamma) > 0$, let

$$\tilde{H}^{1/2}(\partial\omega \setminus \gamma) := \{v \in L^2(\partial\omega) \mid \exists w \in H_\gamma^1(\omega) \text{ with } w|_{\partial\omega} = v\}.$$

The spaces $H^{-1/2}(\partial\omega)$ and $H^{-1/2}(\partial\omega \setminus \gamma)$ denote the dual spaces to $H^{1/2}(\partial\omega)$ and $\tilde{H}^{1/2}(\partial\omega \setminus \gamma)$. The dual pairing is given by $\langle \bullet, \bullet \rangle_{\partial\omega}$.
For any function space $W(\omega; X) := \{f : \omega \to X \text{ is a function}\}$, $W(\omega)$ abbreviates $W(\omega; \mathbb{R})$.

Operators

For sufficiently smooth functions $f : \omega \to \mathbb{R}^M$, $M \in \mathbb{N}$, the first (weak) derivative is denoted by Df and the second weak derivative by $D^2 f$. For $M = 1$, the first (weak) derivative Df is abbreviated by ∇f (also called the gradient of f). If $M = n$, the divergence is given by $\operatorname{div} f := \sum_{j=1}^{n} \partial f_j / \partial x_j$. The Laplacian of $f : \omega \to \mathbb{R}$ reads $\Delta f = \operatorname{div} \nabla f$. Let $f \in L^2(\omega; \mathbb{R}^n)$. If there exists a function $f_{\operatorname{div}} : \omega \to \mathbb{R}$ with

$$\int_\omega f \cdot \nabla \varphi \, \mathrm{d}x = -\int_\omega \varphi f_{\operatorname{div}} \, \mathrm{d}x \quad \text{for all } \varphi \in C_0^\infty(\omega),$$

then f has a weak divergence $\operatorname{div} f := f_{\operatorname{div}}$. The set of L^2 functions with a weak divergence in L^2 is given by

$$H(\operatorname{div}, \omega) := \{f \in L^2(\omega; \mathbb{R}^m) \mid \exists \operatorname{div} f \text{ and } \operatorname{div} f \in L^2(\omega)\}.$$

Let $\gamma \subseteq \partial\omega$ be a finite union of open arcs and let ν denote the outward unit vector along γ, and let $g \in L^2(\gamma)$. Then

$$H_{g,\gamma}(\operatorname{div}, \omega) := \{q \in H(\operatorname{div}, \omega) \mid q \cdot \nu = g \text{ along } \gamma\}. \tag{2.1}$$

If $\gamma = \partial\omega$, the space $H_{g,\partial\omega}(\operatorname{div}, \omega)$ is abbreviated by $H_g(\operatorname{div}, \omega)$. For $\omega \subset \mathbb{R}^2$, the Curl of a function $v \in H^1(\omega)$ is given by $\operatorname{Curl} v := (\partial v/\partial x_2, -\partial v/\partial x_1)$ and equals a rotated gradient, i.e.,

$$\operatorname{Curl} v = \begin{pmatrix} 0 & 1 \\ -1 & 0 \end{pmatrix} \nabla v.$$

2.2. Finite element spaces

On the basis of a shape regular triangulation (see Subsection 2.2.1) this section defines the finite element spaces, which are analyzed in this thesis.

2.2.1. Shape-regular triangulation

Let $\omega \subset \mathbb{R}^2$ be a bounded polygonal Lipschitz domain with boundary $\partial\omega$. The boundary $\partial\omega$ is subdivided into a finite number of disjoint compact arcs $\gamma_1, \ldots, \gamma_J$.

The bounded polygonal Lipschitz domain $\omega \subset \mathbb{R}^2$ is partitioned into triangles forming a triangulation $\mathcal{T}$. The triangles $T \in \mathcal{T}$ are closed and satisfy $\overline{\omega} = \bigcup_{T \in \mathcal{T}} T$. Any two triangles $T, K \in \mathcal{T}$ are either identical, share exactly one edge or one node, or are disjoint. For some triangle $T \in \mathcal{T}$, let $\mathcal{N}(T)$ denote the vertices of T, and $\mathcal{E}(T)$ the edges of T. Let $\mathcal{N} := \bigcup_{T \in \mathcal{T}} \mathcal{N}(T)$ denote the set of vertices of the triangulation $\mathcal{T}$ and $\mathcal{E} := \bigcup_{T \in \mathcal{T}} \mathcal{E}(T)$ the set of all edges of $\mathcal{T}$. Each edge $E \in \mathcal{E}$ has length $|E|$ and midpoint $\operatorname{mid}(E)$. For any $E := \operatorname{conv}\{y, z\} \in \mathcal{E}$ with $y, z \in \mathcal{N}$, let $\mathcal{N}(E) := \{y, z\}$. For any $z \in \mathcal{N}$, let $\mathcal{T}(z) := \{T \in \mathcal{T} \mid z \in \mathcal{N}(T)\}$ denote the set of all elements that have z as a vertex, and $\mathcal{E}(z) := \{E \in \mathcal{E} \mid z \in \mathcal{N}(E)\}$ the set of edges that have z as an endpoint. The set $\mathcal{N}(\omega)$ denotes the set of nodes that lie in the interior of ω, and $\mathcal{E}(\omega)$ denotes the set of edges that lie in the interior of ω. The sets $\mathcal{N}(\partial\omega)$ and $\mathcal{E}(\partial\omega)$ denote the set of vertices, respectively edges that lie on the boundary $\partial\omega$. For $\gamma_j \subseteq \partial\omega$, $j = 1, \ldots, J$, $\mathcal{N}(\gamma_j) := \{z \in \mathcal{N}(\gamma_j) \mid z \in \gamma_j\}$ denotes the

set of all nodes $z \in \mathcal{N}(\partial\omega)$ that lie on γ_j and $\mathcal{E}(\gamma_j) := \{E \in \mathcal{E}(\gamma_j) \mid E \subseteq \gamma_j\}$ denotes the set of all edges $E \in \mathcal{E}(\gamma)$ that are part of γ_j. Any boundary edge $E \in \mathcal{E}(\partial\omega)$ has to satisfy $E \subset \gamma_j$ for some $j \in \{1, \dots, J\}$. For any γ_j, $j = 1, \dots, J$, the endpoints z_{1j}, z_{2j} of γ_j with respect to the boundary $\partial\omega$ satisfy $z_{1j}, z_{2j} \in \mathcal{N}(\partial\omega)$.

The triangulation is assumed to be shape-regular in the sense that there exists some universal constant $\gamma_0 > 0$ such that any interior angle α satisfies $\gamma_0 \leq \alpha$.
The sub-division of each triangle $T \in \mathcal{T}$ into four congruent sub-triangles $T_1, \dots, T_4$ by straight lines through the edges' midpoints results in the red-refined triangulation $\mathrm{red}(\mathcal{T})$, where T_4 denotes the centre triangle.

To minimize technicalities, assume, that the triangulation is not too coarse near convex corners, i.e., each side adjacent to a convex corner contains at least two edges. Furthermore, each triangle has at least one interior node $z \in \mathcal{N}(\omega) \cap \mathcal{N}(T)$.

Based on a shape-regular triangulation $\mathcal{T}$ of ω, the following definitions are fundamental.

Definition 2.2 (piecewise differential operators)**.** *Let $\mathcal{T}$ be a triangulation of $\omega \subset \mathbb{R}^2$. The piecewise action of the gradient is denoted by ∇_{NC}, and defined by*

$$(\nabla_{\mathrm{NC}} v)|_T = \nabla(v|_T) \quad \text{for any } T \in \mathcal{T} \text{ and } v \in H^1(T).$$

Definition 2.3 (piecewise Sobolev space)**.** *Let $\mathcal{T}$ be a triangulation of $\omega \subset \mathbb{R}^2$. Define the piecewise Sobolev space $H^1(\mathcal{T})$ by*

$$H^1(\mathcal{T}) := \{v \in L^2(\omega) \mid v \in H^1(\mathrm{int}(T)) \text{ for } T \in \mathcal{T}\}.$$

Definition 2.4 (mesh-size)**.** *Let $\mathcal{T}$ be a triangulation of $\omega \subset \mathbb{R}^2$. The mesh-size $h_{\mathcal{T}} : \mathcal{T} \to \mathbb{R}$ is defined by*

$$h_T := h_{\mathcal{T}}|_T := \operatorname{diam} T := \sup_{x,y \in T} |y - z|.$$

The mesh-size $h_{\mathcal{E}} : \mathcal{E} \to \mathbb{R}$ is define by

$$h_E := h_{\mathcal{E}}|_E := |E|.$$

Definition 2.5 (patches)**.** *Let $\mathcal{T}$ be a triangulation of $\omega \subset \mathbb{R}^2$. For $z \in \mathcal{N}$, $E \in \mathcal{E}$, and $T \in \mathcal{T}$ define the following patches*

$$\begin{aligned} \omega_z &:= \mathrm{int}\big(\cup_{T \in \mathcal{T}(z)} T\big), \quad \omega_E := \mathrm{int}\big(\cup_{T \in \mathcal{T}(E)} T\big), \\ \Omega_E &:= \mathrm{int}\big(\cup_{z \in \mathcal{N}(E)} \cup_{K \in \mathcal{T}(z)} K\big), \\ \Omega_T &:= \mathrm{int}\big(\cup_{z \in \mathcal{N}(T)} \cup_{K \in \mathcal{T}(z)} K\big). \end{aligned}$$

Definition 2.6 (unit normal, unit tangential)**.** *Each edge is associated with a fixed orientation of the unit normal ν_E. For boundary edges $E \in \mathcal{E}(\partial\omega)$ ν_E is the outer unit normal. For interior edges $E \in \mathcal{E}(\omega)$, the orientation of ν is fixed by the choice of the triangles T_+, T_- with $E := T_+ \cap T_-$ and ν_E is the outward normal of T_+ along the edge $E \in \mathcal{E}(T_+) \cap \mathcal{E}(T_-)$. The unit tangential vector τ_E along an edge $E \in \mathcal{E}$ is given by $\tau_E := (0\,1; -1\,0)\nu_E$.*

Definition 2.7 (jump, average)**.** *Let $\mathcal{T}$ be a triangulation of $\omega \subset \mathbb{R}^2$ and let $f \in H^1(\mathcal{T})$. The jump across an interior edge $E := T_+ \cap T_- \in \mathcal{E}$ is defined by*

$$[f]_E := f|_{T_+} - f|_{T_-}.$$

For a boundary edge $E \in \mathcal{E}(\partial\omega)$, the jump is defined by

$$[f]_E := f.$$

The average along an edge $E := T_+ \cap T_- \in \mathcal{E}$ is defined by

$$\langle f \rangle_E := (f|_{T_+} + f|_{T_-})/2.$$

For a boundary edge $E \in \mathcal{E}(\partial\omega)$, the average is defined by

$$\langle f \rangle_E := f.$$

Definition 2.8 (volume oscillations)**.** *Let $\mathcal{T}$ be a shape-regular triangulation of $\omega \subset \mathbb{R}^2$ and let $\tilde{\omega} \subseteq \omega$. For $f \in L^2(\omega)$ define the oscillations by*

$$\operatorname{osc}^2(f, \tilde{\omega}) := \operatorname{diam}^2(\tilde{\omega}) \left\| f - \fint_{\tilde{\omega}} f \,\mathrm{d}x \right\|^2_{L^2(\tilde{\omega})}.$$

For $z \in \mathcal{N}, E \in \mathcal{E}$, $T \in \mathcal{T}$, and for the subsets $\mathcal{M} \subseteq \mathcal{N}$, $\mathcal{F} \subseteq \mathcal{E}$, and $\mathcal{K} \subseteq \mathcal{T}$ define the following oscillations by

$$\operatorname{osc}^2(f, z) := \operatorname{osc}^2(f, \omega_z) \qquad \operatorname{osc}^2(f, \mathcal{M}) := \sum_{z \in \mathcal{M}} \operatorname{osc}^2(f, z),$$

$$\operatorname{osc}^2(f, E) := \operatorname{osc}^2(f, \omega_E) \qquad \operatorname{osc}^2(f, \mathcal{F}) := \sum_{E \in \mathcal{F}} \operatorname{osc}^2(f, E),$$

$$\operatorname{osc}^2(f, T) := \operatorname{osc}^2(f, T) \qquad \operatorname{osc}^2(f, \mathcal{K}) := \sum_{T \in \mathcal{K}} \operatorname{osc}^2(f, T),$$

$$\operatorname{Osc}^2(f, T) := \operatorname{osc}^2(f, \Omega_T) \qquad \operatorname{Osc}^2(f, \mathcal{K}) := \sum_{T \in \mathcal{K}} \operatorname{Osc}^2(f, T).$$

Definition 2.9 (boundary oscillations)**.** *Let $\mathcal{T}$ be a shape-regular triangulation of $\omega \subset \mathbb{R}^2$ with boundary $\partial\omega$ and $\gamma \subseteq \partial\omega$. For $\psi \in L^2(\partial\omega)$ define the oscillations by*

$$\operatorname{osc}^2_{1/2}(\psi, \gamma) := \operatorname{meas}^2_1(\gamma) \left\| \psi - \fint_{\gamma} \psi \,\mathrm{d}s \right\|^2_{L^2(\gamma)}.$$

For $z \in \mathcal{N}(\partial\omega)$, $\mathcal{M} \subseteq \mathcal{N}(\partial\omega)$, and $\mathcal{F} \subseteq \mathcal{E}(\partial\omega)$ define

$$\operatorname{osc}^2_{1/2}(\psi, z) := \operatorname{osc}^2_{1/2}(\psi, \partial\omega_z \cap \partial\omega) \qquad \operatorname{osc}^2_{1/2}(\psi, \mathcal{M}) := \sum_{z \in \mathcal{M}} \operatorname{osc}^2_{1/2}(\psi, z),$$

$$\operatorname{osc}^2_{1/2}(\psi, \mathcal{F}) := \sum_{E \in \mathcal{F}} \operatorname{osc}^2_{1/2}(\psi, E).$$

2.2.2. Piecewise spaces

This section defines piecewise spaces with respect to the shape-regular triangulation $\mathcal{T}$ of $\omega \subset \mathbb{R}^2$ from Subsection 2.2.1. The basis for the finite element methods employed in this thesis is the set of piecewise polynomials defined in the following.

Definition 2.10 (polynomials)**.** *Let $\omega \subseteq \mathbb{R}^n$. The set of polynomials of degree $\leq k$ is given by*

$$P_k(\omega;\mathbb{R}^m) := \{v \in L^\infty(\omega;\mathbb{R}^m) \mid v_k \text{ is a polynomial of degree } \leq k\}.$$

For a shape-regular triangulation $\mathcal{T}$ of $\omega \subset \mathbb{R}^2$, define the set of piecewise polynomials by

$$P_k(\mathcal{T};\mathbb{R}^m) := \{v_k \in L^\infty(\omega;\mathbb{R}^m) \;\big|\; v_k|_T \in P_k(T;\mathbb{R}^m) \text{ for all } T \in \mathcal{T}\}.$$

Let $\gamma \subset \partial\omega$ with a set $\mathcal{F} \subset \mathcal{E}(\partial\omega)$ such that $\overline{\gamma} = \cup_{E\in\mathcal{F}} E$ and define the set of piecewise polynomials of degree $\leq k$ on these edges by

$$P_k(\mathcal{F};\mathbb{R}^m) := \{v_k \in L^\infty(\cup_{E\in\mathcal{F}} E;\mathbb{R}^m) \;\big|\; v_k|_E \in P_k(E;\mathbb{R}^m) \text{ for all } E \in \mathcal{F}\}$$

If $m = 1$, omit $\mathbb{R}$, i.e., $P_k(\omega;\mathbb{R}) =: P_k(\omega)$ etc.

The L^2 orthogonal projection onto the space $P_k(\mathcal{T})$ (respectively $P_k(\mathcal{T},\mathbb{R}^m)$) is denotes by Π_k and the L^2 orthogonal projection onto the space $P_k(\mathcal{F})$ (respectively $P_k(\mathcal{F};\mathbb{R}^m)$) by Π_k^γ.

2.2.3. Conforming finite element space

This section describes the conforming finite element spaces employed for the Courant finite element method (CFEM). The method was introduced by Courant (1943) and the described properties can be found in e.g. Braess (2007).

Definition 2.11 (conforming finite element space)**.** *Let $\mathcal{T}$ be a shape-regular triangulation of $\omega \subset \mathbb{R}^2$. The space of continuous piecewise polynomials of degree $\leq k$ on $\mathcal{T}$ is defined by*

$$S^k(\mathcal{T}) := P_k(\mathcal{T}) \cap C(\omega).$$

Let $\mathcal{J} \subseteq \{1,\dots,J\}$ and let $\gamma = \cup_{j\in\mathcal{J}}\gamma_j \subseteq \partial\omega$. Define

$$S^k_\gamma(\mathcal{T}) := P_k(\mathcal{T}) \cap C_\gamma(\omega).$$

In case $\gamma = \partial\omega$, abbreviate $S^k_\gamma(\mathcal{T})$ by $S^k_0(\mathcal{T})$ and by $S^k_j(\mathcal{T})$ if $\gamma = \gamma_j$ for $j = 1\dots J$.

Definition 2.12 (nodal basis functions for $k = 1$)**.** *Consider the space $S^1(\mathcal{T})$. For each node $z \in \mathcal{N}$, define the nodal basis functions $\varphi_z \in S^1(\mathcal{T})$ by*

$$\varphi_z(y) := \delta_{y,z}$$

for the Kronecker delta δ and $z \in \mathcal{N}$. The set $\omega_z := \operatorname{int}\big(\cup_{T\in\mathcal{T}(z)} T\big)$ denotes the interior of the support of φ_z.

The space $S^1_\gamma(\mathcal{T})$ is spanned by φ_z for $z \in \mathcal{N}(\omega) \cup \mathcal{N}(\partial\omega \setminus \gamma)$.

2.2.4. Non-conforming finite element space

This section describes the non-conforming finite element space employed for the non-conforming Crouzeix-Raviart finite element method (NCFEM). The method was first introduced by Crouzeix and Raviart (1973) and the properties can be found in e.g. Braess (2007)

Definition 2.13 (non-conforming finite element space)**.** *Let $\mathcal{T}$ be a shape-regular triangulation of $\omega \subset \mathbb{R}^2$. The space of Crouzeix-Raviart functions is defined by*

$$\mathrm{CR}^1(\mathcal{T}) := \left\{ v_{\mathrm{CR}} \in P_1(\mathcal{T}) \mid \fint_E [v_{\mathrm{CR}}]_E \,\mathrm{d}s = 0 \text{ for all } E \in \mathcal{E} \right\}.$$

Let $\mathcal{J} \subseteq \{1, \dots, J\}$ and let $\gamma = \cup_{j \in \mathcal{J}} \gamma_j \subset \partial\omega$. Define

$$\mathrm{CR}^1_\gamma(\mathcal{T}) := \left\{ v_{\mathrm{CR}} \in \mathrm{CR}^1(\mathcal{T}) \mid \fint_E v_{\mathrm{CR}} \,\mathrm{d}s = 0 \text{ for all } E \in \mathcal{E}(\gamma) \right\}$$

Abbreviate $\mathrm{CR}^1_\gamma(\mathcal{T})$ by $\mathrm{CR}^1_0(\mathcal{T})$ if $\gamma = \partial\omega$ and by $\mathrm{CR}^1_j(\mathcal{T})$ if $\gamma = \gamma_j$ for $j = 1, \dots, J$.

Definition 2.14 (non-conforming edge-oriented basis function)**.** *Consider the space $\mathrm{CR}^1(\mathcal{T})$. For each edge $E \in \mathcal{E}$ define the edge-oriented basis function $\psi_E \in \mathrm{CR}^1(\mathcal{T})$ by*

$$\psi_E\big(\operatorname{mid}(F)\big) := \delta_{E,F}$$

for the Kronecker delta δ and $F \in \mathcal{E}$. The set $\omega_E := \operatorname{int}\big(T_+ \cup T_-\big)$ (with $T_+ \cap T_- = E$) is the interior of the support of ψ_E.

The space $\mathrm{CR}^1_\gamma(\mathcal{T})$ is spanned by ψ_E for $E \in \mathcal{E}(\omega) \cup \mathcal{E}(\partial\omega \setminus \gamma)$.

2.2.5. Mixed finite element space

This section describes the function space employed for the mixed lowest-order Raviart-Thomas finite element method (MFEM). This method was first introduced by Raviart and Thomas (1977) and the following properties and definitions can be found in e.g. Braess (2007).

Definition 2.15 (mixed finite element space)**.** *Let $\mathcal{T}$ be a shape-regular triangulation of $\omega \subset \mathbb{R}^2$. The space of lowest-order Raviart-Thomas functions is defined by*

$$\mathrm{RT}_0(\mathcal{T}) := \left\{ q_{\mathrm{RT}} \in H(\mathrm{div}, \omega) \;\middle|\; \begin{array}{l} \forall T \in \mathcal{T}\ \exists (a,b,c) \in \mathbb{R}^3 \\ \quad s.t.\ q_{\mathrm{RT}}|_T := (a,b) + cx \end{array} \right\}.$$

Let $\mathcal{J} \subseteq \{1, \dots, J\}$ with $\gamma = \cup_{j \in \mathcal{J}} \gamma_j \subset \partial\omega$ and let $g \in L^2(\gamma)$. Define

$$\mathrm{RT}_0^{\gamma,g}(\mathcal{T}) := \left\{ q_{\mathrm{RT}} \in \mathrm{RT}_0(\mathcal{T}) \mid q_{\mathrm{RT}} \cdot \nu_E = \fint_E g \,\mathrm{d}s \text{ for all } E \in \mathcal{E}(\gamma) \right\}.$$

For $\gamma = \gamma_j$ for $j = 1, \dots, J$ abbriviate $\mathrm{RT}_0^{\gamma,g}(\mathcal{T})$ by $\mathrm{RT}_0^{j,g}(\mathcal{T})$.

Definition 2.16 (mixed edge-oriented basis functions)**.** *Consider the space $\mathrm{RT}_0(\mathcal{T})$. For each edge $E \in \mathcal{E}$ with $E = T_+ \cap T_-$ ($T_+, T_- \in \mathcal{T}$) define the edge-oriented basis functions $\Psi_E \in \mathrm{RT}_0(\mathcal{T})$ by*

$$\Psi_E(x) := \begin{cases} \pm |E| / (2|T_\pm|)(x - P_\pm) & \text{for } x \in T_\pm \\ 0 & \text{otherwise.} \end{cases}$$

The space $\mathrm{RT}_0(\mathcal{T})$ is spanned by Ψ_E for all $E \in \mathcal{E}(\omega)$.

2.2.6. Interpolation operators

This subsection presents the well-known conforming and non-conforming interpolation operators as well as interpolation error estimates

Definition 2.17 (nodal interpolation operator)**.** *Let $\mathcal{T}$ be a shape-regular triangulation of ω. The conforming interpolation operator I_{C} is given by*

$$I_{\mathrm{C}} : C(\overline{\omega}) \to S^1(\mathcal{T}),\ v \mapsto \sum_{z \in \mathcal{N}} v(z)\varphi_z.$$

Theorem 2.18. *Let $T \in \mathcal{T}$ with a maximal interior angle α. For $v \in H^2(T)$, the conforming interpolation operator satisfies*

$$||h_T^{-1}\nabla(v - I_{\mathrm{C}}v)||_{L^2(T)} \leq \sqrt{\frac{1/4 + 2/j_{1,1}^2}{1 - |\cos(\alpha)|}}||D^2 v||_{L^2(T)}.$$

for the smallest positive root $j_{1,1} \geq 3.8317$ of the Bessel function of the first kind.

Proof. The assertion is contained in Carstensen et al. (2012b, Thm. 3.1). □

Definition 2.19 (non-conforming interpolation operator)**.** *Let $\mathcal{T}$ be a shape-regular triangulation of ω. The non-conforming interpolation operator I_{NC} is given by*

$$I_{\mathrm{NC}} : H^1(\omega) \to \mathrm{CR}^1(\mathcal{T}),\ v \mapsto \sum_{E \in \mathcal{E}} (\fint_E v \,\mathrm{d}s)\psi_E.$$

Theorem 2.20. *For all $v \in H^1(\omega)$, the non-conforming interpolation operator satisfies*

ⓐ $||h_{\mathcal{T}}^{-1}(v - I_{\mathrm{NC}}v)||_{L^2(\omega)} \leq \sqrt{1/48 + 1/j_{1,1}^2}||\nabla_{\mathrm{NC}}(v - I_{\mathrm{NC}}v)||_{L^2(\omega)}$;

ⓑ $\nabla_{\mathrm{NC}} I_{\mathrm{NC}} v = \Pi_0 \nabla v$

for the smallest positive root $j_{1,1} \geq 3.8317$ of the Bessel function of the first kind.

Proof. The proof of ⓐ follows as in Carstensen et al. (2012b) with the improved constant in Carstensen and Gallistl (2014, Thm. 4).
The proof of ⓑ follows from an integration by parts on each triangle and the integral mean property of I_{NC} along each edge $E \in \mathcal{E}$. □

2.3. Frequently used results

This section presents frequently used Theorems.

Theorem 2.21 (Poincaré inequality)**.** *Let $\omega \subset \mathbb{R}^n$ be a Lipschitz domain. Then there exists a constant $C_P(\omega)$, such that for any $v \in H^1(\omega)$ with $\fint_\omega v \,\mathrm{d}x = 0$, it holds*

$$||v||_{L^2(\omega)} \leq C_P(\omega)||Dv||_{L^2(\omega)}.$$

Proof. The proof an be found in Evans (2010, Thm. 1, P. 290). □

Remark 2.22. *Any convex open set $\omega \subset \mathbb{R}^n$ satisfies $C_P(\omega) \leq \operatorname{diam}(\omega)/\pi$ (Payne and Weinberger, 1960). If $\omega \subset \mathbb{R}^2$ is a triangle, the constant is improved to $C_P(\omega) \leq \operatorname{diam}(\omega)/j_{1,1}$ for the fist positive root $j_{1,1} \geq 3.8317$ of the first Bessel function of first kind (Laugesen and Siudeja, 2010).*

Theorem 2.23 (Friedrichs inequality)**.** *Let $\omega \subset \mathbb{R}^n$ be a Lipschitz domain and $\gamma \subseteq \partial\omega$ with $\operatorname{meas}_{n-1}(\gamma) > 0$. Then there exists a constant $C_F(\omega, \gamma)$, such that for any $v \in H^1_\gamma(\omega)$ it holds*

$$||v||_{L^2(\omega)} \leq \operatorname{diam}(\omega) C_F(\omega, \gamma) ||Dv||_{L^2(\omega)}.$$

Proof. The proof can be found in Braess (2007, P. 30). □

Theorem 2.24 (trace inequality)**.** *Let $\omega \subset \mathbb{R}^n$ be a Lipschitz domain. Then there exists a constant C_ω, such that for any $v \in H^1(\omega)$ it holds*

$$||v||_{L^2(\partial\omega)} \leq C_\omega ||v||^{1/2}_{L^2(\omega)} ||Dv||^{1/2}_{L^2(\omega)}.$$

Proof. This follows from Brenner and Scott (2008, Thm. 1.6.6, P. 39). □

Theorem 2.25 (Young's inequality)**.** *Any $a, b \in \mathbb{R}$ and $\varepsilon > 0$ satisfy*

$$ab \leq a^2/2\varepsilon + \varepsilon b^2/2.$$

Proof. This follows from the binomial formula. □

Theorem 2.26 (Helmholtz decomposition)**.** *Let $\omega \subset \mathbb{R}^2$ be a simply connected Lipschitz domain and $\gamma \subset \partial\omega$ with $\operatorname{meas}_{n-1}(\gamma) > 0$. Define $H_{\operatorname{Curl},\partial\omega\setminus\gamma}(\omega) := \{q \in H^1(\omega; \mathbb{R}^2) \mid \operatorname{Curl} q \cdot \nu = 0 \text{ along } \partial\omega \setminus \gamma\}$. Then*

$$L^2(\omega; \mathbb{R}^2) = \nabla H^1_\gamma(\omega) \oplus \operatorname{Curl} H_{\operatorname{Curl},\partial\omega\setminus\gamma}(\omega).$$

Proof. Standard results yield the unique existence of $\alpha \in H^1_\gamma(\omega)$ with $\nabla\alpha = p$ in ω and $\nabla\alpha \cdot \nu = p \cdot \nu$ along $\partial\omega \setminus \gamma$. Set $q := p - \nabla\alpha$ and note that q satisfies $q \in H(\operatorname{div}, \omega)$ with $\operatorname{div} q = 0$ and $q \cdot \nu = 0$ along $\partial\omega \setminus \gamma$. Girault and Raviart (1986, Thm. 3.1, P. 37) show the existence of $\beta \in H_{\operatorname{Curl},\partial\omega\setminus\gamma}(\omega)$ with $\operatorname{Curl}\beta = q$. This concludes the proof. □

2.4. Conforming companions

In many situations it is necessary to obtain a function $v \in H^1_0(\omega)$ from a given Crouzeix-Raviart function $v_{\mathrm{CR}} \in \mathrm{CR}^1_0(\omega)$. Given $v_{\mathrm{CR}} \in \mathrm{CR}^1_0(\omega)$, define $J_1 : \mathrm{CR}^1_0(\omega) \to S^1_0(\omega)$ by

$$J_1 v_{\mathrm{CR}} := \sum_{z \in \mathcal{N}(\omega)} \left(\operatorname{card}(\mathcal{T}(z))^{-1} \sum_{T \in \mathcal{T}(z)} v_{\mathrm{CR}}|_T(z) \right) \varphi_z,$$

where $\operatorname{card}(\mathcal{T}(z))$ denotes the number of triangles in $\mathcal{T}(z)$. For an edge $E \in \mathcal{E}$, define the edge bubble function $b_E := 6\Pi_{z \in \mathcal{N}(E)} \varphi_z$ which satisfies $⨍_E b_E \, \mathrm{d}s = 1$ and

$\operatorname{supp}(b_E) \subseteq \omega_E$. The operator $J_2 : \mathrm{CR}_0^1(\mathcal{T}) \to S_0^2(\mathcal{T})$ is define by

$$J_2 v_{\mathrm{CR}} := J_1 v_{\mathrm{CR}} + \sum_{E \in \mathcal{E}(\omega)} \left(\fint_E (v_{\mathrm{CR}} - J_1 v_{\mathrm{CR}}) \,\mathrm{d}s \right) b_E.$$

For a triangle $T \in \mathcal{T}$, define the cubic volume bubble $b_T := 60 \Pi_{z \in \mathcal{N}(T)} \varphi_z$ which satisfies $\fint_T b_T \,\mathrm{d}x = 1$ and $\operatorname{supp}(b_T) \subseteq T$. The operator $J_3 : \mathrm{CR}_0^1(\mathcal{T}) \to S_0^3(\mathcal{T})$ is given by

$$J_3 v_{\mathrm{CR}} := J_2 v_{\mathrm{CR}} + \sum_{T \in \mathcal{T}} \left(\fint_T (v_{\mathrm{CR}} - J_2 v_{\mathrm{CR}}) \,\mathrm{d}x \right) b_T.$$

These operators fulfil the following properties

Theorem 2.27 (properties of the conforming companions)**.** *The operators* $J_k : \mathrm{CR}_0^1(\mathcal{T}) \to S_0^k(\mathcal{T})$ *for* $k = 1, 2, 3$*, satisfy*

$$\text{ⓐ} \int_T \nabla_{\mathrm{NC}}(v_{\mathrm{CR}} - J_k v_{\mathrm{CR}}) \,\mathrm{d}x = 0 \quad \text{for all } T \in \mathcal{T} \text{ and } k = 2, 3,$$

$$\text{ⓑ} \int_T (v_{\mathrm{CR}} - J_3 v_{\mathrm{CR}}) \,\mathrm{d}x = 0 \quad \text{for all } T \in \mathcal{T},$$

$$\text{ⓒ} \; ||h_{\mathcal{T}}^{-1}(v_{\mathrm{CR}} - J_k v_{\mathrm{CR}}||_{L^2(\omega)} \approx ||\nabla_{\mathrm{NC}}(v_{\mathrm{CR}} - J_k v_{\mathrm{CR}})||_{L^2(\omega)} \approx \min_{\varphi \in H_0^1(\omega)} ||\nabla_{\mathrm{NC}}(v_{\mathrm{CR}} - \varphi)||_{L^2(\omega)}.$$

Proof. The proof follows from Carstensen et al. (2015a). □

2.5. Inhomogeneous boundary conditions

In many practical examples, the Dirichlet boundary conditions cannot be incorporated exactly in the finite element space at hand. The following theorem presents a remedy for this problem.

Theorem 2.28. *Let* $\omega \subset \mathbb{R}^2$ *and* $\gamma_D \subseteq \partial\omega$ *with* $\operatorname{meas}_1(\gamma_D) > 0$*. For any* $v_D \in C(\gamma_D) \cap H^2(\mathcal{E}(\gamma_D))$*, with* $v_D(z) = 0$ *for all* $z \in \mathcal{N}(\gamma_D)$*, there exists a function* $w_D \in H^1(\omega)$ *with* $w_D|_{\gamma_D} = v_D|_{\gamma_D}$*,* $w_D|_E = 0$ *for all* $E \in \mathcal{E}(\omega) \cup \mathcal{E}(\partial\omega \setminus \gamma_D)$*,* $I_{\mathrm{NC}} w_D = 0$*,* $\Pi_0 w_D = 0$*, and*

$$||\nabla w_D||_{L^2(\omega)} \lesssim ||h_{\mathcal{E}}^{3/2} \partial^2 v_D / \partial s^2||_{L^2(\gamma_D)}.$$

Proof. This follows from Theorem 4.2 of Bartels et al. (2004) and Carstensen and Köhler (2016b, Lem. 2.4). □

2.6. Variational inequalities

This section presents the general notation for elliptic variational inequalities of the first and second kind and forms the basis for all problems considered within this thesis. The following description can be found in Glowinski (2008).

Let $(V, (\bullet, \bullet))$ be a real Hilbert space with dual V^* and $a : V \times V \to \mathbb{R}$ a continuous and V-elliptic bilinear form on $V \times V$. Furthermore $F : V \to \mathbb{R}$ is a continuous linear functional and $K \subset V$ is a closed, convex, and non-empty subset of V. The functional $j : V \to \mathbb{R} \cup \{\infty\}$ is proper (i.e., $j(v) > -\infty$ for all $v \in V$ and there exists $w \in V$ with $j(w) \neq \infty$), convex, and lower semi-continuous. Then a *variational inequality of first kind* seeks $u \in K$ such that

$$F(v-u) \leq a(u, v-u) \quad \text{for all } v \in K. \tag{2.2}$$

A *variational inequality of second kind* seeks $u \in V$ such that

$$F(v-u) \leq a(u, v-u) + j(v) - j(u) \quad \text{for all } v \in V. \tag{2.3}$$

Remark 2.29. *Variational inequalities of the first kind can also be formulated as variational inequalities of the second kind, where j is a characteristic function.*

2.7. Common scalar product and norms

This section presents the bilinear forms, scalar products, and norms most commonly used throughout the thesis.

The Sobolev space $H^1(\omega)$ is equipped with a norm $||\bullet||_{H^1(\omega)}$ and the corresponding scalar product. Let $\gamma \subset \partial\omega$ with $\mathrm{meas}_{n-1}(\gamma) > 0$, then the space $H^1_\gamma(\omega)$ is equipped with an alternative energy norm given by

$$\| \bullet \| := ||\nabla \bullet||_{L^2(\omega)}. \tag{2.4}$$

Since the Friedrichs inequality (cf. Theorem 2.23) holds, this is indeed a norm on $H^1_\gamma(\omega)$. This norm is induced by the scalar product

$$a(v, w) := \int_\omega \nabla v \cdot \nabla w \, \mathrm{d}x \quad \text{for all } v, w \in H^1_\gamma(\omega). \tag{2.5}$$

Remark 2.30. *The scalar product can be extended to a bilinear form on $H^1(\omega) \times H^1(\omega)$ and then defines a semi norm $\| \bullet \|^2 = a(\bullet, \bullet)$ on $H^1(\omega)$.*

Let $\mathcal{T}$ be a triangulation of $\omega \subset \mathbb{R}^2$ and define the bilinear form $a_{\mathrm{NC}} : H^1(\mathcal{T}) \times H^1(\mathcal{T})$ by

$$a_{\mathrm{NC}}(v_\mathcal{T}, w_\mathcal{T}) := \int_\omega \nabla_{\mathrm{NC}} v_\mathcal{T} \cdot \nabla_{\mathrm{NC}} w_\mathcal{T} \, \mathrm{d}x \quad \text{for } v_\mathcal{T}, w_\mathcal{T} \in H^1(\mathcal{T}). \tag{2.6}$$

Then $\| \bullet \|^2_{\mathrm{NC}} := a_{\mathrm{NC}}(\bullet, \bullet)$ is a semi norm on $H^1(\mathcal{T})$. Let $\gamma \subseteq \partial\omega$ with $\mathrm{meas}_1(\gamma) > 0$. The discrete Friedrichs inequality (cf. for example (Brenner and Scott, 2008, Thm. 10.6.12)) shows that $\| \bullet \|_{\mathrm{NC}}$ a norm on $\mathrm{CR}^1_\gamma(\mathcal{T}) \subset H^1(\mathcal{T})$ for $\gamma \subseteq \omega$ with $\mathrm{meas}_1(\gamma) \geq 0$.

Definition 2.31 (operator norm)**.** *Let $\omega \subset \mathbb{R}^n$ and $\gamma \subset \partial\omega$ with $\mathrm{meas}_{n-1}(\gamma) > 0$. Let $F \in H^{-1}_\gamma(\omega)$, and define $H^1_\gamma(\mathcal{T}) := \{v \in H^1(\mathcal{T}) \mid \fint_E [v]_E \, \mathrm{d}s = 0 \text{ for } E \in \mathcal{E}(\Omega) \cup \mathcal{E}(\gamma)\}$. Then the operator norm $\|F\|_*$ and semi norm $\|F\|_{\mathrm{NC},*}$ are defined by*

$$\|F\|_* := \sup_{v \in H^1_\gamma(\omega) \setminus \{0\}} F(v)/\|v\|,$$

$$\|F\|_{\mathrm{NC},*} := \sup_{v \in H^1_\gamma(\mathcal{T}) \setminus \{0\}} F(v)/\|v\|_{\mathrm{NC}}.$$

3. Obstacle Problem

This chapter is devoted to the obstacle problem, which is the model problem for variational inequalities. The chapter presents the results of Carstensen and Köhler (2016a) and reports further aspects in the analysis of this model problem.

3.1. Problem formulation

This section introduces the variational inequality that describes the obstacle problem and discusses equivalent formulations.

3.1.1. Mathematical modelling

Let $\Omega \subset \mathbb{R}^d$ be a bounded, simply connected Lipschitz domain with polyhedral boundary $\partial\Omega$, subdivided into the closed subset Γ_D and the open (and possibly empty) subset Γ_N. Set $V := H^1_D(\Omega) := H^1_{\Gamma_D}(\Omega)$. Let the obstacle χ and the Dirichlet boundary value u_D satisfy

$$\chi \in H^1(\Omega) \text{ and } u_D \in H^{1/2}(\Gamma_D) \text{ with } \chi \leq u_D \text{ a.e. along } \Gamma_D, \tag{3.1}$$

so that the closed and convex subset

$$K := \{v \in \mathcal{A} \mid \chi \leq v \text{ a.e. in } \Omega\} \quad \text{of} \quad \mathcal{A} := \{v \in H^1(\Omega) \mid v = u_D \text{ a.e. along } \Gamma_D\}$$

is non-empty. For $f \in L^2(\Omega)$ and $g \in L^2(\Gamma_N)$, define $F \in V^*$ by

$$F(v) := \int_\Omega fv \,\mathrm{d}x + \int_{\Gamma_N} gv \,\mathrm{d}s \quad \text{for all } v \in V.$$

The weak formulation of the obstacle problem seeks $u \in K$ such that

$$F(v-u) \leq a(u, v-u) \quad \text{for all } v \in K. \tag{3.2}$$

Lemma 3.1 (existence of solutions)**.** *Let the conditions* (3.1) *hold. Then there exists a unique solution $u \in K$ to problem* (3.2)*.*

Proof. Since $a(\bullet, \bullet)$ is a scalar product on $H^1_D(\Omega)$, the proof follows after a shift of χ to $\chi - u_D$ and of F to $F - a(u_D, \bullet)$ from Kinderlehrer and Stampacchia (1980, Ch. 2, Thm. 2.1). □

Lemma 3.2 (regularity)**.** *Let $\Gamma_D = \partial\Omega$, $u_D \in H^1(\Omega), \chi \in H^1(\Omega)$ with $\chi \geq u_D$ along $\partial\Omega$ and $\Delta\chi \in L^2(\Omega)$. For $f \in L^2(\Omega)$, the unique solution $u \in K$ to* (3.2) *satisfies $u \in H^1(\Omega)$ and $\Delta u \in L^2(\Omega)$.*

Proof. This follows from (Rodrigues, 1987, Prop. 5:2.2). □

Remark 3.3. *In the case of mixed boundary conditions, i.e., the Dirichlet and Neumann boundary satisfy* $\operatorname{meas}_{n-1}(\Gamma_D), \operatorname{meas}_{n-1}(\Gamma_N) > 0$*, the unique solution* $u \in K$ *is of reduced regularity in general (see Rodrigues, 1987, Thm. 5:3.4). If the obstacle* χ *satisfies* $\nabla\chi \cdot \nu \leq g$ *along* Γ_N*, the regularity of the obstacle problem is related to the regularity of the corresponding linear problem (see Rodrigues, 1987, Ch. 5, Rem. 3.5). If* $u \in K$ *satisfies* $\nabla u \cdot \nu \in L^2(\partial\Omega)$*, Theorem 3.3 in Rodrigues (1987, Ch. 5) shows that* $g = \nabla u \cdot \nu$ *along* Γ_N*.*

Define the linear and bounded form $\Lambda \in V^*$, i.e., the Lagrange multiplier, by

$$\Lambda(v) := F(v) - a(u, v) \quad \text{for all } v \in V. \tag{3.3}$$

Lemma 3.4 (complementary conditions)**.** *Let the conditions* (3.1) *on the obstacle* χ *and the Dirichlet boundary value* u_D *be satisfied. Then the functional* $\Lambda \in V^*$ *from* (3.3) *and the unique solution* $u \in K$ *to* (3.2) *satisfy the following complementary conditions*

$$0 \leq u - \chi,\ \Lambda(u - \chi) = 0,\ \Lambda(\varphi) \leq 0 \text{ for all } \varphi \in V_+ := \{v \in V \mid v \geq 0 \text{ in } \Omega\}. \tag{3.4}$$

Proof. The first inequality follows from $u \in K$. To show orthogonality, let $n \in \mathbb{N}$ and consider the standard mollifier $\varphi_{1/n} \in C_0^\infty(\Omega)$ with $0 \leq \varphi_{1/n} \leq 1$. Define the test functions

$$v := u \pm \varphi_{1/n}(u - \chi) \in K.$$

The variational inequality (3.2) shows

$$\Lambda(v - u) = \pm\Lambda(\varphi_{1/n}(u - \chi)) = \pm F(\varphi_{1/n}(u - \chi)) \mp a(u, \varphi_{1/n}(u - \chi)) \leq 0.$$

Convergence in the sense of distributions shows $\pm\Lambda(u - \chi) \leq 0$ and hence

$$\Lambda(u - \chi) = 0.$$

To show the last inequality, let $\varphi \in V$ with $\varphi \geq 0$ a.e. in Ω and define $v = u + \varphi \in K$. The variational inequality (3.2) shows

$$\Lambda(\varphi) = F(\varphi) - a(u, \varphi) \leq 0$$

and concludes the proof. □

Remark 3.5. *Similar results which do not include mixed boundary conditions or have slightly stronger assumptions on the obstacle (i.e.* $\chi|_{\Gamma_D} = u_D$*) can be found in Kinderlehrer and Stampacchia (1980, Ch. 2, Thm. 6.9) and Rodrigues (1987, Ch. 4, Prop. 5.6).*

Remark 3.6. *In the case of pure Dirichlet boundary conditions, the functional* $\Lambda \in H^{-1}(\Omega)$ *has an* L^2 *representation* $\lambda = f + \Delta u \in L^2(\Omega)$ *which satisfies*

$$0 \leq u - \chi \perp \lambda \leq 0$$

where $a \perp b$ *abbreviates pointwise orthogonality a.e. in* $\mathbb{R}$*, i.e.* $a \perp b$ *signifies* $ab = 0$ *for* $a, b \in \mathbb{R}$*.*

Remark 3.7. *In the case of mixed boundary conditions, i.e. the Dirichlet and Neumann boundary satisfy* $\operatorname{meas}_{n-1}(\Gamma_D), \operatorname{meas}_{n-1}(\Gamma_N) > 0$*, assume, that the data for*

the obstacle problem is regular enough, so that $\Delta u \in L^2(\Omega)$ *and* $\nabla u \cdot \nu \in L^2(\partial\Omega)$. *Then the functional* $\Lambda \in V^*$ *has the following representation*

$$\Lambda(\bullet) = \int_\Omega (\Delta u + f) \bullet \,\mathrm{d}x + \int_{\Gamma_N} (g - \nabla u \cdot \nu) \bullet \,\mathrm{d}s =: \int_\Omega \lambda \bullet \,\mathrm{d}x + \int_{\Gamma_N} \lambda_N \bullet \,\mathrm{d}s.$$

3.1.2. Equivalent formulations

This subsection presents three equivalent formulations for the obstacle problem together with the corresponding complementary conditions. Theorem 3.14 below shows the equivalence of the three formulations under certain regularity assumptions. Assume that the obstacle χ satisfies $\nabla\chi \cdot \nu \in L^2(\Gamma_N)$ and $\nabla\chi \cdot \nu \leq g$ along Γ_N to guarantee the regularity results $\Delta u \in L^2(\Omega)$ and $\nabla u \cdot \nu = g$ along Γ_N from Remark 3.7.

Define the energy functional

$$E(v) := 1/2a(v,v) - F(v) \quad \text{for all } v \in \mathcal{A}.$$

Then the energy formulation of the obstacle problem seeks $u \in K$ such that

$$E(u) = \min_{v \in K} E(v). \tag{3.5}$$

Lemma 3.8 (existence of solutions)**.** *There exists a unique solution* $u \in K$ *to problem* (3.5).

Proof. This follows for example from (Braess, 2007, Prop. 2.5). □

Remark 3.9. *The equivalence of Problem* (3.2) *and Problem* (3.5) *is well established and can be found in Glowinski (2008, Ch. 1, Sec. 3).*

Recall the space $H_{g,N}(\mathrm{div},\Omega) := H_{g,\Gamma_N}(\mathrm{div},\Omega)$ and $H_{0,N}(\mathrm{div},\Omega) := H_{0,\Gamma_N}(\mathrm{div},\Omega)$ from Page 11 and define the convex subset $\mathcal{M} := L^2(\Omega;[0,\infty))$ of $L^2(\Omega)$. For all functions $(q,v) \in H(\mathrm{div},\Omega) \times \mathcal{M}$ consider the following bilinear and linear forms

$$\begin{aligned} b(q,v) &:= \int_\Omega v \,\mathrm{div}\, q \,\mathrm{d}x, \\ H(q) &:= -\int_\Omega \chi \,\mathrm{div}\, q \,\mathrm{d}x + \int_{\partial\Omega} u_D q \cdot \nu \,\mathrm{d}s, \\ G(v) &:= -\int_\Omega f v \,\mathrm{d}x. \end{aligned} \tag{3.6}$$

The mixed formulation of the obstacle problem seeks $(p,w) \in H_{g,N}(\mathrm{div},\Omega) \times \mathcal{M}$ such that

$$\int_\Omega p \cdot q \,\mathrm{d}x + b(q,w) = H(q) \qquad \text{for all } q \in H_{0,N}(\mathrm{div},\Omega), \tag{3.7}$$

$$b(p, v-w) \leq G(v-w) \qquad \text{for all } v \in \mathcal{M} \tag{3.8}$$

Lemma 3.10 (mixed complementary conditions)**.** *Any continuous solution* $(p,w) \in H_{g,N}(\mathrm{div},\Omega) \times \mathcal{M}$ *to* (3.7)–(3.8) *satisfies the mixed complementary conditions*

$$0 \leq w \perp \lambda := \mathrm{div}\, p + f \leq 0.$$

Here, $\perp$ abbreviates pointwise orthogonality a.e. in $\mathbb{R}$, i.e., $a \perp b$ signifies $ab = 0$ for $a, b \in \mathbb{R}$.

Remark 3.11. *Since $p \in H_{g,N}(\operatorname{div}, \Omega)$ satisfies the Neumann boundary conditions exactly, a Lagrange multiplier which corresponds to λ_N does not exist.*

Proof. The definition of $\mathcal{M}$ implies $w \geq 0$ in Ω. To verify the orthogonality, insert the test functions $v = 2w$ and $v = 0 \in \mathcal{M}$ in (3.8). This shows

$$\int_\Omega w(\operatorname{div} p + f)\,\mathrm{d}x = 0.$$

To deduce the last inequality, let $v = w + \varphi \in \mathcal{M}$ for $\varphi \in \mathcal{M}$. Then (3.8) proves $\operatorname{div} p + f \leq 0$ a.e. in Ω. □

Remark 3.12. *The proof of the complementary conditions only employ the inequality* (3.8).

For the dual variational inequality, define the set

$$Q(f) := \{q \in H_{g,N}(\operatorname{div}, \Omega) \mid f + \operatorname{div} q \leq 0 \text{ a.e. in } \Omega\}.$$

The dual variational inequality seeks $p \in Q(f)$ such that

$$H(q - p) \leq \int_\Omega p \cdot (q - p)\,\mathrm{d}x \qquad \text{for all } q \in Q(f). \tag{3.9}$$

Lemma 3.13. *Let Ω be a simply connected domain.*

ⓐ *Any solution $p \in Q(f)$ to* (3.9) *satisfies $p = \nabla\alpha$ for some $\alpha \in K$.*

ⓑ *The function α from ⓐ fulfils the following complementary conditions*

$$0 \leq \alpha - \chi \perp \operatorname{div} p + f \leq 0. \tag{3.10}$$

where $\perp$ abbreviates pointwise orthogonality.

Proof of ⓐ. Given $p \in Q(g, f)$, define $\alpha \in \mathcal{A}$ as the solution to the auxiliary problem

$$\int_\Omega (p - \nabla\alpha) \cdot \nabla\varphi\,\mathrm{d}x = 0 \quad \text{for all } \varphi \in V.$$

Then $p - \nabla\alpha \perp \nabla V$. Since Ω is simply connected, the Helmholtz decomposition in Theorem 2.26 on Page 17 shows, that there exists $\phi \in H^1(\Omega)$ with $\operatorname{Curl}\phi \cdot \nu = 0$ along Γ_N such that

$$p - \nabla\alpha = \operatorname{Curl}\phi.$$

Set $q := p - \operatorname{Curl}\phi \in Q(f)$. Since $p - q = -\operatorname{Curl}\phi$, the dual variational inequality (3.9) and an integration by parts show

$$\begin{aligned}
-\int_{\Gamma_D} u_D \operatorname{Curl}\phi\,\mathrm{d}s = H(-\operatorname{Curl}\phi) &\leq -\int_\Omega p \cdot \operatorname{Curl}\phi\,\mathrm{d}x \\
&= -\int_\Omega (p - \nabla\alpha) \cdot \operatorname{Curl}\phi\,\mathrm{d}x - \int_{\Gamma_D} \alpha \operatorname{Curl}\phi \cdot \nu\,\mathrm{d}s \\
&= -||p - \nabla\alpha||^2_{L^2(\Omega)} - \int_{\Gamma_D} \alpha \operatorname{Curl}\phi \cdot \nu\,\mathrm{d}s.
\end{aligned}$$

Since $\alpha|_{\Gamma_D} = u_D$ it follows

$$0 \leq -||p - \nabla\alpha||^2_{L^2(\Omega)}$$

and hence $p = \nabla\alpha$. It remains to show that $\alpha \in K$. An integration by parts in (3.9) and $p = \nabla\alpha$ shows

$$H(q-p) - \int_\Omega \nabla\alpha\cdot(p-q)\,\mathrm{d}x = \int_\Omega (\alpha-\chi)\,\mathrm{div}(q-p)\,\mathrm{d}x \leq 0 \quad \text{for all } q \in Q(f). \tag{3.11}$$

Since the divergence operator $\mathrm{div} : H_{0,N}(\mathrm{div},\Omega) \to L^2(\Omega)$ is surjective, for all $\mu \in L^2(\Omega;(-\infty,0])$, there exists $\tau \in H_{0,N}(\mathrm{div},\Omega)$ with $\mathrm{div}\,\tau = \mu$. Set $q = p + \tau$ and note that $\mathrm{div}\,q \leq \mathrm{div}\,p \leq f$ and hence $q \in Q(f)$. With $q = p + \tau$ in (3.11) this shows that

$$\int_\Omega (\alpha - \chi)\mu\,\mathrm{d}x \leq 0 \text{ for all } \mu \in L^2(\Omega;(-\infty,0]).$$

Hence $\alpha \in K$. This concludes the proof of ⓐ. □

Proof of ⓑ. The first and second inequality follow from the definition of $\alpha \in K$ and $p = \nabla\alpha \in Q(f)$. To show orthogonality, recall, that the divergence operator $\mathrm{div} : H(\mathrm{div},\Omega) \to L^2(\Omega)$ is surjective. Then there exists $\tau \in H_{0,N}(\mathrm{div},\Omega)$ with

$$\mathrm{div}\,\tau = \mathrm{sgn}(\alpha - \chi)|f + \mathrm{div}\,p|$$

for the sign function sgn. Set $q := p + \tau$ and note that $q \in Q(f)$. Then (3.11) yields

$$\begin{aligned}\int_\Omega (\alpha - \chi)\,\mathrm{div}\,\tau\,\mathrm{d}x &= \int_\Omega (\alpha - \chi)\,\mathrm{sgn}(\alpha - \chi)|f + \mathrm{div}\,p|\,\mathrm{d}x \\ &= \int_\Omega |\alpha - \chi||f + \mathrm{div}\,p|\,\mathrm{d}x \leq 0.\end{aligned}$$

Hence $(\alpha - \chi)(f + \mathrm{div}\,p) = 0$ a.e. in Ω. This concludes the proof of ⓑ. □

Theorem 3.14. *For sufficiently smooth data, i.e., the exact solution $u \in K$ to* (3.2) *satisfies $\Delta u \in L^2(\Omega)$, the three formulations* (3.2), (3.7)–(3.8), *and* (3.9) *are pairwise equivalent in the following sense.*

- ⓐ *Let $u \in K$ solve* (3.2). *Then $(\nabla u, u - \chi) \in H_{g,N}(\mathrm{div},\Omega) \times \mathcal{M}$ solves* (3.7)–(3.8).
- ⓑ *Let $(p, w) \in H_{g,N}(\mathrm{div},\Omega) \times \mathcal{M}$ solve* (3.7)–(3.8). *Then p solves* (3.9).
- ⓒ *Let $p = \nabla\alpha \in Q(f)$ for $\alpha \in K$ solve* (3.9). *Then α solves* (3.2).

Remark 3.15. *For pure Dirichlet boundary conditions, some parts of Theorem 3.14 above are shown in Brezzi et al. (1978). Theorem 2.1 therein states, that if the bilinear form $b(\bullet,\bullet)$ satisfies an* inf sup *condition, i.e., there exists β such that*

$$0 < \beta \leq \inf_{v\in\mathcal{M}} \sup_{q\in H(\mathrm{div},\Omega)} \frac{b(q,v)}{||q||_{H(\mathrm{div},\Omega)}||v||_{L^2(\Omega)}} \tag{3.12}$$

the mixed formulation (3.7)–(3.8) *and the dual variational inequality* (3.9) *are equivalent. Theorem 4.1 in Brezzi et al. (1978) states that if $u \in K$ solves* (3.2), *then*

$p = \nabla u$ *solves* (3.9). *The* inf sup *condition is well known for the spaces* $L^2(\Omega)$ *and* $H(\mathrm{div}, \Omega)$ *and hence follows also for the obstacle problem. This thesis presents a different proof which allows for slightly more general boundary conditions.*

Proof of Theorem 3.14. To prove ⓐ let $u \in K$ be the solution to (3.2). The variational inequality leads to $\nabla u \in H_{g,N}(\mathrm{div}, \Omega)$ and $u - \chi \in \mathcal{M}$. For any $q \in H_{0,N}(\mathrm{div}, \Omega)$, an integration by parts yields

$$\int_\Omega \nabla u \cdot q \,\mathrm{d}x = -\int_\Omega u \,\mathrm{div}\, q \,\mathrm{d}x + \int_{\Gamma_D} u_D q \cdot \nu \,\mathrm{d}s.$$

This results in

$$\int_\Omega \nabla u \cdot q \,\mathrm{d}x + \int_\Omega (u - \chi) \,\mathrm{div}\, q \,\mathrm{d}x = -\int_\Omega \chi \,\mathrm{div}\, q \,\mathrm{d}x + \int_{\Gamma_D} u_D q \cdot \nu \,\mathrm{d}s$$

and (3.7) is satisfied. To show (3.8), compute

$$\begin{aligned} b(\nabla u, v - w) &= \int_\Omega (v - w) \Delta u \,\mathrm{d}x \\ &= \int_\Omega (\Delta u + f)(v - w) \,\mathrm{d}x - \int_\Omega f(v - w) \,\mathrm{d}x \quad \text{for all } v \in \mathcal{M}. \end{aligned}$$

Recall, that $\nabla u \cdot \nu = g$ along Γ_N and hence $\lambda_N = 0$. The complementary conditions (3.4) imply, for $v \in \mathcal{M}$ and $w = u - \chi$, that

$$\int_\Omega (\Delta u + f)(v - w) \,\mathrm{d}x = \int_\Omega (\Delta u + f) v \,\mathrm{d}x \leq 0.$$

This yields (3.8) and concludes the proof of ⓐ. □

To prove ⓑ, suppose that $(p, w) \in H_{g,N}(\mathrm{div}, \Omega) \times \mathcal{M}$ solves (3.7)–(3.8). The mixed complementary conditions in Lemma 3.10 show that $p \in Q(f)$. For $q \in Q(f)$, the mixed complementary conditions (3.10) show that

$$b(q - p, w) = \int_\Omega (\mathrm{div}\, q + f) w \,\mathrm{d}x \leq 0.$$

Hence equation (3.7) leads to

$$\int_\Omega p \cdot (q - p) \,\mathrm{d}x = H(q - p) - b(q - p, w) \geq H(q - p).$$

This shows that $p \in Q(f)$ solves the dual variational inequality (3.9) and concludes the proof of ⓑ. □

For the proof of ⓒ, recall that Lemma 3.13 shows the existence of $\alpha \in K$, such that the solution $p \in Q(f)$ to (3.9) satisfies $p = \nabla \alpha$. Let $v \in K$ and compute $a(\alpha, \alpha - v)$. Since $(\alpha - v)|_{\Gamma_D} = 0$, an integration by parts and $p = \nabla \alpha$ show

$$\begin{aligned} a(\alpha, \alpha - v) &= \int_\Omega p \cdot \nabla(\alpha - v) \,\mathrm{d}x \\ &= -\int_\Omega \mathrm{div}\, p \,(\alpha - v) \,\mathrm{d}x + \int_{\Gamma_N} g(\alpha - v) \,\mathrm{d}s \\ &= -\int_\Omega (\mathrm{div}\, p + f)(\alpha - v) \,\mathrm{d}x + \int_\Omega f(\alpha - v) \,\mathrm{d}x + \int_{\Gamma_N} g(\alpha - v) \,\mathrm{d}s. \end{aligned}$$

Since p and α satisfy the complementary conditions (3.10) and α and $v \in K$, it follows that

$$-\int_\Omega (\operatorname{div} p + f)(\alpha - v)\,\mathrm{d}x = -\int_\Omega (\operatorname{div} p + f)(\chi - v)\,\mathrm{d}x \le 0.$$

Hence

$$a(\alpha, \alpha - v) \le \int_\Omega f(\alpha - v)\,\mathrm{d}x + \int_{\Gamma_N} g(\alpha - v)\,\mathrm{d}s$$

and α satisfies (3.2). This concludes the proof of ©. □

The following theorem comments on the unique existence of solutions to problems (3.7)–(3.8) and (3.9).

Theorem 3.16. ⓐ *There exists a unique solution to problem* (3.7)–(3.8).

ⓑ *There exists a unique solution to problem* (3.9).

Proof. Since the inf sup condition (3.12) is well known and there exists a unique solution to Problem (3.2) (cf. Lemma 3.1), the result follows from Theorems 2.1 and 4.1 in Brezzi et al. (1978). □

3.2. Reliable and efficient error estimate for the obstacle problem

This subsection is devoted to a reliable and efficient error estimate for the obstacle problem. Let $v \in \mathcal{A}$ be some approximation to the exact solution $u \in K$ to (3.2). For any $(\mu, \mu_N) \in L^2(\Omega \times \Gamma_N; (-\infty, 0])$, define the non-positive approximation $M \in V^*$ (non-positive in the sense that $M(\varphi) \le 0$ for all $\varphi \in V_+$, i.e., $\varphi \in V$ with $\varphi \ge 0$ a.e.) to the exact Lagrange multiplier $\Lambda \in V^*$ by

$$M(\varphi) := \int_\Omega \mu\varphi\,\mathrm{d}x + \int_{\Gamma_N} \mu_N\varphi\,\mathrm{d}s \quad \text{for all } \varphi \in V. \tag{3.13}$$

The residual $\operatorname{Res} \in V^*$ is defined by

$$\operatorname{Res}(\varphi) := \int_\Omega (f - \mu)\varphi\,\mathrm{d}x + \int_{\Gamma_N} (g - \mu_N)\varphi\,\mathrm{d}s - a(v, \varphi) \quad \text{for all } \varphi \in V. \tag{3.14}$$

Note that $v \in \mathcal{A}$ does not have to satisfy $v \in K$ and so leads to the following gap function $w \in H^1(\Omega)$, defined by $w := \min\{0, v - \chi\}$. Recall, with $S := \{\varphi \in V \mid |\!|\!|\varphi|\!|\!| = 1\}$ the definitions $|\!|\!| \operatorname{Res} |\!|\!|_* := \sup\{\operatorname{Res}(\varphi) \mid \varphi \in S\}$ and $|\!|\!|\Lambda - M|\!|\!|_* := \sup\{(\Lambda - M)(\varphi) \mid \varphi \in S\}$.

Theorem 3.17. *Suppose $v \in \mathcal{A}$ is some approximation to the exact continuous solution $u \in K$ to* (3.2) *and $M \in V^*$ defined as in* (3.13) *for some $(\mu, \mu_N) \in L^2(\Omega \times \Gamma_N; (-\infty])$ is some non-positive approximation (i.e. $M(\varphi) \le 0$ for all $\varphi \in V_+$) of the Lagrange multiplier $\Lambda \in V^*$. Then the error $e := u - v$ and the gap function $w := \min\{0, v - \chi\}$ satisfy*

ⓐ $(\Lambda - M)(u - v + w) + |\!|\!|e|\!|\!|^2/2 + |\!|\!|e + w|\!|\!|^2/2 = \operatorname{Res}(e + w) + |\!|\!|w|\!|\!|^2/2;$

ⓑ $0 \le M(\chi - u) - \Lambda((v-\chi)_+) = (\Lambda - M)(u - v + w) - M((v-\chi)_+)$;

ⓒ $M(\chi - u) - \Lambda((v-\chi)_+) + |||e|||^2/2 + (1 - 1/t)|||e + w|||^2/2$
$\le t|||\mathrm{Res}|||_*^2/2 - M((v-\chi)_+) + |||w|||^2/2 \quad$ *for all* $\quad 0 < t < \infty$;

ⓓ $\Big|\,|||\Lambda - M|||_* - |||e|||\,\Big| \le |||\mathrm{Res}|||_* \le |||e||| + |||\Lambda - M|||_*$.

Proof. Direct calculations show

$$(\Lambda - M)(u - v + w) = \mathrm{Res}(e + w) - a(e, e + w).$$

This and some straightforward algebra, namely

$$-a(e, e + w) = -|||e|||^2/2 - |||e + w|||^2/2 + |||w|||^2/2,$$

concludes the proof of ⓐ. □

Since $(v - \chi)_+ = \chi - v - w$, ⓑ follows from the continuous complementary conditions (3.4) in Lemma 3.4 and some direct calculations.

The assumption ⓒ follows from the combination of ⓐ and ⓑ with a further evaluation of $\mathrm{Res}(e+w)$. The definition of the operator norm and a Young inequality for $0 < t < \infty$ yield

$$\mathrm{Res}(e + w) \le |||\mathrm{Res}|||_* |||e + w||| \le t|||\mathrm{Res}|||_*^2/2 + |||e + w|||^2/(2t). \qquad \square$$

The assumption ⓓ employs the auxiliary Poisson problem with the exact solution $z \in \mathcal{A}$ to

$$a(z, \varphi) = F(\varphi) - M(\varphi) \qquad \text{for all } \varphi \in V.$$

The continuous solution $u \in K$ to the obstacle problem (3.2) and the definition of the continuous Lagrange multiplier Λ yield

$$a(u - z, \varphi) = (M - \Lambda)(\varphi) \qquad \text{for all } \varphi \in V.$$

In other words, $u - z \in V$ is the Riesz representation of the linear and bounded functional $M - \Lambda$ in the Hilbert space (V, a) and therefore

$$|||u - z||| = |||\Lambda - M|||_*. \tag{3.15}$$

The definition of the residual (3.14) yields

$$\begin{aligned} |||v - z|||^2 &= a(v, v - z) - a(z, v - z) \\ &= a(v, v - z) - F(v - z) + M(v - z) \\ &= \mathrm{Res}(z - v) \le |||\mathrm{Res}|||_* |||v - z|||. \end{aligned}$$

This implies $|||z - v||| \le |||\mathrm{Res}|||_*$. A triangle inequality and (3.15) show

$$\Big|\,|||\Lambda - M|||_* - |||e|||\,\Big| \le |||v - z||| \le |||\mathrm{Res}|||_*.$$

Given any $\varphi \in S$, the definition of Λ in (3.3) shows $\mathrm{Res}(\varphi) = (\Lambda - M)(\varphi) + a(e, \varphi)$ and hence

$$|||\mathrm{Res}|||_* \le \sup_{\varphi \in S} \Big((\Lambda - M)(\varphi) + a(e, \varphi) \Big) \le |||\Lambda - M|||_* + |||e|||.$$

This concludes the proof of ⓓ. □

Given $v \in V$ and $M \in V^*$ as in (3.13), recall the gap function $w := \min\{0, v-\chi\}$ and the error $e := u - v$. Define the total error

$$\mathrm{Err}^2 := M(\chi - u) - \Lambda((v-\chi)_+) + |||e|||^2 + |||e+w|||^2 + |||\Lambda - M|||_*^2.$$

The total error Err is controlled by the estimator

$$\mathrm{Est}^2 := |||\mathrm{Res}|||_*^2 - M((v-\chi)_+) + |||w|||^2.$$

The following theorem is a realization of Theorem A.

Theorem 3.18 (reliability and efficiency)**.** *For any approximation $v \in V$ to the exact solution $u \in K$ to* (3.2) *and any non-positive approximation $M \in V^*$ (i.e. $M(\varphi) \le 0$ for all $\varphi \in V_+$)(cf.* (3.13)*) to the exact Lagrange multiplier $\Lambda \in V^*$ of* (3.3)*, the total error* Err *and the estimator* Est *satisfy*

$$\mathrm{Est}^2/2 \le \mathrm{Err}^2 \le 30\,\mathrm{Est}^2.$$

Remark 3.19. *The guaranteed upper bound* GUB *from* (1.2) *on Page 2 satisfies*

$$\mathrm{GUB} = 30\mathrm{Est}.$$

Proof of reliability. Theorem 3.17.d leads to

$$\mathrm{Err} \le (M(\chi-u))^{1/2} + (-\Lambda((v-\chi)_+))^{1/2} + 2|||e||| + |||e+w||| + |||\mathrm{Res}|||_*. \tag{3.16}$$

The upper bound of (3.16) the scalar product of

$$\Big(M(\chi-u))^{1/2}, (-\Lambda((v-\chi)_+)^{1/2}, |||e|||/\sqrt{2}, |||e+w|||/2, |||\mathrm{Res}|||_*\Big)$$

with $\Big(1,1,2\sqrt{2},2,1\Big)$ in $\mathbb{R}^5$. A Cauchy inequality in $\mathbb{R}^5$ yields

$$\mathrm{Err} \le \sqrt{15}\Big(M(\chi-u) - \Lambda((v-\chi)_+) + |||e|||^2/2 + |||e+w|||^2/4 + |||\mathrm{Res}|||_*^2\Big)^{1/2}. \tag{3.17}$$

Theorem 3.17.c with $t = 2$ shows

$$\begin{aligned} M(\chi-u) - \Lambda((v-\chi)_+) + 1/2|||e|||^2 + 1/4|||e+w|||^2 \\ \le |||\mathrm{Res}|||_*^2 + |||w|||^2/2 - M((v-\chi)_+). \end{aligned}$$

The combination of this and (3.17) leads to

$$\begin{aligned} \mathrm{Err}^2/15 &\le 2|||\mathrm{Res}|||^2 - M((v-\chi)_+) + |||w|||^2/2 \\ &\le 2\mathrm{Est}^2. \end{aligned}$$

□

Proof of efficiency. The key step in the proof of efficiency is the verification of (a refined version) of

$$-M((v-\chi)_+) \le \mathrm{Err}^2. \tag{3.18}$$

Since $w := \min\{0, v-\chi\}$ satisfies $(v-\chi)_+ = (v-\chi) - w$, it follows that

$$-M((v-\chi)_+) = -M(v-\chi) + M(w) = -M(u-\chi) + M(e+w).$$

The last term is split into

$$M(e+w) = (M-\Lambda)(e+w) + \Lambda(e+w). \tag{3.19}$$

Since $e + w \in V$, the dual norm estimate and Young's inequality show

$$2(M-\Lambda)(e+w) \le |||\Lambda - M|||_*^2 + |||e+w|||^2.$$

The complementary conditions (3.4) show, for the last term in (3.19), that

$$\Lambda(e+w) = \Lambda(\chi - v + w) = -\Lambda((v-\chi)_+).$$

Altogether, the left-hand side of (3.18) satisfies

$$-M((v-\chi)_+) \leq \|\Lambda - M\|_*^2/2 + \|e+w\|^2/2 - \Lambda((v-\chi)_+) + M(u-\chi). \quad (3.20)$$

This implies (3.18). Theorem 3.17.d and a triangle inequality lead to

$$\|\mathrm{Res}\|_* + \|w\| \leq \|\Lambda - M\|_* + 2\|e\| + \|e+w\|.$$

The combination of this with (3.20) yields $\mathrm{Est} \leq 2\mathrm{Err}^2$ and concludes the proof. □

Remark 3.20 ($\|\mathrm{Res}\|_*$ and inexact solve)**.** *This remark describes a possibility to compute upper and lower bounds for the term $\|\mathrm{Res}\|_*$ for the residual $\mathrm{Res} \in V^*$ from (3.14). Let $(V_h, a|_{V_h \times V_h})$ be a discrete Hilbert space with $V_h \subset V$. Let u_{Dh} be some approximation to the Dirichlet boundary data u_D which corresponds to the discrete space V_h and assume that $u_h \in u_{Dh} + V_h$ is some discrete approximation to the exact solution $u \in K$ to (3.2) computed for example from a finite element method. Assume, that there exists $w_D \in H^1(\Omega)$ such that the approximation $v \in \mathcal{A}$ satisfies $v = w_D + u_h$. Let $z \in V$ be the Riesz representation of the residual $\mathrm{Res} \in V^*$ and let $z_h \in V_h$ be the Riesz representation of $\mathrm{Res}|_{V_h} \in V_h^*$ in the discrete space. The Riesz isometry and Pythagoras' theorem reveal*

$$\|\mathrm{Res}\|_*^2 = \|z\|^2 = \|z - z_h\|^2 + \|z_h\|^2.$$

With $\psi := z - z_h \in V$, this leads to

$$\|z - z_h\|^2 = a(z,\psi) - a(z_h,\psi) = \mathrm{Res}(\psi) - a(z_h,\psi) =: \mathrm{Res}_h(\psi) - a(w_D,\psi)$$

with the modified residual $\mathrm{Res}_h(\bullet) := \int_\Omega (f-\mu) \bullet \,\mathrm{d}x - a(u_h + z_h, \bullet) \in V^*$. This shows that $\|z - z_h\| \leq \|\mathrm{Res}_h\|_* + \|w_D\|^2$ and so

$$\|\mathrm{Res}\|_*^2 \leq \|z_h\|^2 + \|\mathrm{Res}_h\|_*^2 + \|w_D\|^2.$$

It holds $V_h \subseteq \ker(\mathrm{Res}_h)$ and hence any residual-based a posteriori error estimator for the Poisson model problem may be employed to compute upper and lower bounds of the residual term $\|\mathrm{Res}\|_*$. For the finite element spaces analyzed in this thesis residual-based a posteriori error estimators for the Poisson problem are well known (for the conforming FEM see for example Braess, 2007; Brenner and Scott, 2008; Carstensen, 1999; Carstensen et al., 2001; Carstensen and Merdon, 2010; Repin, 2008; Verfürth, 1996).

3.3. Conforming FEM for the obstacle problem

This section is devoted to the conforming Courant CFEM for the obstacle problem in two space dimensions. The conforming finite element method for the obstacle problem is well studied in the literature, where several choices of discrete Lagrange multipliers (see for example Veeser, 2001; Bartels and Carstensen, 2004; Carstensen and Merdon, 2013b) have been proposed. This section studies the Lagrange multipliers from Veeser (2001) and Bartels and Carstensen (2004) and provides proofs for Theorem B and C in this context. The results of this section are restricted to Dirich-

let boundary conditions $u_D \in H^1(\Omega)$, an obstacle $\chi \in H^1(\Omega)$ with $\chi \leq u_D$ along $\partial\Omega$ and $\Delta\chi \in L^2(\Omega)$, and $f \in L^2(\Omega)$ and the resulting regularity with $\Delta u \in L^2(\Omega)$.

3.3.1. Conforming discretization of the obstacle problem

Given a shape-regular triangulation $\mathcal{T}$ of $\Omega \subset \mathbb{R}^2$ from Subsection 2.2.1 on Page 11, recall the Courant finite element space $V_{\mathrm{C}}(\mathcal{T}) := S^1_0(\mathcal{T})$ from Page 14. To approximate the Dirichlet boundary conditions u_D, define

$$u_{D,\mathrm{C}} := \sum_{z \in \mathcal{N}(\partial\Omega)} u_D(z)\varphi_z \in P_1(\mathcal{T}) \cap C(\Omega).$$

This leads to the discrete subset $\mathcal{A}_{\mathrm{C}}(\mathcal{T}) := u_{D,\mathrm{C}} + S^1_0(\mathcal{T})$ of $S^1(\mathcal{T})$ and the convex and non-empty set

$$K_{\mathrm{C}}(\mathcal{T}) := \{v_{\mathrm{C}} \in \mathcal{A}_{\mathrm{C}}(\mathcal{T}) \mid \forall z \in \mathcal{N}(\Omega), \chi(z) \leq v_{\mathrm{C}}(z)\} \subset \mathcal{A}_{\mathrm{C}}(\mathcal{T}).$$

The discrete solution $u_{\mathrm{C}} \in K_{\mathrm{C}}(\mathcal{T})$ solves the variational inequality

$$F(v_{\mathrm{C}} - u_{\mathrm{C}}) \leq a(u_{\mathrm{C}}, v_{\mathrm{C}} - u_{\mathrm{C}}) \quad \text{for all } v_{\mathrm{C}} \in K_{\mathrm{C}}(\mathcal{T}). \tag{3.21}$$

Lemma 3.21 (existence of solutions)**.** *There exists a unique solution $u_{\mathrm{C}} \in K_{\mathrm{C}}(\mathcal{T})$ to problem* (3.21)*.*

Proof. Since $a(\bullet, \bullet)$ is a scalar product on $S^1_0(\mathcal{T}) \times S^1_0(\mathcal{T})$, the proof follows after a shift of χ to $\chi - u_{D,\mathrm{C}}$ and of F to $F - a(u_{D,\mathrm{C}}, \bullet)$ from Kinderlehrer and Stampacchia (1980, Thm. 2.1). □

Lemma 3.22 (discrete complementary conditions)**.** *The solution $u_{\mathrm{C}} \in K_{\mathrm{C}}(\mathcal{T})$ to* (3.21) *satisfies the discrete complementary conditions*

$$0 \leq u_{\mathrm{C}}(z) - \chi(z) \perp F(\varphi_z) - a(u_{\mathrm{C}}, \varphi_z) := \sigma_{\mathrm{C}}(\varphi_z) \leq 0 \quad \text{for all } z \in \mathcal{N}(\Omega) \tag{3.22}$$

where $\perp$ abbreviates pointwise orthogonality in $\mathbb{R}$, i.e. $a \perp b$ signifies $ab = 0$ for $a, b \in \mathbb{R}^2$.

Proof. The first inequality follows from the definition of $K_{\mathrm{C}}(\mathcal{T})$. For any $z \in \mathcal{N}(\Omega)$, $v_{\mathrm{C}} := u_{\mathrm{C}} + \varphi_z \in K_{\mathrm{C}}(\mathcal{T})$. Hence the discrete variational inequality (3.21) shows $\sigma_{\mathrm{C}}(\varphi_z) \leq 0$. To show the orthogonality, consider the test functions $v_{\mathrm{C}} := (2u_{\mathrm{C}} - \chi)(z)\varphi_z$ and $v_{\mathrm{C}} = \chi(z)\varphi_z$ for $z \in \mathcal{N}(\Omega)$. The discrete variational inequality (3.21) then shows

$$F\big((u_{\mathrm{C}} - \chi)(z)\varphi_z\big) - a\big(u_{\mathrm{C}}, (u_{\mathrm{C}} - \chi)(z)\varphi_z\big) = 0.$$

This concludes the proof. □

3.3.2. Boundary conditions

The discrete solution $u_{\mathrm{C}} \in K_{\mathrm{C}}(\mathcal{T})$ does not match the Dirichlet boundary conditions exactly. Recall Theorem 2.28 on Page 18 and define $w_D \in H^1(\Omega)$ such that $w_D|_{\partial\Omega} = u_D - u_{D,\mathrm{C}}$.

The design of w_D allows the definition of $v \in \mathcal{A}$ from the discrete solution u_C. Since $u_C|_{\partial\Omega} = u_{D,C}$ the function

$$v := w_D + u_C \in \mathcal{A}$$

is an admissible function in Theorem 3.18.

3.3.3. Interpolation operator and boundary modification

The proof of the efficiency of the discrete Lagrange multipliers presented in this subsection is closely related to an appropriate interpolation operator. Carstensen and Verfürth (1999) present the following interpolation operator

$$J\varphi := \sum_{z\in\mathcal{N}(\Omega)} \left(\int_{\omega_z} \varphi\varphi_z \,\mathrm{d}x / \int_{\omega_z} \varphi_z \,\mathrm{d}x \right) \varphi_z \quad \text{for all } \varphi \in H^1(\Omega). \tag{3.23}$$

Carstensen and Verfürth (1999, Lemma 6.2) show that this operator is H^1 stable. To avoid unnecessary boundary terms, the nodal basis functions are modified and at the same time the degrees of freedom are limited to the interior nodes.

For any boundary node $z \in \mathcal{N}(\partial\Omega)$, let $\zeta(z)$ be a neighbouring free node in the sense that z and $\zeta(z)$ belong to the same interior edge of the triangulation $\mathcal{T}$. For all interior nodes $z \in \mathcal{N}(\Omega)$, set $\zeta(z) := z$. Then

$$\psi_z := \sum_{y\in\zeta^{-1}(z)} \varphi_y \in S^1(\mathcal{T}) := P_1(\mathcal{T}) \cap C(\overline{\Omega}) \quad \text{and} \quad \Omega_z := \{\psi_z > 0\}. \tag{3.24}$$

Recall the oscillations from Definition 2.8 on Page 13 and define the oscillations $\mathrm{Osc}(f, \mathcal{N}(\Omega))$ for the patch Ω_z by

$$\mathrm{Osc}^2(f, \mathcal{N}(\Omega)) := \sum_{z\in\mathcal{N}(\Omega)} \mathrm{osc}^2(f, \Omega_z).$$

The quasi-interpolation operator J^* from Carstensen (1999) is given by

$$J^*\varphi := \sum_{z\in\mathcal{N}(\Omega)} \left(\int_{\Omega} \varphi\psi_z \,\mathrm{d}x / \int_{\Omega} \varphi_z \,\mathrm{d}x \right) \varphi_z \quad \text{for any } \varphi \in H^1(\Omega) \tag{3.25}$$

and satisfies a first-order approximation, stability, and orthogonality property presented in the following lemma.

Lemma 3.23 (Carstensen (1999, Thm. 3.1))**.** *There exist positive constants C_{stab} and C_{apx} with $C_{\mathrm{stab}} + C_{\mathrm{apx}} \lesssim 1$ such that any $\varphi \in H^1(\Omega)$ and $f \in L^2(\Omega)$ satisfy*

$$|||J^*\varphi||| \le C_{\mathrm{stab}}|||\varphi||| \quad \textit{and} \quad \int_\Omega f(\varphi - J^*\varphi)\,\mathrm{d}x \le C_{\mathrm{apx}}\mathrm{Osc}(f, \mathcal{N}(\Omega))|||\varphi|||. \qquad \square$$

3.3.4. Two discrete Lagrange multipliers for CFEM

This section presents two discrete Lagrange multipliers $\mu \in S^1(\mathcal{T}; (-\infty, 0])$. With $\sigma_C := F(\bullet) - a(u_C, \bullet)$ from (3.22) and ψ_z from (3.24), Bartels and Carstensen (2004) present the following choice

$$\mu := \lambda_{\mathrm{CB}} := \sum_{z\in\mathcal{N}(\Omega)} \left(\sigma_C(\varphi_z) / \int_\Omega \varphi_z \,\mathrm{d}x \right) \psi_z \in S^1(\mathcal{T}; (-\infty, 0]). \tag{3.26}$$

Another possible discrete Lagrange multiplier (with respect to some optimal discrete right-hand side $f_{h,opt}$ with $ce(f_{h,opt}) = 0$ in Veeser (2001)) from Veeser (2001) reads

$$\mu := \lambda_{\mathrm{V}} := \sum_{z \in \mathcal{N}(\Omega)} \left(\sigma_{\mathrm{C}}(\varphi_z) / \int_\Omega \varphi_z \, \mathrm{d}x \right) \varphi_z \in S^1_0(\mathcal{T}; (-\infty, 0]). \tag{3.27}$$

Remark 3.24. *Veeser (2001) suggests the following boundary modification*

$$\sigma_{\mathrm{C}}(\varphi_z) = \begin{cases} 0 & \text{if } \chi(z) < u_{\mathrm{C}}(z), \\ \min\{0, F(\varphi_z) - a(u_{\mathrm{C}}, \varphi_z) + \int_{\partial\Omega} \varphi_z \nabla u_{\mathrm{C}} \cdot \nu \, \mathrm{d}s\} & \text{otherwise} \end{cases}$$

for $z \in \mathcal{N}(\partial\Omega)$. The efficiency of this estimator will be studied experimentally in Section 6.1.

The discrete complementary conditions (3.22) show, that these discrete Lagrange multipliers satisfy $\mu \leq 0$ in Ω.

Remark 3.25. *Other discrete Lagrange multipliers can be found in the literature, e.g., Λ_h in Carstensen and Merdon (2013b). The efficiency of Λ_h will not be analyzed in this thesis, however, the numerical experiments in Section 6.1 suggest also efficiency for this Lagrange multiplier.*

3.3.5. Efficiency of the discrete Lagrange multipliers for CFEM

Recall the solution $u \in K$ to (3.2) and the Lagrange multiplier Λ from (3.3) with L^2 representation $\lambda = \Delta u + f \in L^2(\Omega; (-\infty, 0])$. The subsequent theorem shows, that the above choices for the discrete Lagrange multipliers ((3.26) and (3.27)) are efficient in the sense of Theorem B.

Theorem 3.26 (efficiency of the discrete Lagrange multipliers)**.** *The discrete solution $u_{\mathrm{C}} \in K_{\mathrm{C}}(\mathcal{T})$ to* (3.21) *and the discrete Lagrange multipliers λ_{CB} from* (3.26) *and λ_{V} from* (3.27) *satisfy*

$$\text{ⓐ } |\!|\!| \lambda - \lambda_{\mathrm{CB}} |\!|\!|_* \lesssim |\!|\!| u - u_{\mathrm{C}} |\!|\!| + \mathrm{Osc}(\lambda, \mathcal{N}(\Omega));$$

$$\text{ⓑ } |\!|\!| \lambda - \lambda_{\mathrm{V}} |\!|\!|_* \lesssim |\!|\!| u - u_{\mathrm{C}} |\!|\!| + \mathrm{Osc}(\lambda, \mathcal{N}(\Omega)) + \sqrt{\sum_{z \in \mathcal{N}(\partial\Omega)} |\omega_z| \, ||\lambda||^2_{L^2(\omega_z)}}.$$

Remark 3.27. *A heuristic argument shows, that the terms* $\mathrm{Osc}(\lambda, \mathcal{N}(\Omega))$ *and* $\sqrt{\sum_{x \in \mathcal{N}(\partial\Omega)} |\omega_z| \, ||\lambda||_{L^2(\omega_z)}}$ *are in fact of higher order. Remark 4.4 of Carstensen and Merdon (2013b) shows that*

$$\mathrm{Osc}(\lambda, \mathcal{N}(\Omega)) \lesssim h^{3/2}_{\max}.$$

The main observation is that for the benchmark examples presented in Section 6.1, the free boundary $\mathcal{F}$ is a one-dimensional sub-manifold where λ is piecewise smooth. With similar arguments it can be shown that $\sqrt{\sum_{x \in \mathcal{N}(\partial\Omega)} |\omega_z| \, ||\lambda||^2_{L^2(\omega_z)}}$ is of higher order. Since λ is piecewise smooth in Ω it follows that

$$||\lambda||^2_{L^2(\omega_z)} \lesssim h^2_{\max}.$$

Assume that the boundary $\partial\Omega$ has length $|\partial\Omega| =: L$ and that the edges $E \in \mathcal{E}(\partial\Omega)$ are enumerated by $E_1, ..., E_J$. Let $t_0, ..., t_J$ be a partition of $[0, L]$ such that for each $j = 1, ..., J$, $|E_j| = t_j - t_{j-1}$. Then it follows that

$$\sum_{z\in\mathcal{N}(\partial\Omega)} |\omega_z|\,||\lambda||^2_{L^2(\omega_z)} \lesssim \sum_{j=1}^{J} |E_j|^4 = \sum_{j=1}^{J} |E_j|^3(t_j - t_{j-1}).$$

Since $|E_j| \le h_{\max}$,

$$\sum_{j=1}^{J} |E_j|^3(t_j - t_{j-1}) \le \int_0^L h^3_{\max}\,\mathrm{d}x.$$

Then $\sqrt{\sum_{z\in\mathcal{N}(\partial\Omega)} |\omega_z|||\lambda||^2_{L^2(\omega_z)}} \lesssim h^{3/2}_{\max}$ is of higher order.

The proof of Theorem 3.26 employs the following lemma, which follows from elementary algebra and the linearity of F and $a(u_{\mathrm{C}}, \bullet)$. The lemma also clarifies the close connection of the discrete Lagrange multiplier λ_{CB} from (3.26) and the interpolation operator J^* from (3.25).

Lemma 3.28. *For all $\varphi \in V$, the discrete Lagrange multiplier λ_{CB} from (3.26) and the interpolation operator J^* from* (3.25) *satisfy*

$$\int_\Omega \lambda_{\mathrm{CB}}\varphi\,\mathrm{d}x = F(J^*\varphi) - a(u_{\mathrm{C}}, J^*\varphi). \qquad \square$$

Proof. Since F and $a(u_{\mathrm{C}}, \bullet)$ are linear forms, the discrete Lagrange multiplier λ_{CB} satisfies

$$\begin{aligned}\int_\Omega \lambda_{\mathrm{CB}}\varphi\,\mathrm{d}x &= \int_\Omega \Big(\sum_{z\in\mathcal{N}(\Omega)} (F(\varphi_z) - a(u_{\mathrm{C}}, \varphi_z))/\Big(\int_\Omega \varphi_z\,\mathrm{d}x\Big)\,\psi_z\varphi \Big)\,\mathrm{d}x \\ &= F\Big(\sum_{z\in\mathcal{N}(\Omega)} \int_\Omega \varphi\psi_z\,\mathrm{d}x/\int_\Omega \varphi_z\,\mathrm{d}x\varphi_z\Big) - a\Big(u_{\mathrm{C}}, \sum_{z\in\mathcal{N}(\Omega)} \int_\Omega \varphi\psi_z\,\mathrm{d}x/\int_\Omega \varphi_z\,\mathrm{d}x\varphi_z\Big) \\ &= F(J^*\varphi) - a(u_{\mathrm{C}}, J^*\varphi).\end{aligned}$$

and concludes the proof. $\square$

Proof of Theorem 3.26. Let $\varphi \in V$ with $\|\!|\varphi|\!\| = 1$. The discrete Lagrange multipliers $\mu = \lambda_{\mathrm{CB}}$ and $\mu = \lambda_{\mathrm{V}}$ and the interpolation operator J^* from (3.25) allow for the split

$$\int_\Omega (\lambda - \mu)\varphi\,\mathrm{d}x = \int_\Omega \lambda(\varphi - J^*\varphi)\,\mathrm{d}x + \int_\Omega (\lambda J^*\varphi - \mu\varphi)\,\mathrm{d}x.$$

Lemma 3.23 shows that

$$\int_\Omega \lambda(\varphi - J^*\varphi)\,\mathrm{d}x \lesssim \mathrm{Osc}(\lambda, \mathcal{N}(\Omega))|\!|\!|\varphi|\!|\!|.$$

For $\mu = \lambda_{\mathrm{CB}}$, the definition of the Lagrange multiplier λ and Lemma 3.28 lead to

$$\int_\Omega (\lambda J^*\varphi - \lambda_{\mathrm{CB}}\varphi)\,\mathrm{d}x = a(u_{\mathrm{C}} - u, J^*\varphi) \le |\!|\!|u - u_{\mathrm{C}}|\!|\!|\,|\!|\!|J^*\varphi|\!|\!|.$$

The combination of the three previous displayed formulas and the stability of the interpolation operator J^* in Lemma 3.23 prove ⓐ. □

To conclude the proof of ⓑ, the definition of the interpolation operator $J^*\varphi$ result in

$$\begin{aligned}\int_\Omega &(\lambda J^*\varphi - \lambda_{\mathrm{V}}\varphi)\,\mathrm{d}x \\ &= \sum_{z\in\mathcal{N}(\Omega)} \left(\int_{\omega_z} \lambda\varphi_z\,\mathrm{d}x - F(\varphi_z) + a(u_{\mathrm{C}},\varphi_z)\right) \int_{\omega_z} \varphi\varphi_z\,\mathrm{d}x \Big/ \int_{\omega_z} \varphi_z\,\mathrm{d}x \\ &\quad + \sum_{z\in\mathcal{N}(\Omega)} \int_{\omega_z} \lambda\varphi_z\,\mathrm{d}x \int_{\Omega_z} (\psi_z - \varphi_z)\varphi\,\mathrm{d}x \Big/ \int_{\omega_z} \varphi_z\,\mathrm{d}x \\ &=: ① + ②.\end{aligned}$$

The stability of the operator J in (3.23) (cf. Carstensen and Verfürth (1999)) and the definition of the Lagrange multiplier λ lead to

$$① = -\,a\,(u - u_{\mathrm{C}}, J\varphi) \lesssim |\!|\!| u - u_{\mathrm{C}} |\!|\!|\, |\!|\!| \varphi |\!|\!| = |\!|\!| u - u_{\mathrm{C}} |\!|\!|.$$

The definition of ψ_z and φ_z and some renaming show that

$$② = \sum_{z\in\mathcal{N}(\partial\Omega)} \int_\Omega \lambda\varphi_{\zeta(z)}\,\mathrm{d}x \int_{\omega_z} \varphi\varphi_z\,\mathrm{d}x \Big/ \int_\Omega \varphi_{\zeta(z)}\,\mathrm{d}x.$$

Since $\varphi \in H^1_0(\Omega)$, a Cauchy and Friedrichs inequality yield

$$② \lesssim \sqrt{\sum_{z\in\mathcal{N}(\partial\Omega)} ||h_z\lambda||^2_{L^2(\omega_z)}}.$$

The combination of the estimates for ① − ② concludes the proof of ⓑ. □

3.3.6. Comments on the complementary condition residual for CFEM in the obstacle problem

This subsection analyzes the efficiency of the computable integral $\int_\Omega(-\mu)(u_{\mathrm{C}} + w_D - \chi)\,\mathrm{d}x$ in Est for an affine obstacle $\chi \in P_1(\Omega)$ and $\mu = \lambda_{\mathrm{CB}}$ and $\mu = \lambda_{\mathrm{V}}$ from (3.26) and (3.27). The integral in Est is a complementary condition residual. Set $\mathcal{N}(\mathcal{T}_I \setminus \mathcal{T}_C) := \{z \in \mathcal{N}(T) \mid T \in \mathcal{T}_I \setminus \mathcal{T}_C\}$ for

$$\begin{aligned}\mathcal{T}_C &:= \{T \in \mathcal{T} \mid u_{\mathrm{C}} = \chi \text{ in } T\};\\ \mathcal{T}_I &:= \{T \in \mathcal{T} \mid \exists y_T, z_T \in \mathcal{N}(\overline{\Omega}_T), \chi(y_T) < u_{\mathrm{C}}(y_T) \text{ and } \chi(z_T) = u_{\mathrm{C}}(z_T)\};\\ \mathcal{T}_{DB} &:= \{T \in \mathcal{T} \;\big|\; |\mathcal{N}(T) \cap \mathcal{N}(\partial\Omega)| = 0\}.\end{aligned}$$

In other words, $\mathcal{T}_C$ contains all triangles T, where the discrete solution u_{C} is in contact, $\mathcal{T}_I$ contains all triangles T, where u_{C} is neither completely in contact nor completely in non-contact. Note that the nodes $y_T, z_T \in \mathcal{N}(\overline{\Omega}_T)$ are preferably chosen as interior nodes. Finally, the set $\mathcal{T}_{DB}$ contains all triangles T, which have at least one node at the boundary of the domain. Recall $v := w_D + u_{\mathrm{C}} \in \mathcal{A}$ where w_D from Theorem 2.28 satisfies $w_D|_{\partial\Omega} = (u_D - u_{D,\mathrm{C}})|_{\partial\Omega}$. The subsequent theorem proves the efficiency of the computable integral in Est in the sense of Theorem C.

Theorem 3.29. *For an affine obstacle $\chi \in P_1(\Omega)$, it holds*

$$\text{ⓐ} \quad \int_\Omega (-\lambda_{\mathrm{CB}})(u_{\mathrm{C}} + w_D - \chi)\,\mathrm{d}x \lesssim |\!|\!| u - u_{\mathrm{C}} |\!|\!|^2 + |\!|\!| \lambda - \lambda_{\mathrm{CB}} |\!|\!|_*^2 + \mathrm{Osc}^2(f, \mathcal{T} \setminus (\mathcal{T}_C \cup \mathcal{T}_{\mathrm{DB}})) + \sum_{T \in \mathcal{T}_{\mathrm{I}} \cap \mathcal{T}_{\mathrm{DB}}} ||h_T f||_{L^2(T)}^2 + |\!|\!| w_D |\!|\!|^2;$$

$$\text{ⓑ} \quad \int_\Omega (-\lambda_{\mathrm{V}})(u_{\mathrm{C}} + w_D - \chi)\,\mathrm{d}x \lesssim |\!|\!| u - u_{\mathrm{C}} |\!|\!|^2 + |\!|\!| \lambda - \lambda_{\mathrm{V}} |\!|\!|_*^2 + \mathrm{Osc}^2(f, \mathcal{T} \setminus (\mathcal{T}_C \cup \mathcal{T}_{\mathrm{DB}})) + \sum_{z \in \mathcal{N}(\partial\Omega)} ||h_z f||_{L^2(\omega_z)}^2 + |\!|\!| w_D |\!|\!|^2.$$

Corollary 3.30. *For $\chi \in P_1(\Omega)$ and $\mu = \lambda_{\mathrm{V}}$ or $\mu = \lambda_{\mathrm{CB}}$, the guaranteed upper bound* $\mathrm{GUB} = 30\mathrm{Est}$ *is efficient with respect to the energy error $|\!|\!| u - u_{\mathrm{C}} |\!|\!|$ and the total error* Err *of Theorem 3.18 in the sense that*

$$|\!|\!| u - u_{\mathrm{C}} |\!|\!| \le \mathrm{Err} \approx \mathrm{GUB} \lesssim |\!|\!| u - u_{\mathrm{C}} |\!|\!| + \text{ higher-order terms.}$$

Proof. The proof follows from the combination of Theorem 3.18, 3.26, and 3.29. □

Remark 3.31. *The estimate in Corollary 3.30 contains the higher-order terms* $\mathrm{osc}(f, \mathcal{T}), \mathrm{osc}(\lambda, \mathcal{T}), \sqrt{\sum_{z \in \mathcal{N}(\partial\Omega)} ||h_z f||_{L^2(\omega_z)}^2}$, $|\!|\!| w_D |\!|\!|$, *and* $\sqrt{\sum_{z \in \mathcal{N}(\partial\Omega)} ||h_z \lambda||_{L^2(\omega_z)}^2}$.

The proof of Theorem 3.29 is based on the following lemma.

Lemma 3.32. *Let $z \in \mathcal{N}(\Omega)$ with a neighbourhood $\Omega(z)$ of z with $\omega_z \subseteq \Omega(z) \subseteq \omega_z^{(2)} := \cup_{y \in \mathcal{N}(\overline{\omega}_z)} \omega_y$. Any $v_{\mathrm{C}} \in S^1(\mathcal{T}(\Omega(z)))$ with $v_{\mathrm{C}}(z) = 0$ and $v_{\mathrm{C}}(y) \ge 0$ for all $y \in \mathcal{N}(\Omega(z))$ satisfies*

$$h_z^{-1} ||v_{\mathrm{C}}||_{L^2(\Omega(z))} \lesssim \sqrt{\sum_{E \in \mathcal{E}(\Omega(z))} |E|\, ||[\nabla v_{\mathrm{C}} \cdot \nu_E]_E||_{L^2(E)}^2}. \tag{3.28}$$

Proof. The left- and right-hand side of (3.28) define semi-norms on $S^1(\mathcal{T}(\Omega(z)))$. Given any $v_{\mathrm{C}} \in S^1(\mathcal{T}(\Omega(z)))$ with $v_{\mathrm{C}}(z) = 0$ and $v_{\mathrm{C}}(y) \ge 0$ for all $y \in \mathcal{N}(\Omega(z))$, the condition $\sum_{E \in \mathcal{E}(\Omega(z))} |E|\, ||[\nabla u_C \cdot \nu_E]_E||_{L^2(E)}^2 = 0$ implies that $v_{\mathrm{C}} \in P_1(\Omega(z))$. Since $v_{\mathrm{C}}(z) = 0$ and $v_{\mathrm{C}}(y) \ge 0$ in $\mathcal{N}(\Omega(z))$ and $z \in \mathrm{conv}\{\mathcal{N}(\Omega(z)) \setminus \{z\}\}$, $v_{\mathrm{C}} \equiv 0$ in $\Omega(z)$. A compactness argument as in the proof of the equivalence of norms shows that (3.28) holds in the cone of all such v_{C}. A scaling argument shows that the generic constant hidden in $\lesssim$ depends on the shape-regularity of the underlying triangulation, but not on the size of the triangles. □

Proof of Theorem 3.29. The proof follows from *Claim 1–3* below.
Claim 1. For some subset $\omega \subset \Omega$, let $\eta^2(\omega) := \sum_{E \in \mathcal{E}(\omega)} |E|\, ||[\nabla u_{\mathrm{C}} \cdot \nu_E]_E||_{L^2(E)}^2$. With Ω_T from Subsection 2.2.1 on Page 11 and a neighbourhood $\Omega(T)$ of T, specified in the proof below, it holds

$$\int_\Omega (-\lambda_{\mathrm{CB}})(u_{\mathrm{C}} + w_D - \chi)\,\mathrm{d}x \le \sum_{T \in \mathcal{T}_I \cap \mathcal{T}_{DB}} ||h_T \lambda_{\mathrm{CB}}||_{L^2(T)} |\!|\!| w_D |\!|\!|_T$$

$$+ \sum_{T\in\mathcal{T}\setminus\mathcal{T}_C} ||h_T^2\nabla\lambda_{\mathrm{CB}}||_{L^2(T)}\eta(\Omega_T) + \sum_{T\in\mathcal{T}_C\cap\mathcal{T}_{DB}} ||h_T\lambda_{\mathrm{CB}}||_{L^2(T)}|||w_D|||_T;$$

$$\int_\Omega(-\lambda_{\mathrm{V}})(u_{\mathrm{C}}+w_D-\chi)\,\mathrm{d}x \le \sum_{T\in(\mathcal{T}_I\cup\mathcal{T}_C)\cap\mathcal{T}_{DB}} ||h_T^2\nabla\lambda_{\mathrm{V}}||_{L^2(T)}|||w_D|||_T + \sum_{T\in\mathcal{T}_I} ||h_T^2\nabla\lambda_{\mathrm{V}}||_{L^2(T)}\eta(\Omega_T).$$

Proof. For $\mu=\lambda_{\mathrm{CB}}$ and $\mu=\lambda_{\mathrm{V}}$, fix $T\in\mathcal{T}$ and analyze the integral $I_T := \int_T(-\mu)(u_{\mathrm{C}}+w_D-\chi)\,\mathrm{d}x$ for each triangle separately. A Cauchy, a triangle, and a Friedrichs inequality show

$$I_T \le ||\mu||_{L^2(T)}||u_{\mathrm{C}}-\chi||_{L^2(T)} + ||h_T\mu||_{L^2(T)}|||w_D|||_T.$$

For $T\in\mathcal{T}_C$, it follows that $||u_{\mathrm{C}}-\chi||_{L^2(T)}=0$ and hence

$$I_T \le ||h_T\mu||_{L^2(T)}|||w_D|||_T.$$

For $T\in\mathcal{T}$ with $u_{\mathrm{C}}>\chi$ in T, the discrete complementary conditions (3.22) guarantee that $\lambda_{\mathrm{CB}}(y)=0$ for $y\in\mathcal{N}(T)\cap\mathcal{N}(\Omega)$ and $\lambda_{\mathrm{V}}(y)=0$ for $y\in\mathcal{N}(T)$. Hence $||\lambda_{\mathrm{CB}}||_{L^2(T)}=0$ for all triangles T with positive distance to the boundary and $||\lambda_{\mathrm{V}}||_{L^2(T)}=0$ for all triangles $T\in\mathcal{T}\setminus(\mathcal{T}_C\cup\mathcal{T}_I)$. Since $u_{\mathrm{C}}-\chi>0$ in T and each triangle has at least one interior node, a Friedrichs inequality shows

$$||\lambda_{\mathrm{CB}}||_{L^2(T)} \lesssim ||h_T\nabla\lambda_{\mathrm{CB}}||_{L^2(T)}.$$

For a triangle T with $z\in\mathcal{N}(T)\cap\mathcal{N}(\partial\Omega)$, consider the case $\lambda_{\mathrm{CB}}(z)\neq 0$. (Otherwise $||\lambda_{\mathrm{CB}}||_{L^2(T)}=0$.) There exists $\zeta(z)\in\mathcal{N}(\omega_z)\cap\mathcal{N}(\Omega)$ with $(u_{\mathrm{C}}-\chi)(\zeta(z))=0$ and Lemma 3.32 applies to $u_{\mathrm{C}}-\chi$ with $\omega_{\zeta(z)}\subseteq\Omega(T):=\Omega(\zeta(z)):=\Omega_T\cup\omega_{\zeta(z)}\subseteq\omega^{(2)}_{\zeta(z)}$. Hence in this case it follows that

$$I_T \lesssim ||h_T^2\nabla\lambda_{\mathrm{CB}}||_{L^2(T)}\left(\sqrt{\sum_{E\in\mathcal{E}(\Omega(T))}|E|\,||[\nabla u_{\mathrm{C}}\cdot\nu_E]_E||^2_{L^2(E)}} + |||w_D|||_T\right)$$

and $I_T=0$ otherwise. In the remaining case, consider $T\in\mathcal{T}_I$. The nodes y_T and z_T are preferably chosen as interior nodes. If $z_T\in\mathcal{N}(\Omega)$, Lemma 3.32 can be applied to $u_{\mathrm{C}}-\chi$ with $\Omega(T):=\Omega(z_T):=\Omega_T\cup\omega_{z_T}\subseteq\omega^{(2)}_{z_T}$ and leads to

$$||u_{\mathrm{C}}-\chi||_{L^2(T)} \lesssim h_T\sqrt{\sum_{E\in\mathcal{E}(\Omega(T))}|E|\,||[\nabla u_{\mathrm{C}}\cdot\nu_E]_E||^2_{L^2(E)}}$$

for $\mu=\lambda_{\mathrm{CB}}$ and $\mu=\lambda_{\mathrm{V}}$. To estimate $||h_T\mu||_{L^2(T)}$, consider two cases. For $T\in\mathcal{T}_I\setminus\mathcal{T}_{\mathrm{DB}}$ there exists $y\in\mathcal{N}(T)$ with $\mu(y)=0$ (for $\mu=\lambda_{\mathrm{CB}}$ and $\mu=\lambda_{\mathrm{V}}$) and hence a Friedrichs inequality yields

$$||h_T\mu||_{L^2(T)} \lesssim ||h_T^2\nabla\mu||_{L^2(T)}.$$

For $T\in\mathcal{T}_{\mathrm{DB}}$ and $\mu=\lambda_{\mathrm{V}}$, the boundary conditions for λ_{V} show that there exists $y\in\mathcal{N}(T)$ such that $\lambda_{\mathrm{V}}(y)=0$. Hence a Friedrichs inequality yields

$$||h_T\mu||_{L^2(T)} \lesssim ||h_T^2\nabla\mu||_{L^2(T)}.$$

For $\mu=\lambda_{\mathrm{CB}}$ such an argument is not possible if y_T cannot be chosen as an interior

node and hence $I_T \lesssim ||h_T\lambda_{\mathrm{CB}}||_{L^2(T)}\,(\eta(\Omega_T) + |||w_D|||_T)$. If z_T cannot be chosen as an interior node, it holds $\{z \in \mathcal{N}(T) \mid (u_{\mathrm{C}} - \chi)(z) = 0\} \subseteq \mathcal{N}(\partial\Omega)$ and hence $\lambda_{\mathrm{CB}} = 0 = \lambda_{\mathrm{V}}$. This concludes the proof of *Claim 1.* □

Claim 2. For $T \in \mathcal{T}$ and $\eta^2(\Omega_T) := \sum_{E\in\mathcal{E}(\Omega_T)\cap\mathcal{E}(\Omega)} |E|\,||[\nabla u_{\mathrm{C}}\cdot\nu_E]_E||^2_{L^2(E)}$ it holds

ⓐ $||h_T\lambda_{\mathrm{CB}}||_{L^2(T)} \lesssim ||h_{\mathcal{T}} f||_{L^2(\Omega_T)} + \eta(\Omega_T)$;

ⓑ $||h_T^2\nabla\lambda_{\mathrm{CB}}||_{L^2(T)} \lesssim \mathrm{Osc}(f,T) + \eta(\Omega_T)$;

ⓒ $||h_T^2\nabla\lambda_{\mathrm{V}}||_{L^2(T)} \lesssim \mathrm{Osc}(f,T) + \sqrt{\sum_{z\in\mathcal{N}(\partial\Omega)\cap\mathcal{N}(T)} ||h_T f||^2_{L^2(\omega_z)}} + \eta(\Omega_T)$.

Proof. The definition of λ_{CB} and the properties of the L^2 norm lead to

$$||h_T\lambda_{\mathrm{CB}}||_{L^2(T)} \le \sum_{z\in\mathcal{N}(T)\cap\mathcal{N}(\Omega)} h_T\Big|\big(F(\varphi_z) - a(u_{\mathrm{C}},\varphi_z)\big)/\int_\Omega \varphi_z\,\mathrm{d}x\Big|\,||\psi_z||_{L^2(T)}.$$

A Cauchy inequality for $F(\varphi_z)$ and an integration by parts of $a(u_{\mathrm{C}},\varphi_z)$ conclude the proof of ⓐ. □

The proofs of ⓑ and ⓒ follow the arguments of the proof of Lemma 8 in Bartels and Carstensen (2004) with a modified analysis of the terms

$$||\sum_{z\in\mathcal{N}(T)\cap\mathcal{N}(\Omega)} \left(\int_{\omega_z} f\varphi_z\,\mathrm{d}x/\int_{\omega_z}\varphi_z\,\mathrm{d}x\right)\nabla\phi_z||_{L^2(T)} \quad \text{for } \phi_z = \psi_z \text{ or } \phi_z = \varphi_z.$$

For the proof of ⓑ let $\mu = \lambda_{\mathrm{CB}}$ and $\phi_z = \psi_z$. Since the modified basis functions $\{\psi_z \mid z \in \mathcal{N}(T)\cap\mathcal{N}(\Omega)\}$ form a partition of unity on T, it follows

$$\begin{aligned}\|\sum_{z\in\mathcal{N}(T)\cap\mathcal{N}(\Omega)} &\left(\int_{\omega_z} f\varphi_z\,\mathrm{d}x/\int_{\omega_z}\varphi_z\,\mathrm{d}x\right)\nabla\psi_z\|_{L^2(T)}\\ &= ||\sum_{z\in\mathcal{N}(T)\cap\mathcal{N}(\Omega)} \left(\int_{\omega_z}(f - \fint_{\Omega_T} f\,\mathrm{d}x)\varphi_z\,\mathrm{d}x/\int_{\omega_z}\varphi_z\,\mathrm{d}x\right)\nabla\psi_z||_{L^2(T)}.\end{aligned}$$

Since $||\varphi_z||_{L^2(\Omega)}/\int_\Omega\varphi_z\,\mathrm{d}x \approx h_z^{-1} \approx h_T^{-1}$ and $||\nabla\psi_z||_{L^2(\Omega)} \approx 1$, a Cauchy inequality completes the proof of ⓑ with

$$h_T^2||\sum_{z\in\mathcal{N}(T)\cap\mathcal{N}(\Omega)} \left(\int_{\omega_z} f\varphi_z\mathrm{d}x/\int_{\omega_z}\varphi_z\,\mathrm{d}x\right)\nabla\psi_z||_{L^2(\Omega_T)} \lesssim h_T||f - \fint_{\Omega_T} f\,\mathrm{d}x||_{L^2(\Omega_T)}.$$

For the proof of ⓒ with $\mu = \lambda_{\mathrm{V}}$ and $\phi_z = \varphi_z$, a triangle inequality leads to

$$\begin{aligned}&||\sum_{z\in\mathcal{N}(T)\cap\mathcal{N}(\Omega)} \left(\int_{\omega_z} f\varphi_z\,\mathrm{d}x/\int_{\omega_z}\varphi_z\,\mathrm{d}x\right)\nabla\varphi_z||_{L^2(T)}\\ &\le ||\sum_{z\in\mathcal{N}(T)} \left(\int_{\omega_z} f\varphi_z\,\mathrm{d}x/\int_{\omega_z}\varphi_z\,\mathrm{d}x\right)\nabla\varphi_z||_{L^2(T)}\\ &\quad + ||\sum_{z\in\mathcal{N}(T)\cap\mathcal{N}(\partial\Omega)} \left(\int_{\omega_z} f\varphi_z\,\mathrm{d}x/\int_{\omega_z}\varphi_z\,\mathrm{d}x\right)\nabla\varphi_z||_{L^2(T)}.\end{aligned}$$

Since $\{\varphi_z | z \in \mathcal{N}(T)\}$ form a partition of unity on T, the first term on the right is estimated as above in the proof of ⓑ. A Cauchy and triangle inequality for the second term lead to

$$\begin{aligned} || \sum_{z\in\mathcal{N}(T)\cap\mathcal{N}(\partial\Omega)} h_T^2 \left(\int_{\omega_z} f\varphi_z \,\mathrm{d}x / \int_{\omega_z} \varphi_z \,\mathrm{d}x \right) \nabla\varphi_z ||_{L^2(T)} \\ \leq \sqrt{\sum_{z\in\mathcal{N}(T)\cap\mathcal{N}(\partial\Omega)} h_T^2 ||f||^2_{L^2(\omega_z)}}. \end{aligned}$$ □

Claim 3. For $\mu = \lambda_{\mathrm{CB}}$ and $\mu = \lambda_{\mathrm{V}}$, it holds (with $\eta(E)^2 := |E| \, ||[\nabla u_{\mathrm{C}} \cdot \nu_E]||^2_{L^2(E)}$)

$$||h_{\mathcal{T}}(f-\mu)||_{L^2(\Omega)} + \sqrt{\sum_{E\in\mathcal{E}(\Omega)} \eta(E)^2} \lesssim |\!|\!| u - u_{\mathrm{C}} |\!|\!| + |\!|\!| \lambda - \mu |\!|\!|_* + \mathrm{osc}(f, \mathcal{T}).$$

Proof. Let $b_T := 60\Pi_{z\in\mathcal{N}(T)}\varphi_z \in H^1_0(T) \cap P_3(T)$ denote the cubic bubble function on the triangle T with $⨍_T b_T \,\mathrm{d}x = 1$. Define $w_T := (\Pi_0 f - \mu) b_T$. The arguments in Verfürth (1996) yield

$$||h_T(\Pi_0 f - \mu)||_{L^2(T)} \lesssim \mathrm{osc}(f, T) + |\!|\!| u - u_{\mathrm{C}} |\!|\!|_T + |\!|\!| \lambda - \mu |\!|\!|_{T,*}.$$

A triangle inequality then shows

$$||h_T(f-\mu)||_{L^2(T)} \lesssim \mathrm{osc}(f, T) + |\!|\!| u - u_{\mathrm{C}} |\!|\!| + |\!|\!| \lambda - \mu |\!|\!|_{*,T}. \tag{3.29}$$

To obtain the global result define w piecewise by $w|_T := w_T$.
For an edge $E \in \mathcal{E}$, define the quadratic bubble function $b_E := 6\Pi_{z\in\mathcal{N}(E)}\varphi_z$ with $⨍_E b_E \,\mathrm{d}s = 1$. Set $w_E := [\nabla u_{\mathrm{C}} \cdot \nu_E]_E b_E$. The arguments in Verfürth (1996) lead to

$$||[\nabla u_{\mathrm{C}} \cdot \nu_E]_E||_{L^2(E)} \lesssim \int_{\omega_E} \nabla(u_{\mathrm{C}} - u) \cdot \nabla w_E \,\mathrm{d}x + \int_{\omega_E} \nabla u \cdot \nabla w_E \,\mathrm{d}x. \tag{3.30}$$

For the first term in the upper bound of (3.30), a Cauchy inequality shows

$$\int_{\omega_E} \nabla(u_{\mathrm{C}} - u) \cdot \nabla w_E \,\mathrm{d}x \leq |\!|\!| u - u_{\mathrm{C}} |\!|\!|_{\omega_E} \, |\!|\!| w_E |\!|\!|_{\omega_E}.$$

An integration by parts and the definition of the continuous and discrete Lagrange multipliers for the second term leads to,

$$\begin{aligned} \int_{\omega_E} \nabla u \cdot \nabla w_E \,\mathrm{d}x &= \int_{\omega_E} (\mu - \lambda) w_E \,\mathrm{d}x + \int_{\omega_E} (f - \mu) w_E \,\mathrm{d}x \\ &\lesssim \left(|\!|\!| \lambda - \mu |\!|\!|_{*,\omega_E} + ||h_T(f-\mu)||_{L^2(\omega_E)} \right) |\!|\!| w_E |\!|\!|_{\omega_E}. \end{aligned}$$

A finite overlap, the estimate (3.29), and the combination of the last three displayed inequalities with $|E| \, |\!|\!| w_E |\!|\!|_{\omega_E} \lesssim ||w_E||_{L^2(\omega_E)} \lesssim ||[\nabla u_{\mathrm{C}} \cdot \nu_E]_E||_{L^2(E)}$ conclude the proof. □

The combination of the three claims concludes the proof of Theorem 3.29. □

3.4. Non-conforming FEM for the obstacle problem

This section is devoted to the analysis of the non-conforming FEM (NCFEM) for the obstacle problem in two space dimensions. Carstensen and Köhler (2016a) suggest

a first choice for a discrete Lagrange multiplier. The efficiency of this particular discrete Lagrange multiplier in the sense of Theorem B is discussed in this section. This section also analyzes the efficiency of the complementary condition residual $\int_\Omega (-\mu)(v-\chi)_+ \,\mathrm{d}x$ for some $v \in \mathcal{A}$ in the sense of Theorem C. The results of this section are restricted to Dirichlet boundary conditions $u_D \in H^1(\Omega)$, an obstacle $\chi \in H^1(\Omega)$ with $\chi \leq u_D$ along $\partial\Omega$ and $\Delta\chi \in L^2(\Omega)$, and $f \in L^2(\Omega)$ and the resulting regularity with $\Delta u \in L^2(\Omega)$.

3.4.1. Non-conforming discretization of the obstacle problem

Given a shape-regular triangulation $\mathcal{T}$ of $\Omega \subset \mathbb{R}^2$ from Subsection 2.2.1 on Page 11, recall the spaces $\mathrm{CR}^1(\mathcal{T})$ and $\mathrm{CR}^1_0(\mathcal{T})$ from Definition 2.13 on Page 15. To approximate the Dirichlet boundary conditions u_D define

$$u_{D,\mathrm{NC}} := \sum_{E \in \mathcal{E}(\partial\Omega)} \fint_E u_D \,\mathrm{d}s \psi_E.$$

This leads to the discrete subset $\mathcal{A}_{\mathrm{NC}}(T) := u_{D,\mathrm{NC}} + \mathrm{CR}^1_0(\mathcal{T})$ of $\mathrm{CR}^1(\mathcal{T})$ and the convex and non-empty subset

$$K_{\mathrm{CR}}(\mathcal{T}) := \{v_{\mathrm{CR}} \in \mathcal{A}_{\mathrm{NC}}(\mathcal{T}) \mid \forall E \in \mathcal{E}(\Omega), \fint_E \chi \mathrm{d}s \leq \fint_E v_{\mathrm{CR}} \mathrm{d}s\}$$

of $\mathcal{A}_{\mathrm{NC}}(\mathcal{T})$. Recall the bilinear form $a_{\mathrm{NC}}(\bullet,\bullet)$ from Page 19. The discrete variational inequality seeks $u_{\mathrm{CR}} \in K_{\mathrm{CR}}(\mathcal{T})$ such that

$$F(v_{\mathrm{CR}} - u_{\mathrm{CR}}) \leq a_{\mathrm{NC}}(u_{\mathrm{CR}}, v_{\mathrm{CR}} - u_{\mathrm{CR}}) \quad \text{for all } v_{\mathrm{CR}} \in K_{\mathrm{CR}}(\mathcal{T}). \tag{3.31}$$

Lemma 3.33 (existence of solutions)**.** *There exists a unique discrete solution $u_{\mathrm{CR}} \in K_{\mathrm{CR}}(\mathcal{T})$ to* (3.31)*.*

Proof. Since $a_{\mathrm{NC}}(\bullet,\bullet)$ is a scalar product on $\mathrm{CR}^1_0(\mathcal{T}) \times \mathrm{CR}^1_0(\mathcal{T})$, the proof follows after a shift of χ to $\chi - u_{D,\mathrm{NC}}$ and of F to $F - a(u_{D,\mathrm{NC}}, \bullet)$ from Kinderlehrer and Stampacchia (1980, Thm. 2.1). □

Lemma 3.34 (discrete complementary conditions)**.** *The solution $u_{\mathrm{CR}} \in K_{\mathrm{CR}}(\mathcal{T})$ to* (3.31) *satisfies the discrete complementary conditions*

$$0 \leq \fint_E (u_{\mathrm{CR}} - \chi)\mathrm{d}s \perp F(\psi_E) - a_{\mathrm{NC}}(u_{\mathrm{CR}}, \psi_E) =: \sigma_{\mathrm{CR}}(\psi_E) \leq 0 \tag{3.32}$$

for all $E \in \mathcal{E}(\Omega)$ where $\perp$ abbreviates pointwise orthogonality in $\mathbb{R}$.

Proof. The first inequality follows from the definition of $K_{\mathrm{CR}}(\mathcal{T})$. For any $E \in \mathcal{E}(\Omega)$, $v_{\mathrm{CR}} := u_{\mathrm{CR}} + \psi_E \in K_{\mathrm{CR}}(\mathcal{T})$. Hence the discrete variational inequality (3.31) shows $\sigma_{\mathrm{CR}}(\psi_E) \leq 0$. To show the orthogonality, consider the test functions $v_{\mathrm{CR}} := \big(2u_{\mathrm{CR}}(\mathrm{mid}(E)) - \fint_E \chi \,\mathrm{d}s\big)\psi_E$ and $v_{\mathrm{CR}} = \fint_E \chi \,\mathrm{d}s \psi_E$ for $E \in \mathcal{E}(\Omega)$. The discrete variational inequality (3.31) then shows

$$F\Big((u_{\mathrm{CR}}(\mathrm{mid}(E)) - \fint_E \chi \,\mathrm{d}s)\psi_E\Big) - a\Big(u_{\mathrm{CR}}, (u_{\mathrm{CR}}(\mathrm{mid}(E)) - \fint_E \chi \,\mathrm{d}s)\psi_E\Big) = 0.$$

This concludes the proof. □

3.4.2. Conforming companion and boundary conditions

To employ Theorem 3.18, a conforming companion $v \in \mathcal{A}$ to the discrete solution u_{CR} to (3.31) needs to be defined. Recall the map $J_2 : \mathrm{CR}^1_0(\mathcal{T}) \to S^2_0(\mathcal{T})$ from Theorem 2.27 and the non-conforming interpolation operator $I_{\mathrm{NC}} : H^1_0(\Omega) \to \mathrm{CR}^1_0(\mathcal{T})$ defined uniquely by

$$\fint_E (w - I_{\mathrm{NC}} w)\mathrm{d}s = 0 \qquad \text{for all } E \in \mathcal{E}(\Omega) \text{ and } w \in H^1_0(\Omega).$$

For an edge $E \in \mathcal{E}$, define the edge-oriented quadratic bubble function $b_E := 6\Pi_{z\in\mathcal{N}(E)}\varphi_z \in H^1_0(\omega_E) \cap P_2(\mathcal{T}(\omega_E))$ which satisfies $\mathrm{supp}(b_E) = \overline{\omega}_E$ and $\fint_E b_E \,\mathrm{d}s = 1$. Given the Dirichlet data $u_D \in C(\partial\Omega)$, the functions $u_{D1} \in P_1(\mathcal{T}) \cap C(\overline{\Omega})$ and $u_{D2} \in P_2(\mathcal{T}) \cap C(\overline{\Omega})$ approximate the non-homogeneous Dirichlet data. The function u_{D1} is defined by the nodal values

$$u_{D1}(z) := \begin{cases} u_D(z) & \text{for } z \in \mathcal{N}(\partial\Omega), \\ 0 & \text{for } z \in \mathcal{N}(\Omega) \end{cases}$$

and the function $u_{D2} \in P_2(\mathcal{T}) \cap C(\overline{\Omega})$ is given by

$$u_{D2} := u_{D1} + \sum_{E\in\mathcal{E}(\partial\Omega)} \fint_E (u_D - u_{D1}) \,\mathrm{d}s\, b_E. \tag{3.33}$$

Any $w_{\mathrm{CR}} \in \mathcal{A}_{\mathrm{NC}}$ satisfies $w_{\mathrm{CR}} = I_{\mathrm{NC}} u_{D2} + (w_{\mathrm{CR}} - I_{\mathrm{NC}} u_{D2})$ and $w_{\mathrm{CR}} - I_{\mathrm{NC}} u_{D2} \in \mathrm{CR}^1_0(\mathcal{T})$. Let w_D in Theorem 2.28 be such that $w_D|_{\partial\Omega} = (u_D - u_{D2})|_{\partial\Omega}$. For the solution $u_{\mathrm{CR}} \in K_{\mathrm{CR}}(\mathcal{T})$ to Problem (3.31) define u_2 and the conforming companion v by

$$u_2 := u_{D2} + J_2(u_{\mathrm{CR}} - I_{\mathrm{NC}} u_{D2}) \in u_{D2} + S^2_0(\mathcal{T}) \quad \text{and} \quad v := w_D + u_2 \in \mathcal{A}. \tag{3.34}$$

3.4.3. Interpolation operator and boundary modification

The proof of efficiency of the proposed discrete Lagrange multiplier presented in this section is closely related an appropriate interpolation operator. To avoid unnecessary boundary terms, the edge-oriented basis functions are modified and at the same time the degrees of freedom are limited to the interior nodes. For any boundary edge $E \in \mathcal{E}(\partial\Omega)$, let $N(E) \in \mathcal{E}(\overline{\omega}_E)$ be a neighbouring interior edge in the sense that E and $N(E)$ are edges of the same triangle. For all interior edges set $N(E) := E$. Then

$$\Psi_E := \sum_{F\in N^{-1}(E)} \psi_F \in \mathrm{CR}^1(\mathcal{T}) \quad \text{and} \quad \omega(E) := \bigcup_{F\in N^{-1}(E)} \omega_F. \tag{3.35}$$

With the modified basis function Ψ_E, define the interpolation operator $J_{\mathrm{NC}} : V \to \mathrm{CR}^1_0(\mathcal{T})$ by

$$J_{\mathrm{NC}}\varphi := \sum_{E\in\mathcal{E}(\Omega} \int_\Omega \varphi\Psi_E \,\mathrm{d}x \psi_E / ||\psi_E||^2_{L^2(\Omega)} \quad \text{for all } \varphi \in V. \tag{3.36}$$

The properties of this operator are summarized in the following theorem.

Theorem 3.35. *Any $f \in L^2(\Omega)$ and any $\varphi \in V$ satisfy*

ⓐ $\|\!| J_{\mathrm{NC}}\varphi |\!\| \lesssim \|\!| \varphi |\!\|$,

ⓑ $\int_\Omega f(\varphi - J_{\mathrm{NC}}\varphi)\,\mathrm{d}x \lesssim \mathrm{osc}(f,\mathcal{T})\|\!| \varphi |\!\|$.

Proof. For the proof of ⓐ recall that $(\psi_E)_{E\in\mathcal{E}}$ is a partition of unity on Ω. Then a triangle inequality shows

$$\begin{aligned}\|\!| J_{\mathrm{NC}}\varphi |\!\| &= \Big\| \sum_{E\in\mathcal{E}(\Omega)} \Big(\int_\Omega \varphi\Psi_E\,\mathrm{d}x/||\psi_E||^2_{L^2(\omega_E)} - \varphi\Big)\nabla\psi_E + \sum_{E\in\mathcal{E}(\partial\Omega)} \varphi\nabla\psi_E\Big\|_{L^2(\Omega)} \\ &\le \sum_{E\in\mathcal{E}(\Omega)} \Big\| \int_\Omega \varphi\Psi_E\,\mathrm{d}x/||\psi_E||^2_{L^W(\omega_E)} - \varphi\Big\|_{L^2(\omega_E)} + \sum_{E\in\mathcal{E}(\partial\Omega)} ||\varphi\nabla\psi_E||_{L^2(\omega_E)}.\end{aligned}$$

Since $|\nabla\psi_E| \lesssim |E|^{-1}$, it follows

$$\begin{aligned}\|\!| J_{\mathrm{NC}}\varphi |\!\| \lesssim \sum_{E\in\mathcal{E}(\Omega)} |E|^{-1}\Big\| \int_\Omega \varphi\Psi_E\,\mathrm{d}x/||\psi_E||^2_{L^2(\omega_E)} - \varphi\Big\|_{L^2(\omega_E)} \\ + \sum_{E\in\mathcal{E}(\partial\Omega)} |E|^{-1}||\varphi||_{L^2(\omega_E)}.\end{aligned}$$

This leads to three different cases. In the first case, consider $E\in\mathcal{E}(\Omega)$ with $\Psi_E = \psi_E$. Then a triangle inequality yields

$$\begin{aligned}&\Big\| \int_\Omega \varphi\psi_E\,\mathrm{d}x/||\psi_E||^2_{L^2(\omega_E)} - \varphi\Big\|_{L^2(\omega_E)} \\ &\quad\le \Big\| \int_\Omega (\varphi - \fint_{\omega_E}\varphi\,\mathrm{d}x)\psi_E\,\mathrm{d}x/||\psi_E||^2_{L^2(\omega_E)}\Big\|_{L^2(\omega_E)} + ||\fint_{\omega_E}\varphi\,\mathrm{d}x - \varphi||_{L^2(\omega_E)}.\end{aligned}$$

A Cauchy and a Poincaré inequality result in

$$\Big\| \int_\Omega \varphi\psi_E\,\mathrm{d}x/||\psi_E||^2_{L^2(\omega_E)} - \varphi\Big\|_{L^2(\omega_E)} + ||\fint_{\omega_E}\varphi\,\mathrm{d}x - \varphi||_{L^2(\omega_E)} \lesssim h_E\|\!|\varphi|\!\|_{\omega_E}.$$

In the second case, consider $E\in\mathcal{E}(\Omega)$ with $\Psi_E \neq \psi_E$. Hence $\Psi_E \neq 0$ on part of the boundary $\partial\Omega$. Since $\varphi = 0$ along $\partial\Omega$, a Cauchy, triangle, and Friedrichs inequality yield

$$\begin{aligned}\Big\| \int_\Omega \varphi\Psi_E\,\mathrm{d}x/||\psi_E||^2_{L^2(\Omega)} - \varphi\Big\|_{L^2(\omega_E)} &\le \Big\| \int_\Omega \varphi\Psi_E\,\mathrm{d}x/||\psi_E||^2_{L^2(\Omega)}\Big\|_{L^2(\omega_E)} + ||\varphi||_{L^2(\omega_E)} \\ &\lesssim h_E\|\!|\varphi|\!\|_{\omega_E}.\end{aligned}$$

Finally, let $E\in\mathcal{E}(\partial\Omega)$. Since $\varphi = 0$ along the boundary $\partial\Omega$ a Friedrichs inequality yields

$$||\varphi||_{L^2(\omega_E)} \lesssim h_E\|\!|\varphi|\!\|_{\omega_E}.$$

The combination of these three cases concludes the proof of ⓐ. □

Since $\{\Psi_E \mid E\in\mathcal{E}(T)\cap\mathcal{E}(\Omega)\}$ define a partition of unity on T for all $T\in\mathcal{T}$, and since $||\psi_E||^2_{L^2(\Omega)} = \int_\Omega \psi_E\,\mathrm{d}x$, it holds, for all $T\in\mathcal{T}$

$$\int_T (\varphi - J_{\mathrm{NC}}\varphi)\,\mathrm{d}x = \int_T \sum_{E\in\mathcal{E}(T)\cap\mathcal{E}(\Omega)} \left(\varphi\Psi_E - \int_\Omega \varphi\Psi_E\,\mathrm{d}x/||\psi_E||^2_{L^2(\Omega)}\psi_E\right)\mathrm{d}x = 0.$$

Then a Cauchy inequality yields

$$\begin{aligned}\int_\Omega f(\varphi - J_{\mathrm{NC}}\varphi)\,\mathrm{d}x &= \int_\Omega (f - \Pi_0 f)(\varphi - J_{\mathrm{NC}}\varphi)\,\mathrm{d}x \\ &\leq ||f - \Pi_0 f||_{L^2(\Omega)}||(1-\Pi_0)(\varphi - J_{\mathrm{NC}}\varphi)||_{L^2(\Omega)}.\end{aligned}$$

A Poincaré inequality shows

$$||(1-\Pi_0)(\varphi - J_{\mathrm{NC}}\varphi)||_{L^2(\Omega)} \lesssim h_{\mathcal{T}}|||\varphi - J_{\mathrm{NC}}\varphi|||_{\mathrm{NC}}.$$

Then the stability in ⓐ concludes the proof of ⓑ. □

3.4.4. Discrete Lagrange multiplier for NCFEM

This section presents a discrete Lagrange multiplier $\mu = \lambda_{\mathrm{CR}}^- \in L^2(\Omega;(-\infty,0])$. It is designed with the aid of an intermediate Lagrange multiplier $\lambda_{\mathrm{CR}} \in \mathrm{CR}^1(\mathcal{T})$ which does not satisfy $\lambda_{\mathrm{CR}} \leq 0$ a.e. in Ω. The resulting discrete Lagrange multiplier λ_{CR}^- is piecewise affine, but not necessarily with respect to the triangulation $\mathcal{T}$. With $\sigma_{\mathrm{CR}}(\psi_E)$ from (3.32), and ψ_E and Ψ_E from (3.35), set

$$\lambda_{\mathrm{CR}} := \sum_{E\in\mathcal{E}(\Omega)} \sigma_{\mathrm{CR}}(\psi_E)\Psi_E/||\psi_E||^2. \tag{3.37}$$

This Lagrange multiplier does not satisfy $\lambda_{\mathrm{CR}} \leq 0$ a.e. on Ω and hence leads to the following split of the triangulation $\mathcal{T} := \mathcal{T}_+ \cup \mathcal{T}'$ with

$$\mathcal{T}_+ := \{T\in\mathcal{T} \mid |\{x\in T \;\Big|\; \lambda_{\mathrm{CR}}(x) > 0\}| > 0\} \text{ and } \mathcal{T}' := \mathcal{T}\setminus\mathcal{T}_+.$$

The goal is to set $\mu = \lambda_{\mathrm{CR}}$ wherever λ_{CR} has the right sign and to modify λ_{CR} only on sections of triangles in $\mathcal{T}_+$. To this end, let $K\in\mathcal{T}_+$ and design some triangle $\hat{T}_K$. Consider the red-refinement $\mathrm{red}(K) = \{T_1,T_2,T_3,T_4\}$ for $K\in\mathcal{T}_+$ and let T_4 denote the central triangle. The discrete complementary conditions (3.32) and the design of λ_{CR} guarantee that $\lambda_{\mathrm{CR}}(\mathrm{mid}(E)) \leq 0$ for all interior edges $E\in\mathcal{E}(\Omega)$. This means that $\lambda_{\mathrm{CR}} \geq 0$ can only happen in one of the sub-triangles T_1,T_2,T_3 of $\mathrm{red}(K)$. Without loss of generality, let this triangle be T_1. The discrete Lagrange multiplier λ_{CR} is affine on $K\in\mathcal{T}_+$ and hence the set $\{x\in K \mid \lambda_{\mathrm{CR}}(x)\geq 0\}$ defines a triangle $T_K := \mathrm{conv}\{A,B,C\} \subseteq T_1$ with $C\in\mathcal{N}(K)$ and $\lambda_{\mathrm{CR}}(C) = \max\lambda_{\mathrm{CR}}|_K$ depicted in Figure 3.1. Let α,β, and γ denote the angles at the corresponding vertices A, B, and C in T_K. The shape-regularity of the triangulation implies $\gamma_0 \leq \gamma$. Without loss of generality, assume $\alpha\leq\beta$ and define $d_K := \mathrm{dist}\{B,C\}$. Consider the line which contains the line segment $\overline{BC}$ and define the point C' on that line such that $d_K := \mathrm{dist}\{B,C\} = \mathrm{dist}\{B,C'\}$. This defines a triangle

$$T_K' := \mathrm{conv}\{A,B,C'\} \subseteq K$$

adjacent to T_K and their union

$$\hat{T}_K := T_K \cup T_K' = \mathrm{conv}\{A,C,C'\}. \tag{3.38}$$

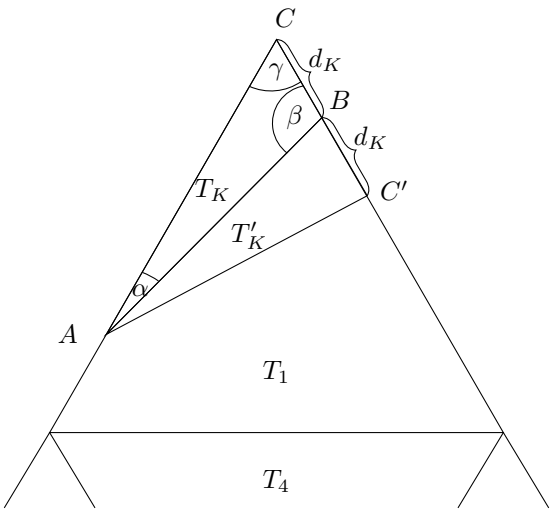

Figure 3.1.: Design of triangle $\hat{T}_K = T_K \cup T'_K$.

With the triangle $\hat{T}_K$, the discrete Lagrange multiplier $\mu = \lambda^-_{\mathrm{CR}} \in L^2(\Omega; (-\infty, 0])$ is defined by

$$\lambda^-_{\mathrm{CR}}(x) := \begin{cases} \lambda_{\mathrm{CR}}(x) & \text{if } x \in \Omega_- := \Omega \setminus \bigcup_{K \in \mathcal{T}_+} \hat{T}_K, \\ 0 & \text{if } x \in \cup_{K \in \mathcal{T}_+} \hat{T}_K. \end{cases} \tag{3.39}$$

The advantage of this special design of $\hat{T}_K$ and the connection to λ^-_{CR} becomes apparent in the following lemma.

Lemma 3.36. *Let $K \in \mathcal{T}_+$ and consider the triangle $\hat{T}_K$ of* (3.38) *and Figure 3.1. Any function $f \in H^1(\hat{T}_K)$ satisfies*

$$\int_{\hat{T}_K} \lambda_{\mathrm{CR}} f \,\mathrm{d}x \leq 2d_K/\pi ||\lambda_{\mathrm{CR}}||_{L^2(\hat{T}_K)} |\!|\!| f |\!|\!|_{\hat{T}_K}.$$

Proof. In a first step, assume that the triangle $T_K := \mathrm{conv}\{A, B, C\}$ has a right angle at the vertex B and choose a local coordinate system such that the triangle $\hat{T}_K = \mathrm{conv}\{A, C, C'\}$ has vertices $(0,0), (L, -d_K), (L, d_K)$ as depicted in Figure 3.2. The triangle $\hat{T}_K$ is parametrized by $(x, y) \in \hat{T}_K$ for $0 \leq x \leq L$ and $-xd_K/L \leq y \leq xd_K/L$. Then

$$\int_{\hat{T}_K} \lambda_{\mathrm{CR}} f \,\mathrm{d}x = \int_0^L \int_{-xd_K/L}^{xd_K/L} (\lambda_{\mathrm{CR}} f)(x, y) \,\mathrm{d}y \,\mathrm{d}x.$$

The point of the design of $\hat{T}_K$ and the choice of the coordinate system is that $\lambda_{\mathrm{CR}} = 0$ for $0 \leq x \leq L$ and $y = 0$. For any fixed $x \in (0, L)$ and $\ell := xd_K/L$, the line segment $\{x\} \times (-\ell, \ell)$ is parallel to the edge $\mathrm{conv}\{C, C'\}$ and the one-dimensional Poincaré inequality yields

$$\int_{-\ell}^{\ell} \lambda_{\mathrm{CR}} f \,\mathrm{d}y \leq 2\ell/\pi \, ||\lambda_{\mathrm{CR}}||_{L^2(-\ell,\ell)} ||\partial f(x, \bullet)/\partial y||_{L^2(-\ell,\ell)}.$$

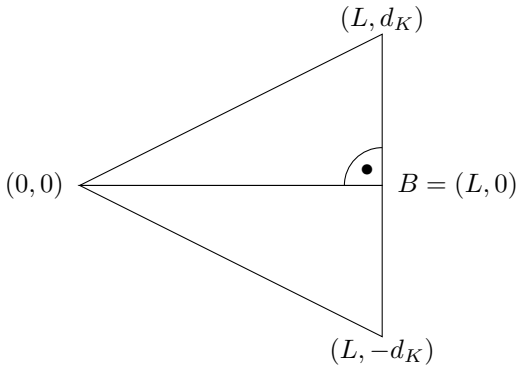

Figure 3.2.: Design of triangle $\hat{T}_K = T_K \cup T_K'$.

An integration of this with respect to $0 \leq x \leq L$ finally results in

$$\int_{\hat{T}_K} \lambda_{\mathrm{CR}} f \,\mathrm{d}x \leq 2d_K/\pi \, ||\lambda_{\mathrm{CR}}||_{L^2(\hat{T}_K)} \|\!| f |\!\|_{\hat{T}_K}.$$

In a second step, consider the general configuration with a general angle β at B. The one-dimensional integration follows affine coordinate systems along lines parallel to $\mathrm{conv}\{C, C'\}$. The arguments above then lead to the result in the general setting. □

There is a strong connection between the two discrete Lagrange multipliers λ_{CR} and λ_{CR}^- identified in the following proposition.

Proposition 3.37. *The discrete Lagrange multipliers* λ_{CR} *and* λ_{CR}^- *from* (3.37) *and* (3.39) *and* $\eta_+^2 := \sum_{K \in \mathcal{T}_+} (4d_K/\pi ||\lambda_{\mathrm{CR}}||_{L^2(T_K)})^2$ *satisfy*

$$\|\!| \lambda_{\mathrm{CR}} - \lambda_{\mathrm{CR}}^- |\!\|_* \leq \|\!| \lambda_{\mathrm{CR}} - \lambda_{\mathrm{CR}}^- |\!\|_{\mathrm{NC},*} \leq \eta_+ \lesssim \|\!| \lambda - \lambda_{\mathrm{CR}} |\!\|_*.$$

Proof. The first inequality follows from $H_0^1(\Omega) \subset \{v \in H^1(\mathcal{T}) \mid \fint_E [v]_E \,\mathrm{d}s = 0 \text{ for all } E \in \mathcal{E}(\Omega)\}$ and the definition of the operator norm in (2.31). To prove the second inequality, let $\varphi \in H^1(K)$ for $K \in \mathcal{T}_+$ with $\|\!| \varphi |\!\|_{\hat{T}_K}$. Lemma (3.36) shows that

$$\int_K (\lambda_{\mathrm{CR}} - \lambda_{\mathrm{CR}}^-)\varphi \,\mathrm{d}x = \int_{\hat{T}_K} \lambda_{\mathrm{CR}} \varphi \,\mathrm{d}x \leq 2d_K/\pi ||\lambda_{\mathrm{CR}}||_{L^2(\hat{T}_K)} \|\!| \varphi |\!\|_{\hat{T}_K}.$$

This and a Cauchy inequality complete the proof of the second inequality. To prove the last inequality, recall that the triangulation $\mathcal{T}$ is shape-regular and hence the angle γ is bounded away from 0 and π. The design of $\hat{T}_K$ proves, that in consequence this also holds for the angle β in T_K. The angle α may be much smaller than $\beta \approx \gamma$. The shape-regularity shows, that the distance $\ell_K := |AB|$ between the vertices A and B satisfies $d_K \lesssim \ell_K$. This, the design of T_K, and the midpoint quadrature rule show

$$d_K ||\lambda_{\mathrm{CR}}||_{L^2(T_K)} \lesssim d_K^{3/2} \ell_K^{1/2} \lambda_{\mathrm{CR}}(C).$$

Given the barycentric coordinates $\lambda_A, \lambda_B, \lambda_C$ on T_K at A, B, and C, define the cubic bubble-function $b_{T_K} := 27\lambda_A\lambda_B\lambda_C$. The function b_{T_K} satisfies $b_{T_K} \in W_0^{1,\infty}(T_K)$

with $0 \le b_{T_K} \le 1$, and $\|\!| b_{T_K} |\!\| = ||\nabla b_{T_K}||_{L^2(T_K)} \le d_K^{1/2}\ell_K^{1/2}||\nabla b_{T_K}||_{L^\infty(T_K)}$. Since $\lambda \le 0 \le \lambda_{\mathrm{CR}}$ on T_K, the arguments in Verfürth (1996) show

$$\lambda_{\mathrm{CR}}(C) d_K \ell_K \approx \int_{T_K} b_{T_K}\lambda_{\mathrm{CR}}\,\mathrm{d}x \le \int_{T_K} b_{T_K}(\lambda_{\mathrm{CR}} - \lambda)\,\mathrm{d}x \le \|\!| b_{T_K} |\!\|\, \|\!| \lambda - \lambda_{\mathrm{CR}} |\!\|_{*,T_K}.$$

The bubble function satisfies $\|\!| b_{T_K} |\!\| \lesssim d_K^{-1/2}\ell_K^{1/2}$ and hence

$$d_K||\lambda_{\mathrm{CR}}||_{L^2(T_K)} \lesssim \|\!| \lambda - \lambda_{\mathrm{CR}} |\!\|_{*,T_K}.$$

The summation over $K \in \mathcal{T}_+$ concludes the proof. □

3.4.5. Efficiency of the discrete Lagrange multiplier for NCFEM

Recall the solution $u \in K$ to (3.2) and the Lagrange multiplier Λ from (3.3) with L^2 representation $\lambda = \Delta u + f \in L^2(\Omega; (-\infty, 0])$. The following theorem shows that the discrete Lagrange multiplier $\lambda_{\mathrm{CR}}^- \in L^2(\Omega; (-\infty, 0])$ from (3.39) is efficient in the sense of Theorem B.

Theorem 3.38. *The discrete solution $u_{\mathrm{CR}} \in K_{\mathrm{CR}}(\mathcal{T})$ to* (3.31) *and the discrete Lagrange multiplier λ_{CR}^- of* (3.39) *satisfy*

$$\|\!| \lambda - \lambda_{\mathrm{CR}}^- |\!\|_* \lesssim \|\!| u - u_{\mathrm{CR}} |\!\|_{\mathrm{NC}} + \mathrm{osc}(f, \mathcal{T}) + \mathrm{osc}(\lambda, \mathcal{T}).$$

The proof of Theorem 3.38 employs the following lemma, which follows from elementary algebra and the linearity of F and $a_{\mathrm{NC}}(u_{\mathrm{CR}}, \bullet)$. It also clarifies the close connection between the discrete Lagrange multiplier λ_{CR} and the interpolation operator J_{NC} from (3.36).

Lemma 3.39. *For all $\varphi \in V$, the discrete Lagrange multiplier λ_{CR} from* (3.37) *and the interpolation operator J_{NC} from* (3.36) *satisfy*

$$\int_\Omega \lambda_{\mathrm{CR}}\varphi\,\mathrm{d}x = F(J_{\mathrm{NC}}\varphi) - a_{\mathrm{NC}}(u_{\mathrm{CR}}, J_{\mathrm{NC}}\varphi).$$

Proof. Since F and $a_{\mathrm{NC}}(u_{\mathrm{CR}}, \bullet)$ are linear, the discrete Lagrange multiplier λ_{CR} satisfies

$$\begin{aligned}
\int_\Omega \lambda_{\mathrm{CR}}\varphi\,\mathrm{d}x &= \int_\Omega \sum_{E\in\mathcal{E}(\Omega)} \Big(\big(F(\psi_E) - a_{\mathrm{NC}}(u_{\mathrm{CR}}, \psi_E)\big)/||\psi_E||^2_{L^2(\Omega)}\Psi_E\Big)\,\varphi\,\mathrm{d}x \\
&= F\left(\sum_{E\in\mathcal{E}(\Omega)} \int_\Omega \varphi\Psi_E\,\mathrm{d}x/||\psi_E||^2_{L^2(\Omega)}\psi_E\right) \\
&\quad - a_{\mathrm{NC}}\left(u_{\mathrm{CR}}, \sum_{E\in\mathcal{E}(\Omega)} \int_\Omega \varphi\Psi_E\,\mathrm{d}x/||\psi_E||^2_{L^2(\Omega)}\psi_E\right) \\
&= F(J_{\mathrm{NC}}\varphi) - a_{\mathrm{NC}}(u_{\mathrm{CR}}, J_{\mathrm{NC}}\varphi).
\end{aligned}$$

□

Proof of Theorem 3.38. Proposition 3.37 shows that $\|\!| \lambda_{\mathrm{CR}} - \lambda_{\mathrm{CR}}^- |\!\|_* \lesssim \|\!| \lambda - \lambda_{\mathrm{CR}} |\!\|_*$. Hence a triangle inequality shows that it remains to estimate $\|\!| \lambda - \lambda_{\mathrm{CR}} |\!\|_*$. Recall the conforming companion operator $J_3 := \mathrm{CR}_0^1(\mathcal{T}) \to P_3(\mathcal{T}) \cap C_0(\overline{\Omega})$ from Theorem

2.27. Given any $v \in H^1_0(\Omega)$ with $\|\!|v|\!\| = 1$, set $v_{\mathrm{CR}} := J_{\mathrm{NC}} v$ and define $v_3 = J_3 v_{\mathrm{CR}}$. Then

$$\int_\Omega (\lambda - \lambda_{\mathrm{CR}}) v \,\mathrm{d}x = \int_\Omega (v - v_3)\lambda \,\mathrm{d}x + \int_\Omega (\lambda v_3 - \lambda_{\mathrm{CR}} v) \,\mathrm{d}x =: ① + ②.$$

The first term satisfies

$$① = \int_\Omega \lambda (v - J_{\mathrm{NC}} v) \,\mathrm{d}x + \int_\Omega (J_{\mathrm{NC}} v - v_3)\lambda \,\mathrm{d}x.$$

Theorem 3.35.b and the integral mean property $\Pi_0(v_3 - J_{\mathrm{NC}} v) = 0$ lead to $① \lesssim \mathrm{osc}(\lambda, \mathcal{T})$. The properties of the continuous Lagrange multiplier λ and Lemma 3.39 yield

$$\begin{aligned} ② &= F(v_3 - I_{\mathrm{NC}} v_3) - a_{\mathrm{NC}}(u - u_{\mathrm{CR}}, v_3) \\ &= \int_\Omega (f - \Pi_0 f)(v_3 - I_{\mathrm{NC}} v_3) \,\mathrm{d}x - a_{\mathrm{NC}}(u - u_{\mathrm{CR}}, v_3). \end{aligned}$$

An interpolation error estimate (Brenner and Scott, 2008; Carstensen et al., 2012b) and the stability of the non-conforming interpolation operator I_{NC} show that

$$② \lesssim \|\!|u - u_{\mathrm{CR}}|\!\|_{\mathrm{NC}} + \mathrm{osc}(f, \mathcal{T})$$

The combination of the estimates of ① and ② conclude the proof. □

3.4.6. Comments on the complementary condition residual for NCFEM in the obstacle problem

This section analyzes the efficiency of the computable integral $\int_\Omega (-\lambda^-_{\mathrm{CR}})(v - \chi)_+ \,\mathrm{d}x$ of Est as a complementary condition residual for an affine obstacle $\chi \in P_1(\Omega)$. Theorem 3.40 proves the efficiency of the computable integral in Est in the sense of Theorem C and employs the following five subsets of $\mathcal{T}$,

$$\begin{aligned} \mathcal{T}_{FC} &:= \{T \in \mathcal{T} \mid u_{\mathrm{CR}} \equiv \chi \text{ in } \Omega_T\}; \\ \mathcal{T}_C &:= \{T \in \mathcal{T} \mid u_{\mathrm{CR}} \equiv \chi \text{ in } T \text{ but } u_{\mathrm{CR}} \not\equiv \chi \text{ in } \Omega_T\}; \\ \mathcal{T}_I &:= \{T \in \mathcal{T} \mid \exists E, F \in \mathcal{E}(T), (u_{\mathrm{CR}} - \chi)(\mathrm{mid}(E)) = 0 < (\chi - u_{\mathrm{CR}})(\mathrm{mid}(F))\}; \\ \mathcal{T}_{DB} &:= \{T \in \mathcal{T} \mid \exists E \in \mathcal{E}(T) \cap \mathcal{E}(\partial\Omega)\}; \\ \mathcal{T}_{CD} &:= \{T \in \mathcal{T} \mid \exists E \in \mathcal{E}(T) \cap \mathcal{E}(\Omega) \text{ such that } A = \mathcal{N}(E) \cap \mathcal{N}(\partial\Omega) \\ &\qquad \text{is a convex corner point}\}. \end{aligned}$$

In other words, $\mathcal{T}_{FC}$ describes elements T with contact in the entire patch Ω_T, $\mathcal{T}_C$ consists of triangles T where u_{CR} is in contact but is not in contact in the entire patch Ω_T, $\mathcal{T}_I$ are the triangles which are neither in contact nor in non-contact, $\mathcal{T}_{DB}$ contains triangles which have a boundary edge, and finally, $\mathcal{T}_{\mathrm{CB}}$ is the set of triangles which lie at convex corner points. Note that $|\mathcal{T}_{\mathrm{CB}}|$ can be bounded by a fixed number, which depends only on the initial triangulation.

The following theorem states the efficiency, in the sense of Theorem C, of the computable integral $\int_\Omega (-\lambda^-_{\mathrm{CR}})(v - \chi)_+ \,\mathrm{d}x$ in Est.

Theorem 3.40. *For $\chi \in P_1(\Omega)$ the function $v := w_D + u_{D2} + J_2(u_{\mathrm{CR}} - u_{D,\mathrm{NC}}) \in \mathcal{A}$*

from (3.34) *satisfies*

$$\int_\Omega (-\lambda_{\mathrm{CR}}^-)(v-\chi)_+ \,\mathrm{d}x \lesssim |\!|\!| u-u_{\mathrm{CR}} |\!|\!|_{\mathrm{NC}}^2 + |\!|\!| \lambda-\lambda_{\mathrm{CR}}^- |\!|\!|_*^2 + \sum_{T\in\mathcal{T}_{CD}} |\!|\!| u-\chi |\!|\!|_T^2$$
$$+\mathrm{Osc}(f,\mathcal{T}_I\cup\mathcal{T}_C)^2 + \sum_{T\in\mathcal{T}_I\cup\mathcal{T}_C} \mathrm{osc}(f,\mathcal{E}(\Omega_T))^2 + \sum_{T\in\mathcal{T}_{DB}} ||h_T f||_{L^2(T)}^2.$$

Corollary 3.41. *For $\chi\in P_1(\Omega)$ and $\mu=\lambda_{\mathrm{CR}}$, the guaranteed upper bound* $\mathrm{GUB}=30\mathrm{Est}$ *is efficient with respect to the energy error $|\!|\!| u-u_{\mathrm{CR}} |\!|\!|_{\mathrm{NC}}$ and the total error* Err *of Theorem 3.18 in the sense that*

$$|\!|\!| u-u_{\mathrm{CR}} |\!|\!|_{\mathrm{NC}} \le \mathrm{Err} + |\!|\!| u_{\mathrm{CR}}-v |\!|\!| \approx \mathrm{GUB} \lesssim |\!|\!| u-u_{\mathrm{CR}} |\!|\!| + \sum_{T\in\mathcal{T}_{CD}} |\!|\!| u-\chi |\!|\!|_T$$
$$+ \text{ higher-order terms.}$$

Proof. The proof follows from the combination of Theorem 3.18, 3.38, and 3.40. □

Remark 3.42. *The term $\sum_{T\in\mathcal{T}_{CD}} |\!|\!| u-\chi |\!|\!|_T$ only appears on a fixed number of elements and hence is at least of first-order. The higher-order terms are given by* $\mathrm{osc}(f,\mathcal{T})$, $\mathrm{osc}(f,\mathcal{E})$, *and* $\sqrt{\sum_{T\in\mathcal{T}_{DB}} ||h_T f||_{L^2(T)}^2}$.

The proof of Theorem 3.40 is based on the following lemma.

Lemma 3.43. *For an edge $E\in\mathcal{E}(\Omega)$ with at most one vertex $\{A\}=\mathcal{N}(E)\cap\mathcal{N}(\partial\Omega)$ at a non-convex corner point or at a part of a straight segment of $\partial\Omega$ any $v_{\mathrm{CR}}\in \mathrm{CR}^1(\mathcal{T})$ with $v_{\mathrm{CR}}(\mathrm{mid}(E))=0$ and $v_{\mathrm{CR}}(\mathrm{mid}(F))\ge 0$ for all $F\in\mathcal{E}(\Omega_E)$ satisfies*

$$h_E^{-1}||v_{\mathrm{CR}}||_{L^2(\Omega_E)} \lesssim \sqrt{\sum_{F\in\mathcal{E}(\Omega_E)} |F|\,|||[\nabla v_{\mathrm{CR}}]_F||_{L^2(F)}^2}. \tag{3.40}$$

The set $\mathcal{E}(\Omega_E)$ contains only the interior edges of Ω_E.

Proof. Observe that the left- and right-hand sides of (3.40) define semi-norms on $\mathrm{CR}^1(\mathcal{T}(\Omega_E))$. Given any $v_{\mathrm{CR}}\in\mathrm{CR}^1(\mathcal{T}(\Omega_E))$, $\sum_{F\in\mathcal{E}(\Omega_E)} |F|\,|||[\nabla v_{\mathrm{CR}}]_F||_{L^2(F)}^2=0$ implies $v_{\mathrm{CR}}\in P_1(\Omega_E)$. Since $v_{\mathrm{CR}}(\mathrm{mid}(E))=0$ and $v_{\mathrm{CR}}(\mathrm{mid}(F))\ge 0$ for all $F\in\mathcal{E}(\Omega_E)$, it follows $v_{\mathrm{CR}}\equiv\chi$. A compactness argument, as in the proof of the equivalence of norms, shows that (3.40) holds in the cone of all such v_{CR}. A scaling argument shows that the constants hidden in $\lesssim$ solely depend on the shape of $\mathcal{T}(\Omega_E)$ and $\mathcal{T}(\Omega(E))$ but not on the mesh-size. □

Remark 3.44. *In case of homogeneous boundary conditions the case that $E\in\mathcal{E}(\Omega)$ has a node $A:=\mathcal{N}(E)\cap\mathcal{N}(\partial\Omega)$ at a convex corner point can also be treated. In this case, assume, that the triangulation $\mathcal{T}$ is not too coarse at convex corner points, i.e., each node at a convex corner point has two adjoining edges $F_1,F_2\in\mathcal{E}(\partial\Omega)$ on a straight line. Then E has a neighbourhood $\Omega(E)$ with $\Omega_E\subseteq\Omega(E)\subseteq\Omega_E^{(2)}$, such that any $v_{\mathrm{CR}}\in K_{\mathrm{CR}}(\mathcal{T})$ with $v_{\mathrm{CR}}(\mathrm{mid}(E))=⨍_E \chi\mathrm{d}s$ satisfies*

$$h_E^{-1}||v_{\mathrm{CR}}-\chi||_{L^2(\Omega(E))} \lesssim \sqrt{\sum_{F\in\mathcal{E}(\Omega(E))} |F|\,|||[\nabla v_{\mathrm{CR}}]_F||_{L^2(F)}^2}.$$

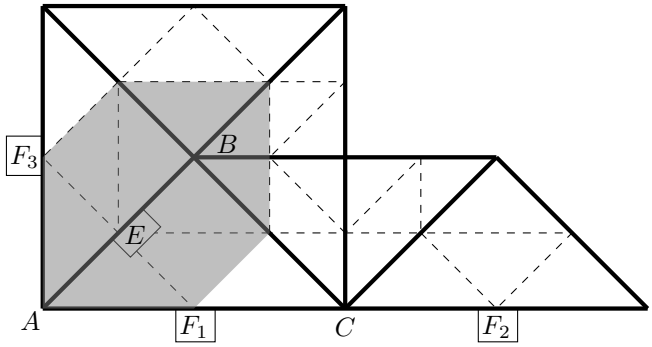

Figure 3.3.: Design of enlarged patch $\Omega(E)$ and its red-refinement.

Proof. *The situation described above is depicted in Figure 3.3. Recall that next to the vertex A there are two boundary edges F_1, F_2 on a straight line. In the situation of Figure 3.3 define* $\Omega(E) := \Omega_E \cup \omega_C$. *Suppose that* $v_{\mathrm{CR}} \in K_{\mathrm{CR}}(\mathcal{T})$ *satisfies* $v_{\mathrm{CR}}(\mathrm{mid}(E))) = \fint_E \chi \mathrm{d}s$ *and* $\rho_2(v_{\mathrm{CR}}) := \sqrt{\sum_{F\in\mathcal{E}(\Omega(E))} |F|\,||[\nabla_{\mathrm{NC}} v_{\mathrm{CR}}]_F||^2_{L^2(F)}} = 0$. *Then* $v_{\mathrm{CR}} \in P_1(\Omega(E))$ *and the boundary conditions at* $\mathrm{mid}(F_j)$ *for* $j = 1, 2, 3$ *imply* $v_{\mathrm{CR}} \equiv 0$ *in* $\Omega(E)$. *The affine function* $v_{\mathrm{CR}} - \chi \equiv -\chi \geq 0$ *is non-negative at all vertices of the patch* $\omega_M^* := \mathrm{conv}\{\mathrm{mid}(\mathcal{E}(\Omega_E)), A\}$ *of* $M = \mathrm{mid}(E)$ *in the red-refined triangulation* $\mathrm{red}(\mathcal{T})$ *depicted in Figure 3.3 as a shaded region. Since* $\chi \leq 0$ *in* ω_M^* *but vanishes at the interior point* $M = \mathrm{mid}(E)$, *the affine function* χ *vanishes on* ω_M^* *and hence also on* $\Omega(E)$. *Consequently* $\rho_1(v_{\mathrm{CR}}) := ||v_{\mathrm{CR}} - \chi||_{L^2(\Omega(E))} = 0$. *An inverse estimate argument implies* $\rho_1(v_{\mathrm{CR}}) \lesssim \rho_2(v_{\mathrm{CR}})$ *for all* $v_{\mathrm{CR}} \in K_{\mathrm{CR}}(\mathcal{T})$ *with* $v_{\mathrm{CR}}(M) = 0$. *A scaling argument shows that the constants hidden in* $\lesssim$ *solely depend on the shape of* $\mathcal{T}(\Omega_E)$ *but not on the mesh-size.* □

Proof of Theorem 3.40. The proof follows from *Claim 1–4* below.
Claim 1. Recall that for all $T \in \mathcal{T}_I$, there exists and edge $E_T \in \mathcal{E}(T)$ with $(u_{\mathrm{CR}} - \chi)(\mathrm{mid}(E)) = 0$ and define $\eta^2(\Omega(E_T)) := \sum_{F\in\mathcal{E}(\Omega(E_T))} |F|\,||[\nabla u_{\mathrm{CR}}]_F||^2_{L^2(F)}$. Then it holds

$$\begin{aligned}
\int_\Omega (-\lambda^-_{\mathrm{CR}})(v-\chi)_+ \,\mathrm{d}x \lesssim{}& \sum_{T\in\mathcal{T}_C\setminus\mathcal{T}_{FC}} ||h_T\lambda^-_{\mathrm{CR}}||_{L^2(T)}\Big(|\!|\!|v-u_{\mathrm{CR}}|\!|\!|_{\mathrm{NC}(T)} + |\!|\!|u-\chi|\!|\!|_T\Big)\\
&+ \sum_{T\in(\mathcal{T}_I\setminus\mathcal{T}_{CD})\setminus\mathcal{T}_{DB}} ||h_T^2\nabla_{\mathrm{NC}}\lambda^-_{\mathrm{CR}}||_{L^2(T)}\Big(|\!|\!|v-u_{\mathrm{CR}}|\!|\!|_{\mathrm{NC}(T)} + \eta(\Omega(E_T))\Big)\\
&+ \sum_{T\in(\mathcal{T}_I\setminus\mathcal{T}_{\mathrm{CD}})\cap\mathcal{T}_{DB}} ||h_T\lambda^-_{\mathrm{CR}}||_{L^2(T)}\Big(|\!|\!|v-u_{\mathrm{CR}}|\!|\!|_{\mathrm{NC}(T)} + \eta(\Omega(E_T))\Big)\\
&+ \sum_{T\in(\mathcal{T}_I\cap\mathcal{T}_{\mathrm{CD}})\setminus\mathcal{T}_{DB}} ||h_T^2\nabla_{\mathrm{NC}}\lambda^-_{\mathrm{CR}}||_{L^2(T)}\Big(|\!|\!|v-u_{\mathrm{CR}}|\!|\!|_{\mathrm{NC}(T)}\\
&\qquad + |\!|\!|u_{\mathrm{CR}}-u|\!|\!|_{\mathrm{NC}(T)} + |\!|\!|u-\chi|\!|\!|_T\Big)
\end{aligned}$$

$$+ \sum_{T\in(\mathcal{T}_I\cap\mathcal{T}_{\mathrm{CD}})\cap\mathcal{T}_{DB}} ||h_T\lambda_{\mathrm{CR}}^-||_{L^2(T)}\Big(|\!|\!|v-u_{\mathrm{CR}}|\!|\!|_{\mathrm{NC}(T)} + |\!|\!|u_{\mathrm{CR}}-u|\!|\!|_{\mathrm{NC}(T)}\Big).$$

Proof. Fix $T\in\mathcal{T}$ and analyze the integral $I := \int_T(-\lambda_{\mathrm{CR}}^-)(v-\chi)_+\,\mathrm{d}x$.
If $\lambda_{\mathrm{CR}}^-\equiv 0$ in T then $I=0$. If $u_{\mathrm{CR}}\equiv\chi$ in Ω_T, then $u_{\mathrm{CR}}=v_2=\chi$ in T and a Cauchy and Friedrichs inequality show $I\lesssim ||h_T\lambda_{\mathrm{CR}}||_{L^2(T)}|\!|\!|w_D|\!|\!|_T$ for $T\in\mathcal{T}_{FC}\cap\mathcal{T}_{DB}$ and zero otherwise. If $T\in\mathcal{T}_C$, the definition of v with $I_{\mathrm{NC}}v=u_{\mathrm{CR}}=\chi$ in T, a Cauchy inequality, and a subsequent interpolation error estimate yield

$$I\le ||\lambda_{\mathrm{CR}}^-||_{L^2(T)}||v-\chi||_{L^2(T)}\lesssim ||h_T\lambda_{\mathrm{CR}}^-||_{L^2(T)}|\!|\!|v-I_{\mathrm{NC}}v|\!|\!|_{\mathrm{NC}(T)}.$$

In all remaining cases, $u_{\mathrm{CR}}\not\equiv\chi$ in T as well as $\lambda_{\mathrm{CR}}^-\not\equiv 0$ in T. A triangle inequality and an interpolation error estimate show

$$I\lesssim ||\lambda_{\mathrm{CR}}^-||_{L^2(T)}\left(h_T|\!|\!|v-I_{\mathrm{NC}}v|\!|\!|_{\mathrm{NC}(T)} + ||u_{\mathrm{CR}}-\chi||_{L^2(T)}\right).$$

For a triangle $T\in\mathcal{T}_I\setminus\mathcal{T}_{CD}$, Lemma 3.43 shows

$$h_T^{-2}||u_{\mathrm{CR}}-\chi||_{L^2(T)}^2\lesssim\sum_{F\in\mathcal{E}(\Omega(E_T))}|F|\,||[\nabla u_{\mathrm{CR}}]_F||_{L^2(F)}^2.$$

For $T\in\mathcal{T}_{CD}$, a Friedrichs inequality and a triangle inequality show

$$||u_{\mathrm{CR}}-\chi||_{L^2(T)}\le h_T(|\!|\!|u_{\mathrm{CR}}-u|\!|\!|_{\mathrm{NC}(T)}+|\!|\!|u-\chi|\!|\!|_T).$$

Recall, that for $T\in\mathcal{T}_I$, the edges E_T and F_T with $(u_{\mathrm{CR}}-\chi)(\mathrm{mid}(E_T))=0<(u_{\mathrm{CR}}-\chi)(\mathrm{mid}(F_T))$ are preferably chosen as interior edges. If E_T cannot be chosen as an interior edge, it follows that $(u_{\mathrm{CR}}-\chi)(\mathrm{mid}(F))>0$ for all $F\in\mathcal{E}(T)\setminus E_T$ and hence $\lambda_{\mathrm{CR}}=0$ in T. If F_T can be chosen as an interior edge, a Friedrichs inequality shows $||\lambda_{\mathrm{CR}}||_{L^2(T)}\le||h_T\nabla\lambda_{\mathrm{CR}}||_{L^2(T)}$. The combination of all estimates for I concludes the proof of *Claim 1.* □

Claim 2. For $T\in\mathcal{T}$ and $\eta(T)^2:=\sum_{E\in\mathcal{E}(T)\cap\mathcal{E}(\Omega)}|E|\,||[\nabla u_{\mathrm{CR}}\cdot\nu_E]_E||_{L^2(E)}^2$ it holds

$$\text{ⓐ } h_T||\lambda_{\mathrm{CR}}^-||_{L^2(T)}\lesssim||h_Tf||_{L^2(\Omega_T)}+\eta(T);$$
$$\text{ⓑ } h_T^2||\nabla\lambda_{\mathrm{CR}}^-||_{L^2(T)}\lesssim\mathrm{Osc}(f,T)+\eta(T).$$

Proof. For all $T\in\mathcal{T}$ it holds that $||\lambda_{\mathrm{CR}}^-||_{L^2(T)}\le||\lambda_{\mathrm{CR}}||_{L^2(T)}$. Since the edge-oriented basis functions $(\psi_E)_{E\in\mathcal{E}}$ are orthogonal in two dimensions the definition of λ_{CR} in (3.37) shows

$$||h_{\mathcal{T}}\lambda_{\mathrm{CR}}||^2\lesssim\sum_{E\in\mathcal{E}(\Omega)}\sigma_{\mathrm{CR}}(\psi_E)^2\lesssim\sum_{E\in\mathcal{E}(\Omega)}F(\psi_E)^2+\sum_{E\in\mathcal{E}(\Omega)}a_{\mathrm{NC}}(u_{\mathrm{CR}},\psi_E)^2.$$

A Cauchy inequality and a piecewise integration by parts lead to

$$F(\psi_E)\lesssim||h_Tf||_{L^2(T)}\quad\text{and}\quad a_{\mathrm{NC}}(u_{\mathrm{CR}},\psi_E)^2\lesssim|E|\,||[\nabla u_{\mathrm{CR}}\cdot\nu_E]_E||_{L^2(E)}^2.\tag{3.41}$$

The combination of the aforementioned estimates concludes the proof of ⓐ.

For all $T\in\mathcal{T}$, the proof of ⓑ follows the arguments in the proof of *Claim 2* of Theorem 3.29. A triangle inequality shows

$$||\nabla\lambda_{\mathrm{CR}}||_{L^2(T)}\le\Big\|\sum_{E\in\mathcal{E}(T)\cap\mathcal{E}(\Omega)}F(\psi_E)\nabla\Psi_E/||\psi_E||_{L^2(\omega_E)}^2\Big\|_{L^2(T)}$$

$$+\Big\| \sum_{E\in\mathcal{E}(T)\cap\mathcal{E}(\Omega)} a_{\mathrm{NC}}(u_{\mathrm{CR}},\psi_E)\nabla\Psi_E/||\psi_E||^2_{L^2(\omega_E)}\Big\|_{L^2(T)} = ① + ②.$$

Recall that $\{\Psi_E \mid E\in\mathcal{E}(T)\cap\mathcal{E}(\Omega)\}$ is a partition of unity on the triangle $T\in\mathcal{T}$. Then it follows

$$\begin{aligned} ① &= \Big\| \sum_{E\in\mathcal{E}(T)\cap\mathcal{E}(\Omega)} \int_\Omega (f - \fint_{\Omega_T} f\,\mathrm{d}x)\psi_E\,\mathrm{d}x/||\psi_E||^2_{L^2(\omega_E)}\nabla\Psi_E\Big\|_{L^2(T)} \\ &\le ||f - \fint_{\Omega_T} f\,\mathrm{d}x||_{L^2(\Omega_T)} \sum_{E\in\mathcal{E}(T)\cap\mathcal{E}(\Omega)} ||\nabla\Psi_E||_{L^2(\omega(E))}/||\psi_E||_{L^2(\omega_E)} \end{aligned}$$

Since $||\nabla\Psi_E||_{L^2(\omega(E))}\approx 1$, it holds $h_T^2① \lesssim \mathrm{osc}(f,\Omega_T)$.
For the second term, an integration by parts and $||\nabla\Psi_E||_{L^2(\omega(E))}\approx 1$ yield

$$② \lesssim \sum_{E\in\mathcal{E}(T)\cap\mathcal{E}(\Omega)} \int_E [\nabla u_{\mathrm{CR}}\cdot\nu_E]\psi_E\mathrm{d}s/||\psi_E||^2_{L^2(\omega_E)}.$$

A Cauchy inequality and the multiplication with the mesh size leads to $h_T^2② \lesssim \eta(T)$. The combination of the two estimates concludes the proof of *Claim 2.b.* □

Claim 3. For each $T\in\mathcal{T}$ and $E\in\mathcal{E}(\Omega)$ it holds

ⓐ $||h_T(f-\lambda_{\mathrm{CR}})||_{L^2(T)} \lesssim |\!|\!|u-u_{\mathrm{CR}}|\!|\!|_{\mathrm{NC}(T)} + |\!|\!|\lambda-\lambda_{\mathrm{CR}}|\!|\!|_{*,T} + \mathrm{osc}(f,\mathcal{T})$;

ⓑ $|E|^{1/2}\,||[\nabla u_{\mathrm{CR}}]_E||_{L^2(E)} \lesssim |\!|\!|u-u_{\mathrm{CR}}|\!|\!|_{\mathrm{NC}(\omega_E)} + |\!|\!|\lambda-\lambda_{\mathrm{CR}}|\!|\!|_{*,\omega_E} + \mathrm{osc}(f,\mathcal{T}(\omega_E))$.

Proof. The proof of ⓐ follows the arguments of Verfürth (1996) for the linear case as described in the proof of Claim 3 in the proof of Theorem 3.29. The technique is adapted to the non-conforming FEM as described in Braess (2009, Lem. 1).
To prove ⓑ, the jump over the gradient is split into the normal and the tangential component. On both components the arguments of Verfürth (1996) apply as described in the proof of Claim 3 in the proof of Theorem 3.29. The adaptation to non-conforming NCFEM in Braess (2009, Lem. 1) allows the application of this technique to the Crouzeix-Raviart FEM and concludes the proof of *Claim 3.* □

Claim 4. For all $T\in\mathcal{T}_C\setminus\mathcal{T}_{FC}$, it holds

$$||h_T f||_{L^2(\Omega_T)} \lesssim |\!|\!|u-u_{\mathrm{CR}}|\!|\!|_{\mathrm{NC}(\Omega_T)} + |\!|\!|\lambda-\lambda_{\mathrm{CR}}|\!|\!|_{*,\Omega_T} + \mathrm{Osc}(f,T) + \mathrm{osc}(f,\mathcal{E}(\Omega_T)).$$

Proof. Since $T\in\mathcal{T}_C\setminus\mathcal{T}_{FC}$, there exists $E\in\mathcal{E}(\Omega_T)\cap\mathcal{E}(\Omega)$ with $\lambda_{\mathrm{CR}}(\mathrm{mid}(E))=0$. The shape-regularity of the triangulation, the finite overlap, and a triangle inequality yield

$$\begin{aligned} ||h_T f||_{L^2(\Omega_T)} \lesssim & ||h_{\mathcal{T}}(f - \fint_{\Omega_T} f\,\mathrm{d}x)||_{L^2(\Omega_T)} + ||h_E(f-\fint_{\omega_E} f\,\mathrm{d}x)||_{L^2(\omega_E)} \\ & + |\omega_E|^{1/2}||\fint_{\omega_E} f\,\mathrm{d}x||_{L^2(\omega_E)}. \end{aligned}$$

The definition of the edge-oriented basis function ψ_E shows

$$|\omega_E|^{1/2}||\fint_{\omega_E} f\,\mathrm{d}x||_{L^2(\omega_E)} \approx \int_{\omega_E}(\fint_{\omega_E} f\,\mathrm{d}x - f)\psi_E\,\mathrm{d}x + F(\psi_E)$$

$$\lesssim |\omega_E|^{1/2} ||(f - \fint_{\omega_E} f \,\mathrm{d}x)||_{L^2(\omega_E)} + F(\psi_E).$$

Since $\lambda_{\mathrm{CR}}(\mathrm{mid}(E)) = 0$, the complementary conditions and (3.41) lead to

$$|F(\psi_E)| = |a_{\mathrm{NC}}(u_{\mathrm{CR}}, \psi_E)| \lesssim |E|^{1/2} ||[\nabla u_{\mathrm{CR}} \cdot \nu_E]_E||_{L^2(E)}.$$

This, *Claim 3*, and the definition of the oscillations in (2.8) conclude the proof of *Claim 4*. □

The combination of the four claims concludes the proof of Theorem 3.40. □

3.5. Mixed FEM for the obstacle problem

This section is devoted to the lowest-order mixed Raviart-Thomas finite element method (MFEM) for the obstacle problem in two space dimensions. As in the linear case (cf. Marini, 1985; Ainsworth, 2007) there is a strong connection between the non-conforming Crouzeix-Raviart NCFEM and the mixed Raviart-Thomas MFEM. This section clarifies this connection in the case of the non-linear obstacle problem. The section introduces a discrete Lagrange multiplier $\lambda_{\mathrm{RT}} \in P_0(\mathcal{T}; (-\infty, 0])$ and shows its efficiency in the sense of Theorem B. Furthermore, the section analyzes the computable integral $\int (-\lambda_{\mathrm{RT}})(v - \chi)_+ \,\mathrm{d}x$ in Est in the sense of Theorem C for some conforming companion $v \in V$. The results of this section are restricted to Dirichlet boundary conditions $u_D \in H^1(\Omega)$, an obstacle $\chi \in H^1(\Omega)$ with $\chi \leq u_D$ along $\partial\Omega$ and $\Delta\chi \in L^2(\Omega)$, and $f \in L^2(\Omega)$ and the resulting regularity with $\Delta u \in L^2(\Omega)$.

3.5.1. Mixed discretization

Given a shape-regular triangulation $\mathcal{T}$ of $\Omega \subset \mathbb{R}^2$ from Subsection 2.2.1 on Page 11, recall the Raviart-Thomas finite element space $\mathrm{RT}_0(\mathcal{T})$ from Definition 2.15 on Page 15 and define $\mathcal{M}_0$ by

$$\mathcal{M}_0 := P_0(\mathcal{T}; [0,\ \infty)) \subseteq L^2(\Omega; [0, \infty)).$$

The discrete mixed formulation utilizes the bilinear and linear forms b, H, and G from (3.6) on Page 23. Then the mixed Raviart Thomas MFEM seeks $(p_{\mathrm{RT}}, w_0) \in \mathrm{RT}_0(\mathcal{T}) \times \mathcal{M}_0$ such that

$$\int_\Omega p_{\mathrm{RT}} \cdot q_{\mathrm{RT}} \,\mathrm{d}x + b(q_{\mathrm{RT}}, w_0) = H(q_{\mathrm{RT}}) \quad \text{for all } q_{\mathrm{RT}} \in \mathrm{RT}_0(\mathcal{T}); \tag{3.42}$$

$$b(p_{\mathrm{RT}}, v_0 - w_0) \leq G(v_0 - w_0) \quad \text{for all } v_0 \in \mathcal{M}_0. \tag{3.43}$$

Lemma 3.45 (existence of solutions)**.** *There exists a unique solution* $(p_{\mathrm{RT}}, w_0) \in \mathrm{RT}_0(\mathcal{T}) \times \mathcal{M}_0$ *to* (3.42)–(3.43).

Proof. The spaces $\mathrm{RT}_0(\mathcal{T})$ and $P_0(\mathcal{T})$ satisfy the following, well-known, inf sup condition

$$0 < \beta_h \leq \inf_{v_0 \in P_0(\mathcal{T}) \setminus \{0\}} \sup_{q_{\mathrm{RT}} \in \mathrm{RT}_0(\mathcal{T}) \setminus \{0\}} \frac{b(v_0, q_{\mathrm{RT}})}{||v_0||_{L^2(\Omega)} ||q_{\mathrm{RT}}||_{H(\mathrm{div},\Omega)}}.$$

Since $\mathcal{M}_0 = P_0(\mathcal{T}; [0,\infty)) \subset P_0(\mathcal{T})$, the inf sup condition also holds for $\mathcal{M}_0$. Hence Theorem 4.4 in Brezzi et al. (1978) shows the unique existence of a discrete solution $(p_{\mathrm{RT}}, w_0) \in \mathrm{RT}_0(\mathcal{T}) \times \mathcal{M}_0$ and concludes the proof. □

Lemma 3.46 (discrete complementary conditions)**.** *The discrete mixed solution* $(p_{\mathrm{RT}}, w_0) \in \mathrm{RT}_0(\mathcal{T}) \times \mathcal{M}_0$ *satisfies the following discrete complementary conditions*

$$0 \le w_0 \perp \lambda_{\mathrm{RT}} := \Pi_0 f + \operatorname{div} p_{\mathrm{RT}} \le 0. \tag{3.44}$$

Proof. The first inequality follows form the definition of $\mathcal{M}_0$. To show the second inequality, let $\varphi_0 \in \mathcal{M}_0$ and define $v_0 = w_0 + \varphi_0 \in \mathcal{M}_0$. Then (3.43) shows

$$\int_\Omega (\operatorname{div} p_{\mathrm{RT}} + \Pi_0 f)\varphi_0 \,\mathrm{d}x \le 0 \quad \text{for all } \varphi_0 \in \mathcal{M}_0.$$

To show the orthogonality, consider the test functions $v_0 = 0$ and $v_0 = 2w_0$ in $\mathcal{M}_0$. Then (3.43) leads to

$$\pm \int_\Omega (\operatorname{div} p_{\mathrm{RT}} + \Pi_0 f) w_0 \,\mathrm{d}x \le 0$$

and hence the orthogonality follows. □

Notice that the piecewise constant variable w_0 from (3.42)–(3.43) approximates $u - \chi$ rather than u.

3.5.2. Efficiency of the discrete Lagrange multiplier for MFEM

Recall the solution $u \in K$ to (3.2) and Λ from (3.3) with L^2 representation $\lambda = \Delta u + f \in L^2(\Omega; (-\infty, 0])$. The subsequent theorem shows, that the Lagrange multiplier λ_{RT} from (3.44) is efficient in the sense of Theorem B.

Theorem 3.47 (efficiency)**.** *The discrete solution* $p_{\mathrm{RT}} \in \mathrm{RT}_0(\mathcal{T})$ *to* (3.42)–(3.43) *and* $\lambda_{\mathrm{RT}} := \operatorname{div} p_{\mathrm{RT}} + \Pi_0 f$ *from* (3.44) *satisfy*

$$|\!|\!| \lambda - \lambda_{\mathrm{RT}} |\!|\!|_* \le \operatorname{osc}(f, \mathcal{T})/j_{1,1} + ||\nabla u - p_{\mathrm{RT}}||.$$

where $j_{1,1} \ge 3.8317$ *is the smallest positive root of the Bessel function of the first kind.*

Proof. Any $\varphi \in H^1_0(\Omega)$ with $|\!|\!|\varphi|\!|\!| = 1$ satisfies

$$\begin{aligned}\int_\Omega (\lambda - \lambda_{\mathrm{RT}})\varphi \,\mathrm{d}x &= \int_\Omega (\lambda - \operatorname{div} p_{\mathrm{RT}} - \Pi_0 f)\varphi \,\mathrm{d}x \\ &= \int_\Omega (f - \Pi_0 f)\varphi \,\mathrm{d}x + \int_\Omega (\Delta u + \operatorname{div} p_{\mathrm{RT}})\varphi \,\mathrm{d}x.\end{aligned}$$

A piecewise Poincaré inequality with the constant $1/j_{1,1}$ from Laugesen and Siudeja (2010) in the first term shows

$$\int_\Omega (f - \Pi_0 f)\varphi \,\mathrm{d}x = \int_\Omega (f - \Pi_0 f)(\varphi - \Pi_0 \varphi) \le \operatorname{osc}(f, \mathcal{T})/j_{1,1}.$$

An integration by parts in the second term proves

$$\int_\Omega (\Delta u + \operatorname{div} p_{\mathrm{RT}})\varphi \,\mathrm{d}x = -\int_\Omega (\nabla u - p_{\mathrm{RT}}) \cdot \nabla \varphi \,\mathrm{d}x \le ||\nabla u - p_{\mathrm{RT}}||.$$

The combination of the displayed estimates concludes the proof. □

3.5.3. Representation by NCFEM

This section presents a non-conforming Crouzeix-Raviart representation of the discrete mixed solution $(p_{\mathrm{RT}}, w_0) \in \mathrm{RT}_0(\mathcal{T}) \times \mathcal{M}_0$ to (3.42)–(3.43) and so generalizes the results in Ainsworth (2007) and Marini (1985) to the obstacle problem. Define $s(\mathcal{T}) \in P_0(\mathcal{T})$ by $s(\mathcal{T})|_T := ||\bullet - \mathrm{mid}(T)||^2_{L^2(T)}/(4|T|)$ for $T \in \mathcal{T}$.

Proposition 3.48. ⓐ *For any $q_{\mathrm{RT}} \in \mathrm{RT}_0(\mathcal{T})$ there exists a unique $\tilde{w}_{\mathrm{CR}} \in \mathcal{A}_{\mathrm{NC}}(T)$ such that*

$$q_{\mathrm{RT}} = \nabla_{\mathrm{NC}} \tilde{w}_{\mathrm{CR}} + \operatorname{div} q_{\mathrm{RT}}/2(\bullet - \mathrm{mid}(\mathcal{T})).$$

ⓑ *The Crouzeix-Raviart function $\tilde{u}_{\mathrm{CR}} \in \mathcal{A}_{\mathrm{NC}}(T)$ from ⓐ satisfies*

$$w_0 = \Pi_0(\tilde{u}_{\mathrm{CR}} - \chi) - s(\mathcal{T}) \operatorname{div} p_{\mathrm{RT}}.$$

ⓒ *The function $v_2 \in P_2(\mathcal{T})$,*

$$v_2|_T := \tilde{u}_{\mathrm{CR}} + 1/2 \operatorname{div} p_{\mathrm{RT}}(|\bullet - \mathrm{mid}(T)|^2/2 - ||\bullet - \mathrm{mid}(T)||^2_{L^2(T)}/|T|) \text{ for } T \in \mathcal{T},$$

with $\tilde{u}_{\mathrm{CR}}$ from ⓐ satisfies $I_{\mathrm{NC}} v_2 = \tilde{u}_{\mathrm{CR}}$, $\Pi_0 v_2 = \Pi_0 \tilde{u}_{\mathrm{CR}} - s(\mathcal{T}) \operatorname{div} p_{\mathrm{RT}}$, and $\nabla_{\mathrm{NC}} v_2 = p_{\mathrm{RT}}$.

Proof. The proof of ⓐ follows from Marini (1985), with the substitution of $\Pi_0 f$ by $-\operatorname{div} p_{\mathrm{RT}}$ and a straightforward adaptation to the boundary conditions at hand. □

To prove ⓑ, an integration by parts, with a careful consideration of the boundary terms, yields

$$\sum_{T\in\mathcal{T}} \int_T \nabla \tilde{u}_{\mathrm{CR}} \cdot q_{\mathrm{RT}} \,\mathrm{d}x = -\sum_{T\in\mathcal{T}} \left(\int_T \tilde{u}_{\mathrm{CR}} \operatorname{div} q_{\mathrm{RT}} \,\mathrm{d}x + \int_{\partial T} \tilde{u}_{\mathrm{CR}} q_{\mathrm{RT}} \cdot \nu_T \,\mathrm{d}s \right) \quad (3.45)$$

for all $q_{\mathrm{RT}} \in \mathrm{RT}_0(\mathcal{T})$. Since $\tilde{u}_{\mathrm{CR}}$ is continuous on $\mathrm{mid}(E)$ for all $E \in \mathcal{E}(\Omega)$ and the jump $[q_{\mathrm{RT}} \cdot \nu_E]_E = 0$ for all $E \in \mathcal{E}(\Omega)$, the boundary terms simplify to

$$\sum_{T\in\mathcal{T}} \int_{\partial T} \tilde{u}_{\mathrm{CR}} q_{\mathrm{RT}} \cdot \nu_T \,\mathrm{d}s = \sum_{E\in\mathcal{E}(\partial\Omega)} \int_E u_{D,\mathrm{NC}} q_{\mathrm{RT}} \cdot \nu_E \,\mathrm{d}s.$$

Since any $q_{\mathrm{RT}} \in \mathrm{RT}_0(\mathcal{T})$ satisfies

$$q_{\mathrm{RT}} = \Pi_0 q_{\mathrm{RT}} + \operatorname{div} q_{\mathrm{RT}}/2(\bullet - \mathrm{mid}(\mathcal{T})),$$

the definition of $\tilde{u}_{\mathrm{CR}}$ and (3.45) lead to

$$\int_\Omega p_{\mathrm{RT}} \cdot q_{\mathrm{RT}} \,\mathrm{d}x = \int_\Omega (s(\mathcal{T}) \operatorname{div} p_{\mathrm{RT}} - \tilde{u}_{\mathrm{CR}}) \operatorname{div} q_{\mathrm{RT}} \,\mathrm{d}x + \sum_{E\in\mathcal{E}(\partial\Omega)} \int_E u_D p_{\mathrm{RT}} \cdot \nu_E \,\mathrm{d}s.$$

This and (3.42) show

$$b(q_{\mathrm{RT}}, w_0) = H(q_{\mathrm{RT}}) - \int_\Omega p_{\mathrm{RT}} \cdot q_{\mathrm{RT}} \,\mathrm{d}x = \int_\Omega (\tilde{u}_{\mathrm{CR}} - \chi - s(\mathcal{T}) \operatorname{div} p_{\mathrm{RT}}) \operatorname{div} q_{\mathrm{RT}} \,\mathrm{d}x.$$

Since the divergence operator $\operatorname{div} : \mathrm{RT}_0(\mathcal{T}) \to P_0(\mathcal{T})$ is surjective, this proves ⓑ.□

Proposition 3.48.a and the arguments in Ainsworth (2007) prove ⓒ. □

Since v_2 from Proposition 3.48.c is not an H^1 function in general, recall u_{D2} from (3.33) and define v as a piecewise quadratic and globally continuous function $v \in P_2(\mathcal{T}) \cap C(\overline{\Omega})$ (cf. Ainsworth (2007)) given by the nodal values

$$v_2(z) := \begin{cases} \left(\sum_{T\in\mathcal{T}(\omega_z)} v_2|_T(z)\right)/|\mathcal{T}(z)| & \text{for } z \in \mathcal{N}(\Omega) \cup \operatorname{mid}(\mathcal{E}(\Omega)), \\ u_{D2}(z) & \text{for } z \in \mathcal{N}(\partial\Omega) \cup \operatorname{mid}(\mathcal{E}(\partial\Omega)) \end{cases}$$

(recall the number $|\mathcal{T}(z)|$ of triangles with vertex z of the patch ω_z from Subsection 2.2.1 on Page 11; $|\mathcal{T}(z)| = 2$ and $\omega_z = \omega_E$ for $z \in \operatorname{mid}(\mathcal{E})$). The conforming companion $v \in \mathcal{A}$ is then given by

$$v := v_2 + w_D$$

for w_D from Theorem 2.28 with $w_D|_{\partial\Omega} = (u_D - u_{D2})|_{\partial\Omega}$.

3.5.4. Comments on the complementary condition residual for MFEM in the obstacle problem

This section analyzes the efficiency of the computable integral $\int_\Omega(-\lambda_{\mathrm{RT}})(v-\chi)_+ \,\mathrm{d}x$ in Est for an affine obstacle $\chi \in P_1(\Omega)$. The integral in Est is a complementary conditions residual.

Theorem 3.49. *For an affine obstacle $\chi \in P_1(\Omega)$ it holds*

$$\int_\Omega (-\lambda_{\mathrm{RT}})(v-\chi)_+ \,\mathrm{d}x \lesssim |\!|\!| \lambda - \lambda_{\mathrm{RT}} |\!|\!|_*^2 + |\!|\!| v - v_2 |\!|\!|_{\mathrm{NC}}^2 + |\!|\!| v_2 - I_{\mathrm{NC}} v_2 |\!|\!|_{\mathrm{NC}}^2 + ||h_{\mathcal{T}} f||^2.$$

Corollary 3.50. *For $\chi \in P_1(\Omega)$ and $\mu = \lambda_{\mathrm{RT}}$ the guaranteed upper bound* $\mathrm{GUB} = 30\mathrm{Est}$ *is efficient with respect to the error $||\nabla u - p_{\mathrm{RT}}||_{L^2(\Omega)}$ and the total error* Err *of Theorem 3.18 in the sense that*

$$\begin{aligned} ||\nabla u - p_{\mathrm{RT}}||_{L^2(\Omega)} &\le \mathrm{Err} + ||p_{\mathrm{RT}} - \nabla v||_{L^2(\Omega)} \approx \mathrm{GUB} + ||p_{\mathrm{RT}} - \nabla v||_{L^2(\Omega)} \\ &\lesssim |\!|\!| u - \tilde{u}_{\mathrm{CR}} |\!|\!| + \text{ first-order terms.} \end{aligned}$$

Proof. The proof follows from Theorem 3.18 and Theorem 3.47 and 3.49. □

Remark 3.51. *The upper bounds in Theorem 3.49 allow the sharp first order of convergence. In case of singular solutions and quasi-uniform meshes, the term $||h_{\mathcal{T}} f||$ is even of higher order.*

The proof of Theorem 3.49 is based on the following lemma.

Lemma 3.52. *Suppose the function $v \in P_2(\mathcal{T})$ satisfies $v(z) \ge 0$ for all $z \in \mathcal{N}(\partial\Omega)$, $v(\operatorname{mid}(E)) \ge 0$ for all $E \in \mathcal{E}(\partial\Omega)$, $\nabla_{\mathrm{NC}} v \in \mathrm{RT}_0(\mathcal{T})$, $\Pi_0 v \ge 0$, and $⨍_T v \,\mathrm{d}x = 0$ for some $T \in \mathcal{T}$ with Ω_T from Subsection 2.2.1 on Page 11. Then it holds*

$$||v||_{L^2(T)} \lesssim h_T \min_{\varphi\in H^1(\Omega_T)} |\!|\!| v - \varphi |\!|\!|_{\Omega_T} + h_T^2 ||\operatorname{div} \nabla_{\mathrm{NC}} v||_{L^2(\Omega_T)}. \tag{3.46}$$

Proof. The left- and right-hand side of (3.46) define semi-norms for all $v \in P_2(\Omega_T)$. If $h_T \min_{\varphi \in H^1(\Omega_T)} |\!|\!| v - \varphi |\!|\!|_{\Omega_T} + h_T^2 ||\operatorname{div} \nabla_{\mathrm{NC}} v||_{L^2(\Omega_T)} = 0$, then $v|_{\Omega_T} \in C(\Omega_T) \cap P_2(\mathcal{T}(\Omega_T))$ and $\operatorname{div} \nabla_{\mathrm{NC}} v = 0$ in Ω_T. It follows $\nabla_{\mathrm{NC}}(v|_{\Omega_T}) \in P_0(\mathcal{T}(\Omega_T); \mathbb{R}^2)$. For each interior edge $E \in \mathcal{E}(\Omega_T)$, the jump $[\nabla_{\mathrm{NC}} v]_E \in P_0(E; \mathbb{R}^2)$ satisfies $[\nabla_{\mathrm{NC}} v]_E \cdot \nu_E = 0$ since $\nabla_{\mathrm{NC}}(v|_{\Omega_T}) \in H(\operatorname{div}, \Omega_T)$ and $[\nabla_{\mathrm{NC}} v]_E \cdot \tau_E = 0$ since $v|_{\Omega_T} \in C(\Omega_T)$. Hence $[\nabla_{\mathrm{NC}} v]_E = 0$ for any interior edge $E \in \mathcal{E}(\Omega_T)$ and so $\nabla v|_{\Omega_T} \in P_0(\Omega_T; \mathbb{R}^2)$; whence $v|_{\Omega_T} \in P_1(\Omega_T)$. If T satisfies $\mathcal{E}(T) \cap \mathcal{E}(\partial\Omega) = \emptyset$, then $v \geq 0$ at all midpoints $\operatorname{mid}(\mathcal{T}(\Omega_T))$ and $v = 0$ at $\operatorname{mid}(T)$ yields $v \equiv 0$ in Ω_T. In the remaining two cases let $F \in \mathcal{E}(T) \cap \mathcal{E}(\partial\Omega)$. In the first case assume $v(\operatorname{mid}(F)) > 0$. From this it follows that v has a change of sign in T. Since $v \in P_1(\Omega_T)$, there exists a triangle $T' \in \mathcal{T}(\Omega_T)$ with $⨍_{T'} v \, \mathrm{d}x < 0$, which is a contradiction and hence it holds $v \equiv 0$ in Ω_T. In the other case $v(\operatorname{mid}(F)) = 0$. Either it immediately holds $v \equiv 0$ in Ω_T or there exists $E \in \mathcal{E}(T)$ with $v(\operatorname{mid}(E)) > 0$. Hence v has a change of sign in T and the same arguments as in the previous case apply. This shows that if the right-hand side $= 0$, it follows that $||v||_{L^2(\Omega_T)} = 0$. A compactness argument as in the proof of the equivalence of norms shows that (3.46) holds in the cone of all such functions v. A scaling argument shows that the generic constant hidden in $\lesssim$ depends on the shape-regularity of the underlying triangulation but not on the size of the triangles. □

Proof of Theorem 3.49. A Cauchy inequality, an interpolation estimate, and a Poincaré inequality lead to

$$\int_\Omega (-\lambda_{\mathrm{RT}})(v - \chi)_+ \, \mathrm{d}x \lesssim \sum_{T \in \mathcal{T}} ||\lambda_{\mathrm{RT}}||_{L^2(T)} \left(|\!|\!| h_{\mathcal{T}}(v - v_2) |\!|\!|_{\mathrm{NC}(T)} + ||v_2 - \chi||_{L^2(T)} \right).$$

Lemma 3.52 shows

$$||v_2 - \chi||_{L^2(T)} \lesssim h_T |\!|\!| v_2 - v |\!|\!| + h_T ||h_{\mathcal{T}}(\lambda_{\mathrm{RT}} - \Pi_0 f)||_{L^2(\Omega_T)}.$$

The arguments in Verfürth (1996) (cf. also the proof of Claim 3 in the proofs of Theorem 3.29 and Theorem 3.40) show

ⓐ $||h_T \lambda_{\mathrm{RT}}||_{L^2(T)} \lesssim |\!|\!| \lambda - \lambda_{\mathrm{RT}} |\!|\!|_{*,T} + |\!|\!| u - \tilde{u}_{\mathrm{CR}} |\!|\!|_{\mathrm{NC}(T)} + ||h_T f||_{L^2(T)}$;

ⓑ $||h_T(\lambda_{\mathrm{RT}} - \Pi_0 f)||_{L^2(T)} \lesssim |\!|\!| \lambda - \lambda_{\mathrm{RT}} |\!|\!|_{*,T} + |\!|\!| u - \tilde{u}_{\mathrm{CR}} |\!|\!|_{\mathrm{NC}(T)} + \operatorname{osc}(f, T)$.

The combination of these estimates and some finite overlap conclude the proof. □

4. Signorini Problem

This chapter is devoted to the analysis of the Signorini model problem for the Laplace operator. The Signorini problem is a model problem for the important contact problem in linear elasticity, which is described as a variational inequality.

4.1. Problem formulation

This section introduces the variational inequality that describes the Signorini problem and discusses equivalent formulations.

4.1.1. Mathematical modelling

Let $\Omega \subset \mathbb{R}^d$ be a bounded simply connected Lipschitz domain with a polyhedral boundary $\partial\Omega$. The boundary $\partial\Omega$ is subdivided into the closed subset Γ_D of positive surface measure $|\Gamma_D| > 0$, an open (and possibly empty) subset Γ_N, and the subset $\Gamma_C := \partial\Omega \setminus (\Gamma_D \cup \Gamma_N)$ of positive surface measure $|\Gamma_C| > 0$. Figure 4.1 clarifies, that it is possible that Γ_C is neither closed nor open, depending on the configuration of Γ_D and Γ_N.

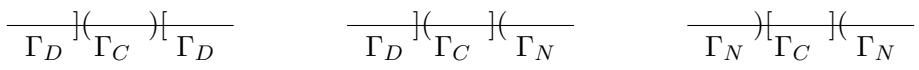

Figure 4.1.: Possible configurations of the boundaries Γ_D, Γ_C, and Γ_N.

Set $V := H^1_D(\Omega) := H^1_{\Gamma_D}(\Omega)$. Let the obstacle and the Dirichlet boundary value u_D satisfy

$$\chi \in H^1(\Omega) \text{ and } u_D \in C(\Gamma_D \cup \Gamma_C) \text{ with } \chi|_{\Gamma_D} = u_D \tag{4.1}$$

so that the closed and convex subset

$$K := \{v \in \mathcal{A} \mid \chi \leq v \text{ a.e. along } \Gamma_C\} \text{ of } \mathcal{A} := \{v \in H^1(\Omega) \mid v = u_D \text{ along } \Gamma_D\}$$

is non-empty. For $f \in L^2(\Omega)$ and $g \in L^2(\Gamma_N \cup \Gamma_C)$, define the linear form $F \in V^*$ by

$$F(v) := \int_\Omega fv \,\mathrm{d}x + \int_{\Gamma_C \cup \Gamma_N} gv \,\mathrm{d}s \quad \text{for all } v \in V.$$

The weak formulation of the Signorini problem seeks $u \in K$ such that

$$F(v - u) \leq a(u, v - u) \quad \text{for all } v \in K. \tag{4.2}$$

Lemma 4.1 (existence of solutions)**.** *Let the conditions* (4.1) *hold. Then the Signorini problem* (4.2) *has a unique solution* $u \in K$*, if and only if* $\Gamma_D \neq \emptyset$ *or* $\int_{\Gamma_N \cup \Gamma_C} g \, \mathrm{d}x < 0$.

Remark 4.2. *This theorem states, that the Dirichlet boundary may also be empty, which is excluded in this thesis.*

Proof. The proof is given in Spann (1993) and employs results from Baiocchi et al. (1986). □

Theorem 4.3 (regularity; Brézis (1972); Spann (1993))**.** *Let* $\Omega \subset \mathbb{R}^2$ *be a bounded domain with a smooth boundary* $\partial\Omega$ *or a convex polygonal domain. If the obstacle* χ *and the Dirichlet boundary value* u_D *satisfy* (4.1) *and* $\chi|_{\Gamma_C \cup \Gamma_D} \in H^{3/2}(\Gamma_C \cup \Gamma_D)$*, then* $u \in H^2(\Omega)$.

Proof. Spann (1993) considers a right-hand side $f = 0$, but a transformation immediately allows the result for the general case. □

Define the bounded linear form $\Lambda \in V^*$, i.e., the Lagrange multiplier, by

$$\Lambda(v) := F(v) - a(u, v) \quad \text{for all } v \in V. \tag{4.3}$$

Lemma 4.4 (complementary conditions)**.** *Let the conditions* (4.1) *on the obstacle* χ *and the Dirichlet boundary value* u_D *be satisfied. The functional* $\Lambda \in V^*$ *from* (4.3) *and the unique solution* $u \in K$ *to* (4.2) *satisfy the following complementary conditions*

$$\begin{aligned} 0 \leq & u - \chi \text{ along } \Gamma_C, \quad \Lambda(u - \chi) = 0, \text{ and} \\ \Lambda(\varphi) \leq 0 \quad & \text{for all } \varphi \in V_+ := \{v \in V \mid v|_{\Gamma_C} \geq 0 \text{ a.e. along } \Gamma_C\}. \end{aligned} \tag{4.4}$$

Proof. The first inequality follows from the definition of $u \in K$. Given any $\varphi \in V_+$, the test function $v := u + \varphi \in K$ in the variational inequality (4.2) results in

$$\Lambda(\varphi) = \Lambda(v - u) = F(v - u) - a(u, v - u) \leq 0.$$

To show orthogonality, insert the test functions $v = \chi \in K$ and $v = 2u - \chi \in K$ in the variational inequality (4.2). This leads to $\Lambda(u - \chi) = 0$. □

Remark 4.5. *If* $u \in H^2(\Omega)$*, an integration by parts shows*

$$\Lambda(v) = -\int_{\Gamma_C} (\nabla u \cdot \nu - g) v \, \mathrm{d}s \,.$$

4.1.2. Equivalent formulations

This subsection presents three equivalent formulations together with the corresponding complementary conditions for a simply connected domain Ω. Theorem 4.10 below shows the equivalence of the three formulations. Define the energy functional

$$E(v) := 1/2 a(v, v) - F(v) \quad \text{for all } v \in \mathcal{A}.$$

The energy formulation of Signorini's problem seeks $u \in K$ such that

$$E(u) = \min_{v \in K} E(v). \tag{4.5}$$

Lemma 4.6 (existence of solutions)**.** *There exists a unique solution $u \in K$ to* (4.5)*.*

Proof. This follows for example from Braess (2007, Prop. 2.5). □

Remark 4.7. *The equivalence of* (4.2) *and* (4.5) *is well established and can be found in Glowinski (2008, Ch. 1, Sec. 3).*

Define $\tilde{H}^{1/2}_{-}(\partial\Omega \setminus \Gamma_D) := \{v|_{\partial\Omega} \;\big|\; -v \in V_+\}$ and set

$$\mathcal{M} := L^2(\Omega) \times \tilde{H}^{1/2}_{-}(\partial\Omega \setminus \Gamma_D). \tag{4.6}$$

Recall, that $\langle \bullet, \bullet \rangle_{\partial\Omega}$ denotes the dual pairing between the spaces $\tilde{H}^{1/2}(\partial\Omega \setminus \Gamma_D)$ and $H^{-1/2}(\partial\Omega \setminus \Gamma_D)$. For all $q \in H(\operatorname{div}, \Omega)$ and $(v, \beta) \in \mathcal{M}$, consider the following bilinear and linear forms

$$\begin{aligned} b(q, (v, \beta)) &:= \int_\Omega v \operatorname{div} q \,\mathrm{d}x + \langle q \cdot \nu, \beta \rangle_{\partial\Omega}, \\ H(q) &:= \langle q \cdot \nu, \chi \rangle_{\partial\Omega}, \\ G((v, \beta)) &:= -\int_\Omega f v \,\mathrm{d}x + \int_{\Gamma_C \cup \Gamma_N} g\beta \,\mathrm{d}s. \end{aligned} \tag{4.7}$$

Note that $\chi|_{\Gamma_D} = u_D|_{\Gamma_D}$ and hence the linear form H includes the Dirichlet boundary conditions. For the mixed formulation, recall the spaces $H_{g,N}(\operatorname{div}, \Omega) := H_{g,\Gamma_N}(\operatorname{div}, \Omega)$ and $H_{0,N}(\operatorname{div}, \Omega) := H_{0,\Gamma_N}(\operatorname{div}, \Omega)$. The mixed formulation of Signorini's problem seeks $(p, (u, \alpha)) \in H_{g,N}(\operatorname{div}, \Omega) \times \mathcal{M}$ such that

$$\int_\Omega p \cdot q \,\mathrm{d}x + b(q, (u, \alpha)) = H(q) \qquad \text{for all } q \in H_{0,N}(\operatorname{div}, \Omega), \tag{4.8}$$

$$b(p, (v - u, \beta - \alpha)) \le G((v - u, \beta - \alpha) \qquad \text{for all } (v, \beta) \in \mathcal{M}. \tag{4.9}$$

Lemma 4.8 (mixed complementary conditions)**.** *Any continuous solution $(p, (u, \alpha)) \in H_{g,N}(\operatorname{div}, \Omega) \times \mathcal{M}$ to* (4.8)–(4.9) *satisfies the following mixed complementary conditions*

$$\alpha \le 0 \text{ along } \Gamma_C, \quad \langle p \cdot \nu - g, \alpha \rangle_{\partial\Omega} = 0, \quad \text{and}$$
$$0 \le \langle p \cdot \nu - g, \varphi \rangle_{\partial\Omega} \quad \text{for all } \varphi \in \tilde{H}^{1/2}_{-}(\partial\Omega \setminus \Gamma_D).$$

Proof. The definition of $\mathcal{M}$ in (4.6) implies $\alpha \le 0$ along Γ_C. To show the orthogonality, insert the test functions $(u, 0)$ and $(u, 2\alpha) \in \mathcal{M}$ in (4.9). This shows

$$\langle p \cdot \nu - g, \alpha \rangle_{\partial\Omega} = 0.$$

To prove the last inequality, let $(u, \varphi + \alpha) \in \mathcal{M}$ for any $\varphi \in \tilde{H}^{1/2}_{-}(\partial\Omega \setminus \Gamma_D)$. Then (4.9) shows

$$\langle p \cdot \nu - g, \varphi \rangle_{\partial\Omega} \le 0 \quad \text{for all } \varphi \in \tilde{H}^{1/2}_{-}(\partial\Omega \setminus \Gamma_D).$$

This concludes the proof. □

For the dual variational inequality let

$$Q(f, g) := \{q \in H_{g,N}(\operatorname{div}, \Omega) \mid f + \operatorname{div} q = 0 \text{ a.e. in } \Omega$$

and $0 \le \langle q \cdot \nu - g, \varphi \rangle_{\partial\Omega}$ for all $\varphi \in \tilde{H}^{1/2}_{-}(\partial\Omega \setminus \Gamma_D)\}$.

The dual variational inequality seeks $p \in Q(f,g)$ such that

$$H(q-p) \le \int_\Omega p \cdot (q-p)\,\mathrm{d}x \qquad \text{for all } q \in Q(f,g). \tag{4.10}$$

Lemma 4.9. *Let Ω be a simply connected bounded domain.*

ⓐ *Any solution $p \in Q(f,g)$ to (4.10) satisfies $p = \nabla v$ for some $v \in K$.*

ⓑ *The function v from ⓐ fulfils the following complementary conditions*

$$\begin{aligned} &0 \le v - \chi \text{ along } \Gamma_C, \quad \langle p \cdot \nu, v - \chi \rangle_{\partial\Omega} = 0, \quad \text{and} \\ &0 \le \langle p \cdot \nu - g, \varphi \rangle_{\partial\Omega} \quad \text{for } \varphi \in \tilde{H}^{1/2}_{-}(\partial\Omega \setminus \Gamma_D). \end{aligned} \tag{4.11}$$

Proof of ⓐ. Given $p \in Q(f,g)$, let $v \in H^1(\Omega)$ be the weak solution to

$$\begin{aligned} -\Delta v &= \operatorname{div} p && \text{in } \Omega, \\ \nabla v \cdot \nu &= p \cdot \nu && \text{along } \Gamma_C \cup \Gamma_N, \\ v &= u_D && \text{along } \Gamma_D. \end{aligned}$$

Hence $v \in H^1(\Omega)$ satisfies

$$\int_\Omega (p - \nabla v) \cdot \nabla \varphi \,\mathrm{d}x = 0 \quad \text{for all } \varphi \in V.$$

Then $p - \nabla v \perp \nabla V$. Since Ω is simply connected, the Helmholtz decomposition in Theorem 2.26 yields the existence of $\phi \in H^1(\Omega)$ with $\operatorname{Curl}\phi \cdot \nu = 0$ along $\Gamma_C \cup \Gamma_N$ such that

$$p - \nabla v = \operatorname{Curl}\phi.$$

Set $q = p - \operatorname{Curl}\phi$. Since $q - p = -\operatorname{Curl}\phi$, the dual variational inequality (4.10) and an integration by parts shows

$$\begin{aligned} -\langle \operatorname{Curl}\phi \cdot \nu, \chi \rangle_{\partial\Omega} = H(-\operatorname{Curl}\phi) &\le \int_\Omega -p \cdot \operatorname{Curl}\phi \,\mathrm{d}x \\ &= -\int_\Omega (p - \nabla v) \cdot \operatorname{Curl}\phi \,\mathrm{d}x - \int_{\partial\Omega} v \operatorname{Curl}\phi \cdot \nu \,\mathrm{d}s \\ &= -||p - \nabla v||^2_{L^2(\Omega)} - \int_{\partial\Omega} v \operatorname{Curl}\phi \cdot \nu \,\mathrm{d}s. \end{aligned}$$

Since $\operatorname{Curl}\phi \cdot \nu = 0$ along $\Gamma_C \cup \Gamma_N$ and $\chi = v = u_D$ along Γ_D, it follows $0 \le -||p - \nabla v||^2_{L^2(\Omega)}$ and hence $p = \nabla v$. It remains to show that $v \in K$. Let $\mu \in L^2(\Gamma_N \cup \Gamma_C)$ such that $\mu \ge 0$ along Γ_C and $\mu = 0$ along Γ_N. Then there exists $\tau \in H(\operatorname{div}, \Omega)$ with $\tau \cdot \nu = \mu$ along $\Gamma_N \cup \Gamma_C$ and $\operatorname{div}\tau = 0$. For $q = \tau + p \in Q(f,g)$, the dual variational inequality (4.10) leads to

$$\begin{aligned} \langle \mu, \chi \rangle_{\partial\Omega} = \langle (q-p) \cdot \nu, \chi \rangle_{\partial\Omega} &\le \int_\Omega p \cdot (q-p)\,\mathrm{d}x = \int_\Omega \nabla v \cdot (q-p)\,\mathrm{d}x \\ &= -\int_\Omega v \operatorname{div}(q-p)\,\mathrm{d}x + \int_{\partial\Omega} v(q-p) \cdot \nu \,\mathrm{d}s. \end{aligned}$$

Since $q - p = \tau$ and $\operatorname{div} \tau = 0$, it follows that

$$\langle \mu, \chi - v \rangle_{\partial\Omega} \leq 0.$$

This holds for all $\mu \in L^2(\Gamma_C)$ with $\mu \geq 0$ along Γ_C and $\mu = 0$ along Γ_N and hence $\chi - v \leq 0$ along Γ_C. This shows that $v \in K$ and concludes the proof of ⓐ. □

Proof of ⓑ. The first and second inequality follow from the definition of $v \in K$ and $p = \nabla v \in Q(f, g)$. To show the orthogonality, let $(\tilde{p}, \tilde{u}) \in H_{p\cdot\nu-g,\Gamma_N\cup\Gamma_C}(\operatorname{div}, \Omega) \times L^2(\Omega)$ solve the following weak Laplace problem

$$\begin{aligned} \int_\Omega \tilde{p} \cdot \tilde{q} \,\mathrm{d}x + \int_\Omega \tilde{u} \operatorname{div} \tilde{q} \,\mathrm{d}x = 0 \qquad & \text{for all } \tilde{q} \in H_{0,N}(\operatorname{div}, \Omega), \\ \int_\Omega \tilde{v} \operatorname{div} \tilde{p} \,\mathrm{d}x = 0 \qquad & \text{for all } \tilde{v} \in L^2(\Omega). \end{aligned}$$

Set $q := p \pm \tilde{p} \in Q(f, g)$. Then the dual variational inequality (4.10) yields

$$\pm \langle \tilde{p} \cdot \nu, \chi - v \rangle_{\partial\Omega} \leq 0.$$

Since $\tilde{p} \in H_{p\cdot\nu-g,\Gamma_N\cup\Gamma_C}(\operatorname{div}, \Omega)$, this concludes the proof of ⓑ. □

Theorem 4.10. *For sufficiently smooth data, i.e., the exact solution $u \in K$ to (4.2) satisfies $u \in H^2(\Omega)$, the three formulations (4.2), (4.8)–(4.9), and (4.10) are pairwise equivalent in the following sense.*

- ⓐ *Let $u \in V$ solve (4.2). Then $(\nabla u, (u, (\chi - u)|_{\partial\Omega})) \in H_{g,N}(\operatorname{div}, \Omega) \times \mathcal{M}$ solves (4.8)–(4.9).*
- ⓑ *Let $(p, (u, \alpha)) \in H(\operatorname{div}, \Omega) \times \mathcal{M}$ solve (4.8)–(4.9). Then p solves (4.10).*
- ⓥ *Let $p = \nabla v \in Q(f, g)$ solve (4.10). Then v solves (4.2).*

Proof. To prove ⓐ, let $u \in K$ be the solution to (4.2). Due to the regularity assumptions, $\nabla u \in H(\operatorname{div}, \Omega)$ and $(u, (\chi - u)|_{\partial\Omega}) \in \mathcal{M}$. For any $q \in H(\operatorname{div}, \Omega)$, an integration by parts shows

$$\int_\Omega \nabla u \cdot q \,\mathrm{d}x = -\int_\Omega u \operatorname{div} q \,\mathrm{d}x + \langle q \cdot \nu, u \rangle_{\partial\Omega}.$$

Hence it holds

$$\int_\Omega \nabla u \cdot q \,\mathrm{d}x + \int_\Omega u \operatorname{div} q \,\mathrm{d}x + \langle q \cdot \nu, \chi - u \rangle_{\partial\Omega} = \langle q \cdot \nu, \chi \rangle_{\partial\Omega}$$

and (4.8) is satisfied.
To show (4.9), observe

$$\begin{aligned} b(\nabla u, (v - u, \beta - (\chi - u)|_{\partial\Omega})) &= \int_\Omega \Delta u (v - u) \,\mathrm{d}x + \langle \nabla u \cdot \nu, \beta - (\chi - u) \rangle_{\partial\Omega} \\ &= -\int_\Omega f (v - u) \,\mathrm{d}x + \langle \nabla u \cdot \nu, \beta - (\chi - u) \rangle_{\partial\Omega}. \end{aligned}$$

The complementary conditions (4.4) show $\langle \nabla u - g \cdot \nu, (\chi - u) \rangle_{\partial\Omega} = 0$ and $\langle \nabla u \cdot \nu - g, \beta \rangle_{\partial\Omega} \leq 0$. Hence

$$-\int_\Omega f (v - u) \,\mathrm{d}x + \langle \nabla u \cdot \nu, \beta - (\chi - u) \rangle_{\partial\Omega}$$

$$\leq -\int_\Omega f(v-u)\,\mathrm{d}x + \int_{\Gamma_C} g(\beta-(\chi-u))\,\mathrm{d}s$$

This completes the proof of ⓐ.

To prove ⓑ, suppose that $(p,(u,\alpha)) \in H_{g,N}(\mathrm{div},\Omega)\times\mathcal{M}$ solves (4.8)–(4.9). The mixed complementary conditions in Lemma 4.8 show that $p \in Q(f,g)$ and $\alpha \leq 0$ along Γ_C. For $q \in Q(f,g)$ the mixed complementary conditions in Lemma 4.8 show, that the bilinear form $b(\bullet,\bullet)$ satisfies

$$b(q-p,(u,\alpha)) = \langle q\cdot\nu - g, \alpha\rangle_{\partial\Omega} \leq 0.$$

Since $p,q \in Q(f,g)$, it holds $p-q \in H_{0,N}(\mathrm{div},\Omega)$ for any $q \in Q(f,g)$. Equation (4.8) leads to

$$\int_\Omega p\cdot(q-p)\,\mathrm{d}x = H(q-p) - b(q-p,(u,\alpha)) \geq H(q-p).$$

Hence $p \in Q(f,g)$ solves the dual variational inequality (4.10). This concludes the proof of ⓑ. □

For the proof of ⓒ, recall the existence of $v \in K$ such that ∇v solves (4.10) (note that $-\Delta v = f$). For $\varphi \in K$ with $\nabla\varphi \in H(\mathrm{div},\Omega)$, an integration by parts shows

$$\begin{aligned}\int_\Omega \nabla v\cdot\nabla(\varphi-v)\,\mathrm{d}x - \int_\Omega f(\varphi-v)\,\mathrm{d}x - \langle g,\varphi-v\rangle_{\partial\Omega} &= \langle\nabla v\cdot\nu - g,\varphi-v\rangle_{\partial\Omega}\\ &= \langle\nabla v\cdot\nu-g,\varphi-\chi\rangle + \langle\nabla v\cdot\nu-g,\chi-v\rangle_{\partial\Omega}.\end{aligned}$$

Since $v-\chi\geq 0$ and $\nabla v\cdot\nu - g = p\cdot\nu - g \geq 0$ along Γ_C, it follows

$$\langle\nabla v\cdot\nu-g,\varphi-\chi\rangle_{\partial\Omega} \geq 0.$$

The dual complementary conditions (4.11) show that $\langle\nabla v\cdot\nu-g,\chi-v\rangle_{\partial\Omega}=0$. This concludes the proof of ⓒ. □

The following theorem comments on the unique existence of solution to (4.8)–(4.9) and (4.10).

Theorem 4.11. ⓐ *Let $(p,(u,\alpha)) \in H_{g,N}(\mathrm{div},\Omega)\times\mathcal{M}$ be the solution to* (4.8)–(4.9). *Then $(p,(u,\alpha|_{\Gamma_C}))$ is unique.*

ⓑ *There exists a unique solution to problem* (4.10).

Proof. Theorem 4.10 and the unique existence of a solution $u \in K$ to (4.2), prove the existence of a solution to (4.8)–(4.9). The uniqueness of the solution $u \in K$ to (4.2) shows the uniqueness of $p \in H_{g,N}(\mathrm{div},\Omega)$. It remains to show the uniqueness of $(u,\alpha|_{\Gamma_C})$. Assume that $(p,(u_1,\alpha_1))$ and $(p,(u_2,\alpha_2)) \in H_{g,N}(\mathrm{div},\Omega)\times\mathcal{M}$ solve (4.8)–(4.9). Then (4.8), for all $q \in H_{0,N}(\mathrm{div},\Omega)$, leads to

$$\begin{aligned}\int_\Omega p\cdot q\,\mathrm{d}x + b(q,(u_1,\alpha_1)) &= H(q),\\ \int_\Omega p\cdot q\,\mathrm{d}x + b(q,(u_2,\alpha_2)) &= H(q).\end{aligned}$$

The difference of those two equations reads

$$\int_\Omega (u_1 - u_2) \operatorname{div} q \,\mathrm{d}x + \langle q \cdot \nu, \alpha_1 - \alpha_2 \rangle_{\partial\Omega} = 0 \quad \text{for all } q \in H_{0,N}(\operatorname{div}, \Omega).$$

It is well-known, that there exits $q \in H_{0,N}(\operatorname{div}, \Omega)$ with $\operatorname{div} q = u_1 - u_2$ and $q \cdot \nu = \alpha_1 - \alpha_2$ along Γ_C. Then it follows that

$$||u_1 - u_2||^2_{L^2(\Omega)} + ||\alpha_1 - \alpha_2||^2_{L^2(\Gamma_C)} = 0.$$

Hence $u_1 = u_2$ and $\alpha_1|_{\Gamma_C} = \alpha_2|_{\Gamma_C}$. This concludes the proof of ⓐ. □

Theorem 4.10 and the unique existence of a solution $u \in K$ to (4.2) prove ⓑ. □

Remark 4.12. *The proof of Theorem 4.11.a is closely related to the proof of Theorem 2.1 in Brezzi et al. (1978).*

4.2. Reliable and efficient a posteriori error estimate for Signorini's problem

This subsection is devoted to a general reliable and efficient error estimate for Signorini's problem. Let $v \in \mathcal{A}$ be any approximation to the exact solution $u \in K$ to (4.2). For any $\mu \in L^2(\Gamma_C; (-\infty, 0])$, define a non-positive approximation $M \in V^*$ (non-positive in the sense that $M(\varphi) \leq 0$ for all $\varphi \in V_+$) to the exact Lagrange multiplier $\Lambda \in V^*$ by

$$M(\varphi) := \int_{\Gamma_C} \mu\varphi \,\mathrm{d}s \quad \text{for all } \varphi \in V. \tag{4.12}$$

The residual $\mathrm{Res} \in V^*$ is defined by

$$\mathrm{Res}(\varphi) := F(\varphi) - M(\varphi) - a(v, \varphi) \quad \text{for all } \varphi \in V. \tag{4.13}$$

Note that $v \in \mathcal{A}$ does not have to satisfy $v \in K$ and hence define a gap function w as the harmonic extension of $\min\{0, v - \chi\} \in L^2(\Gamma_C)$ which satisfies

$$-\Delta w = 0, \quad w|_{\Gamma_C} = \min\{0, v - \chi\}, \quad \text{and} \quad w|_{\Gamma_N \cup \Gamma_D} = 0. \tag{4.14}$$

Contrary to the notation in the other chapters, define $(v - \chi)_+ := v - \chi - w$. Recall the set $S := \{\varphi \in V \mid |\!|\!|\varphi|\!|\!| = 1\}$ and the definitions

$$|\!|\!|\mathrm{Res}|\!|\!|_* := \sup\{\mathrm{Res}(\varphi) \mid \varphi \in S\} \quad \text{and} \quad |\!|\!|\Lambda - M|\!|\!|_* := \sup\{(\Lambda - M)(\varphi) \mid \varphi \in S\}.$$

Theorem 4.13. *Suppose $v \in \mathcal{A}$ is some approximation to the exact continuous solution $u \in K$ to (4.2) and $M \in V^*$, defined as in (4.12) for some $\mu \in L^2(\Gamma_C; (-\infty, 0])$, is some non-positive (i.e., $M(\varphi) \leq 0$ for all $\varphi \in V_+$) approximation to the Lagrange multiplier $\Lambda \in V^*$. Then the error $e := u - v$ and the gap function $w \in V$ from (4.14) satisfy*

ⓐ $(\Lambda - M)(u - v + w) + |\!|\!|e|\!|\!|^2/2 + |\!|\!|e + w|\!|\!|^2/2 = \mathrm{Res}(e + w) + |\!|\!|w|\!|\!|^2/2;$

ⓑ $0 \leq M(\chi - u) - \Lambda((v - \chi)_+) = (\Lambda - M)(u - v + w) - M((v - \chi)_+);$

ⓒ $M(\chi - u) - \Lambda((v - \chi)_+) + |\!|\!|e|\!|\!|^2/2 + (1 - 1/t)|\!|\!|e + w|\!|\!|^2/2$
$\leq t|\!|\!|\mathrm{Res}|\!|\!|_*^2/2 - M((v - \chi)_+) + |\!|\!|w|\!|\!|^2/2 \quad$ *for all* $\quad 0 < t < \infty;$

ⓓ $\left|\|\Lambda - M\|_* - \|e\|\right| \leq \|\mathrm{Res}\|_* \leq \|e\| + \|\Lambda - M\|_*$.

Proof. The proof follows the arguments of the proof of Theorem 3.17 and is repeated here for convenient reading. A direct calculation shows

$$(\Lambda - M)(u - v + w) = \mathrm{Res}(e + w) - a(e, e + w).$$

This and some straightforward algebra, namely

$$-a(e, e + w) = -\|e\|^2/2 - \|e + w\|^2/2 + \|w\|^2/2,$$

conclude the proof of ⓐ. □

Along the boundary Γ_C it holds $(v - \chi)_+ = v - \chi - w$ and hence ⓑ follows from the continuous complementary conditions in Lemma 4.4 and direct calculations. □

The assumption ⓒ follows from the combination of ⓐ and ⓑ with a further evaluation of $\mathrm{Res}(e+w)$. The definition of the operator norm and a Young inequality for $0 < t < \infty$ yield

$$\mathrm{Res}(e + w) \leq \|\mathrm{Res}\|_* \|e + w\| \leq t\|\mathrm{Res}\|_*^2/2 + \|e + w\|^2/(2t).$$ □

The assumption ⓓ employs the auxiliary Poisson problem with the exact solution $z \in \mathcal{A}$ to

$$a(z, \varphi) = F(\varphi) - M(\varphi) \qquad \text{for all } \varphi \in V.$$

The continuous solution $u \in K$ to the Signorini problem (4.2) and the definition of the continuous Lagrange multiplier Λ yield

$$a(u - z, \varphi) = (M - \Lambda)(\varphi) \qquad \text{for all } \varphi \in V.$$

In other words, $u - z \in V$ is the Riesz representation of the linear and bounded functional $M - \Lambda$ in the Hilbert space (V, a) and therefore

$$\|u - z\| = \|\Lambda - M\|_*. \tag{4.15}$$

The definition of the residual (4.13) yields

$$\begin{aligned} \|v - z\|^2 &= a(v, v - z) - a(z, v - z) \\ &= a(v, v - z) - F(v - z) + M(v - z) \\ &= \mathrm{Res}(z - v) \leq \|\mathrm{Res}\|_* \|v - z\|. \end{aligned}$$

This implies $\|z - v\| \leq \|\mathrm{Res}\|_*$. A triangle inequality and (4.15) show

$$\left|\|\Lambda - M\|_* - \|e\|\right| \leq \|v - z\| \leq \|\mathrm{Res}\|_*.$$

Given any $\varphi \in S$, the definition of Λ in (4.3) shows $\mathrm{Res}(\varphi) = (\Lambda - M)(\varphi) + a(e, \varphi)$ and hence

$$\|\mathrm{Res}\|_* \leq \sup_{\varphi \in S} \Big((\Lambda - M)(\varphi) + a(e, \varphi) \Big) \leq \|\Lambda - M\|_* + \|e\|.$$

This concludes the proof of ⓓ. □

Given $v \in \mathcal{A}$ and $M \in V^*$ as in (4.12), recall the gap function w from (4.14) and the error $e := u - v$. Define the total error Err by

$$\mathrm{Err}^2 := M(\chi - u) - \Lambda((v - \chi)_+) + \|e\|^2 + \|e + w\|^2 + \|\Lambda - M\|_*^2.$$

The total error Err is controlled by the estimator

$$\mathrm{Est}^2 := |||\mathrm{Res}|||_*^2 - M((v-\chi)_+) + |||w|||^2.$$

The following Theorem is a realization of Theorem A.

Theorem 4.14 (reliability and efficiency)**.** *For any approximation $v \in \mathcal{A}$ to the exact solution $u \in K$ to* (4.2) *and any non-positive approximation $M \in V^*$ (i.e., $M(\varphi) \leq 0$ for all $\varphi \in V_+$)(cf.* (4.12)*) to the exact Lagrange multiplier $\Lambda \in V^*$, the total error* Err *and the estimator* Est *satisfy*

$$\mathrm{Est}^2/2 \leq \mathrm{Err}^2 \leq 30\,\mathrm{Est}^2.$$

Proof. The proof is analogue to that of Theorem 3.18 and is not recalled here. □

Remark 4.15. *Upper bounds for the residual term $|||\mathrm{Res}|||_*$ can be derived as in Remark* (3.20) *on Page 30.*

Remark 4.16. *The guaranteed upper bound* GUB *from* (1.2) *on Page 2 satisfies*

$$\mathrm{GUB} = 30\mathrm{Est}.$$

4.3. Conforming FEM for Signorini's problem

This section is devoted to the conforming Courant FEM for Signorini's problem in two space dimensions. No discrete Lagrange multiplier has been proposed in the literature. The section proposes a discrete Lagrange multiplier $\mu \in S^1(\mathcal{E}(\Gamma_C); (-\infty, 0])$ and discusses appropriate realizations of Theorems B and C.

4.3.1. Conforming discretization

Given a shape-regular triangulation $\mathcal{T}$ of $\Omega \subset \mathbb{R}^2$ from Subsection 2.2.1 on Page 11, recall the Courant finite element space $V_\mathrm{C} := S^1_D(\mathcal{T})$ from Definition 2.11 on Page 14. To approximate the Dirichlet boundary conditions u_D, define

$$u_{D,\mathrm{C}} := \sum_{z \in \mathcal{N}(\Gamma_D)} u_D(z)\varphi_z \in S^1(\mathcal{T}).$$

This leads to the discrete subset $\mathcal{A}_\mathrm{C}(\mathcal{T}) := u_{D,\mathrm{C}} + S^1_D(\mathcal{T})$ of $S^1(\mathcal{T})$ and the convex and non-empty set

$$K_\mathrm{C}(\mathcal{T}) := \{v_\mathrm{C} \in \mathcal{A}_\mathrm{C}(\mathcal{T}) \mid \forall z \in \mathcal{N}(\overline{\Gamma}_C),\ \chi(z) \leq v_\mathrm{C}(z)\} \subset \mathcal{A}_\mathrm{C}(\mathcal{T}).$$

The discrete problem seeks $u_\mathrm{C} \in K_\mathrm{C}(\mathcal{T})$ such that

$$F(v_\mathrm{C} - u_\mathrm{C}) \leq a(u_\mathrm{C}, v_\mathrm{C} - u_\mathrm{C}) \quad \text{for all } v_\mathrm{C} \in K_\mathrm{C}(\mathcal{T}). \tag{4.16}$$

Lemma 4.17 (existence of solutions)**.** *There exists a unique solution $u_\mathrm{C} \in K_\mathrm{C}(\mathcal{T})$ to problem* (4.16)*.*

Proof. Since $a(\bullet, \bullet)$ is a scalar product on $S^1_D(\mathcal{T}) \times S^1_D(\mathcal{T})$, the proof follows after a shift of χ to $\chi - u_{D,\mathrm{C}}$ and of F to $F - a(u_{D,\mathrm{C}}, \bullet)$ from Kinderlehrer and Stampacchia (1980, Thm. 2.1). □

Lemma 4.18 (discrete complementary conditions)**.** *The discrete solution* $u_C \in K_C(\mathcal{T})$ *to* (4.16) *satisfies the discrete complementary conditions*

$$0 \leq u_C(z) - \chi(z) \perp F(\varphi_z) - a(u_C, \varphi_z) =: \sigma_C(\varphi_z) \leq 0 \quad \text{for all } z \in \mathcal{N}(\Gamma_C) \tag{4.17}$$

where $a \perp b$ *abbreviates pointwise orthogonality in* $\mathbb{R}$*, i.e.,* $a \perp b$ *signifies* $ab = 0$ *for* $a, b \in \mathbb{R}$*.*

Proof. The first inequality follows from the definition of $K_C(\mathcal{T})$. For any $z \in \mathcal{N}(\Gamma_C)$, set $v_C := \varphi_z + u_C \in K_C(\mathcal{T})$. Hence the discrete variational inequality (4.16) shows $\sigma_C(\varphi_z) \leq 0$. To show orthogonality, define the test functions $v_C := (2u_C - \chi)(z)\varphi_z$ and $v_C := \chi(z)\varphi_z$ for $z \in \mathcal{N}(\Gamma_C)$. The discrete variational inequality (4.16) shows

$$\sigma_C(\varphi_z)(u_C(z) - \chi(z)) = F((u_C - \chi)(z)\varphi_z) - a(u_C, (u_C - \chi)(z)\varphi_z) = 0.$$

This concludes the proof. □

4.3.2. Boundary conditions

The discrete solution $u_C \in K_C(\mathcal{T})$ satisfy the Dirichlet boundary conditions in a discrete sense only. Recall Theorem 2.28 on Page 18 and define $w_D \in H^1(\Omega)$ such that $w_D|_{\Gamma_D} = (u_D - u_{D,C})|_{\Gamma_D}$ and $w_D|_{\Gamma_N \cup \Gamma_C} = 0$. This design of w_D allows for the definition of $v \in \mathcal{A}$ by $v := u_C + w_D \in \mathcal{A}$ in Theorem 4.14.

4.3.3. Interpolation operator and boundary modification

The properties of the discrete Lagrange multiplier presented in Subsection 4.3.4 are closely related to an interpolation operator defined in this subsection. This interpolation operator is related to the one in Subsection 3.3.3, but focuses on the contact boundary Γ_C. To accommodate the boundary conditions of the Lagrange multiplier correctly, but at the same time keep the degrees of freedom limited to the interior nodes and the nodes on the Neumann and contact boundary, the nodal basis functions φ_z are modified. Recall, that each component of the boundary $\partial\Omega$ has at least one vertex in its relative interior. For any node $z \in \mathcal{N}(\overline{\Gamma}_C \cap \Gamma_D)$, define $\zeta(z) := y$ for a neighbouring boundary node $y \in \mathcal{N}(\Gamma_C)$. For $z \in \mathcal{N}(\Gamma_C)$, $z \in \mathcal{N}(\Gamma_N)$, and for $z \in \mathcal{N}(\Gamma_D)$ where z is an interior point relative to Γ_D, set $\zeta(z) = z$. With this map define the modified basis functions

$$\psi_z := \sum_{y \in \zeta^{-1}(z)} \varphi_y.$$

This modification includes only boundary nodes on the Dirichlet boundary Γ_D and the contact boundary Γ_C. Note that the modified nodal basis functions, restricted to the boundary Γ_C, define a partition of unity on Γ_C. Let $\Omega_z := \cup_{y \in \zeta^{-1}(z)} \omega_y$ denote the support of the function ψ_z with $\gamma_z := \partial\Omega_z \cap \Gamma_C$. With the modified basis functions ψ_z define the interpolation operator J_C^* for all $\varphi \in V$ by

$$J_C^* \varphi := \sum_{z \in \mathcal{N}(\overline{\Gamma}_C) \setminus \mathcal{N}(\Gamma_D)} \left(\int_{\gamma_z} \varphi \psi_z \, \mathrm{d}s \, / \int_{\Gamma_C} \varphi_z \, \mathrm{d}s \right) \varphi_z$$

$$+ \sum_{z\in\mathcal{N}(\Omega)\cup\mathcal{N}(\Gamma_N)} \left(\int_{\omega_z} \varphi\varphi_z \,\mathrm{d}x \Big/ \int_\Omega \varphi_z \,\mathrm{d}x\right) \varphi_z. \tag{4.18}$$

The properties of this interpolation operator are summarized in the following theorem, which employs the subsequent notion of oscillations. For $\psi \in L^2(\Gamma_C)$ and $z \in \mathcal{N}(\Gamma_C)$ recall the oscillations $\operatorname{osc}_{1/2}^2(\psi,\gamma_z)$ from Definition 2.9 on Page 13 and define the boundary oscillations

$$\begin{aligned}
\operatorname{osc}_{1/2,C}^2(\psi,z) &:= \operatorname{osc}_{1/2}^2(\psi,\gamma_z),\\
\operatorname{osc}_{1/2,C}^2(\psi,\mathcal{N}(\Gamma_C)) &:= \sum_{z\in\mathcal{N}(\Gamma_C)} \operatorname{osc}_{1/2,C}^2(\psi,z),\\
\operatorname{Osc}_{1/2,C}^2(\psi,E) &:= |\partial\Omega_E\cap\Gamma_C|\,||\psi - \fint_{\partial\Omega_E\cap\Gamma_C} \psi\,\mathrm{d}s||_{L^2(\partial\Omega_E\cap\Gamma_C)}^2,\\
\operatorname{Osc}_{1/2,C}^2(\psi,\mathcal{E}(\Gamma_C)) &:= \sum_{E\in\mathcal{E}(\Gamma_C)} \operatorname{Osc}_{1/2,C}^2(\psi,E).
\end{aligned}$$

Theorem 4.19. *Any $\psi \in L^2(\Gamma_C)$ and $\varphi \in V$ satisfy*

$$\begin{aligned}
&\text{ⓐ } |(J_C^*\varphi)(z)|\sqrt{|\gamma_z|} \lesssim \|\varphi\|_{L^2(\gamma_z)} \quad \text{for } z\in\mathcal{N}(\Gamma_C)\setminus\mathcal{N}(\Gamma_D);\\
&\text{ⓑ } \int_{\Gamma_C} \psi(\varphi - J_C^*\varphi)\,\mathrm{d}s \lesssim \operatorname{osc}_{1/2,C}(\psi,\mathcal{N}(\Gamma_C))|\!|\!|\varphi|\!|\!|;\\
&\text{ⓒ } |\!|\!|J_C^*\varphi|\!|\!| \lesssim |\!|\!|\varphi|\!|\!|.
\end{aligned}$$

Proof. For the proof of ⓐ, let $z \in \mathcal{N}(\Gamma_C)$. A Cauchy inequality, $\int_{\gamma_z}\varphi_z\,\mathrm{d}s \approx |\gamma_z|$, and $||\psi_z||_{L^2(\gamma_z)} \approx |\gamma_z|^{1/2}$ show

$$\begin{aligned}
|(J_C^*\varphi)(z)|\sqrt{|\gamma_z|} &= |\gamma_z|^{1/2}\left(\int_{\gamma_z}\varphi_z\,\mathrm{d}s\right)^{-1}\left|\int_{\gamma_z}\varphi\psi_z\,\mathrm{d}s\right|\\
&\le |\gamma_z|^{1/2}\left(\int_{\gamma_z}\varphi_z\,\mathrm{d}s\right)^{-1}||\psi_z||_{L^2(\gamma_z)}||\varphi||_{L^2(\gamma_z)}\\
&\lesssim ||\varphi||_{L^2(\gamma_z)}.
\end{aligned}$$

□

For the proof of ⓑ, recall that the nodal basis functions $\psi_z|_{\Gamma_C}$ form a partition of unity on the boundary Γ_C. Since the basis functions for $z \in \mathcal{N}(\Omega)\cup\mathcal{N}(\Gamma_N)$ do not contribute on the boundary Γ_C, it holds

$$\int_{\Gamma_C}\psi(\varphi - J_C^*\varphi)\,\mathrm{d}s = \sum_{z\in\mathcal{N}(\Gamma_C)}\int_{\gamma_z}\psi\psi_z\left(\varphi - \left(\int_{\gamma_z}\varphi\psi_z\,\mathrm{d}s \Big/ \int_{\Gamma_C}\varphi_z\,\mathrm{d}s\right)\varphi_z/\psi_z\right)\mathrm{d}s\,.$$

Elementary calculations show, for each $z \in \mathcal{N}(\Gamma_C)$, that

$$\int_{\gamma_z}\psi_z\left(\varphi - \left(\int_{\gamma_z}\varphi\psi_z\,\mathrm{d}s \Big/ \int_{\Gamma_C}\varphi_z\,\mathrm{d}s\right)\varphi_z/\psi_z\right)\mathrm{d}s = 0.$$

Hence it holds

$$\int_{\gamma_z}\psi(\varphi - J_C^*\varphi)\,\mathrm{d}s$$

$$= \sum_{z\in\mathcal{N}(\Gamma_C)} \int_{\gamma_z} \left(\psi - \fint_{\gamma_z} \psi \,\mathrm{d}s\right) \psi_z \left(\varphi - \left(\int_{\gamma_z} \varphi\psi_z \,\mathrm{d}s \,/ \int_{\Gamma_C} \varphi_z \,\mathrm{d}s\right) \varphi_z/\psi_z\right) \mathrm{d}s\,.$$

A Cauchy inequality shows

$$\begin{aligned}\int_{\Gamma_C} \psi(\varphi - J_C^*\varphi)\,\mathrm{d}s \;\leq\; &\sum_{z\in\mathcal{N}(\Gamma_C)} ||\psi - \fint_{\gamma_z} \psi \,\mathrm{d}s\,||_{L^2(\gamma_z)} \\ &\times ||\psi_z \left(\varphi - \left(\int_{\gamma_z} \varphi\psi_z \,\mathrm{d}s \,/ \int_{\Gamma_C} \varphi_z \,\mathrm{d}s\right) \varphi_z/\psi_z\right)||_{L^2(\gamma_z)}.\end{aligned}$$

The term $||\psi - \fint_{\gamma_z} \psi \,\mathrm{d}s\,||_{L^2(\gamma_z)}$ on the right-hand side is part of the oscillations and so it remains to estimate

$$||\varphi_z \left(\varphi - \left(\int_{\gamma_z} \varphi\psi_z \,\mathrm{d}s \,/ \int_{\Gamma_C} \varphi_z \,\mathrm{d}s\right) \varphi_z/\psi_z\right)||_{L^2(\gamma_z)}.$$

In the case of $\psi_z = \varphi_z$, note that $0 \leq \varphi_z \leq 1$. With $\overline{\varphi} := \fint_{\omega_z} \varphi \,\mathrm{d}x$, a triangle inequality leads to

$$||\varphi_z\big(\varphi - \int_{\gamma_z} \varphi\varphi_z \,\mathrm{d}s \,/ \int_{\Gamma_C} \varphi_z \,\mathrm{d}s\,\big)||_{L^2(\gamma_z)} \leq ||\varphi - \overline{\varphi}||_{L^2(\gamma_z)} + ||(J_C^*(\fint_{\omega_z} -\varphi))(z)||_{L^2(\gamma_z)}.$$

Claim ⓐ, a trace inequality (cf. Theorem 2.24 on Page 17) and a Poincaré inequality from Theorem 2.21 on Page 16 result in

$$||\varphi_z \left(\varphi - \left(\int_{\gamma_z} \varphi\psi_z \,\mathrm{d}s \,/ \int_{\Gamma_C} \varphi_z \,\mathrm{d}s\right) \varphi_z/\psi_z\right)||_{L^2(\gamma_z)} \lesssim h_z^{1/2} |\!|\!| \varphi |\!|\!|_{\omega_z}. \tag{4.19}$$

In the case $0 \leq \varphi_z \neq \psi_z \leq 1$, a triangle and a Cauchy inequality lead to

$$\begin{aligned}||\psi_z\big(\varphi - \int_{\gamma_z} \varphi\psi_z \,\mathrm{d}s \,/ \int_{\Gamma_C} \varphi_z \,\mathrm{d}s\,\big)||_{L^2(\gamma_z)} &\lesssim ||\varphi - \int_{\gamma_z} \varphi\psi_z \,\mathrm{d}s / \int_{\Gamma_C} \varphi_z \,\mathrm{d}s\,||_{L^2(\Omega)} \\ &\lesssim ||\varphi||_{L^2(\gamma_z)}.\end{aligned}$$

Since $\psi_z > 0$ on a part of the Dirichlet boundary Γ_D, a Friedrichs and a trace inequality (Theorems 2.24 and 2.23 on Page 17) show

$$||\varphi||_{L^2(\gamma_z)} \lesssim h_z^{1/2} |\!|\!| \varphi |\!|\!|_{\Omega_z}.$$

The combination of the aforementioned arguments concludes the proof of ⓑ. □

For the proof of ⓒ, recall that $J_C^*\varphi(z) = 0$ for all nodes $z \in \mathcal{N}(\Gamma_D)$ along the Dirichlet boundary. Since $(\varphi_z)_{z\in\mathcal{N}}$ defines a partition of unity, it holds

$$\begin{aligned}|\!|\!| J_C^*\varphi |\!|\!| =& || \sum_{z\in\mathcal{N}_{L^2(\Omega)}} (J_C^*\varphi(z) - \varphi)\,\nabla\varphi_z || \\ \leq& \sum_{z\in\mathcal{N}(\Gamma_C)} ||\big(\int_{\gamma_z} \varphi\psi_z \,\mathrm{d}s / \int_{\Gamma_C} \varphi_z \,\mathrm{d}s\, - \varphi\big)\nabla\varphi_z||_{L^2(\omega_z)} \\ &+ \sum_{z\in\mathcal{N}(\Omega)\cup\mathcal{N}(\Gamma_N)} ||\big(\int_{\omega_z} \varphi\varphi_z \mathrm{d}x / \int_{\omega_z} \varphi_z \,\mathrm{d}x - \varphi\big)\nabla\varphi_z||_{L^2(\omega_z)} \\ &+ \sum_{z\in\mathcal{N}(\Gamma_D)} ||\varphi\nabla\varphi_z||_{L^2(\omega_z)}.\end{aligned}$$

This leads to four different cases. First consider $z \in \mathcal{N}(\Gamma_C)$ with $\psi_z \equiv \varphi_z$. Then

a triangle inequality leads to

$$\begin{aligned}||\Big(\int_{\gamma_z}\varphi\varphi_z\,\mathrm{d}s\,/\int_{\Gamma_C}\varphi_z\,\mathrm{d}s\,-\varphi\Big)\nabla\varphi_z||_{L^2(\omega_z)}&\\ \leq||\Big(\int_{\gamma_z}(\varphi-\fint_{\omega_z}\varphi\,\mathrm{d}x)\varphi_z\,\mathrm{d}s/\int_{\Gamma_C}\varphi_z\,\mathrm{d}s\Big)\nabla\varphi_z||_{L^2(\omega_z)}&\\ +||\Big(\fint_{\omega_z}\varphi\,\mathrm{d}x-\varphi\Big)\nabla\varphi_z||_{L^2(\omega_z)}.&\end{aligned}\tag{4.20}$$

Since $||\nabla\varphi_z||_{L^2(\omega_z)}\approx 1$ and $||\varphi_z||_{L^2(\gamma_z)}\lesssim h_z^{1/2}$, a Cauchy inequality and (4.19) yield

$$\begin{aligned}\|\Big(\int_{\gamma_z}(\varphi-\fint_{\omega_z}\varphi\,\mathrm{d}x)\varphi_z\,\mathrm{d}s/\int_{\Gamma_C}\varphi_z\,\mathrm{d}s\Big)\nabla\varphi_z\|_{L^2(\omega_z)}&\\ \lesssim h_z^{-1/2}||\varphi-\fint_{\omega_z}\varphi\,\mathrm{d}x||_{L^2(\gamma_z)}\lesssim|\!|\!|\varphi|\!|\!|_{\omega_z}.&\end{aligned}$$

For the first term in (4.20), a Poincaré inequality results in

$$||(\fint_{\omega_z}\varphi\,\mathrm{d}x-\varphi)\nabla\varphi_z||_{L^2(\omega_z)}\lesssim|\!|\!|\varphi|\!|\!|_{\omega_z}.$$

In the second case, let $z\in\mathcal{N}(\Gamma_C)$ with $\psi_z\not\equiv\varphi_z$. Since $|\nabla\varphi_z|\approx h_z^{-1}$, the L^2 norm satisfies

$$\begin{aligned}h_z||(\int_{\gamma_z}\varphi\psi_z\,\mathrm{d}s\,/\int_{\Gamma_C}\varphi_z\,\mathrm{d}s\,-\varphi)\nabla\varphi_z||_{L^2(\omega_z)}&\\ \lesssim\|\int_{\gamma_z}\varphi\psi_z\,\mathrm{d}s\,/\int_{\Gamma_C}\varphi_z\,\mathrm{d}s-\varphi\|_{L^2(\omega_z)}&\\ \leq\|\int_{\gamma_z}\varphi\psi_z\,\mathrm{d}s\,/\int_{\Gamma_C}\varphi_z\,\mathrm{d}s\|_{L^2(\omega_z)}+\|\varphi\|_{L^2(\omega_z)}.&\end{aligned}$$

A Cauchy and a trace inequality for the first term in the upper bound show

$$\|\int_{\gamma_z}\varphi\psi_z\,\mathrm{d}s\,/\int_{\Gamma_C}\varphi_z\,\mathrm{d}s\|_{L^2(\omega_z)}\leq\|\varphi\|_{L^2(\omega_z)}.$$

Since $\psi_z>0$ on part of the Dirichlet boundary Γ_D, a Friedrichs inequality lead to

$$\|\varphi\|_{L^2(\omega_z)}\lesssim h_z|\!|\!|\varphi|\!|\!|_{\Omega_z}.$$

In the third case, let $z\in\mathcal{N}(\Omega)\cup\mathcal{N}(\Gamma_N)$. Recall $|\nabla\varphi_z|\approx h_z^{-1}$. With $\overline{\varphi}:=\fint_{\omega_z}\varphi\,\mathrm{d}x$, a triangle inequality reveals

$$\begin{aligned}||\Big(\int_{\omega_z}\varphi\varphi_z\mathrm{d}x/\int_{\omega_z}\varphi_z\,\mathrm{d}x-\varphi\Big)\nabla\varphi_z||_{L^2(\omega_z)}&\\ \lesssim h_z^{-1}\left(||\int_{\omega_z}(\varphi-\overline{\varphi})\varphi_z\,\mathrm{d}x/\int_{\omega_z}\varphi_z\,\mathrm{d}x||_{L^2(\omega_z)}+||\varphi-\overline{\varphi}||_{L^2(\omega_z)}\right).&\end{aligned}$$

A Cauchy and a Poincaré inequality show

$$||\Big(\int_{\omega_z}\varphi\varphi_z\mathrm{d}x/\int_{\omega_z}\varphi_z\,\mathrm{d}x-\varphi\Big)\nabla\varphi_z||_{L^2(\omega_z)}\lesssim|\!|\!|\varphi|\!|\!|_{\omega_z}.$$

In the last case, let $z\in\mathcal{N}(\Gamma_D)$. It holds $\varphi_z>0$ on part of the Dirichlet boundary

Γ_D. Since $|\nabla\varphi_z| \approx h_z^{-1}$ a Friedrichs inequality yields

$$||\varphi\nabla\varphi_z||_{L^2(\omega_z)} \lesssim |\!|\!|\varphi|\!|\!|_{\omega_z}.$$

The combination of the four cases and the finite overlap argument of $(\Omega_z)_{z\in\mathcal{N}}$ conclude the proof of ©. □

4.3.4. Efficiency of the discrete Lagrange multiplier for CFEM

This section designs a discrete Lagrange multiplier $\mu = \lambda_C \in S^1(\mathcal{E}(\Gamma_C); (-\infty, 0])$. With the modified basis function ψ_z, define a discrete Lagrange multiplier $\lambda_C \in S^1(\mathcal{E}(\Gamma_C); (-\infty, 0])$ by

$$\lambda_C := \sum_{z\in\mathcal{N}(\Gamma_C)} \Big(\sigma_C(\varphi_z)/\int_{\Gamma_C} \varphi_z \,\mathrm{d}s\Big)\psi_z|_{\Gamma_C}. \tag{4.21}$$

The discrete complementary conditions (4.17) show that indeed $\lambda_C \le 0$ along Γ_C.

Recall the solution $u \in K$ to (4.2) and the Lagrange multiplier Λ from (4.3). The subsequent theorem shows efficiency for the discrete Lagrange multiplier $\mu = \lambda_C$. For $\lambda_C \in S^1(\mathcal{E}(\Gamma_C); (-\infty, 0])$ and any $\lambda_0 \in L^2(\Gamma_C)$, define the operators $\Lambda_C, \Lambda_0 \in V^*$ by

$$\Lambda_C(\varphi) := \int_{\Gamma_C} \lambda_C\varphi \,\mathrm{d}s \quad \text{and} \quad \Lambda_0(\varphi) := \int_{\Gamma_C} \lambda_0\varphi \,\mathrm{d}s \text{ for all } \varphi \in V.$$

The discrete Lagrange multiplier λ_C is efficient in the following sense.

Theorem 4.20 (efficiency of the discrete Lagrange multiplier)**.** *The discrete solution $u_C \in K_C(\mathcal{T})$ to (4.16) and the discrete conforming Lagrange multiplier $\lambda_C \in S^1(\mathcal{E}(\Gamma_C); (-\infty, 0])$ in (4.21) satisfy*

$$|\!|\!|\Lambda - \Lambda_C|\!|\!|_* \lesssim |\!|\!|u - u_C|\!|\!| + \min_{\lambda_0\in L^2(\Gamma_C)} |\!|\!|\Lambda - \Lambda_0|\!|\!|_* + \mathrm{osc}_{1/2,C}(\lambda_0, \mathcal{N}(\Gamma_C)).$$

Remark 4.21. *This is not an exact realization of Theorem B, since in general, the exact Lagrange multiplier Λ does not have an L^2 representation $\lambda \in L^2(\Gamma_C)$ and hence an oscillation term cannot be defined. Under the assumptions of Theorem 4.3 however, the exact Lagrange multiplier satisfies $\lambda \in L^2(\Gamma_C)$ and hence*

$$\min_{\lambda_0\in L^2(\Gamma_C)} |\!|\!|\Lambda - \Lambda_0|\!|\!|_* + \mathrm{osc}_{1/2,C}(\lambda_0, \mathcal{N}(\Gamma_C)) = \mathrm{osc}_{1/2,C}(\lambda, \mathcal{N}(\Gamma_C)).$$

The proof of Theorem 4.20 relies on the following lemma, which follows from elementary algebra. The connection between the interpolation operator J_C^* and the discrete Lagrange multiplier becomes apparent.

Lemma 4.22. *For all $\varphi \in V$, the discrete Lagrange multiplier λ_C from (4.21) and the interpolation operator J_C^* from (4.18) satisfy*

$$\int_{\Gamma_C} \lambda_C\varphi \,\mathrm{d}s = a(u_C, J_C^*\varphi) - F(J_C^*\varphi).$$

Proof. Since F and $a(u_{\mathrm{C}}, \bullet)$ are linear forms, which satisfy $F(\varphi_z) = a(u_{\mathrm{C}}, \varphi_z)$ for all $z \in \mathcal{N} \setminus \mathcal{N}(\Gamma_{\mathrm{C}} \cup \Gamma_D)$, the discrete Lagrange multiplier satisfies

$$\begin{aligned}\int_{\Gamma_C} \lambda_{\mathrm{C}} \varphi \,\mathrm{d}s &= \sum_{z \in \mathcal{N}(\overline{\Gamma}_C) \setminus \mathcal{N}(\Gamma_D)} \big(F(\varphi_z) - a(u_{\mathrm{C}}, \varphi_z)\big) \int_{\Gamma_C} \varphi \psi_z \,\mathrm{d}s \,/ \int_{\Gamma_C} \varphi_z \,\mathrm{d}s \\ &= F\Big(\sum_{z \in \mathcal{N}(\overline{\Gamma}_C) \setminus \mathcal{N}(\Gamma_D)} \int_{\Gamma_C} \varphi \psi_z \,\mathrm{d}s \,/ \int_{\Gamma_C} \varphi_z \,\mathrm{d}s \, \varphi_z \Big) \\ &\quad - a\Big(u_{\mathrm{C}}, \sum_{z \in \mathcal{N}(\overline{\Gamma}_C) \setminus \mathcal{N}(\Gamma_D)} \int_{\Gamma_C} \varphi \psi_z \,\mathrm{d}s \,/ \int_{\Gamma_C} \varphi_z \,\mathrm{d}s \, \varphi_z \Big) \\ &= F(J_C^* \varphi) - a(u_{\mathrm{C}}, J_C^* \varphi). \end{aligned}$$

□

Proof of Theorem 4.20. Let $\varphi \in V$ with $|\!|\!|\varphi|\!|\!| = 1$. The interpolation operator J_C^* from Subsection 4.3.3 and the definition of Λ_{C} allow the split

$$(\Lambda - \Lambda_{\mathrm{C}})(\varphi) = \Lambda(\varphi - J_C^* \varphi) + \Lambda(J_C^* \varphi) - \int_{\Gamma_C} \lambda_{\mathrm{C}} \varphi \,\mathrm{d}s \; = ① + ②.$$

For an arbitrary $\lambda_0 \in L^2(\Gamma_C)$, Theorem 4.19.b and c show that

$$\begin{aligned} ① &= \Lambda(\varphi - J_C^* \varphi) - \Lambda_0(\varphi - J_C^* \varphi) + \int_{\Gamma_C} \lambda_0 (\varphi - J_C^* \varphi) \,\mathrm{d}s \\ &\lesssim |\!|\!| \Lambda - \Lambda_0 |\!|\!|_* + \mathrm{osc}_{1/2,C}(\lambda_0, \mathcal{N}(\Gamma_C)). \end{aligned}$$

The definition of the continuous Lagrange multiplier Λ and the interpolation operator J_C^* imply, with Lemma 4.22, that

$$② := \Lambda(J_C^* \varphi) - \int_{\Gamma_C} \lambda_{\mathrm{C}} \varphi \,\mathrm{d}s \lesssim a(u - u_{\mathrm{C}}, J_C^* \varphi).$$

The stability of the interpolation operator J_C^* in Theorem 4.19.c and a Cauchy inequality conclude the proof. □

4.3.5. Comments on the complementary condition residual

This subsection analyzes the efficiency of the computable integral $\int_{\Gamma_C} (-\lambda_{\mathrm{C}})(u_{\mathrm{C}} - \chi) \,\mathrm{d}s$ in Est, which is a complementary condition residual. Let Ω be a convex polygonal domain and define a set of Dirichlet edges which is close to the contact boundary Γ_C by

$$\mathcal{E}(\Gamma_C \cap \Gamma_D) := \{E \in \mathcal{E}(\partial\Omega) \mid \exists z \in \mathcal{N}(E) \cap \mathcal{N}(\overline{\Gamma}_C) \cap \mathcal{N}(\Gamma_D)\}.$$

Extend the contact boundary Γ_C to

$$\tilde{\Gamma}_C := \Gamma_C \cup \bigcup_{E \in \mathcal{E}(\Gamma_C \cap \Gamma_D)} E$$

and define

$$\omega_C := \mathrm{int}\{T \in \mathcal{T}(z) \mid z \in \mathcal{N}(\tilde{\Gamma}_C)\}.$$

The subsequent theorem proves efficiency up to higher-order terms for an obstacle $\chi \in H^1(\Omega)$ with (4.1) and

$$\chi|_{\Gamma_C \cup \Gamma_D} \in H^{2/3}(\Gamma_C \cup \Gamma_D) \text{ and } \chi|_{\omega_C} \in P_1(\omega_C).$$

Remark 4.23. *The assumptions on the obstacle and the domain Ω guarantee that $u \in H^2(\Omega)$ and hence $\lambda \in L^2(\Gamma_C; (-\infty, 0])$ (cf. Theorem 4.3.)*

The following theorem employs the subsets $\mathcal{E}_C$ and $\mathcal{E}_{DC}$ of $\mathcal{E}(\Gamma_C)$ given by

$$\begin{aligned}\mathcal{E}_C &:= \{E \in \mathcal{E}(\Gamma_C) \mid \exists z \in \mathcal{N}(E) \cap \mathcal{N}(\Gamma_C) \text{ with an interior angle } \omega \neq \pi \text{ at } z \\ &\qquad \text{or } z \in \mathcal{N}(\Gamma_C) \cap \mathcal{N}(\overline{\Gamma}_N)\}, \\ \mathcal{E}_{DC} &:= \{E \in \mathcal{E}(\Gamma_C) \mid \mathcal{N}(E) \cap \mathcal{N}(\Gamma_D) \neq \emptyset\}.\end{aligned}$$

In other words, $\mathcal{E}_C$ denotes the edges in $\mathcal{E}(\Gamma_C)$ at convex corner points or at the Neumann boundary Γ_N and $\mathcal{E}_{DC}$ describes edges $E \in \mathcal{E}(\Gamma_C)$ which have a neighbouring Dirichlet edge $F \in \mathcal{E}(\Gamma_D)$.

Theorem 4.24. *For an obstacle $\chi \in H^1(\Omega)$ with (4.1), $\chi|_{\Gamma_C \cup \Gamma_D} \in H^{3/2}(\Gamma_C \cup \Gamma_D)$, and $\chi \in P_1(\omega_C)$, it holds*

$$\begin{aligned}\int_{\Gamma_C} (-\lambda_{\mathrm{C}})(u_{\mathrm{C}} - \chi)\,\mathrm{d}s \lesssim |\!|\!| u - u_{\mathrm{C}} |\!|\!|^2 + \operatorname{osc}^2(f, \mathcal{T}) + \operatorname{Osc}^2_{1/2,C}(\lambda, \mathcal{E}(\Gamma_C)) \\ + \sum_{E \in \mathcal{E}_C} |\!|\!| u - \chi |\!|\!|^2_{\omega_E} + \sum_{E \in \mathcal{E}_{DC}} ||h_E^{1/2} \lambda||^2_{L^2(E)}.\end{aligned}$$

Remark 4.25. *The terms $\sum_{E \in \mathcal{E}_C(\Gamma_C)} |\!|\!| u - \chi |\!|\!|^2_{\omega_E}$ and $\sum_{E \in \mathcal{E}_{DC}} ||h_E \lambda||^2_{L^2(E)}$ appear only for a bounded number of edges. Since the assumptions on the domain Ω and the obstacle χ guarantee that $u \in H^2(\Omega)$,*

$$|\!|\!| u - \chi |\!|\!|^2_{\omega_E} \lesssim h^2_{\max} \quad \text{and} \quad ||h_E^{1/2} \lambda||^2_{L^2(E)} \lesssim h^2_{\max}$$

holds for all $E \in \mathcal{E}$. Hence

$$\sum_{E \in \mathcal{E}_C} |\!|\!| u - \chi |\!|\!|^2_{\omega_E} \lesssim h^2_{\max} \quad \text{and} \quad \sum_{E \in \mathcal{E}_{DC}} ||h_E^{1/2} \lambda||^2_{L^2(E)} \lesssim h^2_{\max}$$

are of first order.

Corollary 4.26. *For $\chi \in H_1(\Omega)$ which satisfies (4.1), $\chi|_{\Gamma_C \cup \Gamma_D} \in H^{3/2}(\Gamma_C \cup \Gamma_D)$ and $\chi|_{\omega_C} \in P_1(\omega_z)$ and $\mu = \lambda_{\mathrm{C}}$, the guaranteed upper bound* GUB = 30Est *is efficient with respect to the energy error $|\!|\!| u - u_{\mathrm{C}} |\!|\!|$ and the total error* Err *of Theorem 4.14 in the sense that*

$$\begin{aligned}|\!|\!| u - u_{\mathrm{C}} |\!|\!|^2 \leq \mathrm{Err}^2 \approx \mathrm{GUB}^2 \lesssim |\!|\!| u - u_{\mathrm{C}} |\!|\!|^2 + \sum_{E \in \mathcal{E}_C} |\!|\!| u - \chi |\!|\!|^2_{\omega_E} \\ + \sum_{E \in \mathcal{E}_{DC}} ||h_E^{1/2} \lambda||^2_{L^2(E)} + \textit{higher-order terms.}\end{aligned}$$

Proof. The proof follows from a combination of Theorems 4.14, 4.20, and 4.24. □

Remark 4.27. *The higher-order terms in Corollary 4.26 consist of the oscillation terms* $\operatorname{osc}(f, \mathcal{T})$ *and* $\operatorname{Osc}_{1/2,C}(\lambda, \mathcal{E}(\Gamma_C))$.

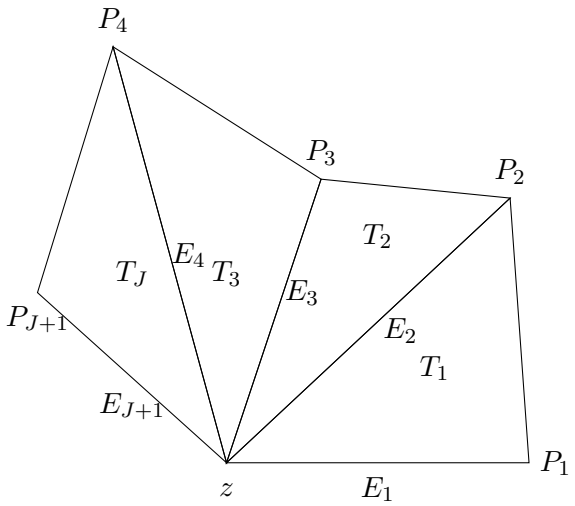

Figure 4.2.: Enumeration of triangles in the patch ω_z.

The following two lemmas characterize the constants in Theorem 4.24. They employ the following notation, displayed in Figure 4.2. For a node $z \in \mathcal{N}(\partial\Omega)$, the set $\mathcal{T}(z)$ contains $\mathcal{T}(z) := \{T_1, ..., T_J\}$. For $j = 1, ..., J+1$, the edges $E_j \in \mathcal{E}(z)$ are given by $E_j := \mathrm{conv}\{z, P_j\}$ for the vertices $P_1, ..., P_{J+1}$. Define the set $\mathcal{E}'(z) := \{E \in \mathcal{E}(z) \mid E \text{ is an interior edge}\}$ and $h(z) := \max\{|E| \;\big|\; E \in \mathcal{E}(z)\}$.

Lemma 4.28. *For a node $z \in \mathcal{N}(\partial\Omega)$ with $\mathcal{T}(z) = \{T_1, ..., T_J\}$ and edges $E_j := \mathrm{conv}\{z, P_j\}$ for $j = 1, ..., J+1$ as above, it holds*

$$\left|\nabla v_{\mathrm{C}}|_{T_J} - \nabla v_{\mathrm{C}}|_{T_1}\right| \leq \sqrt{\sum_{E\in\mathcal{E}'(z)} |E|^{-2}} \sqrt{\sum_{E\in\mathcal{E}'(z)} |E| \|[\partial v_{\mathrm{C}}/\partial\nu_E]_E\|^2_{L^2(E)}}.$$

Proof. A triangle inequality followed by a weighted Cauchy inequality in $\mathbb{R}^{J-1}$ shows

$$\begin{aligned}
\left|\nabla v_{\mathrm{C}}|_{T_J} - \nabla v_{\mathrm{C}}|_{T_1}\right| &\leq \sum_{j=1}^{J-1} \left|\nabla v_{\mathrm{C}}|_{T_{j+1}} - \nabla v_{\mathrm{C}}|_{T_j}\right| \\
&\leq \sum_{j=1}^{J-1} \left(\left|[\partial v_{\mathrm{C}}/\partial\nu_{E_{j+1}}]_{E_{j+1}}\right| |E_{j+1}|\right) \left(|E_{j+1}|^{-1}\right) \\
&\leq \sqrt{\sum_{E\in\mathcal{E}'(z)} |E|^{-2}} \sqrt{\sum_{E\in\mathcal{E}'(z)} |E| \, \|[\partial v_{\mathrm{C}}/\partial\nu_E]_E\|^2_{L^2(E)}}. \qquad \square
\end{aligned}$$

Lemma 4.29. *For a node $z \in \mathcal{N}(\partial\Omega)$ with an interior angle equal to π at $z \in \mathcal{N}(\partial\Omega)$, any $v_{\mathrm{C}} \in S^1(\mathcal{T})$ with $v_{\mathrm{C}}(z) = 0 \leq v_{\mathrm{C}}|_{E_1\cup E_{J+1}}$ satisfies*

$$||\nabla v_{\mathrm{C}} \cdot \tau||^2_{L^2(\gamma_z)} \leq C(\gamma_0) \sum_{F\in\mathcal{E}'(z)} |F| \, \|[\nabla v_{\mathrm{C}} \cdot \nu_F]_F\|^2_{L^2(F)}.$$

The constant $C(\gamma_0) > 0$, only depends on the shape-regularity of the triangulation $\mathcal{T}$ and τ denotes the tangential unit vector.

Proof. Set $A_j := \nabla v_C|_{T_j}$ for $j = 1, ..., J$ and compute

$$||\nabla v_C \cdot \tau||^2_{L^2(\gamma_z)} = |E_1|\,|A_1 \cdot \tau_{E_1}|^2 + |E_{J+1}|\,|A_J \cdot \tau_{E_{J+1}}|^2.$$

Since $v_C(z) = 0 \leq v_C|_{E_1 \cup E_{J+1}}$, it holds $\nabla v_C|_{T_1} \cdot \tau_{E_1} = A_1 \cdot \tau_{E_1} \leq 0 \leq \nabla v_C|_{T_J} \cdot \tau_{E_{J+1}} = A_J \cdot \tau_{E_{J+1}}$. This leads to

$$||\nabla v_C \cdot \tau||^2_{L^2(\gamma_z)} \leq h(z)|(A_1 - A_J) \cdot \tau|^2$$

for the tangential vector τ along γ_z. Recall that $A_1 = \nabla v_C|_{T_1}$ and $A_J = \nabla v_C|_{T_J}$ and note that there exists a constant $C(\gamma_0)$ which only depends on the shape-regularity of the triangulation $\mathcal{T}$ such that $\sqrt{\sum_{E \in \mathcal{E}'(z)} |E|^{-2}} \leq C(\gamma_0) h(z)^{-1}$. This and Lemma 4.28 conclude the proof. □

Proof of Theorem 4.24. The proof follows from *Claim 1–3* below.

Claim 1. It holds

$$\begin{aligned}\int_{\Gamma_C} (-\lambda_C)(u_C - \chi)\,\mathrm{d}s \lesssim & \sum_{E \in \mathcal{E}(\Gamma_C) \setminus \mathcal{E}_{DC}} \|h_E^{3/2} \partial \lambda_C / \partial s\|^2_{L^2(E)} \\ & + \sum_{F \in \mathcal{E}(\Omega)} |F| \|[\nabla u_C \cdot \nu_F]_{L^2(F)}\|^2_F \\ & + \sum_{E \in \mathcal{E}_C} |\!|\!| u_C - \chi |\!|\!|^2_{\omega_E} + \sum_{E \in \mathcal{E}_{DC}} ||h_E^{1/2} \lambda_C||^2_{L^2(E)}.\end{aligned}$$

Proof. Consider the integral $I_E := \int_E (-\lambda_C)(u_C - \chi)\,\mathrm{d}s$ for each edge $E \in \mathcal{E}(\Gamma_C)$ separately. The complementary conditions reduce the analysis to the case of an edge $E := \mathrm{conv}\{y, z\} \in \mathcal{E}(\Gamma_C)$ with $(u_C - \chi)(z) = 0 < (u_C - \chi)(y)$. If $y, z \in \mathcal{N}(\overline{\Gamma}_C \setminus \Gamma_D)$, it follows that $\lambda_C(y) = 0$ and hence a Cauchy inequality followed by a Friedrichs inequality shows

$$I_E \lesssim \|h_E \partial \lambda_C / \partial s\|_{L^2(E)} \|u_C - \chi\|_{L^2(E)}.$$

If $y \in \mathcal{N}(\Gamma_D)$, the modification of the nodal basis functions and the definition of λ_C, show that λ_C is constant along E, and hence

$$I_E \leq ||\lambda_C||_{L^2(E)} ||u_C - \chi||_{L^2(E)}.$$

Since $(u_C - \chi)(z) = 0 < (u_C - \chi)(y)$, a Friedrichs inequality results in

$$||u_C - \chi||_{L^2(E)} \lesssim |E| ||\nabla(u_C - \chi) \cdot \tau_E||_{L^2(E)}.$$

The combination of the three last displayed estimates leads to

$$\begin{aligned}\int_{\Gamma_C} & (-\lambda_C)(u_C - \chi)\,\mathrm{d}s \\ & \lesssim \sum_{E \in \mathcal{E}(\Gamma_C) \setminus \mathcal{E}_{DC}} |E|\,||h_E \partial \lambda_C / \partial s||_{L^2(E)} ||\nabla(u_C - \chi) \cdot \tau_E||_{L^2(E)} \\ & \quad + \sum_{E \in \mathcal{E}_{DC}} |E|\,||\lambda_C||_{L^2(E)} ||\nabla(u_C - \chi) \cdot \tau_E||_{L^2(E)}. \qquad (4.22)\end{aligned}$$

To estimate $||\nabla(u_C - \chi)\cdot\tau_E||_{L^2(E)}$ consider two cases for $E := \mathrm{conv}\{y,z\}$ with $(u_C-\chi)(z) = 0 \le (u_C-\chi)(y)$. In the first case, suppose that there exists a neighbouring node $y' \in \mathcal{N}(\Gamma_C)$ such that $\mathrm{conv}\{y',z\} \in \mathcal{E}(\Gamma_C)$ with an angle equal to π at z, i.e., $E \in \mathcal{E}(\Gamma_C)\setminus\mathcal{E}_C$. Then Lemma 4.29 shows

$$||\nabla(u_C-\chi)\cdot\tau_E||_{L^2(E)} \lesssim \sqrt{\sum_{F\in\mathcal{E}'(z)} |F|\,||[\nabla u_C\cdot\nu_F]_F||^2_{L^2(F)}}.$$

In the second case, $E\in\mathcal{E}_C$, a trace inequality shows

$$||\nabla(u_C-\chi)\cdot\tau_E||_{L^2(E)} \lesssim |||u_C-\chi|||_{\omega_E} \le |||u-u_C|||_{\omega_E} + |||u-\chi|||_{\omega_E}.$$

The combination of the last two displayed estimates with (4.22) and a Young inequality complete the proof of *Claim 1.* □

Claim 2. ⓐ For $E\in\mathcal{E}(\Gamma_C)$, it holds

$$\|h_E^{3/2}\partial\lambda_C/\partial s\|_E \lesssim |||u-u_C|||_{\omega_E} + \mathrm{Osc}_{1/2,C}(\lambda,E).$$

ⓑ For $E\in\mathcal{E}_{DC}$ it holds

$$||h_E^{1/2}\lambda_C||_{L^2(E)} \lesssim ||h_E^{1/2}\lambda||_{L^2(E)} + |||u-u_C|||_{\omega_E}.$$

Proof. The discrete Lagrange multiplier satisfies

$$\begin{aligned}(\partial\lambda_C/\partial s)|_E &= \sum_{z\in\mathcal{N}(E)\cap\mathcal{N}(\Gamma_C)} \Big((F(\varphi_z)-a(u_C,\varphi_z))/\int_{\Gamma_C}\varphi_z\,\mathrm{d}s\Big)(\partial\psi_z/\partial s)|_E\\ &= \sum_{z\in\mathcal{N}(E)\cap\mathcal{N}(\Gamma_C)} \Big((F(\varphi_z)-a(u_C-u,\varphi_z)-a(u,\varphi_z))/\int_{\Gamma_C}\varphi_z\,\mathrm{d}s\Big)(\partial\psi_z/\partial s)|_E\\ &= \sum_{z\in\mathcal{N}(E)\cap\mathcal{N}(\Gamma_C)} \Big((\Lambda(\varphi_z)-a(u_C-u,\varphi_z))/\int_{\Gamma_C}\varphi_z\,\mathrm{d}s\Big)(\partial\psi_z/\partial s)|_E.\end{aligned}$$

Recall, that the assumptions on the data guarantee that $\Lambda(\varphi_z) = -\int_{\Gamma_C}(\nabla u\cdot\nu - g)\varphi_z\,\mathrm{d}s$. Since the discrete functions $(\psi_z|_E)_{z\in\mathcal{N}(E)\cap\mathcal{N}(\Gamma_C)}$ form a partition of unity on the edge E, it holds

$$\begin{aligned}||h_E^{3/2}\partial\lambda_C/\partial s||_{L^2(E)} =& \|h_E^{3/2}\sum_{z\in\mathcal{N}(E)\cap\mathcal{N}(\Gamma_C)} \Big((\int_{\Gamma_C}\lambda\varphi_z\,\mathrm{d}s - a(u_C-u,\varphi_z))/\int_{\Gamma_C}\varphi_z\,\mathrm{d}s\\ &- \fint_{\partial\Omega_E\cap\Gamma_C}\lambda\,\mathrm{d}s\Big)\partial\psi_z/\partial s\|_{L^2(E)}.\end{aligned}$$

Since $||\partial\psi_z/\partial s||_{L^2(E)} \lesssim h_z^{-1/2} \approx |E|^{-1/2}$ and $1/\int_{\Gamma_C}\varphi_z\,\mathrm{d}s \lesssim |E|^{-1}$, a Cauchy inequality proves

$$||h_E^{3/2}\partial\lambda_C/\partial s||_{L^2(E)} \lesssim |||u-u_C|||_{\omega_z} + \mathrm{Osc}_{1/2}(\lambda,E).$$

This concludes the proof of ⓐ. □

For the proof of ⓑ, let $E := \mathrm{conv}\{y,z\}$ with $z\in\mathcal{N}(\overline{\Gamma}_C\cap\Gamma_D)$. Note that λ_C is

constant along E with $\lambda_C = \lambda_C(y)$. Then it holds

$$\begin{aligned}||h_E^{1/2}\lambda_C||_{L^2(E)} &= |E|\left|F(\varphi_y) - a(u_C, \varphi_y)\right| / \int_{\Gamma_C} \varphi_y \,\mathrm{d}s \\ &= |E|\left|F(\varphi_y) - a(u_C - u, \varphi_y) - a(u, \varphi_y)\right| / \int_{\Gamma_C} \varphi_y \,\mathrm{d}s.\end{aligned}$$

Since $\int_{\Gamma_C} \varphi_y \,\mathrm{d}s \approx |E|$, a Cauchy inequality and the definition of the exact Lagrange multiplier λ result in

$$||h_E^{1/2}\lambda_C||_{L^2(E)} \lesssim ||h_E^{1/2}\lambda||_{L^2(E)} + |||u - u_C|||_{\omega_E}.$$

This concludes the proof of ⓑ. □

Claim 3. It holds

$$\begin{aligned} ||h_{\mathcal{T}} f||_{L^2(T)} &\lesssim \operatorname{osc}(f, T) + |||u - u_C|||_T && \text{for all } T \in \mathcal{T}, \\ |E|||[\nabla u_C \cdot \nu_E]_E||_{L^2(E)} &\lesssim |||u - u_C|||_{\omega_E} + \operatorname{osc}(f, \omega_E) && \text{for all } E \in \mathcal{E}(\Omega). \end{aligned}$$

Proof. To prove ⓐ, let $b_T := 60\Pi_{z\in\mathcal{N}(T)}\varphi_z \in H_0^1(T) \cap P_3(T)$ denote the cubic bubble function on the triangle $T \in \mathcal{T}$ with $⨍_T b_T \,\mathrm{d}x = 1$. Define $w_T := \Pi_0 f b_T$. Since the contact boundary is not involved, the arguments in Verfürth (1996) yield

$$||h_T f||_{L^2(T)} \lesssim \operatorname{osc}(f, T) + |||u - u_C|||_T.$$

To prove ⓑ, let $b_E := 6\Pi_{z\in\mathcal{N}(E)}\varphi_z \in H_0^1(\omega_E) \cap P_2(\omega_E)$ denote the quadratic edge bubble with $⨍_E \,\mathrm{d}s = 1$. Define $w_E := [\nabla u_C \cdot \nu_E]_E b_E$. Since $E \in \mathcal{E}(\Omega)$ is an interior edge, the arguments in Verfürth (1996) result in

$$|E|^{1/2}||[\nabla u_C \cdot \nu_E]_E||_{L^2(E)} \lesssim ||h_E f||_{L^2(\omega_E)} + |||u - u_C|||_{\omega_E}.$$

The combination with ⓐ concludes the proof. □

The combination of *Claim 1–3* concludes the proof. □

4.4. Non-conforming FEM for Signorini's problem

This section is devoted to the analysis of the non-conforming Crouzeix-Raviart FEM for Signorini's problem in two space dimensions. It suggests a discrete Lagrange multiplier $\mu = \lambda_{CR} \in P_0(\mathcal{E}(\Gamma_C); (-\infty, 0])$ and proves its efficiency in the sense of Theorem B. For some $v \in \mathcal{A}$, this section also analyzes the efficiency of the complementary condition residual $\int_{\Gamma_C}(-\lambda_{CR})(v-\chi)_+ \,\mathrm{d}s$ in the sense of Theorem C.

4.4.1. Non-conforming discretization

Given a shape-regular triangulation $\mathcal{T}$ of $\Omega \subset \mathbb{R}^2$ from Subsection 2.2.1 on Page 11, recall the non-conforming Crouzeix-Raviart spaces $\mathrm{CR}^1(\mathcal{T})$ and $\mathrm{CR}^1_D(\mathcal{T})$ from Definition 2.13 on Page 15. To approximate the Dirichlet boundary conditions, define

$$u_{D,\mathrm{NC}} := \sum_{E\in\mathcal{E}(\Gamma_D)} ⨍_E u_D \,\mathrm{d}s \,\psi_E.$$

This leads to the discrete subset

$$\mathcal{A}_{\mathrm{NC}}(\mathcal{T}) := u_{D,\mathrm{NC}} + \mathrm{CR}^1_D(\mathcal{T})$$

of $\mathrm{CR}^1(\mathcal{T})$ and the non-empty and convex subset of $\mathcal{A}_{\mathrm{NC}}(\mathcal{T})$

$$K_{\mathrm{CR}}(\mathcal{T}) := \{v_{\mathrm{CR}} \in \mathcal{A}_{\mathrm{NC}}(\mathcal{T}) \mid \fint_E \chi \,\mathrm{d}s \le \fint_E v_{\mathrm{CR}} \,\mathrm{d}s \text{ for all } E \in \mathcal{E}(\Gamma_C)\}. \quad (4.23)$$

Recall the bilinear form $a_{\mathrm{NC}}(\bullet,\bullet)$ from (2.6) on Page 19. The discrete variational inequality seeks $u_{\mathrm{CR}} \in K_{\mathrm{CR}}(\mathcal{T})$ such that

$$F(v_{\mathrm{CR}} - u_{\mathrm{CR}}) \le a_{\mathrm{NC}}(u_{\mathrm{CR}}, v_{\mathrm{CR}} - u_{\mathrm{CR}}) \quad \text{for all } v_{\mathrm{CR}} \in K_{\mathrm{CR}}(\mathcal{T}). \quad (4.24)$$

Lemma 4.30 (existence of solutions)**.** *There exists a unique discrete solution $u_{\mathrm{CR}} \in K_{\mathrm{CR}}(\mathcal{T})$ to (4.24).*

Proof. Since $a_{\mathrm{NC}}(\bullet,\bullet)$ is a scalar product on $\mathrm{CR}^1_D(\mathcal{T}) \times \mathrm{CR}^1_D(\mathcal{T})$ the proof follows after a shift of χ to $\chi - u_{D,\mathrm{NC}}$ and of F to $F + a_{\mathrm{NC}}(u_{D,\mathrm{NC}}, \bullet)$ from Kinderlehrer and Stampacchia (1980, Thm. 2.1). □

Lemma 4.31 (discrete complementary conditions)**.** *The solution $u_{\mathrm{CR}} \in K_{\mathrm{CR}}(\mathcal{T})$ to (4.24) satisfies the discrete complementary conditions*

$$0 \le \fint_E (u_{\mathrm{CR}} - \chi) \,\mathrm{d}s \perp F(\psi_E) - a_{\mathrm{NC}}(u_{\mathrm{CR}}, \psi_E) =: \sigma_{\mathrm{CR}}(\psi_E) \le 0 \quad (4.25)$$

for all $E \in \mathcal{E}(\Gamma_C)$, where $\perp$ abbreviates pointwise orthogonality in $\mathbb{R}$, i.e., $a \perp b$ signifies $ab = 0$ for $a, b \in \mathbb{R}$.

Proof. The first inequality follows from the definition of $K_{\mathrm{CR}}(\mathcal{T})$. For any $E \in \mathcal{E}(\Gamma_C)$, $v_{\mathrm{CR}} := u_{\mathrm{CR}} + \psi_E \in K_{\mathrm{CR}}(\mathcal{T})$. Hence the discrete variational inequality (4.24) shows $\sigma_{\mathrm{CR}}(\psi_E) \le 0$. To prove orthogonality, consider the test functions $v_{\mathrm{CR}} := \fint_E (2u_{\mathrm{CR}} - \chi) \,\mathrm{d}s\, \psi_E$ and $v_{\mathrm{CR}} = \fint_E \chi \,\mathrm{d}s\, \psi_E$ for all $E \in \mathcal{E}(\Gamma_C)$. The discrete variational inequality (4.24) yields

$$\sigma_{\mathrm{CR}}(\psi_E) \fint_E (u_{\mathrm{CR}} - \chi) \,\mathrm{d}s = F(\fint_E (u_{\mathrm{CR}} - \chi) \,\mathrm{d}s \psi_E) - a_{\mathrm{NC}}(u_{\mathrm{CR}}, \fint_E (u_{\mathrm{CR}} - \chi) \,\mathrm{d}s\, \psi_E) = 0$$

and concludes the proof. □

4.4.2. Conforming companion and boundary conditions

To employ Theorem 4.14, a conforming companion $v \in \mathcal{A}$ to the discrete solution $u_{\mathrm{CR}} \in K_{\mathrm{CR}}(\mathcal{T})$ to (4.24) needs to be defined. This section presents a modification of the conforming companion operator $J_2 : \mathrm{CR}^1_0(\mathcal{T}) \to S^2_0(\mathcal{T})$ from Theorem 2.27 on Page 18, which allows for the correct treatment along the contact boundary. For each edge $E \in \mathcal{E}$, define the edge-oriented quadratic bubble function $b_E := 6\Pi_{z \in \mathcal{N}(E)} \varphi_z \in H^1_0(\omega_E) \cap P_2(\mathcal{T}(\omega_E))$, which satisfies $\mathrm{supp}(b_E) = \overline{\omega}_E$ and $\fint_E b_E \,\mathrm{d}s = 1$. For $z \in \mathcal{N}(\Gamma_C)$, note that the set $\mathcal{E}(z) \cap \mathcal{E}(\Gamma_C)$ contains either one or two edges. For each edge $E \in \mathcal{E}(z) \cap \mathcal{E}(\Gamma_C)$ set

$$\Theta_E(z) := |E| / \sum_{F \in \mathcal{E}(z) \cap \mathcal{E}(\Gamma_C)} |F|.$$

The definition of the conforming companions J_1^C and J_2^C below is a modification of the conforming functions J_1, J_2 presented in Theorem 2.27 on Page 18. Given $v_{\mathrm{CR}} \in \mathrm{CR}^1_D(\mathcal{T})$ define

$$J_1^C v_{\mathrm{CR}}(z) := \sum_{T\in\mathcal{T}(z)} v_{\mathrm{CR}}|_T(z)/|\mathcal{T}(z)| \quad \text{for } z \in \mathcal{N}(\Omega)\cup\mathcal{N}(\Gamma_N),$$

$$J_1^C v_{\mathrm{CR}}(z) := \sum_{E\in\mathcal{E}(z)\cap\mathcal{E}(\Gamma_C)} \Theta_E(z)\, v_{\mathrm{CR}}(\mathrm{mid}(E)) \quad \text{for } z \in \mathcal{N}(\Gamma_C).$$

Recall that $\mathcal{T}(z) := \{T \in \mathcal{T} \mid z \in \mathcal{N}(T)\}$ with cardinality $|\mathcal{T}(z)|$. The function $J_1^C v_{\mathrm{CR}} \in S^1_D(\mathcal{T})$ is given by the linear interpolation of its nodal values from above. For all $v_{\mathrm{CR}} \in \mathrm{CR}^1_D(\mathcal{T})$, the operator $J_2^C : \mathrm{CR}^1_D(\mathcal{T}) \to S^2_D(\mathcal{T})$ is defined by

$$J_2^C v_{\mathrm{CR}} := J_1^C v_{\mathrm{CR}} + \sum_{E\in\mathcal{E}(\Omega)\cup\mathcal{E}(\Gamma_N\cup\Gamma_C)} \fint_E (v_{\mathrm{CR}} - J_1^C v_{\mathrm{CR}})\,\mathrm{d}s\, b_E.$$

Proposition 4.32. *For all $v_{\mathrm{CR}} \in \mathrm{CR}^1_D(\mathcal{T})$, the conforming companion operators J_1^C and J_2^C satisfy*

ⓐ $h_{\mathcal{T}}^{-1}||J_k^C v_{\mathrm{CR}} - v_{\mathrm{CR}}||_{L^2(\Omega)} + |\!|\!| J_k^C v_{\mathrm{CR}} - v_{\mathrm{CR}} |\!|\!|_{\mathrm{NC}} \lesssim \min_{v\in H^1_D(\Omega)} |\!|\!| v - v_{\mathrm{CR}} |\!|\!|_{\mathrm{NC}}$ *for $k = 1, 2$;*

ⓑ $I_{\mathrm{NC}} J_2^C v_{\mathrm{CR}} = v_{\mathrm{CR}}$.

Proof. The proof of ⓐ follows in two steps. For each triangle $T \in \mathcal{T}$, the definition of $J_1^C v_{\mathrm{CR}}$ and a triangle inequality show

$$\|h_{\mathcal{T}}^{-1}(J_1^C v_{\mathrm{CR}} - v_{\mathrm{CR}})\|^2_{L^2(T)} \lesssim \sum_{z\in\mathcal{N}(T)} |(J_1^C v_{\mathrm{CR}} - v_{\mathrm{CR}})(z)|^2.$$

The sum over all triangles reads

$$\sum_{T\in\mathcal{T}}\sum_{z\in\mathcal{N}(T)} |(J_1^C v_{\mathrm{CR}} - v_{\mathrm{CR}})(z)|^2 = \sum_{z\in\mathcal{N}}\sum_{T\in\mathcal{T}(z)} |(J_1^C v_{\mathrm{CR}} - v_{\mathrm{CR}}|_T)(z)|^2.$$

For any $z \in \mathcal{N}(\Omega)$, Carstensen et al. (2012a, Thm. 5.1) show

$$\sum_{T\in\mathcal{T}(z)} |(J_1^C v_{\mathrm{CR}} - v_{\mathrm{CR}}|_T)(z)|^2 \lesssim \sum_{E\in\mathcal{E}(z)} |E|\, \|[\nabla v_{\mathrm{CR}}\cdot\tau_E]_E\|^2_{L^2(E)}.$$

For $z \in \mathcal{N}(\Gamma_N)$, let $\mathcal{E}'(z) := \mathcal{E}(z)\cap\mathcal{E}(\Omega)$. The arguments in Carstensen et al. (2012a, Thm. 5.1) show

$$\sum_{T\in\mathcal{T}(z)} |(J_1^C v_{\mathrm{CR}} - v_{\mathrm{CR}}|_T)(z)|^2 \lesssim \sum_{E\in\mathcal{E}'(z)} |E|\, \|[\nabla v_{\mathrm{CR}}\cdot\tau_E]_E\|^2_{L^2(E)}. \tag{4.26}$$

Note that the right-hand side of (4.26) includes only the jumps over the interior edges. For each edge $E \in \mathcal{E}(z)\cap\mathcal{E}(\Gamma_C)$ let $E := \mathrm{conv}\{z, y_E\}$ with $y_E \in \mathcal{N}(\partial\Omega)$. The patch ω_E consists only of one triangle $\omega_E \in \mathcal{T}$. Then

$$\sum_{T\in\mathcal{T}(z)} \left| J_1^C v_{\mathrm{CR}}(z) - v_{\mathrm{CR}}|_T(z) \right|^2$$
$$= \sum_{T\in\mathcal{T}(z)} \Big| \sum_{E\in\mathcal{E}(z)\cap\mathcal{E}(\Gamma_C)} \Theta_E(z) v_{\mathrm{CR}}(\mathrm{mid}(E)) - v_{\mathrm{CR}}|_T(z) \Big|^2.$$

For $E := \mathrm{conv}\{z, y_E\}$, it holds $v_{\mathrm{CR}}(\mathrm{mid}(E)) = 1/2(v_{\mathrm{CR}}|_{\omega_E}(z) + v_{\mathrm{CR}}|_{\omega_E}(y_E))$. The definition of the midpoint shows

$$\begin{aligned}&\left|\sum_{E\in\mathcal{E}(z)\cap\mathcal{E}(\Gamma_C)} \Theta_E(z) v_{\mathrm{CR}}(\mathrm{mid}(E)) - v_{\mathrm{CR}}|_T(z)\right|^2\\ &= \left|\sum_{E\in\mathcal{E}(z)\cap\mathcal{E}(\Gamma_C)} \Theta_E(z)/2\Big(v_{\mathrm{CR}}|_{\omega_E}(z) + v_{\mathrm{CR}}|_{\omega_E}(y_E)\Big) - v_{\mathrm{CR}}|_T(z)\right|^2.\end{aligned}$$

It holds $\sum_{E\in\mathcal{E}(z)\cap\mathcal{E}(\Gamma_C)} \Theta_E(z) = 1$ and hence

$$\begin{aligned}&\left|\sum_{E\in\mathcal{E}(z)\cap\mathcal{E}(\Gamma_C)} \Theta_E(z)/2\Big(v_{\mathrm{CR}}|_{\omega_E}(z) + v_{\mathrm{CR}}|_{\omega_E}(y_E)\Big) - v_{\mathrm{CR}}|_T(z)\right|^2\\ &= \left|\sum_{E\in\mathcal{E}(z)\cap\mathcal{E}(\Gamma_C)} \Theta_E(z)/2\Big(v_{\mathrm{CR}}|_{\omega_E}(z) + v_{\mathrm{CR}}|_{\omega_E}(y_E) - 2v_{\mathrm{CR}}|_T(z)\Big)\right|^2.\end{aligned}$$

A triangle inequality leads to

$$\begin{aligned}&\left|\sum_{E\in\mathcal{E}(z)\cap\mathcal{E}(\Gamma_C)} \Theta_E(z)/2\Big(v_{\mathrm{CR}}|_{\omega_E}(z) + v_{\mathrm{CR}}|_{\omega_E}(y_E) - 2v_{\mathrm{CR}}|_T(z)\Big)\right|^2\\ &\le \sum_{E\in\mathcal{E}(z)\cap\mathcal{E}(\Gamma_C)} \Theta_E(z)\left(\Big|v_{\mathrm{CR}}|_{\omega_E}(z) - v_{\mathrm{CR}}|_T(z)\Big|^2 + \Big|v_{\mathrm{CR}}|_{\omega_E}(y_E) - v_{\mathrm{CR}}|_T(z)\Big|^2\right).\end{aligned}$$

A further triangle inequality results in

$$\begin{aligned}&\sum_{E\in\mathcal{E}(z)\cap\mathcal{E}(\Gamma_C)} \Theta_E(z)\Big|v_{\mathrm{CR}}|_{\omega_E}(y_E) - v_{\mathrm{CR}}|_T(z)\Big|^2\\ &\le 2\sum_{E\in\mathcal{E}(z)\cap\mathcal{E}(\Gamma_C)} \Theta_E(z)\left(\Big|v_{\mathrm{CR}}|_{\omega_E}(y_E) - v_{\mathrm{CR}}|_{\omega_E}(z)\Big|^2 + \Big|v_{\mathrm{CR}}|_{\omega_E}(z) - v_{\mathrm{CR}}|_T(z)\Big|^2\right).\end{aligned}$$

The combination of the previous estimates leads to

$$\begin{aligned}&\sum_{T\in\mathcal{T}(z)} \Big|J_1^C v_{\mathrm{CR}}(z) - v_{\mathrm{CR}}|_T(z)\Big|^2\\ &\le \sum_{T\in\mathcal{T}(z)}\sum_{E\in\mathcal{E}(z)\cap\mathcal{E}(\Gamma_C)} \Big(3\Theta_E(z)\Big|v_{\mathrm{CR}}|_{\omega_E}(z) - v_{\mathrm{CR}}|_T(z)\Big|^2\\ &\qquad + 2\Big|v_{\mathrm{CR}}|_{\omega_E}(z) - v_{\mathrm{CR}}|_{\omega_E}(z)\Big|^2\Big)\\ &\le \max\{\Theta_E(z) \mid E\in\mathcal{E}(z)\cap\mathcal{E}(\Gamma_C)\}\Big(3\sum_{T\in\mathcal{T}(z)}\sum_{K\in\mathcal{T}(z)} \Big|v_{\mathrm{CR}}|_K(z) - v_{\mathrm{CR}}|_T(z)\Big|^2\\ &\qquad + 2\sum_{T\in\mathcal{T}(z)}\sum_{E\in\mathcal{E}(z)\cap\mathcal{E}(\Gamma_C)} \Big|v_{\mathrm{CR}}|_{\omega_E}(y_E) - v_{\mathrm{CR}}|_{\omega_E}(z)\Big|^2\Big).\end{aligned}$$

The first term leads to tangential jumps of the gradient as in Carstensen et al. (2012a, Thm. 5.1). To analyze the second term, recall that, since $E \in \mathcal{E}(z) \cap \mathcal{E}(\Gamma_C)$ is a boundary edge, ω_E consists of only one triangle. Since v_{CR} is an affine function along any edge E, the definition of the tangential derivative immediately leads to the necessary jump terms along the boundary. Altogether

$$||h_{\mathcal{T}}(J_1^C v_{\mathrm{CR}} - v_{\mathrm{CR}})||_{L^2(\Omega)} \lesssim \sum_{z\in\mathcal{N}} \sum_{E\in\mathcal{E}(z)} |E|\, \|[\nabla v_{\mathrm{CR}} \cdot \tau_E]_E\|^2_{L^2(E)}.$$

Hence, the arguments in Carstensen et al. (2012a, Thm. 5.1) show

$$h_{\mathcal{T}}^{-1}\|v_{\mathrm{CR}} - J_1^C v_{\mathrm{CR}}\|_{L^2(\Omega)} \lesssim \min_{v\in H^1_D(\Omega)} \|\nabla_{\mathrm{NC}}(v_{\mathrm{CR}} - v)\|_{L^2(\Omega)}.$$

The stability property $\|\!|v_{\mathrm{CR}} - J_1^C v_{\mathrm{CR}}|\!\| \lesssim \min_{v\in H^1_D(\Omega)} |\!|\!| v - v_{\mathrm{CR}} |\!|\!|$ follows from an inverse estimate argument.
For the second step, note that the design of J_2^C (with J_1^C instead of J_1) is analogue to the design of J_2 in Carstensen et al. (2015a). The proof of

$$h_{\mathcal{T}}^{-1}||J_2^C v_{\mathrm{CR}} - v_{\mathrm{CR}}||_{L^2(\Omega)} + |\!|\!| J_2^C v_{\mathrm{CR}} - v_{\mathrm{CR}} |\!|\!| \lesssim \min_{v\in H^1_D(\Omega)} |\!|\!| v - v_{\mathrm{CR}} |\!|\!|$$

is contained in Carstensen et al. (2015a).
Straightforward calculations prove ⓑ. □

For each edge $E := \mathrm{conv}\{A, B\} \in \mathcal{E}(\Gamma_D)$ define $b_E := 6\varphi_A\varphi_B \in H^1_0(\omega_E) \cap P_2(\omega_E)$ with $⨍_E b_E \,\mathrm{d}s = 1$. Given the Dirichlet boundary condition u_D, define u_{D1} and u_{D2} as in Subsection 3.4.2 only restricted to the Dirichlet boundary, i.e.,

$$u_{D1}(z) := \begin{cases} u_D(z) & \text{for } z \in \mathcal{N}(\Gamma_D), \\ 0 & \text{otherwise,} \end{cases}$$

$$u_{D2} := u_{D1} + \sum_{E\in\mathcal{E}(\Gamma_D)} ⨍_E (u_D - u_{D1})\,\mathrm{d}s b_E.$$

Any $w_{\mathrm{CR}} \in \mathcal{A}_{\mathrm{NC}}$ satisfies $w_{\mathrm{CR}} = I_{\mathrm{NC}}u_{D2} + (w_{\mathrm{CR}} - I_{\mathrm{NC}}u_{D2})$ and $w_{\mathrm{CR}} - I_{\mathrm{NC}}u_{D2} \in \mathrm{CR}^1_D(\mathcal{T})$. Let w_D in Theorem 2.28 be such that $w_D|_{\Gamma_D} = (u_D - u_{D2})|_{\Gamma_D}$ and $w_D|_{\Gamma_N\cup\Gamma_C} = 0$. For the solution $u_{\mathrm{CR}} \in K_{\mathrm{CR}}(\mathcal{T})$ to Problem (3.31) define u_2 and the conforming companion v by

$$u_2 := u_{D2} + J_2^C(u_{\mathrm{CR}} - I_{\mathrm{NC}}u_{D2}) \in u_{D2} + S^2_D(\mathcal{T}) \quad \text{and} \quad v := w_D + u_2 \in \mathcal{A}. \tag{4.27}$$

Remark 4.33. *In the very particular situation of discrete contact along Γ_C and $\mathrm{dist}\{\Gamma_C, \Gamma_N\} > 0$, one aims at $J_2 u_{\mathrm{CR}} = \chi$ along Γ_C. The following modification of J_1 for $\mathrm{dist}\{\Gamma_C, \Gamma_N\} > 0$ guarantees this property. Recall that $\chi = u_D$ along Γ_D and re-define $J_1^C v_{\mathrm{CR}}$ at $z \in \mathcal{N}(\Gamma_C)$ by $J_1^C u_{\mathrm{CR}}(z) = 0$. Set $u_{D1} \in S^1(\mathcal{T})$ to*

$$u_{D1}(z) := \begin{cases} \chi(z) & \text{for } z \in \mathcal{N}(\Gamma_C \cup \Gamma_D), \\ 0 & \text{otherwise} \end{cases}$$

and set $u_{D2} := u_{D1} + \sum_{E\in\mathcal{E}(\Gamma_D\cup\Gamma_C)} ⨍(\chi - u_{D1})\,\mathrm{d}s\, b_E$. The design of w_D in Theorem 2.28 on Page 18 is extended to $\Gamma_C \cup \Gamma_D$ with $w_D|_{\Gamma_D\cup\Gamma_C} = \chi - u_{D2}$. In this special case, the conforming companions are defined as above and v from (4.27) satisfies $I_{\mathrm{NC}}v = u_{\mathrm{CR}}$.

4.4.3. Efficiency of the discrete Lagrange multiplier for NCFEM

This subsection defines a discrete Lagrange multiplier $\lambda_{\mathrm{CR}} \in P_0(\mathcal{E}(\Gamma_C); (-\infty, 0])$ and shows its efficiency in the sense of Theorem B. Given $\sigma_{\mathrm{CR}}(\psi_E)$ from (4.25), the discrete Lagrange multiplier $\lambda_{\mathrm{CR}} \in P_0(\mathcal{E}(\Gamma_C); (-\infty, 0])$ reads

$$\lambda_{\mathrm{CR}}|_E := \sigma_{\mathrm{CR}}(\psi_E)/|E| \quad \text{for } E \in \mathcal{E}(\Gamma_C). \tag{4.28}$$

Remark 4.34. *Since $\sigma_{\mathrm{CR}}(\psi_E) = 0$ for $E \in \mathcal{E}(\Gamma_N)$, the Lagrange multiplier λ_{CR} can be extended to edges $E \in \mathcal{E}(\Gamma_N)$ and satisfies $\lambda_{\mathrm{CR}}|_E = 0$ for all $E \in \mathcal{E}(\Gamma_N)$.*

The discrete Lagrange multiplier $\Lambda_{\mathrm{CR}} \in V^*$ with $\Lambda_{\mathrm{CR}}(\varphi) := \int_{\Gamma_C \cup \Gamma_N} \lambda_{\mathrm{CR}} \varphi \, \mathrm{d}s$ for all $\varphi \in V$, is efficient in the sense of Theorem B.

Theorem 4.35 (efficiency of the discrete Lagrange multiplier)**.** *The discrete solution $u_{\mathrm{CR}} \in K_{\mathrm{CR}}(\mathcal{T})$ to* (4.24) *and the discrete Lagrange multiplier λ_{CR} satisfy*

$$|||\Lambda - \Lambda_{\mathrm{CR}}|||_* \lesssim |||u - u_{\mathrm{CR}}|||_{\mathrm{NC}} + \operatorname{osc}(f, \mathcal{T}) + \operatorname{osc}_{1/2}(g, \mathcal{E}(\Gamma_C \cup \Gamma_N)).$$

Remark 4.36. *Contrary to the estimate of this type for CFEM in Theorem 4.20, the present estimate does not include oscillations of the exact continuous Lagrange multiplier Λ from* (4.3) *and requires no further regularity.*

The proof of Theorem 4.35 relies on the following observation, which shows the close connection between the non-conforming interpolation operator I_{NC} and the discrete Lagrange multiplier λ_{CR} from (4.28).

Lemma 4.37. *For any $\varphi \in V$, the discrete Lagrange multiplier λ_{CR} from* (4.28) *satisfies*

$$\int_{\Gamma_C} \lambda_{\mathrm{CR}} \varphi \, \mathrm{d}x = F(I_{\mathrm{NC}}\varphi) - a_{\mathrm{NC}}(u_{\mathrm{CR}}, \varphi).$$

Proof. The discrete variational inequality (4.24) and the definition of $K_{\mathrm{CR}}(\mathcal{T})$ in (4.23) show

$$a_{\mathrm{NC}}(u_{\mathrm{CR}}, \psi_E) = F(\psi_E) \quad \text{for all } E \in \mathcal{E} \setminus \mathcal{E}(\Gamma_C \cup \Gamma_D). \tag{4.29}$$

The definition of λ_{CR} results in

$$\int_{\Gamma_C} \lambda_{\mathrm{CR}} \varphi \, \mathrm{d}s = \sum_{E \in \mathcal{E}(\Gamma_C)} \Big(F(\psi_E) - a_{\mathrm{NC}}(u_{\mathrm{CR}}, \psi_E) \Big) \fint_E \varphi \, \mathrm{d}s \,.$$

This and (4.29) prove

$$\int_{\Gamma_C} \lambda_{\mathrm{CR}} \varphi \, \mathrm{d}s = F(I_{\mathrm{NC}}\varphi) - a_{\mathrm{NC}}(u_{\mathrm{CR}}, I_{\mathrm{NC}}\varphi) = F(I_{\mathrm{NC}}\varphi) - a_{\mathrm{NC}}(u_{\mathrm{CR}}, \varphi). \qquad \square$$

Proof of Theorem 4.35. Given any $\varphi \in V$ with $|||\varphi||| = 1$, Lemma 4.37 and the definition of $\Lambda \in V^*$ show

$$\Lambda(\varphi) - \int_{\Gamma_C} \lambda_{\mathrm{CR}} \varphi \, \mathrm{d}s = a_{\mathrm{NC}}(u_{\mathrm{CR}} - u, \varphi) + F(\varphi - I_{\mathrm{NC}}\varphi)$$

The interpolation error estimate in Brenner and Scott (2008); Carstensen et al. (2012b), and a trace inequality show

$$F(\varphi - I_{\mathrm{NC}}\varphi) \lesssim ||h_{\mathcal{T}} f|| + \mathrm{osc}_{1/2}(g, \mathcal{E}(\Gamma_C \cup \Gamma_N)).$$

To estimate $||h_{\mathcal{T}} f||_{L^2(\Omega)}$, define the cubic bubble function $b_T := 60\Pi_{z\in\mathcal{N}(T)}\varphi_z \in H^1_0(T)\cap P_3(T)$ for $T \in \mathcal{T}$, which satisfies $\mathrm{supp}(b_T) = T$ and $\fint_T b_T \,\mathrm{d}x$. The efficiency of $||h_{\mathcal{T}} f||_{L^2(T)}$ employs the arguments in Verfürth (1996), which yield

$$||h_{\mathcal{T}} f||_{L^2(\Omega)} \lesssim |||u - u_{\mathrm{CR}}|||_{\mathrm{NC}} + \mathrm{osc}(f, \mathcal{T}).$$

This concludes the proof. □

4.4.4. Comments on the complementary condition residual

This subsection analyzes the efficiency of the computable integral $\int_{\Gamma_C}(-\lambda_{\mathrm{CR}})(v - \chi)_+ \,\mathrm{d}s$ of Est as a complementary condition residual for an obstacle $\chi \in H^1(\Omega)$ which satisfies (4.1), $\chi|_{\Gamma_C\cup\Gamma_D} \in H^{3/2}(\Gamma_C \cup \Gamma_D)$, and $\chi|_{\Gamma_C} \in P_1(\Gamma_C)$ and v from (4.27). Theorem 4.38 below proves the efficiency of the computable integral in Est in the sense of Theorem C and employs the following three subsets of $\mathcal{E}(\Gamma_C)$

$$\begin{aligned}
\mathcal{E}_C &:= \{E \in \mathcal{E}(\Gamma_C) \mid (u_{\mathrm{CR}} - \chi)(\mathrm{mid}(E)) = 0\},\\
\mathcal{E}_{FC} &:= \{E \in \mathcal{E}_C \mid \mathcal{E}(\partial\Omega_E) \cap \mathcal{E}(\partial\Omega) \subseteq \mathcal{E}_C\\
&\qquad \text{and } \forall F \in \mathcal{E}(\partial\Omega_E) \cap \mathcal{E}(\partial\Omega) \text{ lie on a straight line}\},\\
\mathcal{E}_{DC} &:= \{E \in \mathcal{E}_C \mid \exists F_1 \in \mathcal{E}_C, F_2 \in \mathcal{E}(\Gamma_D) \text{ such that}\\
&\qquad F_1 \cap E \neq \emptyset \neq F_2 \cap E \text{ and } F_1 \text{ and } E \text{ lie on a straight line}\}.
\end{aligned}$$

In other words, the set $\mathcal{E}_C$ denotes the set of edges in $\mathcal{E}(\Gamma_C)$ with discrete contact, the set $\mathcal{E}_{FC}$ describes the areas of full contact, where it holds $v = \chi$ along $E \in \mathcal{E}_{FC}$, and finally $\mathcal{E}_{DC}$ denotes the set of contact edges near the Dirichlet boundary and hence it also holds $v = \chi$ along $E \in \mathcal{E}_{DC}$.

Theorem 4.38. *For an obstacle $\chi \in H^1(\Omega)$ which satisfies (4.1), $\chi|_{\Gamma_C\cup\Gamma_D} \in H^{3/2}(\Gamma_C \cup \Gamma_D)$, and $\chi|_{\Gamma_C} \in P_1(\Gamma_C)$, the function $v = w_D + u_{D2} + J_2^C(u_{\mathrm{CR}} - I_{\mathrm{NC}}u_{D2}) \in \mathcal{A}$ satisfies*

$$\begin{aligned}
\int_{\Gamma_C}(-\lambda_{\mathrm{CR}})(v - \chi)_+ \,\mathrm{d}s \lesssim{}& |||u - u_{\mathrm{CR}}|||^2_{\mathrm{NC}} + |||w|||^2 + \mathrm{osc}^2(f, \mathcal{T})\\
&+ \mathrm{osc}^2_{1/2}(g, \mathcal{E}(\Gamma_C)) + \mathrm{Osc}^2_{1/2,C}(\lambda, \mathcal{E}(\Gamma_C)).
\end{aligned}$$

Remark 4.39. *The conditions on the obstacle ensure that the exact solution $u \in K$ to (4.2) satisfies $u \in H^2(\Omega)$ and hence there exists an L^2 representation $\lambda \in L^2(\Gamma_C; (-\infty, 0])$ of the exact Lagrange multiplier Λ (cf. Theorem 4.3).*

Corollary 4.40. *For $\chi \in H^1(\Omega)$ which satisfies (4.1), $\chi|_{\Gamma_C\cup\Gamma_D} \in H^{3/2}(\Gamma_C \cup \Gamma_D)$, and $\chi|_{\Gamma_C} \in P_1(\Gamma_C)$, the guaranteed upper bound* $\mathrm{GUB} = 30\mathrm{Est}$ *is efficient with respect to the error $|||u - u_{\mathrm{CR}}|||_{\mathrm{NC}}$ and the total error* Err *of Theorem 4.14 in the sense that*

$$|||u - u_{\mathrm{CR}}|||_{\mathrm{NC}} \leq \mathrm{Err} + |||v - u_{\mathrm{CR}}|||_{\mathrm{NC}} \approx \mathrm{GUB} + |||v - u_{\mathrm{CR}}|||_{\mathrm{NC}} \lesssim |||u - u_{\mathrm{CR}}|||_{\mathrm{NC}}$$

$+$*higher-order terms.*

Proof. The proof follows from a combination of Theorems 4.14, 4.35, and 4.38. □

Remark 4.41. *The higher-order terms in Corollary 4.40 are given by* $|||w|||$*, and the oscillation terms* $\operatorname{osc}(f,\mathcal{T})$*,* $\operatorname{osc}_{1/2}(g,\mathcal{E}(\Gamma_C))$*, and* $\operatorname{Osc}_{1/2,C}(\lambda,\mathcal{E}(\Gamma_C))$*.*

Proof. The proof of Theorem 4.38 follows from *Claim 1–3* below. It is only necessary to consider the cases where $\mathcal{E}_C \neq \mathcal{E}(\Gamma_C)$ and Γ_C is adjacent to part of the Neumann boundary or that there exists $E \in \mathcal{E}(\Gamma_C)$ with $\lambda_{\mathrm{CR}}|_E = 0$. In all other cases it holds $v = \chi$ along Γ_C (cf. Remark 4.33) and the integral $\int_{\Gamma_C}(-\lambda_{\mathrm{CR}})(v-\chi)_+\,\mathrm{d}s$ vanishes.
Claim 1. It holds

$$\int_{\Gamma_C}(-\lambda_{\mathrm{CR}})(v-\chi)_+\,\mathrm{d}s \lesssim \sum_{E\in\mathcal{E}_C\setminus(\mathcal{E}_{FC}\cup\mathcal{E}_{DC})} \|h_E^{1/2}\lambda_{\mathrm{CR}}\|_{L^2(E)}|||w|||_{\omega_E}.$$

Proof. For each $E \in \mathcal{E}(\Gamma_C)\setminus\mathcal{E}_C$, $\lambda_{\mathrm{CR}}|_E = 0$ and so $\int_E \lambda_{\mathrm{CR}}(v-\chi)_+\,\mathrm{d}s = 0$. For $E \in \mathcal{E}_{FC}\cup\mathcal{E}_{DC}$, the definition of v shows that $v \equiv \chi$ along E and hence the integral vanishes. In the other case $E \in \mathcal{E}_C\setminus(\mathcal{E}_{FC}\cup\mathcal{E}_{DC})$, recall that $\lambda_{\mathrm{CR}} \in P_0(\mathcal{E}(\Gamma_C))$ and that $⨍_E J_2^C u_{\mathrm{CR}}\,\mathrm{d}s = ⨍_E u_{\mathrm{CR}}\,\mathrm{d}s = u_{\mathrm{CR}}(\mathrm{mid}(E))$. This shows

$$\int_E(-\lambda_{\mathrm{CR}})(v-\chi)_+\,\mathrm{d}s = \int_E \lambda_{\mathrm{CR}}\min\{0,v-\chi\}\,\mathrm{d}s = \int_E \lambda_{\mathrm{CR}}w\,\mathrm{d}s\,.$$

A Cauchy inequality leads to

$$\int_E(-\lambda_{\mathrm{CR}})(v-\chi)_+\,\mathrm{d}s \le ||\lambda_{\mathrm{CR}}||_{L^2(E)}||w||_{L^2(E)}.$$

As a result of the design of the conforming companion v in (4.27), $v|_{\Gamma_C} \in P_2(\mathcal{E}(\Gamma_C))$. This and the condition on the obstacle $\chi|_{\Gamma_C} \in P_1(\Gamma_C)$ show that the edge $E \in \mathcal{E}_C$ can be subdivided into at most two intervals E_1 and E_2 with $w|_{E_j} < 0$ for $j = 1,2$. For each of these intervals there exists $x \in \partial E_j$, $j = 1,2$, such that $w(x) = 0$. Hence a Friedrichs and a subsequent trace inequality (in the form of Theorem 2.24 on Page 17) show

$$||w||_{L^2(E)} \lesssim |E|\,||\partial w/\partial s||_{L^2(E)} \lesssim |E|^{1/2}|||w|||_{\omega_E}.$$

This completes the proof of *Claim 1.* □

Claim 2. For each edge $E \in \mathcal{E}_C\setminus(\mathcal{E}_{FC}\cup\mathcal{E}_{DC})$, the discrete Lagrange multiplier satisfies

$$\|h_E^{1/2}\lambda_{\mathrm{CR}}\|_E \lesssim \operatorname{osc}(f,\omega_E) + \operatorname{osc}_{1/2}(g,E) + |||u-u_{\mathrm{CR}}|||_{\omega_E} + \|h_E^{1/2}\lambda\|_E.$$

Proof. The definition of the discrete Lagrange multiplier yields

$$\|h_E^{1/2}\lambda_{\mathrm{CR}}\|_E = |F(\psi_E) - a_{\mathrm{NC}}(u_{\mathrm{CR}},\psi_E)|.$$

Let $E := \operatorname{conv}\{y,z\}$ with $w_E := \operatorname{conv}\{y,z,A\}$. The bubble function $b_E := 6\varphi_y\varphi_z - 10\varphi_y\varphi_z\varphi_A$ satisfies $\int_{\omega_E}\psi_E\,\mathrm{d}x = \int_{\omega_E} b_E\,\mathrm{d}x$ and $\int_E \psi_E\,\mathrm{d}s = \int_E b_E\,\mathrm{d}s$. Since u_{CR} satisfies $a_{\mathrm{NC}}(u_{\mathrm{CR}},b_E) = a_{\mathrm{NC}}(u_{\mathrm{CR}},I_{\mathrm{NC}}b_E) = a_{\mathrm{NC}}(u_{\mathrm{CR}},\psi_E)$, it follows

$$\|h_E^{1/2}\lambda_{\mathrm{CR}}\|_E = |F(\psi_E) - a_{\mathrm{NC}}(u_{\mathrm{CR}}-u,b_E) - a(u,b_E)|.$$

The continuous variational inequality (4.2) shows

$$a(u, b_E) = F(b_E) - \int_{\Gamma_C} \lambda b_E \,\mathrm{d}s\,.$$

Since $\int_{\omega_E} b_E \,\mathrm{d}x = \int_{\omega_E} \psi_E \,\mathrm{d}x$ and $\int_E b_E \,\mathrm{d}s = \int_E \psi_E \,\mathrm{d}s$, a Cauchy inequality shows

$$\|h_E^{1/2}\lambda_{\mathrm{CR}}\|_E \lesssim \mathrm{osc}(f, \omega_E) + \mathrm{osc}_{1/2}(g, E) + ||\nabla_{\mathrm{NC}}(u - u_{\mathrm{CR}})||_{L^2(T)} + ||h_E^{1/2}\lambda||_{L^2(E)}.$$

This concludes the proof of *Claim 2*. □

Claim 3. The continuous Lagrange multiplier λ satisfies

$$\sum_{E\in\mathcal{E}_C\setminus(\mathcal{E}_{FC}\cup\mathcal{E}_{DC})} ||h_E^{1/2}\lambda||_{L^2(E)} \lesssim \mathrm{Osc}_{1/2,C}(\lambda, \mathcal{E}(\Gamma_C)) + |||\lambda - \lambda_{\mathrm{CR}}|||_*.$$

Proof. For any edge $E \in \mathcal{E}_C \setminus (\mathcal{E}_{FC} \cup \mathcal{E}_{DC})$ a triangle inequality shows

$$\begin{aligned} ||h_E^{1/2}\lambda||_{L^2(E)} \lesssim & ||h_E^{1/2}\big(\lambda - \fint_{\partial\Omega_E\cap\Gamma_C} \lambda \,\mathrm{d}s\big)||^2_{L^2(E)} \\ & + ||h_E^{1/2}\big(\fint_{\partial\Omega_E\cap\Gamma_C} \lambda - \fint_F \lambda \,\mathrm{d}s\big)||^2_{L^2(F)} + ||h_F^{1/2} \fint_F \lambda \,\mathrm{d}s||^2_{L^2(F)} \end{aligned}$$

where $F \in \mathcal{E}(\Gamma_C)$ is a neighbouring edge of E. For arbitrary neighbouring edges $F \in \mathcal{E}(\Gamma_C)$, the first two terms lead to the desired oscillations. The choice of the neighbouring edge $F \in \mathcal{E}(\Gamma_C)$ becomes important in the analysis of the third term. Consider two different cases. In a first case, assume that there exists a neighbouring edge $F \in \mathcal{E}(\Gamma_C) \setminus \mathcal{E}_C$. This means that $\lambda_{\mathrm{CR}}|_F = 0$. Define the quadratic bubble function $b_F := 6\Pi_{z\in\mathcal{N}(F)}\varphi_z \in H_0^1(\omega_F) \cap P_2(\omega_F)$, which satisfies $\mathrm{supp}(b_F) = \overline{w}_F$ and $\fint_F b_F \,\mathrm{d}s = 1$. Then the bubble function methodology in Verfürth (1996) with $w_F = \fint_F \lambda \,\mathrm{d}s\, b_F \leq 0$ yields

$$\|h_F^{1/2} \fint_F \lambda \,\mathrm{d}s\,\|^2_F \lesssim h_F \int_F (\fint_F \lambda \,\mathrm{d}s - \lambda) w_F \,\mathrm{d}s + \int_F (\lambda - \lambda_{\mathrm{CR}}) w_F \,\mathrm{d}s\,. \tag{4.30}$$

A Cauchy inequality and the definition of w_F yield the claim in this case. In the second case, recall that the set $\mathcal{E}_C \setminus (\mathcal{E}_{FC} \cup \mathcal{E}_{DC})$ consists of contact edges that either have a non-contact neighbouring edge, touch a corner of the domain, or touch the Neumann boundary and hence the edge E has no neighbouring edge $F \in \mathcal{E}(\Gamma_C) \setminus \mathcal{E}_C$ and any neighbouring edge F either touches the boundary Γ_N or a corner or the domain. Since either $\mathcal{E}(\Gamma_C) \neq \mathcal{E}_C$ or $\Gamma_C \cap \Gamma_N \neq \emptyset$, (otherwise the design of v shows $(v - \chi) = 0$ and the claim of Theorem 4.38 is immediately satisfied) in both cases there exists a sequence of neighbouring edges $F_j \in \mathcal{E}(\Gamma_C)$, $j = 1, ..., J$ such that $\lambda_{\mathrm{CR}}|_{F_j} < 0$ for $j = 1, ..., J-1$ and $\lambda_{\mathrm{CR}}|_{F_J} = 0$. An estimate as in (4.30) can be repeated until F_J is reached. For $j = 1, ..., J-1$ it then holds

$$\|h_{F_j}^{1/2} \fint_{F_j} \lambda \,\mathrm{d}s\,\|^2_{L^2(F_j)} \lesssim h_{F_j} \int_{F_j} (\fint_{F_j} \lambda \,\mathrm{d}s - \lambda) w_{F_j} \,\mathrm{d}s + \int_{F_j} (\lambda - \fint_{F_{j+1}} \lambda \,\mathrm{d}s\,) w_{F_j} \,\mathrm{d}s\,.$$

Again, a Cauchy inequality and the definition of w_{F_j} (analogue to the definition of w_F above) yield

$$\|h_{F_j}^{1/2} \fint_{F_j} \lambda \,\mathrm{d}s\,\|^2_{L^2(F_j)} \lesssim \mathrm{osc}(\lambda, F_j) + \|h_{F_{j+1}}^{1/2} \fint_{F_{j+1}} \lambda \,\mathrm{d}s\,\|^2_{L^2(F_{j+1})}.$$

For $j = J$ the analysis in (4.30) applies. This procedure is possible since the number of edges which touch the boundary of Γ_C or lie at a corner of the domain Ω is fixed a priori and only depends on the geometry of the domain. This finite number is hidden in the notation $\lesssim$. The combination of the two cases concludes the proof of *Claim 3.* □

The combination of these three claims concludes the proof of Theorem 4.38. □

4.5. Mixed FEM for Signorini's problem

This section is devoted to the mixed formulation for the Signorini problem in two space dimensions and the corresponding lowest-order Raviart-Thomas finite element method. The mixed FEM for Signorini's problem is equivalent to the non-conforming Crouzeix-Raviart FEM, in the spirit of Marini (1985). This section shows this equivalence and introduces a discrete Lagrange multiplier $\lambda_{\mathrm{RT}} \in P_0(\mathcal{E}(\Gamma_C); (-\infty, 0])$. It shows the efficiency of the discrete Lagrange multiplier in the sense of Theorem B and studies the efficiency of the complementary condition residual $\int_\Omega (-\lambda_{\mathrm{RT}})(v - \chi)_+$ (for an appropriate conforming companion $v \in \mathcal{A}$) in the sense of Theorem C.

4.5.1. Mixed discretization

Given a shape-regular triangulation $\mathcal{T}$ of $\Omega \subset \mathbb{R}^2$ from Subsection 2.2.1 on Page 11, recall the Raviart-Thomas finite element space $\mathrm{RT}_0(\mathcal{T})$ from Definition 2.15 from Page 15 and define

$$\mathcal{M}_0 := \mathcal{M}_0(\mathcal{T}) \times \mathcal{M}_0(\Gamma_C \cup \Gamma_N) := P_0(\mathcal{T}) \times P_0(\mathcal{E}(\Gamma_C); (-\infty, 0]) \subseteq \mathcal{M}.$$

The discrete mixed formulation utilizes the linear and bilinear forms from (4.7) and seeks $(p_{\mathrm{RT}}, (u_0, \alpha_0)) \in \mathrm{RT}_0^{N,g}(\mathcal{T}) \times \mathcal{M}_0 := \mathrm{RT}_0^{\Gamma_N,g}(\mathcal{T}) \times \mathcal{M}_0$ such that

$$\int_\Omega p_{\mathrm{RT}} \cdot q_{\mathrm{RT}} \,\mathrm{d}x + b(q_{\mathrm{RT}}, (u_0, \alpha_0)) = H(q_{\mathrm{RT}}) \tag{4.31}$$

$$b(p_{\mathrm{RT}}, (v_0 - u_0, \beta_0 - \alpha_0)) \le G((v_0 - u_0, \beta_0 - \alpha_0)) \tag{4.32}$$

for all $(q_{\mathrm{RT}}, (v_0, \beta_0)) \in \mathrm{RT}_0^{N,0}(\mathcal{T}) \times \mathcal{M}_0 := \mathrm{RT}_0^{\Gamma_N,0}(\mathcal{T}) \times \mathcal{M}_0$.

Lemma 4.42 (discrete complementary conditions)**.** *The discrete mixed solution* $(p_{\mathrm{RT}}, (u_0, \alpha_0)) \in \mathrm{RT}_0^{N,g}(\mathcal{T}) \times \mathcal{M}_0$ *to* (4.31)–(4.32) *satisfies the following discrete complementary conditions*

$$0 \le p_{\mathrm{RT}} \cdot \nu_E - \Pi_0^C g \perp \alpha_0 \le 0 \quad \text{for all } E \in \mathcal{E}(\Gamma_C). \tag{4.33}$$

Here, $\perp$ *abbreviates orthogonality in* $\mathbb{R}$*, i.e.,* $a \perp b$ *means* $ab = 0$ *for* $a, b \in \mathbb{R}$*.*

Proof. To show the first inequality, consider the test function $v_0 = u_0 \in \mathcal{M}_0$ in (4.32). This yields

$$\langle p_{\mathrm{RT}} \cdot \nu, \beta_0 - \alpha_0 \rangle_{\partial\Omega} \le \int_{\Gamma_C \cup \Gamma_N} g(\beta_0 - \alpha_0) \,\mathrm{d}s \text{ for all } \beta_0 \in M_0(\Gamma_C \cup \Gamma_N).$$

Choose the function $\varphi_0 \in \mathcal{M}_0(\Gamma_C \cup \Gamma_N)$ with $\varphi_0 = -\varepsilon$ for any $\varepsilon > 0$ along $E \in \mathcal{E}(\Gamma_C)$ and 0 otherwise and set $\beta_0 = \alpha_0 + \varphi_0 \in \mathcal{M}_0(\Gamma_C \cup \Gamma_N)$ to prove

$$\langle p_{\mathrm{RT}} \cdot \nu - \Pi_0^C g, \varphi_0 \rangle_{\partial\Omega} \leq 0 \text{ for all } \varepsilon > 0.$$

The second inequality follows from the definition of $\alpha_0 \in \mathcal{M}(\Gamma_C \cup \Gamma_N)$. To show orthogonality, choose $\beta_0 = 0$ and $\beta_0 = 2\alpha_0$. This results in

$$\pm\langle p_{\mathrm{RT}} \cdot \nu - g, \alpha_0 \rangle_{\partial\Omega} \leq 0$$

and hence the asserted orthogonality. □

4.5.2. Equivalence NCFEM and MFEM for Signorini's problem

This subsection generalizes the equivalence of the Crouzeix-Raviart NCFEM and the lowest-order Raviart-Thomas MFEM for the Poisson problem in Marini (1985) to the Signorini problem for simply connected domains. Introduce the set

$$\begin{aligned} Q(\mathcal{T}; \Pi_0 f, \Pi_0^N g) := \{ q_{\mathrm{RT}} \in \mathrm{RT}_0^{N,g}(\mathcal{T}) \mid \operatorname{div} q_{\mathrm{RT}} = -\Pi_0 f, \\ \text{and } q_{\mathrm{RT}} \cdot \nu_E - \Pi_0^C g \geq 0 \text{ for all } E \in \mathcal{E}(\Gamma_C) \}. \end{aligned}$$

The discrete dual variational inequality seeks $\tilde{p}_{\mathrm{RT}} \in Q(\mathcal{T}; \Pi_0 f, \Pi_0^N g)$ with

$$\int_{\Gamma_C} \chi(q_{\mathrm{RT}} - \tilde{p}_{\mathrm{RT}}) \cdot \nu \, \mathrm{d}s \leq \int_\Omega \tilde{p}_{\mathrm{RT}} \cdot (q_{\mathrm{RT}} - \tilde{p}_{\mathrm{RT}}) \, \mathrm{d}x \tag{4.34}$$

for all $q_{\mathrm{RT}} \in Q(\mathcal{T}; \Pi_0 f, \Pi_0^N g)$.

Lemma 4.43. *ⓐ There exists $w_{\mathrm{CR}} \in K_{\mathrm{CR}}(\mathcal{T})$ such that the discrete solution $p_{\mathrm{RT}} \in Q(\mathcal{T}; \Pi_0 f, \Pi_0^N g)$ to (4.34) satisfies $p_{\mathrm{RT}} = \nabla_{\mathrm{NC}} w_{\mathrm{CR}} - \Pi_0 f/2(\bullet - \mathrm{mid}(\mathcal{T}))$.*

ⓑ The function w_{CR} from ⓐ satisfies the following discrete complementary conditions

$$0 \leq \fint_E (w_{\mathrm{CR}} - \chi) \, \mathrm{d}s \perp (\Pi_0^C g - p_{\mathrm{RT}} \cdot \nu_E) \leq 0 \quad \text{for all } E \in \mathcal{E}(\Gamma_C)$$

where $\perp$ abbreviates orthogonality in $\mathbb{R}$, i.e., $a \perp b$ signifies $ab = 0$ for $a, b \in \mathbb{R}$.

The proof utilizes the following discrete Helmholtz decomposition.

Lemma 4.44. *Let Ω be a simply connected domain and $\mathcal{T}$ a triangulation of Ω. Consider the space $V_{CN}(\mathcal{T}) := \{ v_{\mathcal{T}} \in P_1(\mathcal{T}) \cap C(\overline{\Omega}) \mid \partial v_{\mathcal{T}}/\partial s = 0 \text{ along } \Gamma_C \cup \Gamma_N \}$. Then*

$$P_0(\mathcal{T}; \mathbb{R}^2) = \nabla_{\mathrm{NC}} \mathrm{CR}_D^1(\mathcal{T}) \oplus \operatorname{Curl} V_{CN}(\mathcal{T})/\mathbb{R}.$$

Proof. To prove the orthogonality of this decomposition, consider an edge-oriented basis function $\psi_E \in \mathrm{CR}_D^1(\mathcal{T})$ and a function $v_{\mathcal{T}} \in V_{CN}(\mathcal{T})$. A piecewise integration by parts leads to

$$\begin{aligned} \int_\Omega \operatorname{Curl} v_{\mathcal{T}} \cdot \nabla_{\mathrm{NC}} \psi_E \, \mathrm{d}x &= \sum_{T \in \mathcal{T}} \left(\int_{\partial T} \operatorname{Curl} v_{\mathcal{T}} \psi_E \cdot \nu_{\mathcal{T}} \, \mathrm{d}s \right) \\ &= \sum_{F \in \mathcal{E}(\Omega) \cup \mathcal{E}(\Gamma_C \cup \Gamma_N)} \int_F [\psi_E \operatorname{Curl} v_{\mathcal{T}} \cdot \nu_F]_F \, \mathrm{d}s \end{aligned}$$

$$=1/2 \sum_{F\in\mathcal{E}(\Omega)\cup\mathcal{E}(\Gamma_C\cup\Gamma_N)} \Big(\langle \operatorname{Curl} v_{\mathcal{T}}\cdot\nu_F\rangle_F[\psi_E]_F + [\operatorname{Curl} v_{\mathcal{T}}\cdot\nu_F]_F\langle\psi_E\rangle_F\Big).$$

Since $v_{\mathcal{T}}\in C(\Omega)$ and ψ_E is continuous at the edges midpoints it holds

$$[\operatorname{Curl} v_{\mathcal{T}}\cdot\nu_F]_F = 0 \text{ and } [\psi_E]_F = 0 \quad \text{for all } F\in\mathcal{E}(\Omega).$$

Since $\partial v_{\mathcal{T}}/\partial s = 0$ along $\Gamma_C\cup\Gamma_N$

$$\langle \operatorname{Curl} v_{\mathcal{T}}\cdot\nu_F\rangle_F = 0 \text{ and } [\operatorname{Curl} v_{\mathcal{T}}\cdot\nu_F]_F = 0 \quad \text{along } \Gamma_N.$$

This proves

$$\int_\Omega \operatorname{Curl}\varphi_z\cdot\nabla_{\mathrm{NC}}\psi_E\,\mathrm{d}x = 0.$$

A dimension argument proves the equality. Euler's formula for the simply connected domain Ω proves

$$\dim(P_0(\mathcal{T};\mathbb{R}^2)) = 2|\mathcal{T}| = |\mathcal{N}| + |\mathcal{E}(\Omega)| - 1.$$

Since the coefficient matrix for the Crouzeix-Raviart FEM is regular, it holds

$$\dim(\mathrm{CR}^1_D(\mathcal{T})) = |E(\Omega)| + |\mathcal{E}(\Gamma_C\cup\Gamma_N)|.$$

Assume $\Gamma_C\cup\Gamma_N = \Gamma_1\cup\ldots\cup\Gamma_J$ has J connected components. The function $v_{\mathcal{T}} = c_j$ is constant on each component Γ_j, $j = 1,\ldots,J$. Without loss of generality, set the first constant $c_1 = 0$. For the space $V_{CN}(\mathcal{T})$, one degree of freedom is counted for each interior node $z\in\mathcal{N}(\Omega)$, one for each node $z\in\mathcal{N}(\partial\Omega\setminus\overline{\Gamma_C\cup\Gamma_N})$, and one for each connected component of $\Gamma_C\cup\Gamma_N$, where the constant c_j is not fixed. This leads to

$$\dim(V_{CN}(\mathcal{T})/\mathbb{R}) = |\mathcal{N}(\Omega)| + |\mathcal{N}(\partial\Omega\setminus\overline{\Gamma_C\cup\Gamma_N})| + J - 1.$$

Since $|\mathcal{E}(\Gamma_N)| + |\mathcal{N}(\partial\Omega\setminus\overline{\Gamma}_N)| + J = \mathcal{N}(\partial\Omega)$,

$$\dim(\mathrm{CR}^1_D(\mathcal{T})) + \dim(V_{CN}(\mathcal{T})/\mathbb{R}) = \dim P_0(\mathcal{T};\mathbb{R}^2).$$

This computation completes the proof. □

Proof of Lemma 4.43. Let $w_{\mathrm{CR}}\in\mathrm{CR}^1_D(\mathcal{T})$ solve the following auxiliary Poisson model problem

$$a_{\mathrm{NC}}(w_{\mathrm{CR}},v_{\mathrm{CR}}) = \int_\Omega \Pi_0 f v_{\mathrm{CR}}\,\mathrm{d}x + \int_{\Gamma_N\cup\Gamma_C}\Pi_0^C g v_{\mathrm{CR}}\,\mathrm{d}s + \int_{\Gamma_C} v_{\mathrm{CR}}p_{\mathrm{RT}}\cdot\nu_E\,\mathrm{d}s \quad (4.35)$$

for all $v_{\mathrm{CR}}\in\mathrm{CR}^1_D(\mathcal{T})$. Set $\tilde{q}_{\mathrm{RT}} := \nabla_{\mathrm{NC}}w_{\mathrm{CR}} - \Pi_0 f/2(\bullet - \mathrm{mid}(T))$. The definition of the piecewise divergence operator $\mathrm{div}_{\mathrm{NC}}$ shows

$$\mathrm{div}_{\mathrm{NC}}\,\tilde{q}_{\mathrm{RT}} = -\Pi_0 f.$$

To verify that $\tilde{q}_{\mathrm{RT}}\in\mathrm{RT}^{N,g}_0(\mathcal{T})$, an integration by parts shows, for all $E\in\mathcal{E}(\Omega)$,

$$\int_E [\nabla_{\mathrm{NC}}w_{\mathrm{CR}}\cdot\nu_E]_E\,\mathrm{d}s = a_{\mathrm{NC}}(w_{\mathrm{CR}},\psi_E) = \Pi_0 f\big|_{T_+}|T_+|/3 + \Pi_0 f\big|_{T_-}|T_-|/3.$$

Note that for $T\in\mathcal{T}(E)$, $(x-\mathrm{mid}(T))\cdot\nu_E = h_E^T/3$ for all $x\in E$, where h_E^T is the height of T with respect to the edge E. This shows that

$$\int_E \Pi_0 f/2(\bullet - \mathrm{mid}\,T)\cdot\nu_E\,\mathrm{d}s = \Pi_0 f\big|_{T_+}|T_+|/3 + \Pi_0 f\big|_{T_-}|T_-|/3$$

and hence it follows that $[\tilde{q}_{\mathrm{RT}} \cdot \nu_E]_E = 0$ for all $E \in \mathcal{E}(\Omega)$. For $E \in \mathcal{E}(\Gamma_N \cup \Gamma_C)$ an integration by parts as above and the auxiliary Poisson model problem (4.35) shows $\tilde{q}_{\mathrm{RT}} \cdot \nu_E = p_{\mathrm{RT}} \cdot \nu_E$.
To show that $\tilde{q}_{\mathrm{RT}} = p_{\mathrm{RT}}$ it remains to show that $\nabla_{\mathrm{NC}} w_{\mathrm{CR}} = \Pi_0 p_{\mathrm{RT}}$. An integration by parts in (4.35) leads to

$$\nabla_{\mathrm{NC}} w_{\mathrm{CR}} - \Pi_0 p_{\mathrm{RT}} \perp \nabla_{\mathrm{NC}} \mathrm{CR}^1_D(\mathcal{T}). \tag{4.36}$$

The discrete Helmholtz decomposition in Lemma 4.44 yields the existence of $v_{\mathcal{T}} \in V_{CN}(\mathcal{T})$ such that $\nabla_{\mathrm{NC}} w_{\mathrm{CR}} - \Pi_0 p_{\mathrm{RT}} = \operatorname{Curl} v_{\mathcal{T}}$. Notice that $\operatorname{Curl} v_{\mathcal{T}} \in Q(\mathcal{T}; 0, 0)$ and hence $q_{\mathrm{RT}} = p_{\mathrm{RT}} \pm \operatorname{Curl} v_{\mathcal{T}} \in Q(\mathcal{T}; \Pi_0 f, \Pi_0^N g)$. Since $\operatorname{Curl} v_{\mathcal{T}} \cdot \nu_E = 0$ for $E \in \mathcal{E}(\Gamma_C)$, the discrete dual variational inequality (4.34) yields

$$0 = \int_{\Gamma_C} \chi \operatorname{Curl} v_{\mathcal{T}} \cdot \nu \, \mathrm{d}s = \int_{\Omega} p_{\mathrm{RT}} \cdot \operatorname{Curl} v_{\mathcal{T}} \, \mathrm{d}x.$$

Since $\operatorname{Curl} v_{\mathcal{T}} = \nabla_{\mathrm{NC}} u_{\mathrm{CR}} - \Pi_0 p_{\mathrm{RT}}$ and (4.36), it follows

$$0 = ||\Pi_0 p_{\mathrm{RT}} - \nabla_{\mathrm{NC}} w_{\mathrm{CR}}||^2_{L^2(\Omega)}.$$

Consequently $\Pi_0 p_{\mathrm{RT}} = \nabla_{\mathrm{NC}} w_{\mathrm{CR}}$ and so $p_{\mathrm{RT}} = \tilde{q}_{\mathrm{RT}}$.

The discrete dual variational inequality (4.34) shows, after an integration by parts, that

$$\int_{\Gamma_C} (\chi - w_{\mathrm{CR}})(q_{\mathrm{RT}} - p_{\mathrm{RT}}) \cdot \nu \, \mathrm{d}s \leq 0 \quad \text{for all } q_{\mathrm{RT}} \in Q(\mathcal{T}; \Pi_0 f, \Pi_0^N g). \tag{4.37}$$

To prove that $w_{\mathrm{CR}} \in K_{\mathrm{CR}}(\mathcal{T})$, set $q_{\mathrm{RT}} := p_{\mathrm{RT}} + \tau_{\mathrm{RT}}$ for some $\tau_{\mathrm{RT}} \in \mathrm{RT}_0(\mathcal{T})$ with $\tau_{\mathrm{RT}} \cdot \nu = \mu$ for $\mu \in L^2(\partial\Omega)$ with $\mu \geq -|p_{\mathrm{RT}} \cdot \nu - \Pi_0^C g|$ along Γ_C. Choose $\mu = |p_{\mathrm{RT}} \cdot \nu - \Pi_0^C g| + (\chi - w_{\mathrm{CR}})_+$ along Γ_C and $\mu = 0$ along $\partial\Omega \setminus \Gamma_C$. Then

$$\int_{\Gamma_C} (\Pi_0^C (\chi - w_{\mathrm{CR}})_+)^2 \leq 0$$

Consequently $\Pi_0^C(\chi - w_{\mathrm{CR}}) \leq 0$. This concludes the proof of ⓐ. □
To prove ⓑ, it remains to show the orthogonality

$$0 = \int_{\Gamma_C} (w_{\mathrm{CR}} - \chi)(p_{\mathrm{RT}} \cdot \nu - \Pi_0^C g) \, \mathrm{d}s \, .$$

To this end, set $q_{\mathrm{RT}} := p_{\mathrm{RT}} + \tau_{\mathrm{RT}}$ for some $\tau_{\mathrm{RT}} \in \mathrm{RT}_0(\mathcal{T})$ with $\tau_{\mathrm{RT}} \cdot \nu = \mu$ for some $\mu \in L^2(\partial\Omega)$ with $\mu \geq -|p_{\mathrm{RT}} \cdot \nu - \Pi_0^C g|$ along Γ_C, and $\mu = 0$ along $\partial\Omega \setminus \Gamma_C$. Choose $\mu = \pm|p_{\mathrm{RT}} \cdot \nu - \Pi_0^C g|$ along Γ_C. This definition and (4.37) show

$$\int_{\Gamma_C} |\chi - w_{\mathrm{CR}}| \, |p_{\mathrm{RT}} \cdot \nu - \Pi_0^C g| = 0.$$

Since $p_{\mathrm{RT}} \in Q(\mathcal{T}; \Pi_0 f, \Pi_0^N g)$ and $w_{\mathrm{CR}} \in K_{\mathrm{CR}}(\mathcal{T})$, this implies ⓑ. □

Let $s(\mathcal{T})$ be defined by $s(\mathcal{T})|_T := \|\bullet - \mathrm{mid}(T)\|^2_{L^2(T)}/(4|T|)$ for all $T \in \mathcal{T}$.

Theorem 4.45 (discrete equivalence)**.** *The discrete variational inequality* (4.24)*, the discrete mixed system* (4.31)–(4.32)*, and the dual variational inequality* (4.34) *are equivalent in the following sense.*

ⓐ *Let $\tilde{u}_{\mathrm{CR}} \in K_{\mathrm{CR}}(\mathcal{T})$ denote the solution to the discrete variational inequality* (4.24) *with the right-hand side $\Pi_0 f$ and define $\tilde{\alpha}_0$ by $\tilde{\alpha}_0|_{\Gamma_C} := \Pi_0^{\Gamma_C}(\chi - \tilde{u}_{\mathrm{CR}})$*

and $\tilde\alpha_0|_{\Gamma_N} = 0$. *Then*
$(\nabla_{\rm NC}\tilde u_{\rm CR} - \Pi_0 f/2(\bullet - \mathrm{mid}(\mathcal{T})), (\Pi_0\tilde u_{\rm CR} + s(\mathcal{T})\Pi_0 f, \tilde\alpha_0)) \in \mathrm{RT}_0^{N,g}(\mathcal{T}) \times \mathcal{M}_0$
solves the discrete mixed problem (4.31)–(4.32).

ⓑ *Let* $(p_{\rm RT}, (u_0, \alpha_0)) \in \mathrm{RT}_0^{N,g}(\mathcal{T}) \times \mathcal{M}_0$ *solve* (4.31)–(4.32). *Then* $p_{\rm RT}$ *solves the discrete dual variational inequality* (4.34).

ⓒ *Let* $p_{\rm RT} = \nabla_{\rm NC} w_{\rm CR} - \Pi_0 f/2(\bullet - \mathrm{mid}(\mathcal{T})) \in Q(\mathcal{T}; \Pi_0 f, \Pi_0^N g)$ *with* $w_{\rm CR} \in K_{\rm CR}(\mathcal{T})$ *solve the discrete dual variational inequality* (4.37). *Then* $w_{\rm CR} \in K_{\rm CR}(\mathcal{T})$ *solves the discrete variational inequality* (4.24).

Proof. To prove ⓐ, set $\tilde p_{\rm RT} := \nabla_{\rm NC}\tilde u_{\rm CR} - \Pi_0 f/2(\bullet - \mathrm{mid}(\mathcal{T}))$. An integration by parts shows, for all $E \in \mathcal{E}(\Omega) \cup \mathcal{E}(\Gamma_N)$,

$$\int_E [\nabla_{\rm NC}\tilde u_{\rm CR} \cdot \nu_E]_E \,\mathrm{d}s = a_{\rm NC}(\tilde u_{\rm CR}, \psi_E).$$

Since $E \in \mathcal{E}(\Omega) \cup \mathcal{E}(\Gamma_N)$ is a free edge, $v_{\rm CR} := \tilde u_{\rm CR} \pm \psi_E \in K_{\rm CR}(\mathcal{T})$. Hence the variational inequality (4.24) leads to

$$\begin{aligned} a_{\rm NC}(\tilde u_{\rm CR}, \psi_E) &= \int_{\omega_E} \Pi_0 f \psi_E \,\mathrm{d}x + \int_E g \,\mathrm{d}s \\ &= \Pi_0 f\big|_{T_+} |T_+|/3 + \Pi_0 f\big|_{T_-} |T_-|/3 + \int_E g \,\mathrm{d}s \end{aligned}$$

where the term $\int_E g\,\mathrm{d}s$ only appears for $E \in \mathcal{E}(\Gamma_N)$. Note that for $T \in \mathcal{T}(E)$, $(x - \mathrm{mid}\, T)\cdot\nu_E = h_E^T/3$ for all $x \in E$ (h_E^T = height of T on E). This shows that

$$\int_E \Pi_0 f/2(\bullet - \mathrm{mid}\, T)\cdot\nu_E \,\mathrm{d}s = \Pi_0 f\big|_{T_+}|T_+|/3 + \Pi_0 f\big|_{T_-}|T_-|/3$$

and hence it follows that $[\tilde p_{\rm RT}\cdot\nu_E]_E = 0$ for all $E \in \mathcal{E}(\Omega)$, $\tilde p_{\rm RT}\cdot\nu_E = \fint_E g\,\mathrm{d}s$ for all $E \in \mathcal{E}(\Gamma_N)$, and $\tilde p_{\rm RT} \in \mathrm{RT}_0^{N,\Pi_0 g}(\mathcal{T})$. The definition of $K_{\rm CR}(\mathcal{T})$ immediately guarantees

$$(\Pi_0\tilde u_{\rm CR} + s(\mathcal{T})\Pi_0(f), \tilde\alpha_0) \in \mathcal{M}_0.$$

To verify (4.31), note that any $q_{\rm RT} \in \mathrm{RT}_0(\mathcal{T})$ can be decomposed as $q_{\rm RT} = \Pi_0 q_{\rm RT} + \mathrm{div}\, q_{\rm RT}/2(\bullet - \mathrm{mid}(\mathcal{T}))$ with $(\bullet - \mathrm{mid}(\mathcal{T})) \perp P_0(\mathcal{T})$. This and an integration by parts lead to

$$\begin{aligned} \int_\Omega \tilde p_{\rm RT}\cdot q_{\rm RT}\,\mathrm{d}x &= \int_\Omega (\nabla_{\rm NC}\tilde u_{\rm CR} - \Pi_0 f/2(\bullet - \mathcal{T}))\cdot q_{\rm RT}\,\mathrm{d}x \\ &= -\int_\Omega (\tilde u_{\rm CR} + \Pi_0 f/4(\bullet - \mathrm{mid}(\mathcal{T}))^2)\,\mathrm{div}\, q_{\rm RT}\,\mathrm{d}x + \int_{\Gamma_C} \tilde u_{\rm CR} q_{\rm RT}\cdot\nu\,\mathrm{d}s \end{aligned}$$

for all $q_{\rm RT} \in \mathrm{RT}_0^{N,0}(\mathcal{T})$. Hence

$$\int_\Omega \tilde p_{\rm RT}\cdot q_{\rm RT}\,\mathrm{d}x + b(q_{\rm RT}, (\Pi_0\tilde u_{\rm CR} + s(T)\Pi_0 f, \tilde\alpha_0)) = H(q_{\rm RT})$$

for all $q_{\rm RT} \in \mathrm{RT}_0^{N,0}(\mathcal{T})$. To show (4.32), notice that $\mathrm{div}\,\tilde p_{\rm RT} = -\Pi_0 f$. Since

$q_{\mathrm{RT}} \cdot \nu = 0$ along Γ_N, it remains to verify

$$\int_{\Gamma_C} (\beta_0 - \tilde{\alpha}_0)\tilde{p}_{\mathrm{RT}} \cdot \nu \,\mathrm{d}s \leq \langle g, \beta_0 - \Pi_0^C(\chi - \tilde{u}_{\mathrm{CR}})\rangle_{\partial\Omega} \tag{4.38}$$

for all $\beta_0 \in \mathcal{M}_0(\Gamma_C \cup \Gamma_N)$. Let $E \in \mathcal{E}(\Gamma_C)$ and $\beta_0 \in \mathcal{M}_0(\Gamma_C \cup \Gamma_N)$. Since $\psi_E|_E = 1$, $\beta_0 \in \mathcal{M}_0(\Gamma_C \cup \Gamma_N)$ satisfies

$$\begin{aligned}\int_E (\beta_0 - \Pi_0^{\Gamma_C}(\chi - \tilde{u}_{\mathrm{CR}}))\nabla_{\mathrm{NC}}\tilde{u}_{\mathrm{CR}} \cdot \nu_E \,\mathrm{d}s \\ = \int_E (\beta_0 - (\chi - \tilde{u}_{\mathrm{CR}})(\mathrm{mid}(E)))\psi_E \nabla_{\mathrm{NC}}\tilde{u}_{\mathrm{CR}} \cdot \nu_E \,\mathrm{d}s\,.\end{aligned}$$

Set v_{CR} such that $\tilde{u}_{\mathrm{CR}} - v_{\mathrm{CR}} = (\beta_0 - (\chi - \tilde{u}_{\mathrm{CR}})(\mathrm{mid}(E))\psi_E$. Then $v_{\mathrm{CR}} \in K_{\mathrm{CR}}(\mathcal{T})$ and hence an integration by parts and the discrete variational inequality show

$$\begin{aligned}\int_E \big(\beta_0 - \Pi_0^{\Gamma_C}(\chi - \tilde{u}_{\mathrm{CR}})\big)\nabla_{\mathrm{NC}}\tilde{u}_{\mathrm{CR}} \cdot \nu_E \,\mathrm{d}s \\ &= a_{\mathrm{NC}}(\tilde{u}_{\mathrm{CR}}, (\beta_0 - (\chi - \tilde{u}_{\mathrm{CR}})(\mathrm{mid}(E)))\psi_E) \\ &\leq \int_{T(E)} \Pi_0 f(\beta_0 - (\chi - \tilde{u}_{\mathrm{CR}})(\mathrm{mid}(E)))\psi_E \,\mathrm{d}x \\ &\quad + \int_E g(\beta_0 - (\chi - \tilde{u}_{\mathrm{CR}})(\mathrm{mid}(E))\psi_E \,\mathrm{d}s.\end{aligned}$$

Since $\tilde{p}_{\mathrm{RT}} = \nabla_{\mathrm{NC}}\tilde{u}_{\mathrm{CR}} - \Pi_0 f(\bullet - \mathrm{mid}(\mathcal{T}))$ and $(x - \mathrm{mid}(\mathcal{T})) \cdot \nu_E = h_E^T/3$ for all $x \in E$ (h_E^T is the height of T with respect to the edge E), it follows

$$\begin{aligned}\int_E \big(\beta_0 - \Pi_0^{\Gamma_C}(\chi - \tilde{u}_{\mathrm{CR}})\big)\Pi_0 f(\bullet - \mathrm{mid}(\mathcal{T})) \cdot \nu_E \,\mathrm{d}s \\ &= (\beta_0 - \Pi_0^{\Gamma_C}(\chi - \tilde{u}_{\mathrm{CR}}))\Pi_0 f|T(E)|/3 \\ &= \int_\Omega \Pi_0 f\big(\beta_0 - \Pi_0^{\Gamma_C}(\chi - \tilde{u}_{\mathrm{CR}})\big)\psi_E \,\mathrm{d}x.\end{aligned}$$

The combination of those estimates yields (4.38) and concludes the proof of ⓐ. □

To prove ⓑ, choose $\beta_0 = \alpha_0$ and $v_0 = 0$ and $v_0 = 2u_0$ in (4.32) to show that $p_{\mathrm{RT}} \in Q(\mathcal{T}; \Pi_0 f, \Pi_0^C g)$. For any $q_{\mathrm{RT}} \in Q(\mathcal{T}; \Pi_0 f, \Pi_0^C g)$, an integration by parts and the complementary conditions (4.33) show

$$b(q_{\mathrm{RT}} - p_{\mathrm{RT}}, (u_0, \alpha_0)) = \int_{\Gamma_C} \alpha_0(q_{\mathrm{RT}} - p_{\mathrm{RT}}) \cdot \nu \,\mathrm{d}s = \int_{\Gamma_C} \alpha_0 q_{\mathrm{RT}} \cdot \nu \,\mathrm{d}s \leq 0.$$

The previous estimate and (4.32) lead to

$$\int_\Omega p_{\mathrm{RT}} \cdot (q_{\mathrm{RT}} - p_{\mathrm{RT}}) \,\mathrm{d}x = H(q_{\mathrm{RT}} - p_{\mathrm{RT}}) - b(q_{\mathrm{RT}} - p_{\mathrm{RT}}, (u_0, \alpha_0)) \geq H(q_{\mathrm{RT}} - p_{\mathrm{RT}}).$$

This concludes the proof of ⓑ.

For the proof of ⓒ, recall the decomposition $p_{\mathrm{RT}} = \nabla_{\mathrm{NC}} w_{\mathrm{CR}} - \Pi_0 f/2(\bullet - \mathrm{mid}(\mathcal{T}))$ for $w_{\mathrm{CR}} \in K_{\mathrm{CR}}(\mathcal{T})$ in Lemma 4.43 where $w_{\mathrm{CR}} \in K_{\mathrm{CR}}(\mathcal{T})$ solves the auxiliary Poisson model problem (4.35). Since p_{RT} satisfies the complementary conditions in

Lemma 4.43.b,

$$\int_{\Gamma_C} p_{\mathrm{RT}} \cdot \nu_E(v_{\mathrm{CR}} - w_{\mathrm{CR}})\,\mathrm{d}s \leq \int_{\Gamma_C} p_{\mathrm{RT}} \cdot \nu_E(v_{\mathrm{CR}} - \chi)\,\mathrm{d}s \leq 0$$

holds for all all $v_{\mathrm{CR}} \in K_{\mathrm{CR}}(\mathcal{T})$. This concludes the proof of ⓒ. □

Theorem 4.46. ⓐ *Let* $(p_{\mathrm{RT}}, (u_0, \alpha_0)) \in \mathrm{RT}_0^{N,g}(\mathcal{T}) \times \mathcal{M}_0$ *solve* (4.31)–(4.32). *Then* $(p_{\mathrm{RT}}, (u_0, \alpha_0|_{\Gamma_C}))$ *is unique.*

ⓑ *There exists a unique solution to* (4.34).

Proof. Theorem 4.45 and the unique existence of a solution $u_{\mathrm{CR}} \in K_{\mathrm{CR}}(\mathcal{T})$ to (4.24), prove the existence of a solution to (4.31)–(4.32). The uniqueness of the solution $u_{\mathrm{CR}} \in K_{\mathrm{CR}}(\mathcal{T})$ to (4.24) shows the uniqueness of $p_{\mathrm{RT}} \in \mathrm{RT}_0^{N,g}(\mathcal{T})$. It remains to show the uniqueness of $(u_0, \alpha_0|_{\Gamma_C})$. Assume that $(p_{\mathrm{RT}}, (u_1, \alpha_1))$ and $(p_{\mathrm{RT}}, (u_2, \alpha_2)) \in \mathrm{RT}_0^{N,g}(\mathcal{T}) \times \mathcal{M}_0$ solve (4.31)–(4.32). Then (4.31), for all $q_{\mathrm{RT}} \in \mathrm{RT}_0^{N,0}(\mathcal{T})$, leads to

$$\int_\Omega p_{\mathrm{RT}} \cdot q\,\mathrm{d}x + b(q_{\mathrm{RT}}, (u_1, \alpha_1)) = H(q_{\mathrm{RT}}),$$
$$\int_\Omega p_{\mathrm{RT}} \cdot q\,\mathrm{d}x + b(q_{\mathrm{RT}}, (u_2, \alpha_2)) = H(q_{\mathrm{RT}}).$$

The difference of those two equations reads

$$\int_\Omega (u_1 - u_2)\,\mathrm{div}\, q_{\mathrm{RT}}\,\mathrm{d}x + \langle q_{\mathrm{RT}} \cdot \nu, \alpha_1 - \alpha_2\rangle_{\partial\Omega} = 0 \quad \text{for all } q_{\mathrm{RT}} \in \mathrm{RT}_0^{N,0}(\mathcal{T}).$$

It is well-known, that there exits $q_{\mathrm{RT}}^{N,0} \in \mathrm{RT}_0(\mathcal{T})$ with $\mathrm{div}\, q_{\mathrm{RT}} = u_1 - u_2$ and $q_{\mathrm{RT}} \cdot \nu = \alpha_1 - \alpha_2$ along Γ_C. Then it follows that

$$||u_1 - u_2||^2_{L^2(\Omega)} + ||\alpha_1 - \alpha_2||^2_{L^2(\Gamma_C)} = 0.$$

Hence $u_1 = u_2$ and $\alpha_1|_{\Gamma_C} = \alpha_2|_{\Gamma_C}$. This concludes the proof of ⓐ. □

Theorem 4.45 and the unique existence of a solution $u_{\mathrm{CR}} \in K_{\mathrm{CR}}(\mathcal{T})$ to (4.24) prove ⓑ. □

Remark 4.47. *The proof of Theorem 4.46 is closely related to the proof of Theorem 2.1 in Brezzi et al. (1978).*

4.5.3. Efficiency of the discrete Lagrange multiplier for MFEM

Define the discrete Lagrange multiplier by

$$\lambda_{\mathrm{RT}} = -p_{\mathrm{RT}} \cdot \nu + \Pi_0^{\Gamma_C \cup \Gamma_N} g \in P_0(\mathcal{E}(\Gamma_C); (-\infty, 0]) \tag{4.39}$$

and $\Lambda_{\mathrm{RT}} \in V^*$ by $\Lambda_{\mathrm{RT}}(\varphi) := \int_{\Gamma_C} \lambda_{\mathrm{RT}} \varphi\,\mathrm{d}s$ for all $\varphi \in V$.

Theorem 4.48. *The discrete solution* $(p_{\mathrm{RT}}, (u_0, \alpha_0)) \in \mathrm{RT}_0^{N,g}(\mathcal{T}) \times \mathcal{M}_0$ *to* (4.31)–(4.32) *and the discrete Lagrange multiplier* Λ_{RT} *satisfies*

$$|||\Lambda - \Lambda_{\mathrm{RT}}|||_* \lesssim \mathrm{osc}(f, \mathcal{T}) + \mathrm{osc}(g, \mathcal{E}(\Gamma_C \cup \Gamma_N)) + \|\nabla u - p_{\mathrm{RT}}\|.$$

Proof. Let $\varphi \in H^1_D(\Omega)$ with $\|\!|\varphi|\!\| = 1$. Since $p_{\mathrm{RT}} \cdot \nu - \Pi_0^{\Gamma_C \cup \Gamma_N} g \in P_0(\mathcal{E}(\Gamma_C))$, an integration by parts shows

$$\begin{aligned}
&\Lambda(\varphi) - \langle p_{\mathrm{RT}} \cdot \nu - \Pi_0^{\Gamma_C \cup \Gamma_N} g, \varphi \rangle_{\partial\Omega} \\
&\quad = F(\varphi) - a(u, \varphi) - \int_\Omega \Pi_0 f I_{\mathrm{NC}} \varphi \,\mathrm{d}x - \int_{\Gamma_C \cup \Gamma_N} \Pi_0^{\Gamma_C \cup \Gamma_N} g \varphi \,\mathrm{d}s + \int_\Omega p_{\mathrm{RT}} \cdot \nabla \varphi \,\mathrm{d}x \\
&\quad = \int_\Omega (f - \Pi_0 f) \varphi \,\mathrm{d}x + \int_\Omega \Pi_0 f (1 - I_{\mathrm{NC}}) \varphi \,\mathrm{d}x + \int_{\Gamma_C \cup \Gamma_N} (g - \Pi_0^{\Gamma_C \cup \Gamma_N} g) \varphi \,\mathrm{d}s \\
&\qquad - \int_\Omega (\nabla u - p_{\mathrm{RT}}) \cdot \nabla \varphi \,\mathrm{d}x.
\end{aligned}$$

A Cauchy inequality shows

$$\|\!|\Lambda - \Lambda_{\mathrm{RT}}|\!\|_* \lesssim \mathrm{osc}(f, \mathcal{T}) + \mathrm{osc}_{1/2}(g, \mathcal{E}(\Gamma_C \cup \Gamma_N)) + ||h_{\mathcal{T}} f||_{L^2(\Omega)} + ||\nabla u - p_{\mathrm{RT}}||.$$

Since the cubic bubble functions $b_T := 60 \Pi_{z \in \mathcal{N}(T)} \varphi_z \in H^1_0(T) \cap \in P_3(T)$, with $\mathrm{supp}(b_T) = T$ and $⨍_T b_T \,\mathrm{d}x = 1$ have zero boundary conditions for each triangle $T \in \mathcal{T}$, the bubble function methodology Verfürth (1996) and the continuous variational inequality (4.2) show

$$||h_T \Pi_0 f||_{L^2(T)} \lesssim \mathrm{osc}(f, T) \text{ for all } T \in \mathcal{T}.$$

This concludes the proof. □

4.5.4. Comments on the complementary condition residual

This section comments on the efficiency of the computable integral $\int_{\Gamma_C} (-\lambda_{\mathrm{RT}})(v - \chi)_+ \,\mathrm{d}s$ of the estimator Est as a complementary condition residual for $v := w_D + u_{D2} + J_2^C(\tilde{u}_{\mathrm{CR}} - I_{\mathrm{NC}} u_{D2})$ from (4.27) with u_{CR} replaced by the solution $\tilde{u}_{\mathrm{CR}} \in K_{\mathrm{CR}}(\mathcal{T})$ to (4.24) with right-hand side $\Pi_0 f$. The integral is efficient for obstacles $\chi \in H^1(\Omega)$ which satisfy (4.1), $\chi|_{\Gamma_C \cup \Gamma_D} \in H^{3/2}(\Gamma_C \cup \Gamma_N)$, and $\chi|_{\Gamma_C} \in P_1(\Gamma_C)$ in the sense of Theorem C.

Theorem 4.49. *For an obstacle $\chi \in H^1(\Omega)$ which satisfies (4.1), $\chi|_{\Gamma_C \cup \Gamma_D} \in H^{3/2}(\Gamma_C \cup \Gamma_N)$, and $\chi|_{\Gamma_C} \in P_1(\Gamma_C)$, the function $v = w_D + u_{D2} + J_2^C(\tilde{u}_{\mathrm{CR}} - I_{\mathrm{NC}} u_{D2}) \in \mathcal{A}$ from (4.27) allows for*

$$\begin{aligned}
\int_{\Gamma_C} (-\lambda_{\mathrm{RT}})(v - \chi)_+ \,\mathrm{d}s \lesssim &\|\!|u - \tilde{u}_{\mathrm{CR}}|\!\|^2 + \|\!|w|\!\|^2 + \mathrm{osc}(f, \mathcal{T})^2 \\
&+ \mathrm{osc}^2_{1/2}(g, \mathcal{E}(\Gamma_C \cup \Gamma_N)) + \mathrm{Osc}^2_{1/2,C}(\lambda, \mathcal{E}(\Gamma_C)).
\end{aligned}$$

Remark 4.50. *The conditions on the obstacle ensure that the exact solution $u \in K$ to (4.2) satisfies $u \in H^2(\Omega)$ and hence there exists an L^2 representation $\lambda \in L^2(\Gamma_C; (-\infty, 0])$ of the exact Lagrange multiplier Λ (cf. Theorem 4.3).*

Corollary 4.51. *For $\chi \in H^1(\Omega)$ which satisfies (4.1), $\chi|_{\Gamma_C \cup \Gamma_D} \in H^{3/2}(\Gamma_C \cup \Gamma_N)$, and $\chi|_{\Gamma_C} \in P_1(\Gamma_C)$, the guaranteed upper bound* GUB = 30Est *is efficient with respect to the error $||\nabla u - p_{\mathrm{RT}}||_{L^2(\Omega)}$ and the total error* Err *of Theorem 4.14 in the sense that*

$$||\nabla u - p_{\mathrm{RT}}||_{L^2(\Omega)} \leq \mathrm{Err} + ||\nabla v - p_{\mathrm{RT}}||_{L^2(\Omega)} \approx \mathrm{GUB} + ||\nabla v - p_{\mathrm{RT}}||_{L^2(\Omega)}$$

$$\lesssim |\!|\!| u - \tilde{u}_{\mathrm{CR}} |\!|\!| + \textit{higher-order terms}.$$

Proof. The proof follows from a combination of Theorems 4.14, 4.48, and 4.49 □

Remark 4.52. *The higher-order terms in Corollary 4.51 are the terms* $|\!|\!| w |\!|\!|$, $\operatorname{osc}(f, \mathcal{T})$, $\operatorname{osc}_{1/2}(g, \mathcal{E}(\Gamma_C \cup \Gamma_N))$, *and* $\operatorname{Osc}_{1/2,C}(\lambda, \mathcal{E}(\Gamma_C))$.

Proof of Theorem 4.49. The equivalence of the non-conforming and mixed problems show that the proof of Theorem 4.49 is the same as that of Theorem 4.38. □

Remark 4.53. *Estimates as in Carstensen et al. (2012c, Thm. 2.3) and the bubble-function methodology show, that the term* $|\!|\!| u - \tilde{u}_{\mathrm{CR}} |\!|\!|$ *can be replaced by the error* $||\nabla u - p_{\mathrm{RT}}||_{L^2(\Omega)}$ *plus oscillations* $\operatorname{osc}(f, \mathcal{T})$.

5. Bingham flow problem

This chapter is devoted to the analysis of the Mosolov problem, which describes the unidirectional flow of a Bingham fluid, and leads to a variational inequality of the second kind.

5.1. Problem formulation

This section introduces the mathematical modeling and discusses equivalent formulations

5.1.1. Mathematical modelling

In order to describe the unidirectional flow of a Bingham fluid, let $\Omega \subset \mathbb{R}^2$ be a bounded Lipschitz domain with a polygonal boundary $\partial\Omega$. The domain Ω can be considered as the cross section of a pipe, where the generator of the pipe coincides with the x_3 axis. This formulation of the Bingham problem is also known as Mosolov's problem (cf. Falk and Mercier (1977)). The fluid's behaviour is described by the viscosity $\mu > 0$ and the yield limit $g > 0$. Throughout the thesis, a scaling of these parameters allows for the choice of $\mu = 1$ (i.e., $g := g/\mu$, and $f := f/\mu$) to simplify the notation. This leads to the following potential function

$$W(F) := |F|^2/2 + g|F| \quad \text{for all } F \in \mathbb{R}^2.$$

Define

$$j(q) := g \int_\Omega |q| \,\mathrm{d}x \quad \text{for } q \in L^2(\Omega;\mathbb{R}^2).$$

The variational problem seeks some velocity $u \in H^1_0(\Omega)$ with

$$E(u) = \min_{v \in H^1_0(\Omega)} E(v) \tag{5.1}$$

for the energy

$$E(v) := \int_\Omega W(\nabla v)\,\mathrm{d}x - \int_\Omega fv\,\mathrm{d}x = \int_\Omega |\nabla v|^2/2\,\mathrm{d}x + j(\nabla v) - \int_\Omega fv\,\mathrm{d}x.$$

Theorem 5.1 (existence of solutions)**.** *Mosolov's problem* (5.1) *has a unique solution* $u \in H^1_0(\Omega)$*.*

Proof. Recall $a(v,w) := \int_\Omega \nabla v \cdot \nabla w\,\mathrm{d}x$ from (2.5) on Page 19. Then $E(v) := 1/2a(v,v) + j(\nabla v) - \int_\Omega fv\mathrm{d}x$. Since $a(v,w)$ is a symmetric, continuous, and $H^1_0(\Omega)$ elliptic bilinear form, and j is convex, lower semi-continuous, and proper, Glowinski (2008, Ch. 1, Lem. 4.1) shows that the energy $E(v)$ has a unique minimizer $u \in H^1_0(\Omega)$. □

Lemma 4.1 in Glowinski (2008, Ch. 1) shows that (5.1) is equivalent to the following variational inequality of second kind, which seeks $u \in H_0^1(\Omega)$ such that

$$\int_\Omega f(v-u)\,\mathrm{d}x \le a(u, v-u) + j(\nabla v) - j(\nabla u) \quad \text{for all } v \in H_0^1(\Omega). \tag{5.2}$$

Theorem 5.2 (regularity; Brézis (1971))**.** *Let $\Omega \subset \mathbb{R}^2$ be a bounded domain with a smooth boundary $\partial\Omega$ or a convex polygonal domain. If $f \in L^2(\Omega)$, the solution to* (5.2) *satisfies*

$$u \in H_0^1(\Omega) \cap H^2(\Omega).$$

Theorem 5.3 (Euler-Lagrange equations)**.** *The solution $u \in H_0^1(\Omega)$ to* (5.2) *satisfies the Euler-Lagrange equations in the sense that there exists $\sigma \in H(\mathrm{div}, \Omega) \cap \partial W(\nabla u)$ with*

$$\int_\Omega \sigma \cdot \nabla\varphi\,\mathrm{d}x = \int_\Omega f\varphi\,\mathrm{d}x \quad \textit{for all } \varphi \in H_0^1(\Omega).$$

Proof. The proof follows from Glowinski (2008, Ch. 2, Thm. 6.3) and Mosolov and Miasnikov (1966, Thm. 1.1). □

5.1.2. Equivalent formulations

This subsection presents three equivalent formulations of the Bingham flow problem. Define the set $\mathcal{M} := \{\mu \in L^2(\Omega; \mathbb{R}^2) \mid |\mu| \le 1 \text{ a.e.}\}$. The Lagrange multiplier formulation seeks $(u, \lambda) \in H_0^1(\Omega) \times \mathcal{M}$ such that

$$a(u, v) + g\int_\Omega \lambda \cdot \nabla v\,\mathrm{d}x = \int_\Omega fv\,\mathrm{d}x \quad \text{for all } v \in H_0^1(\Omega), \tag{5.3}$$

$$\lambda \cdot \nabla u = |\nabla u| \quad \text{a.e. in } \Omega. \tag{5.4}$$

Lemma 5.4 (existence of solutions)**.** *There exists a solution $(u, \lambda) \in H_0^1(\Omega) \times \mathcal{M}$ to* (5.3)–(5.4).

Proof. The proof follows for example from Glowinski (2008, Thm. 6.3, Ch. II), Mosolov and Miasnikov (1966, Thm. 1.1), or Theorem 5.3 . □

Remark 5.5 (Non-uniqueness of λ)**.** *Consider the following example with known exact solution from (Glowinski et al., 1981, Sec. 2.3, Ch. 5). Let $\Omega := \{(x, y) \in \mathbb{R}^2 |\ x^2 + y^2 = R^2\}$ for some $R \ge 0$ and $f = C \in \mathbb{R}$. If $g \ge CR/2$, then the exact solution $u_g = 0$. For $g < CR/2$, the exact solution in polar coordinates reads*

$$u_g(r, \varphi) := \begin{cases} C(R^2 - r^2)/4 + g(R - r) & \textit{for } 2g/C \le r \le R, \\ C(R - 2g/C)^2/4 & \textit{for } 0 \le r \le 2g/C. \end{cases}$$

Glowinski et al. (1981, Sec. 2.3, Ch. 5) prove that there exist an infinite number of

Lagrange multipliers $\lambda \in \mathcal{M}$, given in polar coordinates by

$$\lambda(r,\varphi) = \begin{cases} -\begin{pmatrix} \cos\varphi \\ \sin\varphi \end{pmatrix} & \text{for } 2g/C \le r \le R \\ -Cr/(2g)\begin{pmatrix} \cos\varphi \\ \sin\varphi \end{pmatrix} + \beta(r)\begin{pmatrix} -\sin\varphi \\ \cos\varphi \end{pmatrix} & \text{for } 0 \le r \le 2g/C. \end{cases}$$

It follows, that for any $\beta(r) \in L^\infty(0, 2g/C)$ with $|\beta(r)| \le \sqrt{1-(Cr/(2g))^2}$ a.e. on $(0, 2g/C)$, the pair $(u,\lambda) \in H^1_0(\Omega) \times \mathcal{M}$ is a solution to (5.3)–(5.4). Hence the Lagrange multiplier is not unique.

Remark 5.6 (Euler-Lagrange equations)**.** *For some differentiable potential function W, the minimization of the energy $E(v) := \int_\Omega W(\nabla v)\,\mathrm{d}x/2 - \int_\Omega f v\,\mathrm{d}x$ is equivalent to the fulfilment of the Euler-Lagrange equation*

$$\int_\Omega \nabla v \cdot DW(\nabla u)\,\mathrm{d}x = \int_\Omega f v\,\mathrm{d}x \quad \text{for all } v \in H^1_0(\Omega).$$

In the case at hand, $W(F) := |F|^2/2 + g|F|$ consists of a differentiable part $W_1(F) := |F|^2/2$ and a non-differentiable part $W_2(F) := g|F|$. Since the absolute value of any $F \in \mathbb{R}^2$ can be written as $|F| := \sup_{\mu\in\mathcal{M}} \mu \cdot F$, (5.4) implies

$$g\lambda \cdot \nabla(v-u) \le g|\nabla v| - g|\nabla u|.$$

Hence $\nabla u + g\lambda \in \partial W(\nabla u)$. This shows that (5.3)–(5.4) is a generalization of the Euler-Lagrange equations.

The three-field formulation in Carstensen et al. (2015b) employs the bilinear form

$$b((v,q),\tau) := -\int_\Omega v \operatorname{div}\tau\,\mathrm{d}x - \int_\Omega q\cdot\tau\,\mathrm{d}x$$

for all $((v,q),\tau) \in L^2(\Omega)\times L^2(\Omega;\mathbb{R}^2)\times H(\operatorname{div},\Omega)$. It seeks $(u,p) \in L^2(\Omega)\times L^2(\Omega;\mathbb{R}^2)$ and $\sigma \in H(\operatorname{div},\Omega)$ such that

$$\int_\Omega f(v-u)\,\mathrm{d}x \le \int_\Omega p\cdot(q-p)\,\mathrm{d}x + j(q) - j(p) + b((v-u,q-p),\sigma), \tag{5.5}$$

$$b((u,p),\tau) = 0 \tag{5.6}$$

for all $(v,q) \in L^2(\Omega)\times L^2(\Omega;\mathbb{R}^2)$ and $\tau \in H(\operatorname{div},\Omega)$.

Remark 5.7 (Non-uniqueness of σ; (Carstensen et al., 2015b))**.** *The stress $\sigma \in H(\operatorname{div},\Omega)$ is not unique. Let $\Omega \subset \mathbb{R}^2$ and $f \equiv 0$. The solution to the three-field-formulation (5.5)–(5.6) equals $(0,0,\sigma)$ for $\sigma \in H(\operatorname{div},\Omega)$ with*

$$\operatorname{div}\sigma = 0 \text{ and } \int_\Omega q\cdot\sigma\,\mathrm{d}x \le j(q) \quad \text{for all } q \in L^2(\Omega,\mathbb{R}^2). \tag{5.7}$$

Any $\alpha \in H^1_0(\Omega)$ satisfies $\operatorname{Curl}\alpha = (-\partial\alpha/\partial y, \partial\alpha/\partial x) \in H(\operatorname{div},\Omega)$ with $\operatorname{div}\operatorname{Curl}\alpha = 0$. Therefore any $\sigma = g\operatorname{Curl}\alpha/||\operatorname{Curl}\alpha||_{L^\infty(\Omega)}$ for $\alpha \in H^1_0(\Omega)$ with $\operatorname{Curl}\alpha \in L^\infty(\Omega)$ and $\operatorname{Curl}\alpha \neq 0$ satisfies (5.7).

The following result shows the equivalence of the three different formulations for the Bingham problem.

Theorem 5.8 (equivalence)**.** *The three formulations* (5.2)*,* (5.5)–(5.6)*, and* (5.3)–(5.4) *are pairwise equivalent in the following sense.*

- ⓐ *Let* $u \in H^1_0(\Omega)$ *solve* (5.2)*. Then there exists* $\lambda \in \mathcal{M}$ *such that* $(u, \lambda) \in H^1_0(\Omega) \times \mathcal{M}$ *solve* (5.3)–(5.4)*.*
- ⓑ *Let* $(u, \lambda) \in H^1_0(\Omega) \times \mathcal{M}$ *solve* (5.3)–(5.4)*. Then* $(u, \nabla u, g\lambda + \nabla u) \in L^2(\Omega) \times L^2(\Omega; \mathrm{R}^2) \times H(\mathrm{div}, \Omega)$ *solve* (5.5)–(5.6)*.*
- ⓒ *Let* $(u, p, \sigma) \in L^2(\Omega) \times L^2(\Omega; \mathbb{R}^2) \times H(\mathrm{div}, \Omega)$ *solve* (5.5)–(5.6)*. Then* u *solves* (5.2) *and* $p = \nabla u$*.*

Proof. Theorem 6.3 in Glowinski (2008) shows ⓐ. □

To show ⓑ, note that (5.3) implies, that $g\lambda + \nabla u$ satisfies

$$\int_\Omega (g\lambda + \nabla u) \cdot \nabla v \,\mathrm{d}x = \int_\Omega f v \,\mathrm{d}x \quad \text{for all } v \in H^1_0(\Omega).$$

Hence $\sigma := g\lambda + \nabla u \in H(\mathrm{div}, \Omega)$ with $-\mathrm{div}\,\sigma = f$. For any $v \in H^1_0(\Omega)$, $q \in H(\mathrm{div}, \Omega)$, the computation of $b((v - u, q - \nabla u), \sigma)$ yields

$$\begin{aligned} b((v - u, q - \nabla u), g\lambda + \nabla u) = &\int_\Omega f(v - u) \,\mathrm{d}x - \int_\Omega \nabla u \cdot (q - \nabla u) \,\mathrm{d}x \\ &- g \int_\Omega \lambda \cdot (q - \nabla u) \,\mathrm{d}x. \end{aligned}$$

Since $|F| = \sup_{\mu \in \mathcal{M}} \mu \cdot F$, it follows that $-g \int_\Omega \lambda \cdot q \,\mathrm{d}x \geq -j(q)$ for all $q \in H(\mathrm{div}, \Omega)$. Equation (5.4) shows that $g \int_\Omega \lambda \nabla u \,\mathrm{d}x = j(\nabla u)$. Hence (5.5) is satisfied. An integration by parts of $-\int_\Omega \nabla u \cdot \tau \,\mathrm{d}x$ for all $\tau \in H(\mathrm{div}, \Omega)$ shows

$$b((u, \nabla u), \tau) = 0.$$

Hence (5.6) holds with $p = \nabla u$. This concludes the proof of ⓑ. □

The proof of ⓒ is included in Carstensen et al. (2015b, Thm. 2.1). □

Theorem 5.9. ⓐ *The solution* $u \in H^1_0(\Omega)$ *to* (5.2) *is unique.*

- ⓑ *Let* $(u, \lambda) \in H^1_0(\Omega) \times \mathcal{M}$ *solve* (5.3)–(5.4)*. Then* u *is unique.*
- ⓑ *Let* $(u, p, \sigma) \in L^2(\Omega) \times L^2(\Omega; \mathbb{R}^2) \times H(\mathrm{div}, \Omega)$ *solve* (5.5)–(5.6)*. Then* (u, p) *is unique.*

Proof. The proof follows from the unique existence of a minimizer $u \in H^1_0(\Omega)$ of the energy E in (5.1), the equivalence of (5.1) and (5.2), and Theorem 5.8. □

5.2. Reliable and efficient error estimate for the Bingham flow problem

This subsection is devoted to the reliable and efficient error analysis for the Bingham flow problem. Let $(v, \mu) \in H^1_0(\Omega) \times \mathcal{M}$ be any approximation to the solution (u, λ)

to (5.3)–(5.4) and define the residual $\mathrm{Res} \in H^{-1}(\Omega)$ by

$$\mathrm{Res}(\varphi) := \int_\Omega f\varphi \,\mathrm{d}x - g\int_\Omega \mu\cdot\nabla\varphi\,\mathrm{d}x - a(v,\varphi) \quad \text{for all } \varphi\in H^1_0(\Omega). \tag{5.8}$$

With $S := \{\varphi\in H^1_0(\Omega) \mid |\!|\!|\varphi|\!|\!| = 1\}$ set

$$|\!|\!|\mathrm{Res}|\!|\!|_* := \sup\left\{\mathrm{Res}(\varphi) \;\middle|\; \varphi\in S\right\}$$

and

$$|\!|\!|g\,\mathrm{div}(\lambda-\mu)|\!|\!|_* = \sup\left\{g\int_\Omega(\lambda-\mu)\cdot\nabla\varphi\,\mathrm{d}x \mid \varphi\in S\right\}.$$

Theorem 5.10. *Suppose $(v,\mu)\in H^1_0(\Omega)\times\mathcal{M}$ is some approximation to an exact solution $(u,\lambda)\in H^1_0(\Omega)\times\mathcal{M}$ to (5.3)–(5.4) (recall that the Lagrange multiplier is not unique). Then*

$$\begin{aligned}
&\text{ⓐ}\quad g\int_\Omega(\lambda-\mu)\cdot\nabla(u-v)\,\mathrm{d}x + |\!|\!|u-v|\!|\!|^2 = \mathrm{Res}(u-v);\\
&\text{ⓑ}\quad 0 \le g\int_\Omega(\lambda-\mu)\cdot\nabla(u-v)\,\mathrm{d}x - g\int_\Omega\mu\cdot\nabla v\,\mathrm{d}x + j(\nabla v)\\
&\qquad\quad = j(\nabla u) - g\int_\Omega\mu\cdot\nabla u\,\mathrm{d}x + j(\nabla v) - g\int_\Omega\lambda\cdot\nabla v\,\mathrm{d}x;\\
&\text{ⓒ}\quad j(\nabla u) - g\int_\Omega\mu\cdot\nabla u\,\mathrm{d}x + j(\nabla v) - g\int_\Omega\lambda\cdot\nabla v\,\mathrm{d}x + (1-1/2t)|\!|\!|u-v|\!|\!|^2\\
&\qquad\quad \le t|\!|\!|\mathrm{Res}|\!|\!|_*^2/2 + j(\nabla v) - g\int_\Omega\mu\cdot\nabla v\,\mathrm{d}x \quad \textit{for all} \quad 0<t<\infty;\\
&\text{ⓓ}\quad \Big||\!|\!|g\,\mathrm{div}(\lambda-\mu)|\!|\!|_* - |\!|\!|u-v|\!|\!|\Big| \le |\!|\!|\mathrm{Res}|\!|\!|_* \le |\!|\!|u-v|\!|\!| + |\!|\!|g\,\mathrm{div}(\lambda-\mu)|\!|\!|_*.
\end{aligned}$$

Remark 5.11. *Although the Lagrange multiplier λ is not unique, all terms in Theorem 5.10 which include λ are, i.e., for two distinct Lagrange multipliers λ_1 and λ_2 which satisfy (5.3)–(5.4), and any $v\in H^1_0(\Omega)$ it holds*

$$\int_\Omega\lambda_1\cdot\nabla v\,\mathrm{d}x = \int_\Omega\lambda_2\cdot\nabla v\,\mathrm{d}x.$$

Proof. The properties of the continuous Lagrange multiplier (5.3)–(5.4) show

$$g\int_\Omega(\lambda-\mu)\cdot\nabla(u-v)\,\mathrm{d}x = \int_\Omega f(u-v)\,\mathrm{d}x - a(u,u-v) - g\int_\Omega\mu\cdot\nabla(u-v)\,\mathrm{d}x.$$

The definition of the residual leads to

$$\int_\Omega g(\lambda-\mu)\cdot\nabla(u-v)\,\mathrm{d}x = \mathrm{Res}(u-v) - a(u-v,u-v).$$

This concludes the proof of ⓐ. □

Equation (5.4) shows that $g\int_\Omega\lambda\cdot\nabla u\,\mathrm{d}x = j(\nabla u)$. This and straight forward algebraic manipulations prove the equality in ⓑ. Since

$$j(\nabla\varphi) = \sup_{\mu\in\mathcal{M}} g\int_\Omega\mu\cdot\nabla\varphi\,\mathrm{d}x \quad \text{for all } \varphi\in H^1_0(\Omega),$$

the sign condition follows and completes the proof of ⓑ. □

The assertion ⓒ follows from ⓐ−ⓑ with a further evaluation of $\mathrm{Res}(u-v)$. The definition of the operator norm and a Young inequality for $0 < t < \infty$ yield

$$\mathrm{Res}(u-v) \le \|\mathrm{Res}\|_* \|u-v\| \le t\|\mathrm{Res}\|_*^2/2 + \|u-v\|^2/(2t). \qquad \square$$

The proof of ⓓ employs an auxiliary problem with the exact solution $z \in H_0^1(\Omega)$ to

$$a(z,\varphi) = \int_\Omega f\varphi \,\mathrm{d}x - g\int_\Omega \mu\cdot\nabla\varphi \,\mathrm{d}x \qquad \text{for all } \varphi \in H_0^1(\Omega).$$

The continuous solution $(u,\lambda) \in H_0^1(\Omega)\times\mathcal{M}$ to (5.3)–(5.4) yields

$$a(u-z,\varphi) = g\int_\Omega (\mu-\lambda)\cdot\nabla\varphi \,\mathrm{d}x \qquad \text{for all } \varphi \in H_0^1(\Omega).$$

In other words, $u-z \in H_0^1(\Omega)$ is the Riesz representation of the linear and bounded functional $\mu-\lambda$ in the Hilbert space $(H_0^1(\Omega), a)$ and therefore

$$\|u-z\| = \|g\,\mathrm{div}(\lambda-\mu)\|_*. \tag{5.9}$$

The definition of the residual in (5.8) yields

$$\begin{aligned}\|v-z\|^2 &= a(v,v-z) - a(z,v-z)\\ &= a(v,v-z) - \int_\Omega f(v-z)\,\mathrm{d}x + \int_\Omega g\mu\cdot\nabla(v-z)\,\mathrm{d}x\\ &= \mathrm{Res}(z-v) \le \|\mathrm{Res}\|_*\|z-v\|.\end{aligned}$$

This implies $\|z-v\| \le \|\mathrm{Res}\|_*$. A triangle inequality and (5.9) shows

$$\Big|\|g\,\mathrm{div}(\lambda-\mu)\|_* - \|u-v\|\Big| \le \|v-z\| \le \|\mathrm{Res}\|_*.$$

Given any $\varphi \in S := \{\varphi \in H_0^1(\Omega) \mid \|\varphi\| = 1\}$, (5.3)–(5.4) shows $\mathrm{Res}(\varphi) = g\int_\Omega(\lambda-\mu)\cdot\nabla\varphi\,\mathrm{d}x + a(u-v,\varphi)$ and hence

$$\|\mathrm{Res}\|_* \le \sup_{\varphi\in S}\Big(g\int_\Omega(\lambda-\mu)\cdot\nabla\varphi\,\mathrm{d}x + a(e,\varphi)\Big) \le \|g\,\mathrm{div}(\lambda-\mu)\|_* + \|u-v\|.$$

This concludes the proof of ⓓ. □

Given any approximation $(v,\mu) \in H_0^1(\Omega)\times\mathcal{M}$ to the solution $(u,\lambda) \in H_0^1(\Omega)\times\mathcal{M}$ to (5.3)–(5.4), set $e := u-v$ and define the total error

$$\begin{aligned}\mathrm{Err}^2 :=& j(\nabla u) - g\int_\Omega \mu\cdot\nabla u\,\mathrm{d}x + j(\nabla v) - g\int_\Omega \lambda\cdot\nabla v\,\mathrm{d}x\\ &+ \|u-v\|^2 + \|g\,\mathrm{div}(\lambda-\mu)\|_*^2.\end{aligned}$$

This total error Err is controlled by the estimator

$$\mathrm{Est}^2 := \|\mathrm{Res}\|_*^2 + j(\nabla v) - g\int_\Omega \mu\cdot\nabla v\,\mathrm{d}x.$$

Theorem 5.12 (reliability and efficiency)**.** *It holds*

$$(2/3)\,\mathrm{Est}^2 \le \mathrm{Err}^2 \le 33/2\,\mathrm{Est}^2\,.$$

Remark 5.13. *The guaranteed upper bound* GUB *from* (1.2) *on Page 2 satisfies*
$$\mathrm{GUB} = 33/2\mathrm{Est}.$$

Proof of reliability. Theorem 5.10.d leads to
$$\begin{aligned}\mathrm{Err} \leq & 2\|\!|u-v|\!\| + \|\!|\mathrm{Res}|\!\|_* + \Big(j(\nabla u) - g\int_\Omega \mu\cdot\nabla u\,\mathrm{d}x\Big)^{1/2} \\ & + \Big(j(\nabla v) - g\int_\Omega \lambda\cdot\nabla v\,\mathrm{d}x\Big)^{1/2}.\end{aligned}$$
This can be written as a scalar product of $\Big(2\sqrt{2},1,1,1\Big)$ in $\mathbb{R}^4$ with
$$\Big(\|\!|u-v|\!\|/\sqrt{2}, \|\!|\mathrm{Res}|\!\|_*, \Big(j(\nabla u) - g\int_\Omega \mu\cdot\nabla u\,\mathrm{d}x\Big)^{1/2}, \Big(j(\nabla v) - g\int_\Omega \lambda\cdot\nabla v\,\mathrm{d}x\Big)^{1/2}\Big).$$
A Cauchy inequality followed by Theorem 5.10.c with $t=1$ leads to
$$\begin{aligned}\mathrm{Err}^2/11 \leq & \|\!|u-v|\!\|^2/2 + \|\!|\mathrm{Res}|\!\|_*^2 + j(\nabla u) - g\int_\Omega \mu\cdot\nabla u\,\mathrm{d}x \\ & + j(\nabla v) - g\int_\Omega \lambda\cdot\nabla v\,\mathrm{d}x \\ \leq & 3/2\|\!|\mathrm{Res}|\!\|_*^2 + j(\nabla v) - g\int_\Omega \mu\cdot\nabla v\,\mathrm{d}x.\end{aligned}$$
Since $j(\nabla v) - g\int_\Omega \mu\cdot\nabla v\,\mathrm{d}x \geq 0$, it holds
$$3/2\|\!|\mathrm{Res}|\!\|_*^2 + j(\nabla v) - g\int_\Omega \mu\cdot\nabla v\,\mathrm{d}x \leq 3/2\mathrm{Est}^2.$$
This proves
$$\mathrm{Err}^2 \leq 33/2\,\mathrm{Est}^2.$$ □

Proof of efficiency. Straightforward algebraic manipulations and (5.4) show
$$\begin{aligned}j(\nabla v) - g\int_\Omega \mu\cdot\nabla v\,\mathrm{d}x = & j(\nabla v) - g\int_\Omega \lambda\cdot\nabla v\,\mathrm{d}x + j(\nabla u) - g\int_\Omega \mu\cdot\nabla u\,\mathrm{d}x \\ & + g\int_\Omega (\lambda-\mu)\cdot\nabla(v-u)\,\mathrm{d}x.\end{aligned}$$
A Cauchy and a Young inequality result in
$$\begin{aligned}j(\nabla v) - g\int_\Omega \mu\cdot\nabla v\,\mathrm{d}x \leq & j(\nabla v) - g\int_\Omega \lambda\cdot\nabla v\,\mathrm{d}x + j(\nabla u) - g\int_\Omega \mu\cdot\nabla u\,\mathrm{d}x \\ & + \|\!|u-v|\!\|^2/2 + \|\!|g\,\mathrm{div}(\lambda-\mu)|\!\|_*^2/2.\end{aligned}$$
Hence Theorem 5.10.d shows
$$\begin{aligned}\mathrm{Est}^2 \leq & 3/2\|\!|u-v|\!\|^2 + 3/2\|\!|g\,\mathrm{div}(\lambda-\mu)|\!\|_*^2 + j(\nabla v) \\ & - g\int_\Omega \lambda\cdot\nabla v\,\mathrm{d}x + j(\nabla u) - g\int_\Omega \mu\cdot\nabla u\,\mathrm{d}x.\end{aligned}$$
Since $j(\nabla v) - g\int_\Omega \mu\cdot\nabla v\,\mathrm{d}x \geq 0$, it follows
$$\mathrm{Est}^2 \leq 3/2\Big(\|\!|u-v|\!\|^2 + \|\!|g\,\mathrm{div}(\lambda-\mu)|\!\|_*^2 + j(\nabla v) - g\int_\Omega \lambda\cdot\nabla v\,\mathrm{d}x$$

$$+ j(\nabla u) - g \int_\Omega \mu \cdot \nabla u \, \mathrm{d}x \Big)$$
$$= 3/2 \mathrm{Err}^2.$$

This concludes the proof of efficiency. □

5.3. Conforming FEM for the Bingham flow problem

This section is devoted to the conforming Courant FEM for the Bingham problem. The results in the literature, i.e., Glowinski et al. (1981, App. 5) and Glowinski (2008, Thm. 6.6) show that for general Bingham problems, this method has a reduced convergence rate of $h^{1/2}$. For a particular example (see Glowinski (2008, Sec. 6.8)) on a circular domain Ω with a constant right-hand side $f = c \in L^2(\Omega)$ the convergence rate can be improved to $h\sqrt{\log 1/h}$. This section suggests a discrete Lagrange multiplier $\mu \in \mathcal{M}$ and comments on its efficiency in the sense of Theorem B.

5.3.1. Conforming discretization of the Bingham flow problem

Given a shape-regular triangulation from Subsection 2.2.1, recall the Courant finite element space $S^1_0(\mathcal{T})$ from Definition 2.11 on Page 14. The discrete variational inequality seeks $u_\mathrm{C} \in S^1_0(\mathcal{T})$ such that

$$F(v_\mathrm{C} - u_\mathrm{C}) \leq a(u_\mathrm{C}, v_\mathrm{C} - u_\mathrm{C}) + j(\nabla v_\mathrm{C}) - j(\nabla u_\mathrm{C}) \text{ for all } v_\mathrm{C} \in S^1_0(\mathcal{T}). \tag{5.10}$$

Lemma 5.14 (existence of solutions)**.** *There exists a unique solution to* (5.10)

Proof. The proof is given in Lions and Stampacchia (1967, Thm. 2.1'). □

Define the set

$$\mathcal{M}_0 := \{\mu_\mathrm{C} \in P_0(\mathcal{T}; \mathbb{R}^2) \;\big|\; |\mu_\mathrm{C}| \leq 1\}.$$

Following Glowinski (2008), this leads to the following equivalent formulation.

Theorem 5.15. ⓐ *Let $u_\mathrm{C} \in S^1_0(\mathcal{T})$ solve* (5.10)*. Then there exists $\lambda_0 \in \mathcal{M}_0(\mathcal{T})$ such that $(u_\mathrm{C}, \lambda_0)$ solve*

$$a(u_\mathrm{C}, v_\mathrm{C}) + g \int_\Omega \lambda_0 \cdot \nabla v_\mathrm{C} \, \mathrm{d}x = \int_\Omega f v_\mathrm{C} \mathrm{d}x \quad \text{for all } v_\mathrm{C} \in S^1_0(\mathcal{T}) \tag{5.11}$$

$$\int_\Omega \lambda_0 \cdot \nabla u_\mathrm{C} \mathrm{d}x = \int_\Omega |\nabla u_\mathrm{C}| \mathrm{d}x. \tag{5.12}$$

ⓑ *Let $(u_\mathrm{C}, \lambda_0) \in S^1_0(\mathcal{T}) \times \mathcal{M}_0(\mathcal{T})$ solve* (5.11)–(5.12)*, then u_C solves* (5.10)*.*

Proof. The proof follows with the techniques from (Glowinski, 2008, Thm. 6.3). □

5.3.2. Discrete Lagrange multiplier for CFEM

The characterization (5.11)–(5.12) immediately yields some discrete Lagrange multiplier $\lambda_0 \in \mathcal{M}_0(\mathcal{T})$, which solves the discrete problem (5.11)–(5.12) *exactly*. This shows that $j(\nabla u_C) - g\int_\Omega \lambda_0 \cdot \nabla u_C \,\mathrm{d}x = 0$ and hence the terms in Theorem C on Page 3 vanish. With this Lagrange multiplier the residual Res satisfies $\mathrm{Res}(\varphi_C) = 0$ for any $\varphi_C \in S^1_0(\mathcal{T})$ and hence

$$\|\!|\mathrm{Res}|\!\|_*^2 \lesssim ||h_\mathcal{T} f||^2_{L^2(\Omega)} + \sum_{E\in\mathcal{E}(\Omega)} |E|\,||[(\nabla u_C + \lambda_C)\cdot\nu]_E||_{L^2(E)}. \tag{5.13}$$

5.3.3. Remarks on the efficiency of the discrete Lagrange multiplier for CFEM

The results for the problems in the previous chapters present discrete Lagrange multipliers μ, which allow estimates of the type

$$|\!|\!|\lambda - \mu|\!|\!|_* \lesssim |\!|\!|u - u_h|\!|\!| + \mathrm{apx}(\lambda) + \text{higher-order terms}$$

where $\mathrm{apx}(\lambda)$ present approximation terms to the exact Lagrange multiplier λ. Throughout the thesis, the proof of such estimates is possible because there exists some interpolation operator $J : H^1(\Omega) \to V_h$, where V_h is an appropriate discrete space with the following properties.

ⓐ The interpolation operator is H^1 stable, i.e., $|\!|\!|J\varphi|\!|\!| \lesssim |\!|\!|\varphi|\!|\!|$ for all $\varphi \in H^1(\Omega)$.

ⓑ Let $\langle\bullet,\bullet\rangle$ be a dual pairing between W (the unconstrained vector space where the Lagrange multiplier is found, i.e., $L^2(\Omega)$ for the obstacle problem, $L^2(\Gamma_C)$ for Signorini's problems, and $L^2(\Omega;\mathbb{R}^2)$ for the Bingham problem) and V (the homogeneous space associated to the primal variable , i.e., $V = H^1_D(\Omega)$ for the obstacle problem and Signorini's problem and $H^1_0(\Omega)$ for the Bingham problem). For $f \in W$ the interpolation operator J allows for the estimate $\langle f, \varphi - J\varphi\rangle \lesssim \mathrm{apx}(f)|\!|\!|\varphi|\!|\!|$ for all $\varphi \in V$.

ⓒ If $u_h \in V_h$ denotes the discrete solution to a variational inequality and λ_h the corresponding Lagrange multiplier, J satisfies $\langle\lambda_h, \varphi\rangle = a(u_h, J\varphi) - F(J\varphi)$ for all $\varphi \in V$.

This subsection shows that the existence of such an interpolation operator for the case at hand with the solution $(u_C, \lambda_0) \in S^1_0(\mathcal{T}) \times \mathcal{M}_0(\mathcal{T})$ to the discrete Bingham problem (5.11)–(5.12) is impossible.

Assume, that $I : H^1_0(\Omega) \to S^1_0(\mathcal{T})$ is such an interpolation operator with ⓐ – –ⓒ. Since $\lambda_0 \in P_0(\mathcal{T};\mathbb{R}^2)$ is part of the solution (u_C, λ_0) to (5.11)–(5.12), the interpolation operator I has to satisfy

$$\Pi_0 \nabla\varphi = \nabla I\varphi \quad \text{for all } \varphi \in H^1(\Omega).$$

Then

$$\int_\Omega \lambda_0 \cdot \nabla v \,\mathrm{d}x = F(Iv) - a(u_C, Iv)$$

holds for all $v \in H^1_0(\Omega)$. A dimension argument proves that such an operator cannot exist. The non-conforming interpolation operator I_{NC} from Definition 2.19 from Page 16 satisfies $\Pi_0 \nabla v = \nabla_{\mathrm{NC}} I_{\mathrm{NC}} v$ for all $v \in H^1_0(\Omega)$, and since the stiffness matrix for the Crouzeix-Raviart FEM is regular and since there exists a conforming companion operator J_2 from Section 2.4, it holds

$$\dim(\Pi_0 \nabla H^1_0(\Omega)) = \dim(\mathrm{CR}^1_0(\mathcal{T})) = |\mathcal{E}(\Omega)|. \tag{5.14}$$

The Courant space satisfies $\dim(S^1_0(\mathcal{T})) = |\mathcal{N}(\Omega)|$. Since $I : H^1_0(\Omega) \to S^1_0(\mathcal{T})$, the interpolation operator I satisfies

$$\dim(I H^1_0(\Omega)) \leq \dim(S^1_0(\mathcal{T}))$$

and hence also (since the stiffness matrix for the Courant FEM is regular)

$$\dim(\nabla I H^1_0(\Omega)) \leq \dim(S^1_0(\mathcal{T})) = |\mathcal{N}(\Omega)|.$$

Together with (5.14) this shows

$$|\mathcal{E}(\Omega)| \leq |\mathcal{N}(\Omega)|.$$

Since $|\mathcal{N}(\partial\Omega)| = |\mathcal{E}(\partial\Omega)|$, the Euler formula (for Ω simply connected)

$$|\mathcal{N}| + |\mathcal{T}| = 1 + |\mathcal{E}|$$

shows that $\dim(S^1_0(\mathcal{T})) = |\mathcal{N}(\Omega)| < |\mathcal{E}(\Omega)|$ for $|\mathcal{T}| > 1$. This contradiction shows that an efficiency estimate cannot be derived with the methodology of the previous chapters. The efficiency will therefore be studied experimentally in Section 6.3.

5.4. Non-conforming and mixed FEM for the Bingham flow problem

This section is devoted to the non-conforming and mixed finite element discretization of the Bingham flow problem. The two finite element methods are treated in the same chapter, since the two methods are equivalent. The foundation for the mixed method is given in Carstensen et al. (2015b). This section recalls the equivalence of the two methods and suggests a discrete Lagrange multiplier $\lambda_{\mathrm{CR}} \in P_0(\mathcal{T}; \mathbb{R}^2) \cap \mathcal{M}$. With this Lagrange multiplier a realization of Theorem B is proven and comments on a realization of Theorem C are provided.

5.4.1. Non-conforming and mixed discretization of the Bingham flow problem

Given a shape-regular triangulation from Subsection 2.2.1 on Page 11, recall the non-conforming Crouzeix-Raviart and the mixed Raviart-Thomas finite element spaces $\mathrm{CR}^1_0(\mathcal{T})$ from Definition 2.13 on Page 15 and $\mathrm{RT}_0(\mathcal{T})$ from Definition 2.15 on Page 15. The discrete non-conforming finite element method seeks $u_{\mathrm{CR}} \in \mathrm{CR}^1_0(\mathcal{T})$ such that

$$F(v_{\mathrm{CR}} - u_{\mathrm{CR}}) \leq a(u_{\mathrm{CR}}, v_{\mathrm{CR}} - u_{\mathrm{CR}}) + j(\nabla v_{\mathrm{CR}}) - j(\nabla u_{\mathrm{CR}}) \tag{5.15}$$

for all $v_{\mathrm{CR}} \in \mathrm{CR}^1_0(\mathcal{T})$.

Lemma 5.16 (existence of solutions)**.** *There exists a unique solution* $u_{\mathrm{CR}} \in \mathrm{CR}^1_0(\mathcal{T})$ *to* (5.15)*.*

Proof. Since $\mathrm{CR}^1_0(\mathcal{T})$ is a Hilbert space, $a_{\mathrm{NC}}(\bullet,\bullet)$ is a coercive and $\mathrm{CR}^1_0(\mathcal{T})$-elliptic bilinear form, $F|_{\mathrm{CR}^1_0(\mathcal{T})}$ is linear and continuous, and j is convex, lower semi continuous, and proper the proof follows from Lions and Stampacchia (1967). □

The discretization of the three field formulation (5.5)–(5.6) seeks $(u_0, p_0, \sigma_{\mathrm{RT}}) \in P_0(\mathcal{T}) \times P_0(\mathcal{T};\mathbb{R}^2) \times \mathrm{RT}_0(\mathcal{T})$ such that

$$\int_\Omega f(v_0 - u_0)\,\mathrm{d}x \le \int_\Omega p_0 \cdot (q_0 - p_0)\,\mathrm{d}x + j(q_0) - j(p_0) + b((v_0 - u_0, q_0 - p_0), \sigma_{\mathrm{RT}}) \tag{5.16}$$

$$b((u_0, p_0), \tau_{\mathrm{RT}}) = 0 \tag{5.17}$$

for all $(v_0, q_0, \tau_{\mathrm{RT}}) \in P_0(\mathcal{T}) \times P_0(\mathcal{T};\mathbb{R}^2) \times \mathrm{RT}_0(\mathcal{T})$. The equivalence of the two discretizations is shown in Carstensen et al. (2015b) and the results are repeated here for completeness.

Theorem 5.17 (discrete Euler-Lagrange equations)**.** *The solution* $u_{\mathrm{CR}} \in \mathrm{CR}^1_0(\mathcal{T})$ *to* (5.15)*, with the right-hand side* $f \in L^2(\Omega)$*, satisfies the Euler-Lagrange equations in the following sense. There exists* $\tau_{\mathrm{CR}} \in P_0(\mathcal{T};\mathbb{R}^2) \cap \partial W(\nabla_{\mathrm{NC}} u_{\mathrm{CR}})$ *such that*

$$\int_\Omega \tau_{\mathrm{CR}} \cdot \nabla_{\mathrm{NC}} v_{\mathrm{CR}}\,\mathrm{d}x = \int_\Omega f v_{\mathrm{CR}}\,\mathrm{d}x \text{ for all } v_{\mathrm{CR}} \in \mathrm{CR}^1_0(\mathcal{T}).$$

Proof. The proof follows for example from (Glowinski, 2008, Chapter II, Thm. 6.3) or Mosolov and Miasnikov (1966, Thm. 1.1). □

Theorem 5.18 (equivalence of (5.15) and (5.16)–(5.17))**.**

ⓐ *Let* $u_{\mathrm{CR}} \in \mathrm{CR}^1_0(\mathcal{T})$ *solve* (5.15) *with piecewise constant right-hand side* $\Pi_0 f$ *and let* $\sigma_{\mathrm{CR}} \in P_0(\mathcal{T};\mathbb{R}^2) \cap \partial W(\nabla_{\mathrm{NC}} u_{\mathrm{CR}})$ *satisfy*

$$\int_\Omega \sigma_{\mathrm{CR}} \cdot \nabla_{\mathrm{NC}} v_{\mathrm{CR}}\,\mathrm{d}x = \int_\Omega \Pi_0 f v_{\mathrm{CR}}\,\mathrm{d}x \quad \text{for all } v_{\mathrm{CR}} \in \mathrm{CR}^1_0(\Omega).$$

Then $(\Pi_0 u_{\mathrm{CR}}, \nabla_{\mathrm{NC}} u_{\mathrm{CR}}, \sigma_{\mathrm{CR}} - \Pi_0 f/2(\bullet - \mathrm{mid}(T)))$ *solves* (5.16)–(5.17)*.*

ⓑ *Let* $(u_0, p_0, \sigma_{\mathrm{RT}}) \in P_0(\mathcal{T}) \times P_0(\mathcal{T};\mathbb{R}^2) \times \mathrm{RT}_0(\mathcal{T})$ *be a solution to* (5.16)–(5.17)*, then* $u_{\mathrm{CR}} := u_0 + p_0 \cdot (\bullet - \mathrm{mid}(\mathcal{T})) \in \mathrm{CR}^1_0(\mathcal{T})$ *solves* (5.15) *with piecewise constant right-hand side* $\Pi_0 f$*.*

Proof. The proof is presented in Theorem 3.1 of Carstensen et al. (2015b). □

5.4.2. Discrete Lagrange multiplier for NCFEM

Another equivalent formulation concerns the discrete Lagrange multiplier in the set $\mathcal{M}_0(\mathcal{T}) := \{\mu_0 \in P_0(\mathcal{T};\mathbb{R}^2) \mid |\mu_0| \le 1\}$.

Theorem 5.19. *The following statements are equivalent*

ⓐ *Let* $u_{\mathrm{CR}} \in \mathrm{CR}^1_0(\mathcal{T})$ *solve* (5.15). *Then there exists* $\lambda_{\mathrm{CR}} \in \mathcal{M}_0(\mathcal{T})$ *such that* $(u_{\mathrm{CR}}, \lambda_{\mathrm{CR}})$ *satisfy*

$$a_{\mathrm{NC}}(u_{\mathrm{CR}}, v_{\mathrm{CR}}) + g \int_\Omega \lambda_{\mathrm{CR}} \cdot \nabla_{\mathrm{NC}} v_{\mathrm{CR}} \,\mathrm{d}x = \int_\Omega f v_{\mathrm{CR}} \,\mathrm{d}x, \tag{5.18}$$

$$\int_\Omega \lambda_{\mathrm{CR}} \cdot \nabla_{\mathrm{NC}} u_{\mathrm{CR}} \,\mathrm{d}x = \int_\Omega |\nabla_{\mathrm{NC}} u_{\mathrm{CR}}| \,\mathrm{d}x \tag{5.19}$$

for all $v_{\mathrm{CR}} \in \mathrm{CR}^1_0(\mathcal{T})$.

ⓑ *Let* $(u_{\mathrm{CR}}, \lambda_{\mathrm{CR}}) \in \mathrm{CR}^1_0(\mathcal{T}) \times \mathcal{M}_0(\mathcal{T})$ *solve* (5.18)– (5.19), *then* u_{CR} *solves* (5.15).

Proof. The proof follows as in Chapter II, Thm. 6.3 of Glowinski (2008). □

Remark 5.20. *The solution to* (5.18)–(5.19) *satisfies*

$$|||\mathrm{Res}|||_* \lesssim \sqrt{1/48 + 1/j_{1,1}^2}\, ||h_{\mathcal{T}} f||_{L^2(\Omega)} + |||u_{\mathrm{CR}} - v|||. \tag{5.20}$$

This follows from the definition of the residual and the properties of the non-conforming interpolation operator in Theorem 2.20 on Page 16.

5.4.3. Efficiency of the discrete Lagrange multiplier for NCFEM

The discrete Lagrange multiplier from (5.18)–(5.19) is efficient in the following sense.

Theorem 5.21. *Let* $(u_{\mathrm{CR}}, \lambda_{\mathrm{CR}}) \in \mathrm{CR}^1_0(\mathcal{T}) \times \mathcal{M}_0(\mathcal{T})$ *solve* (5.18)–(5.19). *Then the Lagrange multiplier* λ_{CR} *satisfies*

$$|||g \operatorname{div}(\lambda - \lambda_{\mathrm{CR}})|||_* \lesssim |||u - u_{\mathrm{CR}}|||_{\mathrm{NC}} + ||\sigma - \Pi_0 \sigma||_{L^2(\Omega)} + \operatorname{osc}(f, \mathcal{T}).$$

Remark 5.22. *The result holds for any* σ *which satisfies the Euler Lagrange equations as in Theorem 5.3.*

Proof. Since $\lambda_{\mathrm{CR}} \in \mathcal{M}_0(\mathcal{T}) \subset P_0(\mathcal{T}; \mathbb{R}^2)$, the properties of the non-conforming interpolation operator I_{NC} show that

$$\int_\Omega \lambda_{\mathrm{CR}} \cdot \nabla v \,\mathrm{d}x = \int_\Omega \lambda_{\mathrm{CR}} \cdot \nabla_{\mathrm{NC}} I_{\mathrm{NC}} v \,\mathrm{d}x.$$

For all $v \in H^1_0(\Omega)$ with $|||v||| = 1$ this, (5.3), (5.18), and $a_{\mathrm{NC}}(u_{\mathrm{CR}}, v - I_{\mathrm{NC}} v) = 0$ lead to

$$\int_\Omega (\lambda - \lambda_{\mathrm{CR}}) \cdot \nabla v \,\mathrm{d}x = \int_\Omega f(v - I_{\mathrm{NC}} v) \,\mathrm{d}x - a_{\mathrm{NC}}(u - u_{\mathrm{CR}}, v).$$

A Cauchy inequality and the interpolation error estimate from Subsection 2.2.6 lead to

$$|||g \operatorname{div}(\lambda - \lambda_{\mathrm{CR}})|||_* \lesssim |||u - u_{\mathrm{CR}}||| + ||h_{\mathcal{T}} f||_{L^2(\Omega)}.$$

The term $||h_{\mathcal{T}} f||_{L^2(\Omega)}$ is estimated for each triangle separately. For any $T \in \mathcal{T}$, define the cubic bubble function $b_T := 60 \Pi_{z \in \mathcal{N}(T)} \varphi_z \in H^1_0(T) \cap P_3(T)$ with $⨍_T b_T \,\mathrm{d}x = 1$. With $w_T := \Pi_0 f b_T$ the bubble function methodology due to Verfürth (1996) leads to

$$||h_T f||^2_{L^2(T)} \lesssim ||h_T (f - \Pi_0 f)||^2_{L^2(T)} + h_{\mathcal{T}}^2 \int_T \Pi_0 f w_T \,\mathrm{d}x$$

$$\lesssim ||h_T(f-\Pi_0 f)||^2_{L^2(T)} + h_{\mathcal{T}}^2 \int_\Omega f w_T \,\mathrm{d}x.$$

The Euler Lagrange equations in Theorem 5.3 show that there exists $\sigma \in H(\mathrm{div},\Omega)\cap \partial W(\nabla u)$ such that

$$\int_\Omega f w_T \,\mathrm{d}x = \int_T \sigma \nabla w_T \,\mathrm{d}x = \int_T (\sigma - \Pi_0\sigma)\nabla w_T \,\mathrm{d}x.$$

A Cauchy inequality and an inverse estimate show that

$$||h_{\mathcal{T}} f||_{L^2(\Omega)} \lesssim \mathrm{osc}(f,\mathcal{T}) + ||\sigma - \Pi_0\sigma||_{L^2(\Omega)}$$

and concludes the proof. □

5.4.4. Comments on the guaranteed upper bound

This subsection is devoted to the guaranteed upper bound Est in Theorem 5.12. In comparison to the conforming finite element method in Section 5.3, any conforming companion $v \in H^1_0(\Omega)$ to $u_{\mathrm{CR}} \in \mathrm{CR}^1_0(\mathcal{T})$ leads to the additional term

$$j(\nabla v) - g\int_\Omega \lambda_{\mathrm{CR}} \cdot \nabla v \,\mathrm{d}x$$

in the guaranteed upper bound Est. It appears to be desirable to modify the discrete Lagrange multiplier $\mu = \lambda_{\mathrm{CR}}$ with respect to the chosen conforming companion $v \in H^1_0(\Omega)$, so that the term $j(\nabla v) - g\int_\Omega \mu \cdot \nabla v \,\mathrm{d}x$ becomes as small as possible and Theorem 5.21 is fulfilled to a maximum extend. This subsection shall present some heuristic ideas for such modifications, that will be explored with respect to their performance in the numerical experiments of Subsection 6.3.

For any $v \in H^1_0(\Omega)$, the term $j(\nabla v) - g\int_\Omega \mu \cdot \nabla v \,\mathrm{d}x$ vanishes for

$$\mu := \begin{cases} \nabla v/|\nabla v| & \text{if } \nabla v \neq 0, \\ B_1(0) & \text{otherwise} \end{cases}$$

and so seems to present a possibility to choose v and μ with respect to each other.

Assume, that some $\mu \in \mathcal{M}$ is chosen. Then to estimate $\|\!|g\,\mathrm{div}(\lambda-\mu)|\!\|_*$ it suffices to estimate $\|\!|g\,\mathrm{div}(\lambda_{\mathrm{CR}}-\mu)|\!\|_*$. For the discrete Crouzeix-Raviart solution u_{CR} set $v := J_1 u_{\mathrm{CR}}$, where J_1 is the conforming companion operator from Subsection 2.2.6. If $\nabla_{\mathrm{NC}} u_{\mathrm{CR}} \neq 0 \neq \nabla v$ on some triangle $T \in \mathcal{T}$, it follows that $\lambda_{\mathrm{CR}}|_T = \nabla_{\mathrm{NC}} u_{\mathrm{CR}}/|\nabla_{\mathrm{NC}} u_{\mathrm{CR}}|$ and hence the difference $\left|\lambda_{\mathrm{CR}}|_T - \nabla v|_T/|\nabla v|\right|$ satisfies

$$\left|\lambda_{\mathrm{CR}}|_T - \nabla v|_T/|\nabla v|\right| \leq 2|\nabla_{\mathrm{NC}} u_{\mathrm{CR}} - \nabla v|/(|\nabla_{\mathrm{NC}} u_{\mathrm{CR}}| + |\nabla v|).$$

(This follows essentially from the binomial formulas and can be found in Glowinski (2008, Ch. 2, Lem. 6.1).) This only leads to a useful estimate if $|\nabla v| + |\nabla_{\mathrm{NC}} u_{\mathrm{CR}}| >> 1$ and hence the factor $2/(|\nabla u_{\mathrm{CR}}| + |\nabla v|)$ can be controlled by a constant. Given $v = J_1 u_{\mathrm{CR}}$, this observation suggests the following algorithmic modification of $\mu = \lambda_{\mathrm{CR}}$.

Algorithm 1 Algorithm for the modification of the non-conforming Lagrange multiplier for the Bingham problem.

for $T \in \mathcal{T}$ **do**
  if $\left|\nabla v|_T\right| = 0$ **then**
    $\mu|_T = \lambda_{\mathrm{CR}}|_T$
  else
    Compute $\alpha := \min\Big\{ j(\nabla v) - g \int_\Omega \lambda_{\mathrm{CR}} \cdot \nabla v \,\mathrm{d}x,$
      $\left|\nabla_{\mathrm{NC}} u_{\mathrm{CR}}|_T - \nabla v|_T\right| / \Big(\left|\nabla_{\mathrm{NC}} u_{\mathrm{CR}}|_T\right| + \left|\nabla v|_T\right|\Big)\Big\}$
    if $\alpha = j(\nabla v) - g \int_\Omega \lambda_{\mathrm{CR}} \cdot \nabla v \,\mathrm{d}x$ **then**
      $\mu|_T = \lambda_{\mathrm{CR}}|_T$
    else
      $\mu|_T = \nabla v|_T / \left|\nabla v|_T\right|$
    end if
  end if
end for

This approach leads to the minimization of the critical terms, both on the side of the error terms, as well as on the side of the terms in Est. Unfortunately, from an analytical point of view, it is impossible to show efficiency, and hence the numerical experiments in Subsection 6.3 will clarify the question of efficiency for certain model scenarios.

6. Numerical experiments

This chapter presents numerical experiments for the three model problems; the obstacle problem, the Signorini model problem, and the Bingham flow problem. Each of the three Sections 6.1, 6.2, and 6.3 studies the convergence of the presented finite element methods and the presented estimators as well as their efficiency for representative benchmark problems on uniformly and adaptively refined meshes. Recall that for each problem and each finite element method there exists an estimator Est. Assume that for any triangulation $\mathcal{T}$, this estimator satisfies $\mathrm{Est}^2 = \sum_{T\in\mathcal{T}} \mathrm{Est}^2(T)$ for local contributions $\mathrm{Est}^2(T)$ of Est. Then the following algorithm drives the adaptive mesh-refinement.

Algorithm 2 Adaptive algorithm

INPUT: initial triangulation $\mathcal{T}_0$ and parameter $0 < \Theta \leq 1$
for $\ell = 0$ until termination **do**
SOLVE: Compute the discrete solution
ESTIMATE: Compute local contributions of Est
MARK (Dörfler marking): Choose minimal subset $\mathcal{M}_\ell \subseteq \mathcal{T}_\ell$ such that

$$\Theta \sum_{T\in\mathcal{T}_\ell} \mathrm{Est}^2(T) \leq \sum_{K\in\mathcal{M}_\ell} \mathrm{Est}^2(K).$$

REFINE: Generate the smallest shape-regular triangulation $\mathcal{T}_{\ell+1}$ of $\mathcal{T}_\ell$ in which at least all triangles of $\mathcal{M}_\ell$ are refined
end for
OUTPUT: Sequence of discrete solutions, error estimators, and triangulations

Remark 6.1. *The local contributions of* Est *depend on the choice of the error estimator for the corresponding residual term* $|\!|\!|\mathrm{Res}|\!|\!|_*$. *This quantity depends on the problem (obstacle, Signorini, Bingham) and the finite element method (CFEM, NCFEM, MFEM), and will be defined in each of the Sections 6.1, 6.2, and 6.3.*

Throughout this chapter, the conforming FEM is represented with a diamond marker ($\Diamond$), the non-conforming FEM with a square marker ($\square$), and the mixed FEM with a circular marker ($\bigcirc$). In plots where both error and estimator terms are presented, markers for error terms are connected by a solid lines, and markers for estimator terms by a dashed one. Essentially two types of plots are presented, convergence history plots and plots which demonstrate the efficiency of the finite element methods.

convergence plots The convergence plots have a double logarithmic scale and plot error terms, e.g., the total error Err or the error in the energy norm $|||u - v|||$, and estimator terms, e.g., the estimator Est or parts of it, against the number of degrees of freedom (`ndof`). The standard setting is to plot the error and the estimator to demonstrate that both have the same convergence rate (cf. Figure 6.2). The legend at the side names the plotted quantities. The type of refinement is demonstrated by the colour of the markers, white markers abbreviate uniform mesh-refinement, shaded markers imply adaptive mesh refinement.

efficiency plots The efficiency plots have a logarithmically scaled x-axis and plot the ratio of an error estimator and the error against the number of degrees of freedom (`ndof`). The legend at the side names the plotted quantities. The type of refinement is demonstrated by the colour of the markers, white markers abbreviate uniform mesh-refinement, shaded markers imply adaptive mesh refinement.

unknown exact solution Several of the following examples concern unknown exact solutions. To approximate the exact solution, assume for the moment, that the discrete system is solved with the conforming FEM. After each level, the triangulation is red-refined twice and the problem is then solved with the non-conforming FEM. This new non-conforming approximation serves as an approximation to the exact solution. In case that the non-conforming or mixed FEMs are employed to solve the discrete problem, the conforming FEM on a twice red-refined triangulation serves as an approximation to the exact solution. In each case, a different finite element method is employed to eliminate errors that are numerical artefacts of the finite element method at hand.

The code to compute the discrete solutions, the error estimators, and the error terms is based on the Matlab software package AFEM (Carstensen et al, 2009) maintained at the Humboldt-Universität. The details for the new routines can be found in Appendix B. The complete software can be found in Appendix C. The numerical experiments are implemented with the Matlab version 7.14.0.739 (R2012a) (The MathWorks, 2012).

6.1. Obstacle problem

This section presents five different numerical benchmark examples for the obstacle problem, discretized with the conforming Courant CFEM, the non-conforming Crouzeix-Raviart NCFEM, and the mixed Raviart-Thomas MFEM. For a given triangulation, recall the conforming discrete Lagrange multipliers λ_{CB} and λ_V from Subsection 3.3.4 and define λ_{V2} with the coefficients from Remark 3.24 on Page 33 (Veeser, 2001) and let λ_{CM} denote the discrete Lagrange multiplier from Carstensen and Merdon (2013b). Recall the non-conforming Lagrange multiplier is $\lambda_{\mathrm{CR}}^{-}$ from (3.39) on Page 44 and the mixed Lagrange multiplier is λ_{RT} from (3.44) on Page 53.

For each finite element method, recall the approximation $v \in \mathcal{A}$ to the exact solution $u \in K$ and the residual

$$\operatorname{Res}(\varphi) = \int_\Omega (f-\mu)\varphi \,\mathrm{d}x - a(v,\varphi) \quad \text{for all } \varphi \in H^1_0(\Omega)$$

where μ abbreviates any of the above discrete Lagrange multipliers. Recall, that for each discrete Lagrange multiplier μ, the estimator splits into three components

$$\operatorname{Est}^2 = \|\operatorname{Res}\|_*^2 + \int_\Omega (-\mu)(v-\chi)_+ \,\mathrm{d}x + \|\min\{0, v-\chi\}\|^2.$$

The terms $\eta^2_{\mathrm{CC},\mu} := \int_\Omega (-\mu)(v-\chi)_+ \,\mathrm{d}x$ and $\eta^2_{\mathrm{w},\mu} := \|\min\{0, v-\chi\}\|^2$ are computable element wise and satisfy

$$\eta^2_{\mathrm{CC},\mu} = \sum_{T\in\mathcal{T}} \eta^2_{\mathrm{CC},\mu}(T) \quad \text{and} \quad \eta^2_{\mathrm{w},\mu} = \sum_{T\in\mathcal{T}} \eta^2_{\mathrm{w},\mu}(T).$$

To find a computable bound for $\|\operatorname{Res}\|_*^2$, recall Remark 3.20 and let $z_{\mathrm{C}} \in S^1_0(\mathcal{T})$ denote the Riesz-representation of $\operatorname{Res}|_{S^1_0(\mathcal{T})}$ (for an arbitrary but fixed Lagrange multiplier λ_{CB}, λ_V, λ_{V2}, or λ_{CM}) and let $z_2 \in S^2_0(\mathcal{T})$ denote the Riesz representation of $\operatorname{Res}|_{S^2_0(\mathcal{T})}$ for the non-conforming Lagrange multiplier λ^-_{CR}. Let $w_D \in H^1(\Omega)$ from Theorem 2.28 on Page 18 be the function which corrects the boundary conditions in accordance to the finite element method. For $T \in \mathcal{T}$, this leads to the following computable element wise upper bounds of $\|\operatorname{Res}\|_*^2 \le \eta^2_{\mathrm{Res},\mu} = \sum_{T\in\mathcal{T}} \eta^2_{\mathrm{Res},\mu}(T)$ (cf. for example Braess (2007)) for

$$\begin{aligned}
\eta^2_{\mathrm{Res},\mu}(T) :=& ||h_T(f-\mu)||^2_{L^2(T)} + \sum_{E\in\mathcal{E}(T)} |E| \, ||[\nabla(u_{\mathrm{C}} + z_{\mathrm{C}})\cdot\nu_E]_E||^2_{L^2(E)} \\
&+ \|w_D\|_T + \|z_{\mathrm{C}}\|_T^2 \quad \text{for } \mu = \lambda_{\mathrm{CB}}, \lambda_V, \lambda_{V2}, \lambda_{\mathrm{CM}}, \\
\eta^2_{\mathrm{Res},\lambda^-_{\mathrm{CR}}}(T) :=& ||h_T(f-\lambda^-_{\mathrm{CR}})||^2_{L^2(T)} + \sum_{E\in\mathcal{E}(T)} |E| \, ||[\nabla I_{\mathrm{C}}(v+z_2)\cdot\nu_E]_E||^2_{L^2(E)} \\
&+ \|(1-I_{\mathrm{C}})v\|_T + \|w_D\|_T + \|z_2\|_T, \\
\eta^2_{\mathrm{Res},\lambda_{\mathrm{RT}}}(T) :=& \operatorname{osc}^2(f,\mathcal{T}) + ||p_{\mathrm{RT}} - \nabla v||^2_{L^2(\Omega)}.
\end{aligned}$$

To clarify the notation of the legends, let $\eta^2_\mu := \eta^2_{\mathrm{Res},\mu} + \eta^2_{\mathrm{CC},\mu} + \eta^2_{\mathrm{w},\mu}$ for any of the six discrete Lagrange multipliers above denote the error estimator and let $\operatorname{Err}(\mu, \mathrm{FEM})$ denote the total error Err from Theorem 3.18 for a given discrete Lagrange multiplier and FEM=CFEM, NCFEM, or MFEM.

The adaptive algorithm on Page 109, employs the local estimators $\eta_{\lambda_{\mathrm{CB}}}$ for CFEM, $\eta_{\lambda^-_{\mathrm{CR}}}$ for NCFEM, and $\eta_{\lambda_{\mathrm{RT}}}$ for MFEM.

6.1.1. Square domain

The first experiment from Nochetto et al. (2003) concerns the constant obstacle $\chi \equiv 0$ on the square domain $\Omega := (-1,1)^2$. It is subject to the Dirichlet data

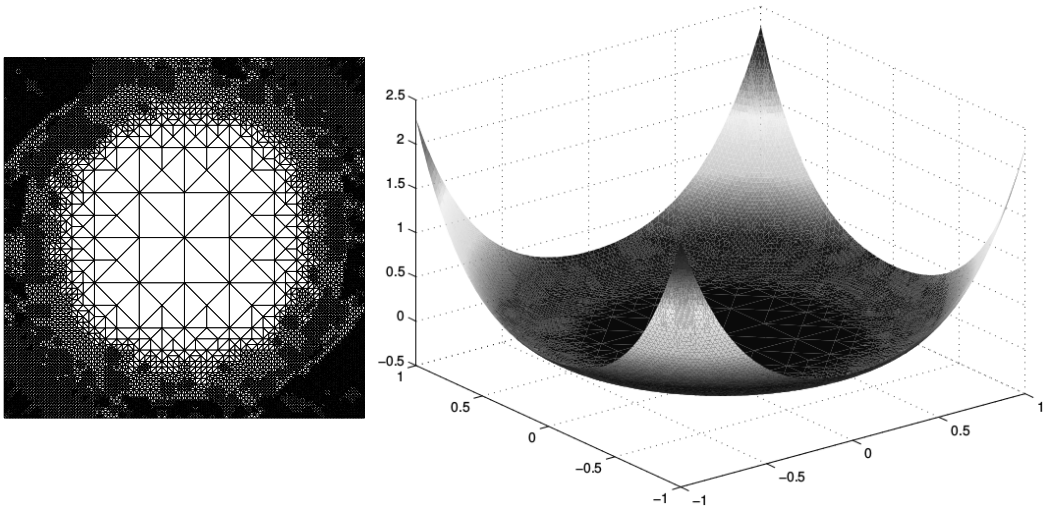

Figure 6.1.: Triangulation (left) and solution after 13 levels of adaptive refinement (right) for NCFEM for the experiment from Subsection 6.1.1.

$u_D(r,\varphi) := r^2 - 0.49$ and the right-hand side

$$f(r,\varphi) := \begin{cases} -16r^2 + 3.92 & \text{for } r > 0.7, \\ -5.8408 + 3.92r^2 & \text{for } r \leq 0.7. \end{cases}$$

The exact solution reads

$$u(r,\varphi) := \max\{0, r^2 - 0.49\}^2.$$

The contact zone is a circle of radius 0.7 centred at the origin (cf. Figure 6.1 right). Figure 6.1 left depicts the adaptive mesh after 13 levels of refinement for NCFEM and shows that the boundary of the contact zone is well refined, whereas the contact zone, where it holds $u_{\mathrm{CR}} = \chi = 0$, is not. Figure 6.2 displays the total error and the estimators for the conforming CFEM with the Lagrange multiplier $\mu = \lambda_{\mathrm{CB}}$, the non-conforming NCFEM, and the mixed MFEM both on adaptive and uniform meshes. The experiment reproduces the expected convergence rate of -0.5 with respect to the number of degrees of freedom (`ndof`), both for adaptive and uniformly refined meshes. The efficiency indices for these methods, for adaptive and uniform meshes are displayed in Figure 6.3. The efficiency index for the conforming finite element method at 4.7 is well above that for the non-conforming NCFEM at 2.5 and that for the mixed MFEM at 1.2. Figure 6.4 shows that the residual term of the error estimator for the mixed Raviart-Thomas FEM is smaller than that of the other two methods. The analysis in Section 3.5 shows that in the case of the Raviart-Thomas MFEM, the residual does not have to be estimated, but can be computed directly and leads to oscillations $\mathrm{osc}(f, \mathcal{T})$ of the right-hand side f and the error $||p_{\mathrm{RT}} - v||_{L^2(\Omega)}$, where v is the conforming companion. Figure 6.5 implies that the error estimator is dominated by the residual term and the error

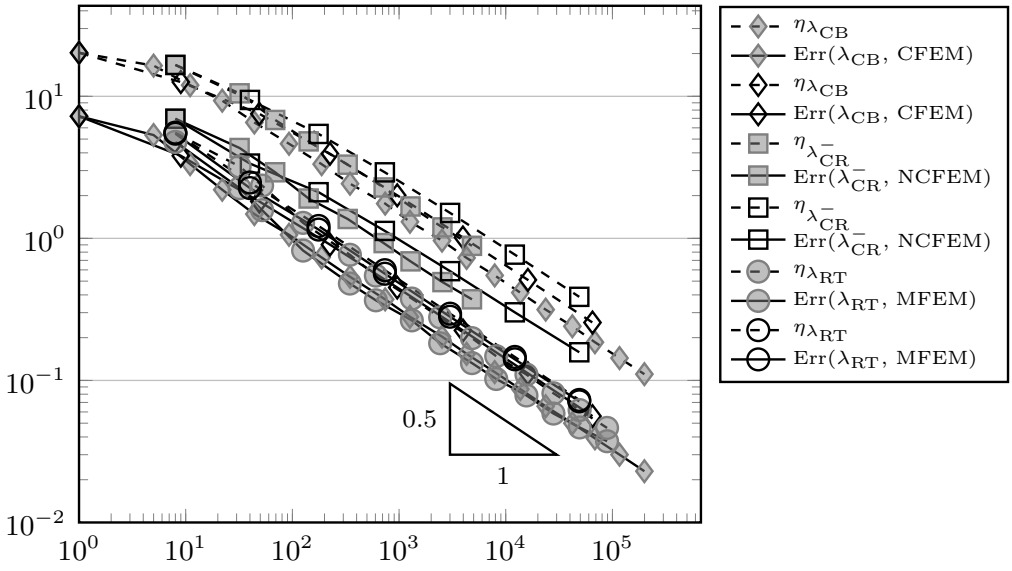

Figure 6.2.: Total error and error estimators for CFEM with $\mu = \lambda_{\mathrm{CB}}$, NCFEM, and MFEM for the experiment from Subsection 6.1.1 for adaptive (grey) and uniform (white) mesh-refinement.

by the error in the primal variables for CFEM. The other terms converge with a higher rate of convergence. The same behaviour can be observed for the other two methods (undisplayed). Figures 6.6 and 6.7 highlight the results of Corollaries 3.30, 3.41, and 3.50. Figure 6.6 shows, that the errors of the primal variable in the energy norm and the corresponding estimators (with the additional terms $\|\!|v - u_{\mathrm{CR}}|\!\|$ for NCFEM and $||\nabla v - p_{\mathrm{RT}}||_{L^2(\Omega)}$ for MFEM, in accordance with Corollaries 3.41, and 3.50) converge with the expected optimal convergence rate of -0.5 with respect to the number of degrees of freedom. Figure 6.7 depicts the resulting efficiency indices, which are higher than those in Figure 6.3 since only a part of the total error is considered. Figure 6.8 presents a comparison of the different estimators for the conforming CFEM. They show identical behaviour which is expected, since the exact solution u is not in contact at the boundary and hence the exact Lagrange multiplier satisfies $\lambda = 0$ along the boundary $\partial\Omega$.

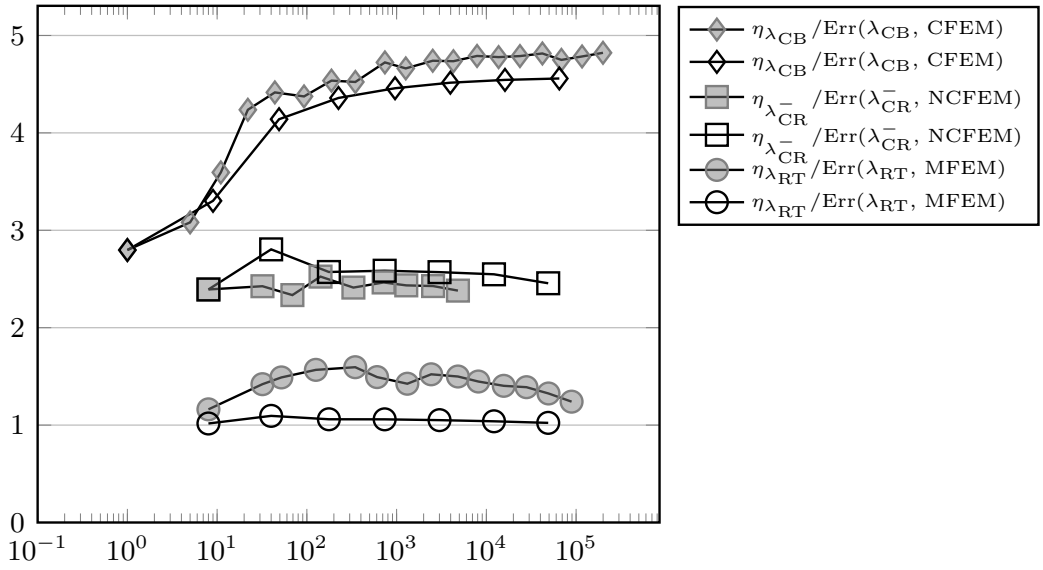

Figure 6.3.: Efficiency indices for the total error for CFEM with $\mu = \lambda_{\mathrm{CB}}$, NCFEM, and MFEM for the experiment from Subsection 6.1.1 for adaptive (grey) and uniform (white) mesh-refinement.

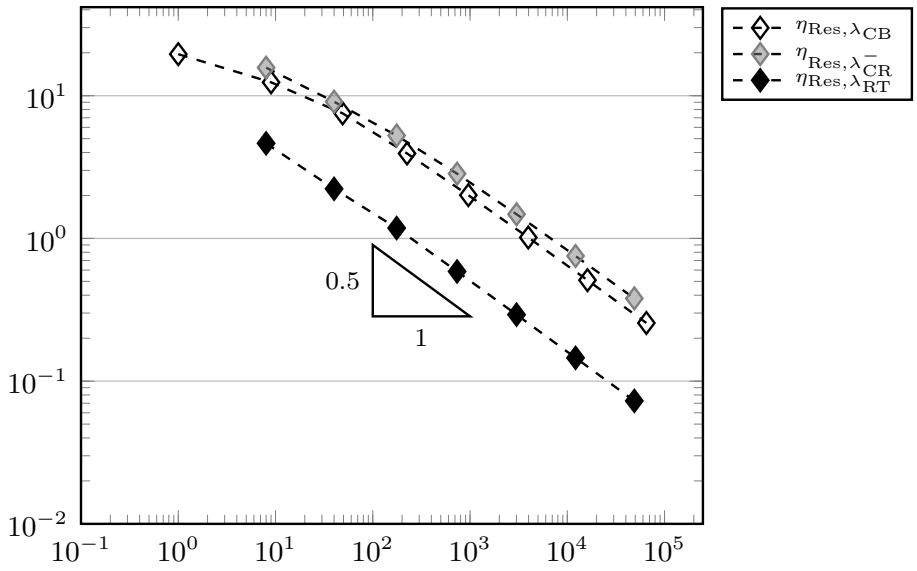

Figure 6.4.: Residual component of the estimator for CFEM with $\mu = \lambda_{\mathrm{CB}}$, NCFEM, and MFEM for the experiment from Subsection 6.1.1 for uniform mesh-refinement.

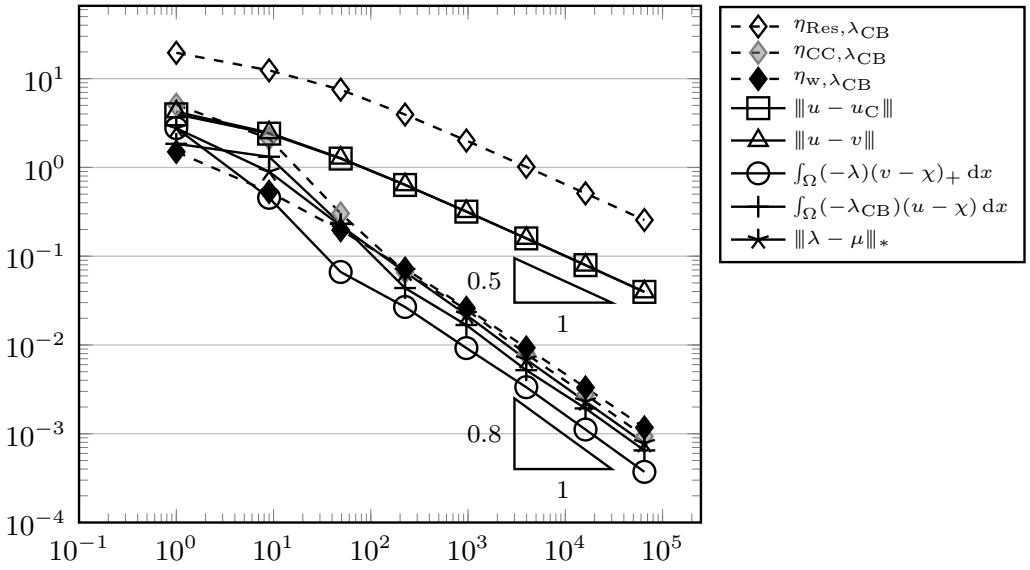

Figure 6.5.: Comparison of different error and estimator components for CFEM for the experiment from Subsection 6.1.1 for uniform mesh-refinement.

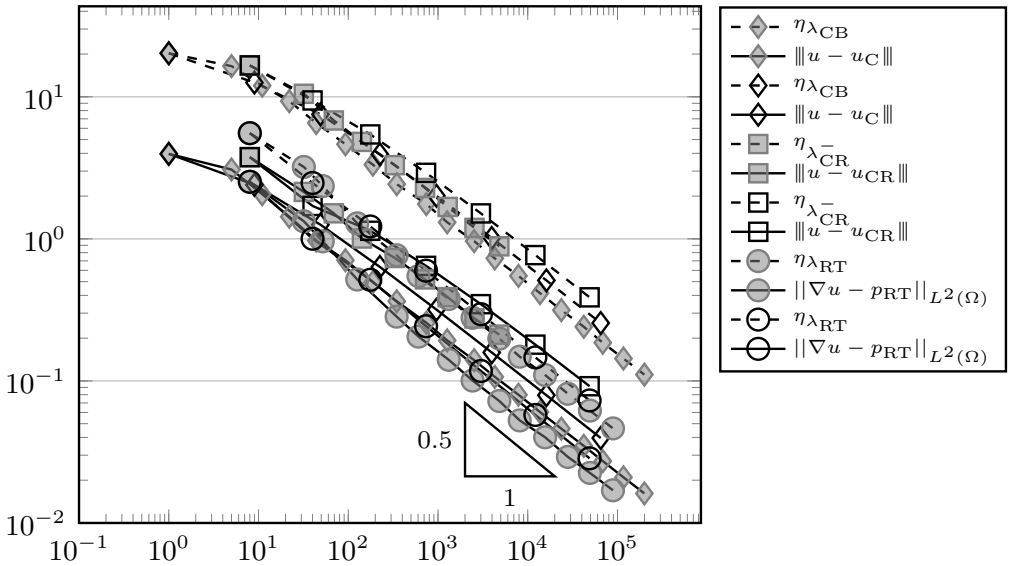

Figure 6.6.: Error of the primal variable in the energy norm and error estimators for CFEM with $\mu = \lambda_{\mathrm{CB}}$, NCFEM, and MFEM for the experiment from Subsection 6.1.1 for adaptive (grey) and uniform (white) mesh-refinement.

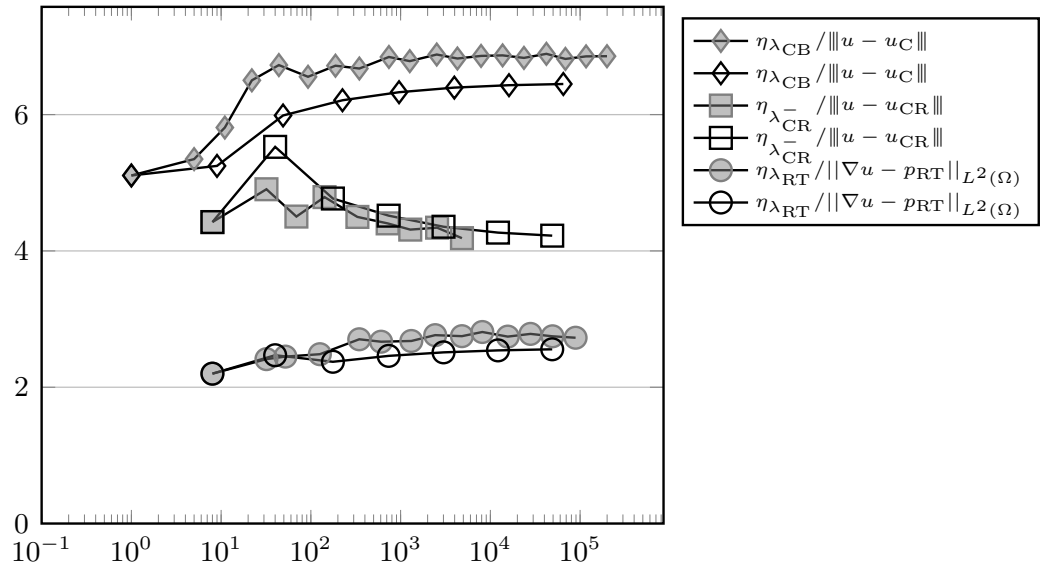

Figure 6.7.: Efficiency indices for the error of the primal variable in the energy norm for CFEM with $\mu = \lambda_{\mathrm{CB}}$, NCFEM, and MFEM for the experiment from Subsection 6.1.1 for adaptive (grey) and uniform (white) mesh-refinement.

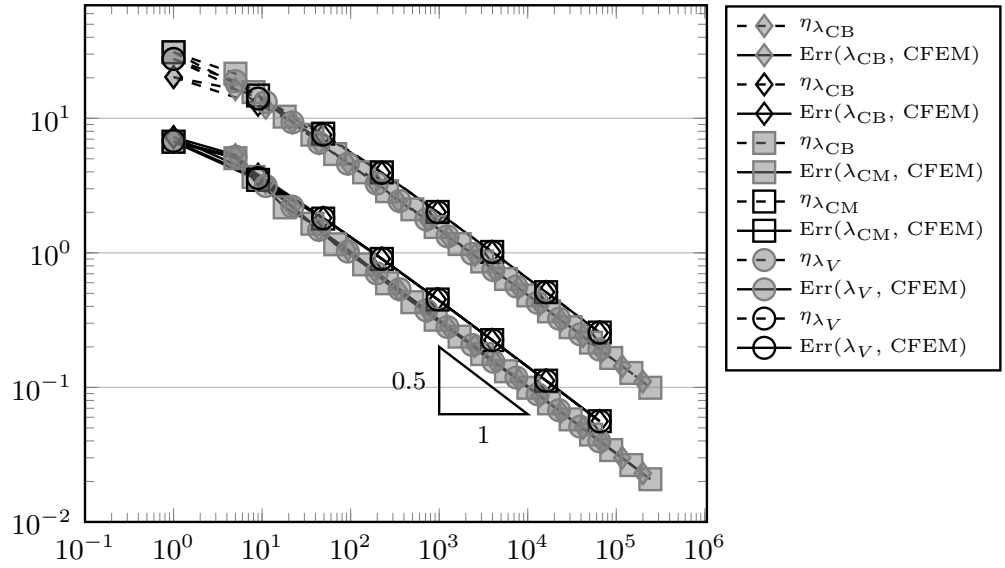

Figure 6.8.: Comparison of estimators and total errors for $\mu = \lambda_{\mathrm{CB}}$, λ_{CM} and λ_V for CFEM for the experiment from Subsection 6.1.1 for adaptive (grey) and uniform (white) mesh-refinement.

6.1.2. L-shaped domain

The second benchmark test is takes from Bartels and Carstensen (2004) and involves a typical corner singularity. It concerns the domain $\Omega := (-2,2)^2 \setminus ([0,2] \times [-2,0])$, the homogeneous Dirichlet boundary condition $u_D = 0$, the constant obstacle $\chi \equiv 0$, and the right-hand side

$$f(r,\varphi) := -r^{2/3}\sin(2\varphi/3)((\partial g(r)/\partial r)/(3r) + (\partial^2 g(r)/\partial r^2)) - H(r-5/4),$$
$$g(r,\varphi) := \max\{0, \min\{1, -6s^6 + 15s^4 - 10s^2 + 1\}\}$$

for $s := 2(r-1/4)$ and the Heaviside function H.

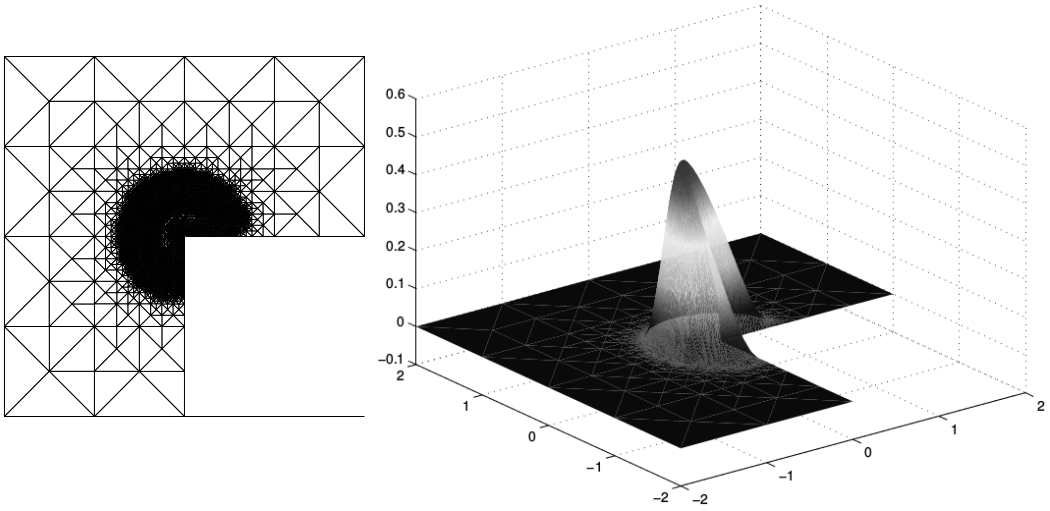

Figure 6.9.: Triangulation (left) and solution after 12 levels of adaptive refinement (right) for NCFEM for the experiment from Subsection 6.1.2.

The exact solution displayed in Figure 6.9 right reads

$$u(r,\varphi) := r^{2/3} g(r) \sin(2\varphi/3).$$

The re-entrant corner of the domain leads to a reduced convergence rate for uniformly refined meshes. Figure 6.9 left shows that the adaptive algorithm refines the area of the singularity. The reduced rate of -0.4 for uniform meshes can be seen Figures 6.10 and 6.12. Although the convergence rate is reduced, it is still higher than expected. The same effect can be witnessed for example in Carstensen and Merdon (2013b) and is a pre-asymptotic effect. Figures 6.10 and 6.12 also show that adaptively refined meshes lead to an improvement of the convergence rate to the expected optimal value of -0.5 with respect to the number of degrees of freedom. Figures 6.10 and 6.11 consider the total error, whereas Figures 6.13 and 6.12 focus only on the error of the primal variables in the energy norm, in accordance with Corollaries 3.30, 3.41, and 3.50. The efficiency indices for the total error vary from 1.05 for MFEM on uniform meshes to 4 for CFEM on uniform and adaptive meshes (cf. Figure 6.11). The efficiency indices for the error of the primal variable in the

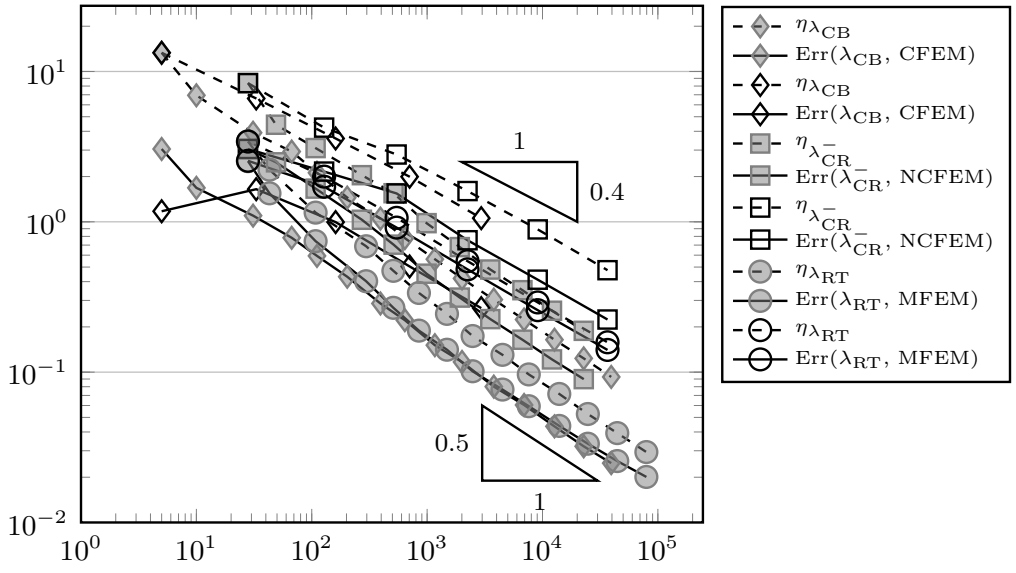

Figure 6.10.: Total error and error estimators for CFEM with $\mu = \lambda_{\mathrm{CB}}$, NCFEM, and MFEM for the experiment from Subsection 6.1.2 for adaptive (grey) and uniform (white) mesh-refinement.

energy norm in Figure 6.13 are at 2.3 for MFEM, 4 for NCFEM, and 5 for CFEM. Figure 6.14 shows that all error estimators refine the area of the singularity as well as the boundary of the contact zone at $r = 3/4$. For the error estimator η_V an extra layer of refinement takes place at the boundary of the domain. In this area the exact Lagrange multiplier λ equals -1, but is approximated by λ_{V} which has zero boundary conditions. However, since this concerns only a fine layer of triangles at the boundary, the effect is not visible in Figure 6.15 where the total error $\mathrm{Err}(\mu, \mathrm{CFEM})$ and error estimator λ_μ are compared for $\mu = \lambda_{\mathrm{CB}}$, λ_{CM}, λ_V, λ_{V2}. Figure 6.16 shows that the estimator is dominated by the residual. The other terms converge with an even higher convergence rate. A similar behaviour is observed for the other methods (undisplayed). The residual term is lowest for the Raviart-Thomas MFEM (cf. Figure 6.17) and hence explains the lower efficiency indices for this method (cf. Figures 6.11 and 6.13). Figure 6.16 also shows that the error is dominated by the error $u - u_h$ in the energy norm, which is in accordance with the results of Corollaries 3.30, 3.41, and 3.50.

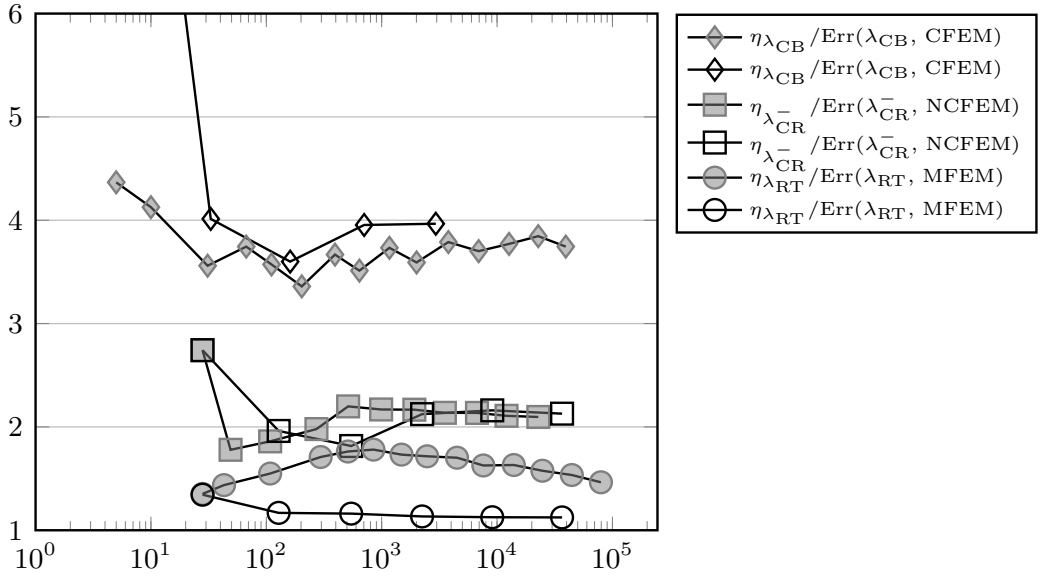

Figure 6.11.: Efficiency indices for the total error for CFEM with $\mu = \lambda_{\mathrm{CB}}$, NCFEM, and MFEM for the experiment from Subsection 6.1.2 for adaptive (grey) and uniform (white) mesh-refinement.

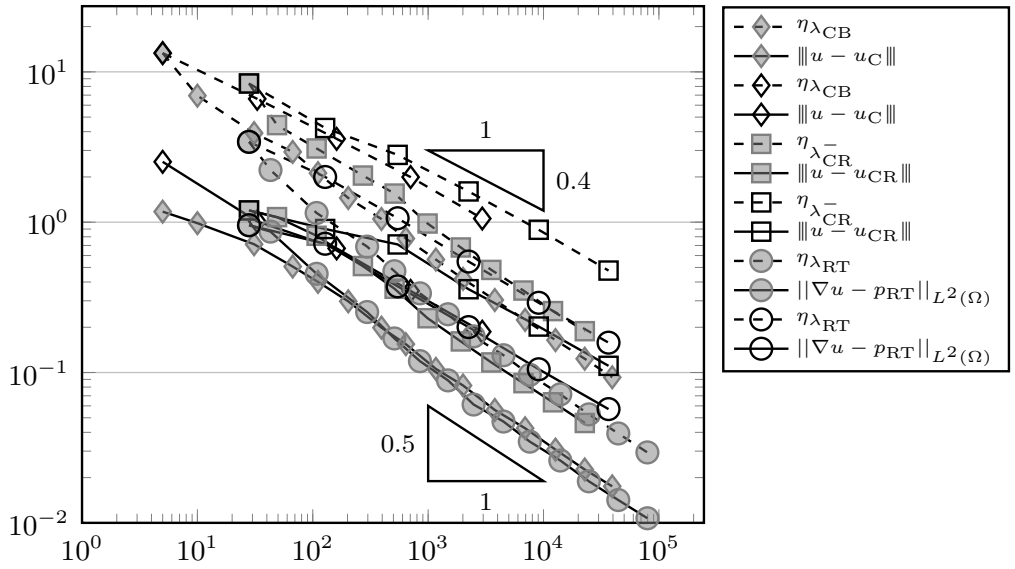

Figure 6.12.: Error of the primal variable in the energy norm and error estimators for CFEM with $\mu = \lambda_{\mathrm{CB}}$, NCFEM, and MFEM for the experiment from Subsection 6.1.2 for adaptive (grey) and uniform (white) mesh-refinement.

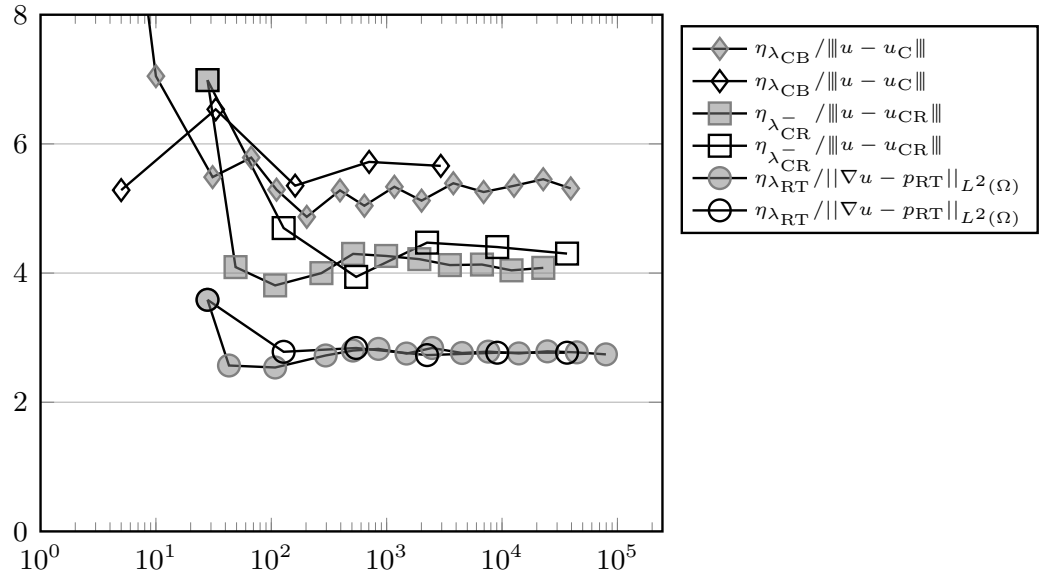

Figure 6.13.: Efficiency indices for the error of the primal variable in the energy norm for CFEM with $\mu = \lambda_{\mathrm{CB}}$, NCFEM, and MFEM for the experiment from Subsection 6.1.2 for adaptive (grey) and uniform (white) mesh-refinement.

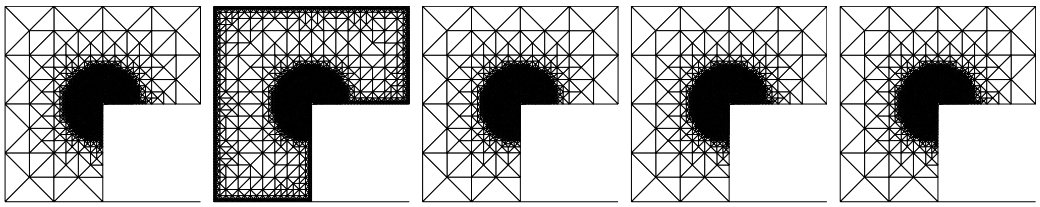

Figure 6.14.: Adaptively refined meshes for η_{CB}, η_{V}, η_{V2}, η_{NC}, η_{RT} (from left to right) for the experiment from Subsection 6.1.2.

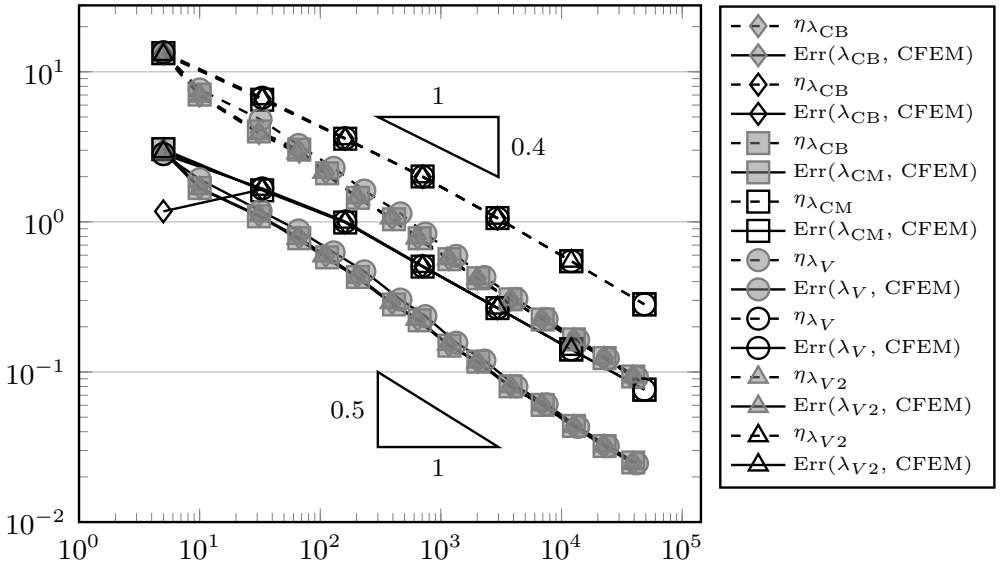

Figure 6.15.: Comparison of estimators and total errors for $\mu = \lambda_{\mathrm{CB}}$, λ_{CM}, λ_V, and λ_{V2} for CFEM for the experiment from Subsection 6.1.2 for adaptive (grey) and uniform (white) mesh-refinement.

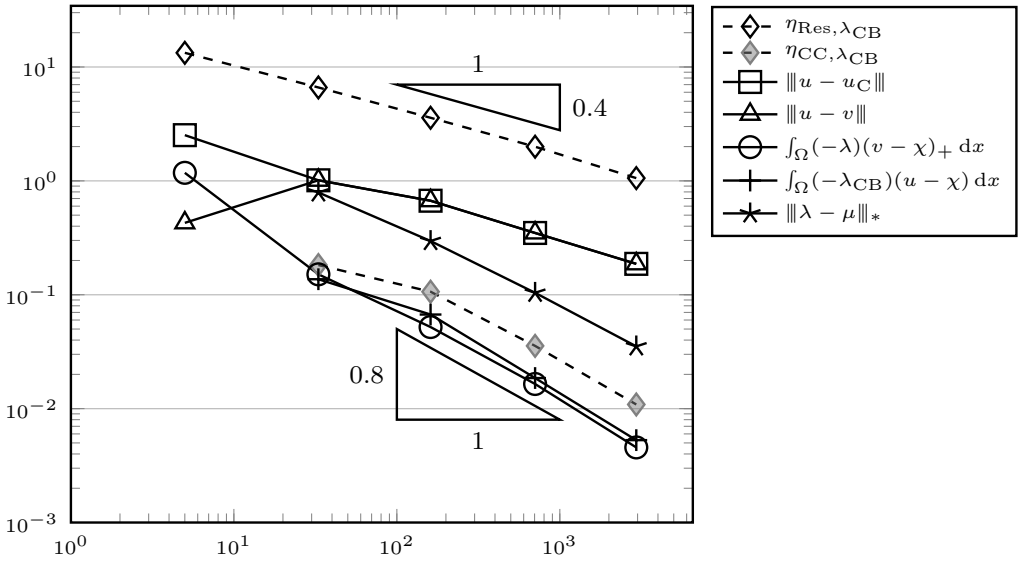

Figure 6.16.: Comparison of different error and estimator components for CFEM, with $\mu = \lambda_{\mathrm{CB}}$, for the experiment from Subsection 6.1.2 for uniform mesh-refinement.

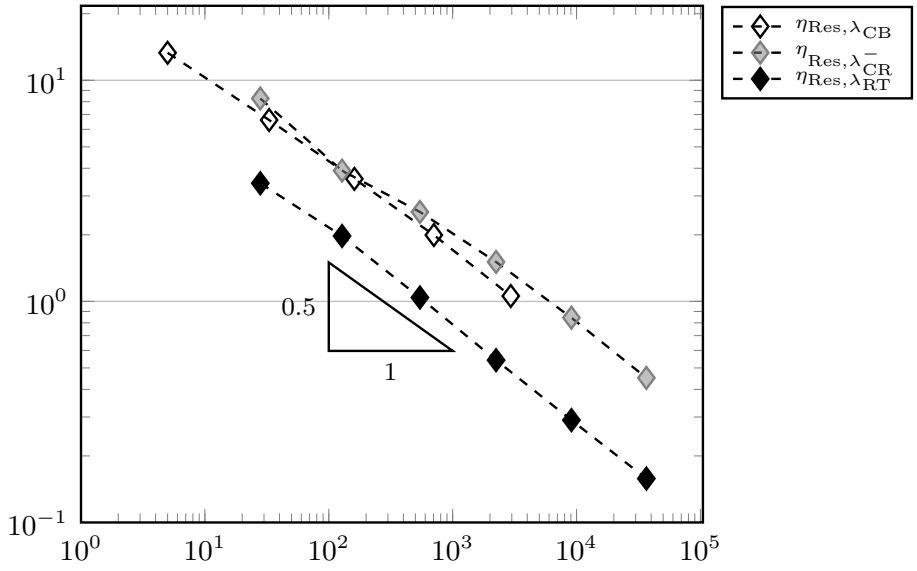

Figure 6.17.: Residual component of the estimator for CFEM with $\mu = \lambda_{\mathrm{CB}}$, NCFEM, and MFEM for the experiment from Subsection 6.1.2 for uniform mesh-refinement.

6.1.3. Pyramid obstacle on square domain

This benchmark problem from Bartels and Carstensen (2004) concerns the square domain $\Omega := (-1,1)^2$, the right-hand side $f \equiv 1$, the Dirichlet boundary $u_D \equiv 0$, and the non-affine obstacle

$$\chi := \operatorname{dist}((x,y), \partial\Omega).$$

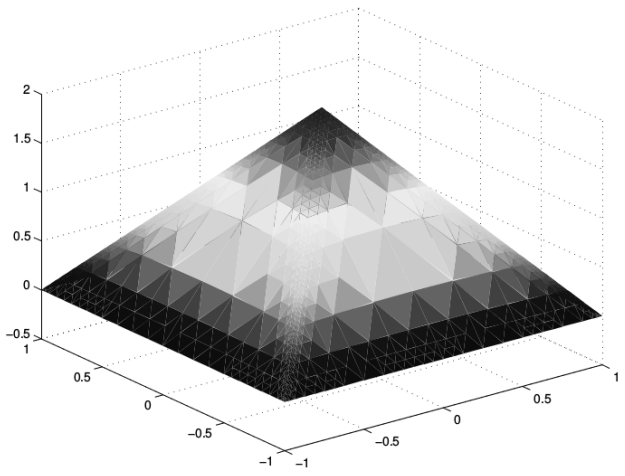

Figure 6.18.: Solution after 10 levels of adaptive refinement for NCFEM for the experiment from Subsection 6.1.3.

The exact solution is unknown and has to be approximated as described on Page 110. An approximation is displayed in Figure 6.18.

The obstacle satisfies the conditions of Theorem 3.18. This is reflected in Figures 6.19 and 6.20, where it can be seen, that the error estimator is efficient and reliable with respect to the total error. Figure 6.19 shows a reduced convergence rate of -0.3 with respect to the number of degrees of freedom for uniform mesh-refinement and the expected convergence rate of -0.5 with respect to the number of degrees of freedom for adaptive mesh-refinement. The efficiency indices in Figure 6.20 range from almost 1 for MFEM to 6 for the conforming CFEM. This is due to the good approximation of the residual $\|\!|\operatorname{Res}|\!\|_*$ for the mixed Raviart-Thomas MFEM (see Figure 6.21). The analysis in Subsections 3.3, 3.4, and 3.5 however, assumes that the exact Lagrange multiplier Λ has an L^2 representation $\lambda \in L^2(\Omega)$. The regularity results in Lemma 3.2 show that the exact solution does not satisfy $u \in H^1(\Omega)$ with $\Delta u \in L^2(\Omega)$ and hence the Lagrange multiplier Λ does not have an L^2 representation $\lambda \in L^2(\Omega)$. The effect of this can be seen in Figure 6.22. For uniform mesh refinement, the conforming and non-conforming error of the primal variables in the energy norm converge with a rate of -0.5 with respect to the number of degrees of freedom, but the estimator (with $\|\!|u_{\mathrm{CR}} - v|\!\|$ resp. $||p_{\mathrm{RT}} - \nabla v||_{L^2(\Omega)}$ added to Est for NCFEM and MFEM) only converges with a rate of -0.3. This leads to unbounded efficiency indices for CFEM and NCFEM on uniform meshes in Figure 6.23. Figure 6.24 shows, that the error term $\|\!|\lambda - \mu|\!\|_*$ is not equivalent to the error term $\|\!|u - v|\!\|$ but has a worse convergence rate. This is due to the fact, that in this case, the Lagrange multiplier is not an L^2 function, but a measure defined on the edges of the pyramid, and hence the oscillations $\operatorname{osc}(\lambda, \mathcal{T})$ are not of higher order. This effect disappears for adaptive mesh-refinement. The effect does not occur for the mixed method, since this method approximates the dual variable $p = \nabla u$ rather than the primal variable u. The discrete Lagrange multiplier $\lambda_{\mathrm{RT}} := \Pi_0 f + \operatorname{div} p_{\mathrm{RT}}$ mimics the behaviour of the exact Lagrange multiplier. Theorem 3.47 shows that $\|\!|\lambda - \lambda_{\mathrm{RT}}|\!\|_*$ is estimated by the error $||\nabla u - p_{\mathrm{RT}}||_{L^2(\Omega)}$ without oscillations of the exact Lagrange multiplier. For all methods the estimator leads to a refinement of the edges of the pyramid shown in Figure 6.26 and hence the area where the error of the Lagrange multiplier is large. This leads to the optimal rate of convergence for adaptive mesh-refinement.

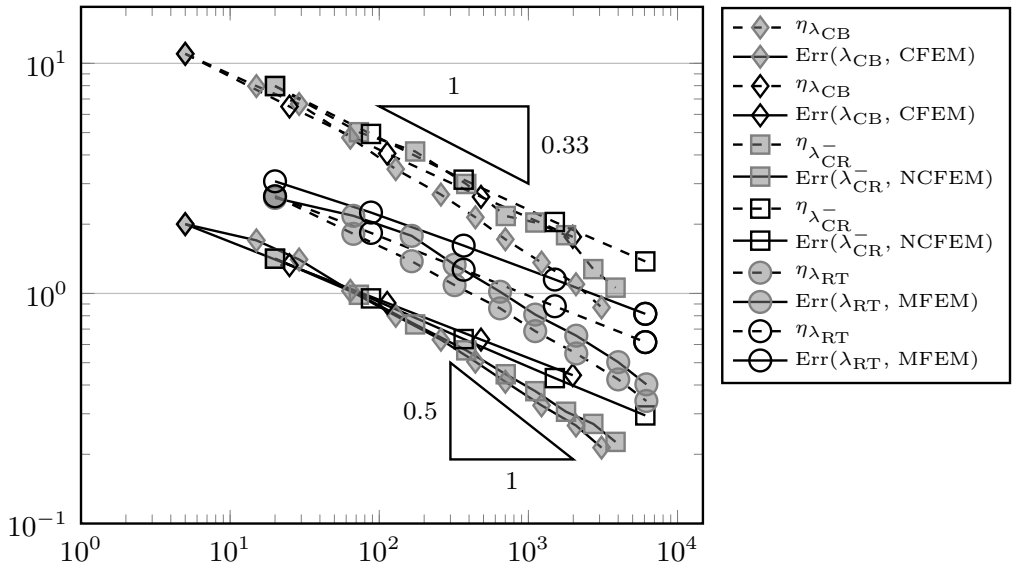

Figure 6.19.: Total error and error estimators for CFEM with $\mu = \lambda_{\mathrm{CB}}$, NCFEM, and MFEM for the experiment from Subsection 6.1.3 for adaptive (grey) and uniform (white) mesh-refinement.

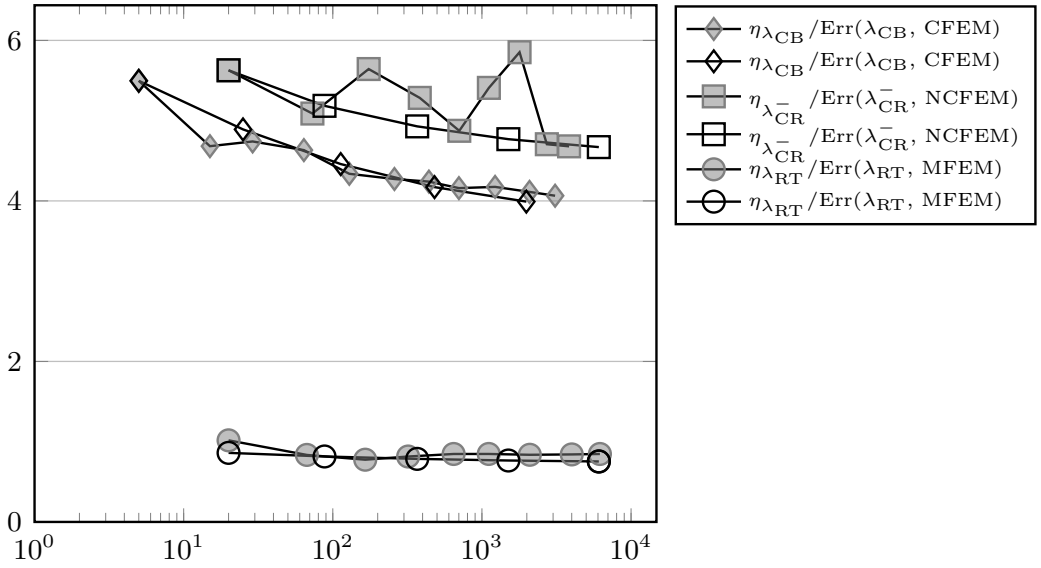

Figure 6.20.: Efficiency indices for the total error for CFEM with $\mu = \lambda_{\mathrm{CB}}$, NCFEM, and MFEM for the experiment from Subsection 6.1.3 for adaptive (grey) and uniform (white) mesh-refinement.

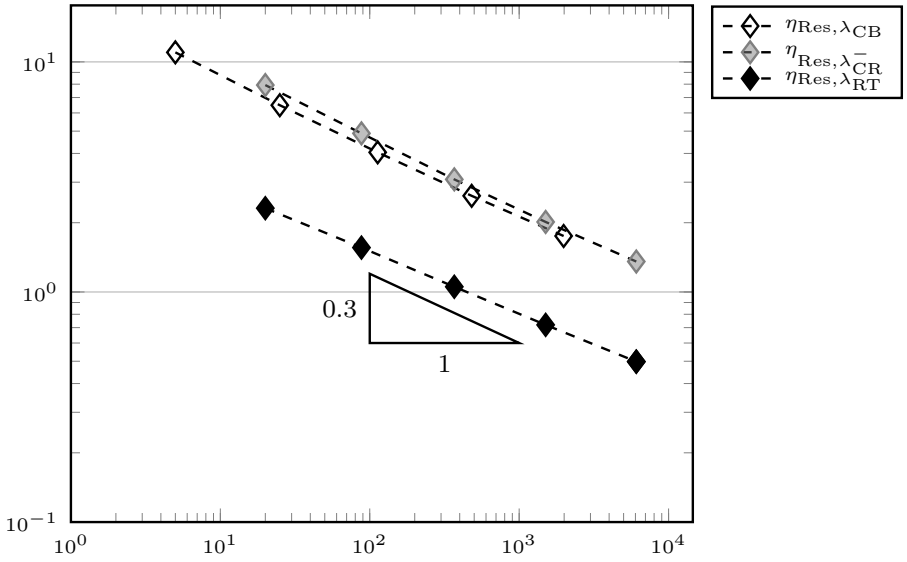

Figure 6.21.: Residual component of the estimator for CFEM with $\mu = \lambda_{\mathrm{CB}}$, NCFEM, and MFEM for the experiment of Subsection 6.1.3 on uniform meshes.

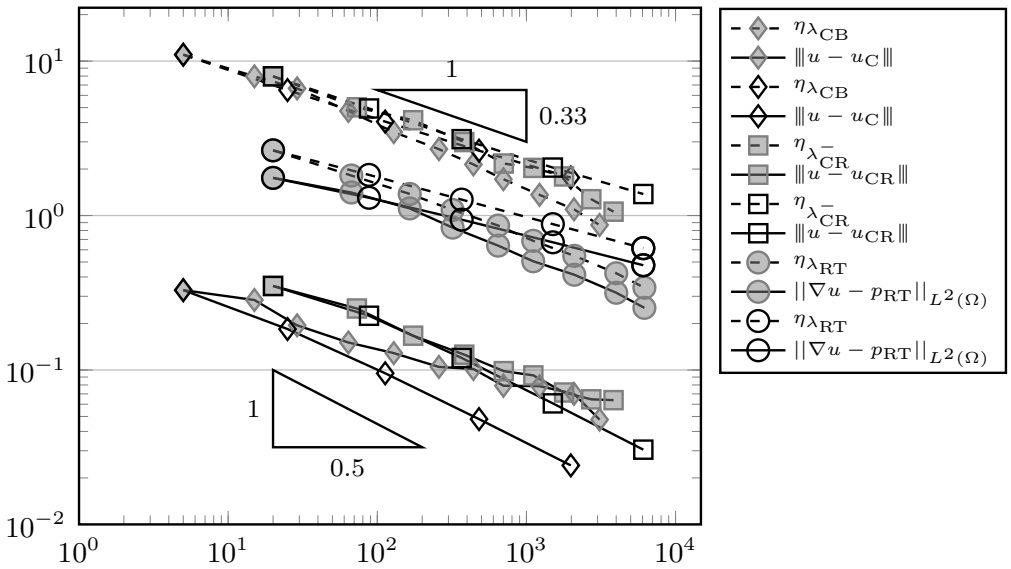

Figure 6.22.: Error of the primal variable in the energy norm and error estimators for CFEM with $\mu = \lambda_{\mathrm{CB}}$, NCFEM, and MFEM for the experiment from Subsection 6.1.3 for adaptive (grey) and uniform (white) mesh-refinement.

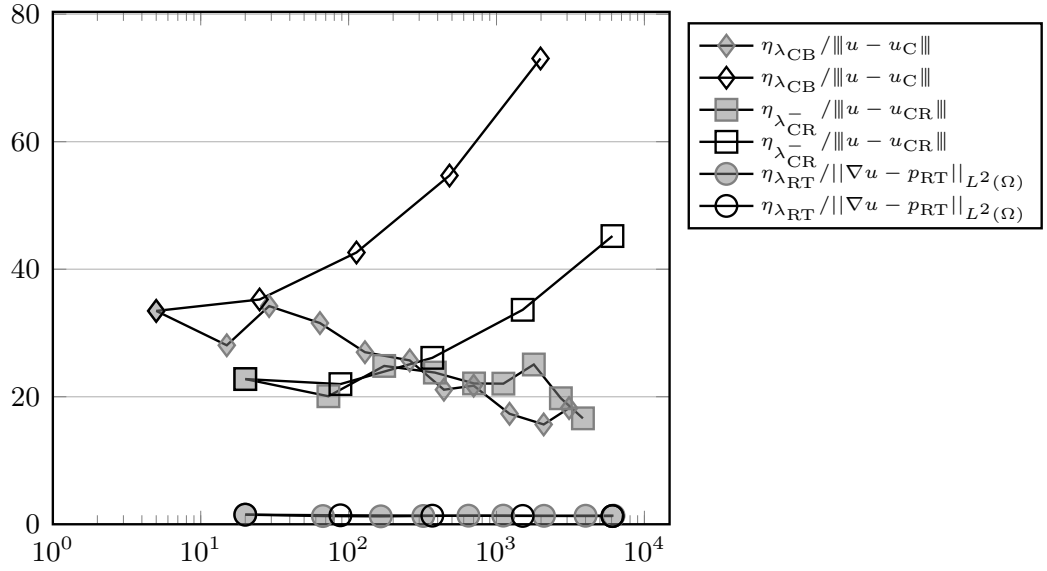

Figure 6.23.: Efficiency indices for the error of the primal variable in the energy norm for CFEM with $\mu = \lambda_{\mathrm{CB}}$, NCFEM, and MFEM for the experiment from Subsection 6.1.3 for adaptive (grey) and uniform (white) mesh-refinement.

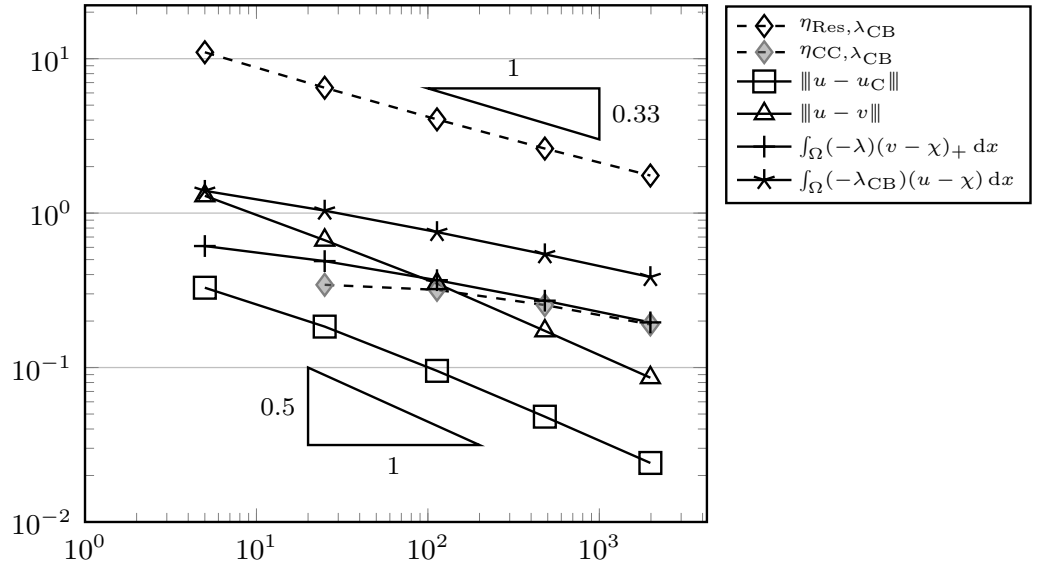

Figure 6.24.: Comparison of different error and estimator components for CFEM, with $\mu = \lambda_{\mathrm{CB}}$, for the experiment from Subsection 6.1.3 for uniform mesh-refinement.

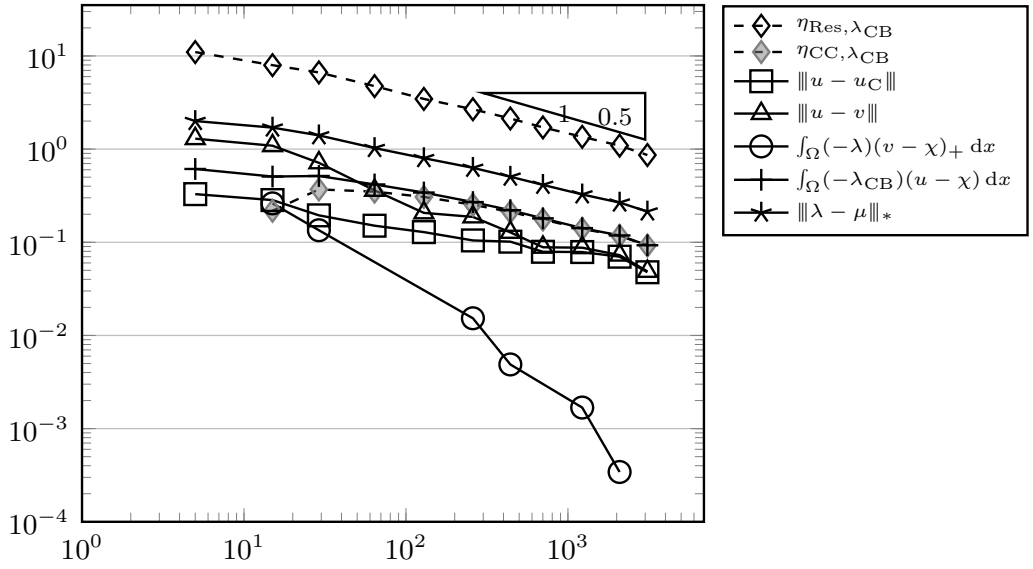

Figure 6.25.: Comparison of different error and estimator components for CFEM, with $\mu = \lambda_{\mathrm{CB}}$, for the experiment from Subsection 6.1.3 for adaptive mesh-refinement.

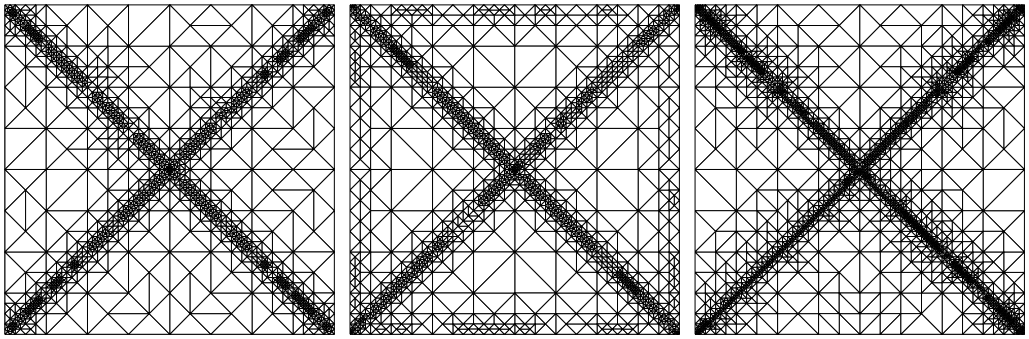

Figure 6.26.: Adaptively refined meshes for η_{CB}, η_{NC}, η_{RT} (from left to right) for the experiment from Subsection 6.1.3.

6.1.4. Cusp obstacle on square domain

This benchmark example from Nochetto et al. (2003) considers the domain Ω, the right-hand side f, the Dirichlet data u_D from Subsection 6.1.1, and the obstacle

$$\chi(x,y) := \max\{-2, 1 - 50\max\{|x|,|y|\}\}.$$

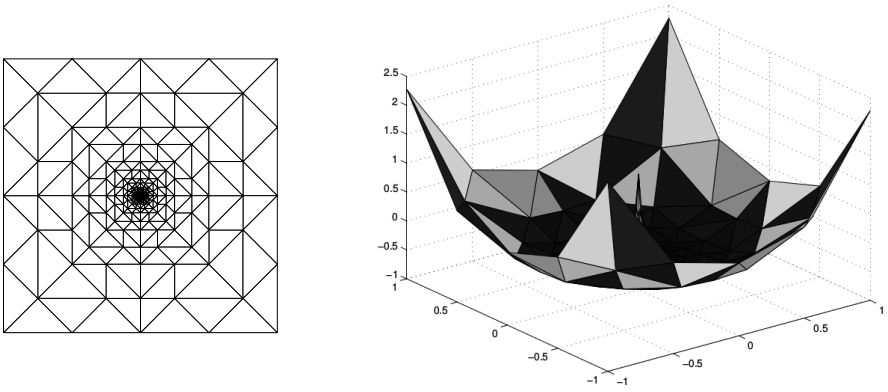

Figure 6.27.: Initial triangulation (left) and solution after 5 levels of uniform refinement (right) for the experiment from Subsection 6.1.4.

The exact solution is not known and is approximated as described on Page 110. The obstacle is piecewise affine, but not on the initial triangulation in Figure 6.27 on the left, although the initial triangulation is already chosen with a strong refinement towards the centre. The right-hand side of Figure 6.27 depicts the discrete conforming solution on the initial triangulation. Figure 6.28 shows that the total errors and the corresponding error estimators recover the optimal empirical convergence rate of -0.5 with respect to the number of degrees of freedom, both for uniform and adaptive meshes. The efficiency indices with respect to the total error in Figure 6.29 lie at 0.95 for MFEM and 3.5 for CFEM. Recall that Theorem 3.18 implies that the efficiency indices are between $1/\sqrt{30}$ and $\sqrt{2}$ if the residual $\|\!|\mathrm{Res}|\!\|_*$ is evaluated exactly. Figure 6.32 shows that the error estimator is dominated by $\eta_{\mathrm{Res},\mu}$ for CFEM. Similar results are obtained for NCFEM and MFEM (undisplayed). Together with the results presented in Figure 6.33, which show that $\eta_{\mathrm{Res},\lambda_{\mathrm{RT}}}$ is smaller than $\eta_{\mathrm{Res},\lambda^-_{\mathrm{CR}}}$ and $\lambda_{\mathrm{Res},\lambda_{\mathrm{CB}}}$, this explains the lower efficiency indices for MFEM. Figure 6.30 concerns the convergence of the error of the primal variable in the energy norm. This error and the corresponding error estimator (with $\|\!|u_{\mathrm{CR}} - v|\!\|$ resp. $||p_{\mathrm{RT}} - \nabla v||_{L^2(\Omega)}$ added to Est for NCFEM and MFEM) converge with the expected convergence rate of -0.5 with respect to the number of degrees of freedom and lead to the efficiency indices between 1.7 for MFEM and 8 for CFEM in Figure 6.31.

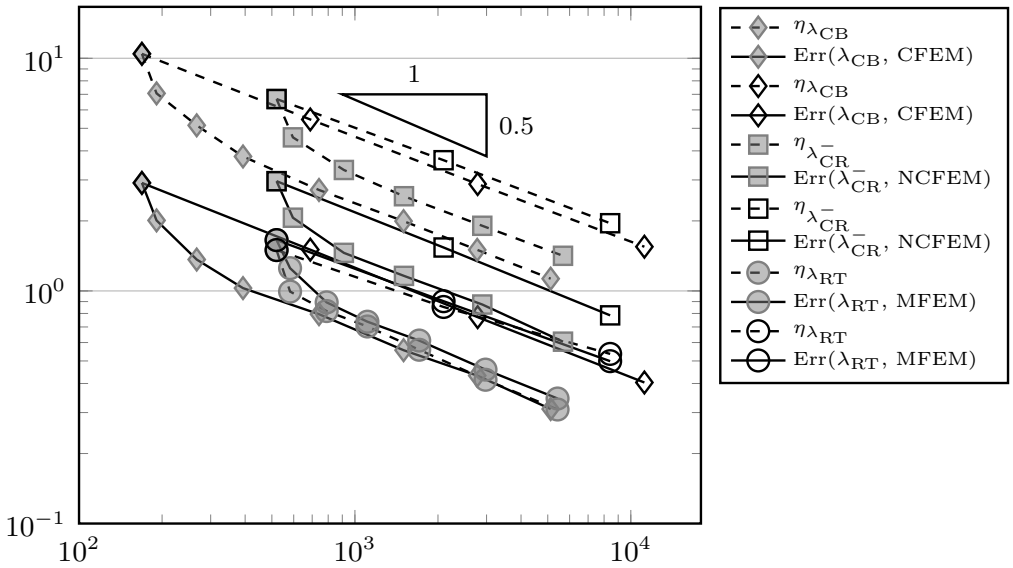

Figure 6.28.: Total error and error estimators for CFEM with $\mu = \lambda_{\mathrm{CB}}$, NCFEM, and MFEM for the experiment from Subsection 6.1.4 for adaptive (grey) and uniform (white) mesh-refinement.

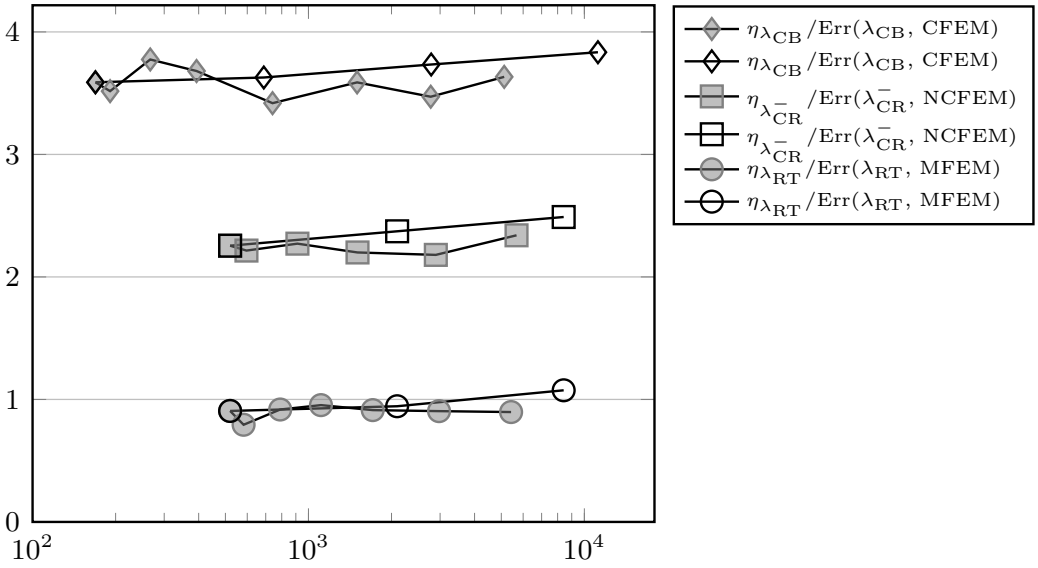

Figure 6.29.: Efficiency indices for the total error for CFEM with $\mu = \lambda_{\mathrm{CB}}$, NCFEM, and MFEM for the experiment from Subsection 6.1.4 for adaptive (grey) and uniform (white) mesh-refinement.

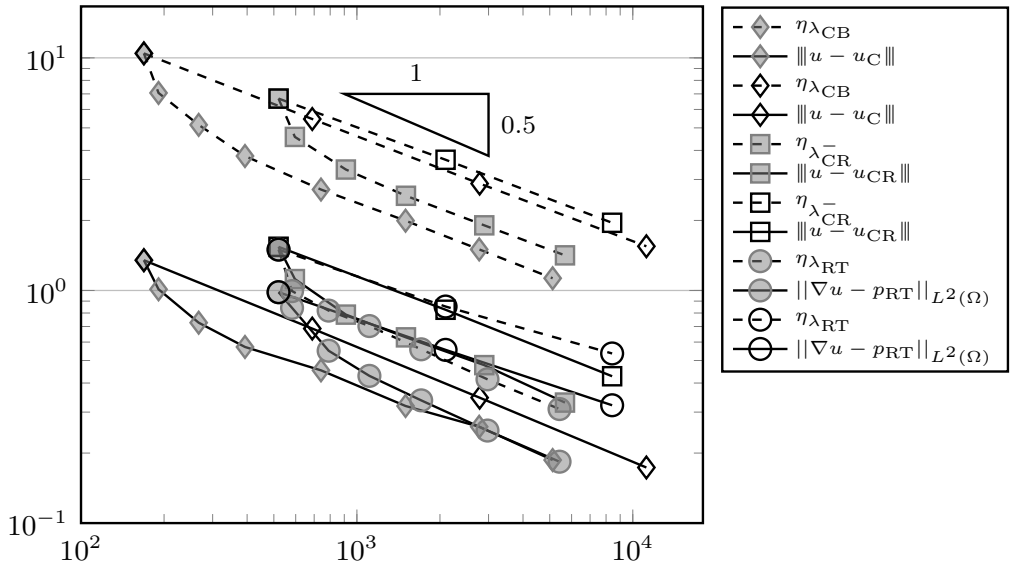

Figure 6.30.: Error of the primal variable in the energy norm and error estimators for CFEM with $\mu = \lambda_{\mathrm{CB}}$, NCFEM, and MFEM for the experiment from Subsection 6.1.4 for adaptive (grey) and uniform (white) mesh-refinement.

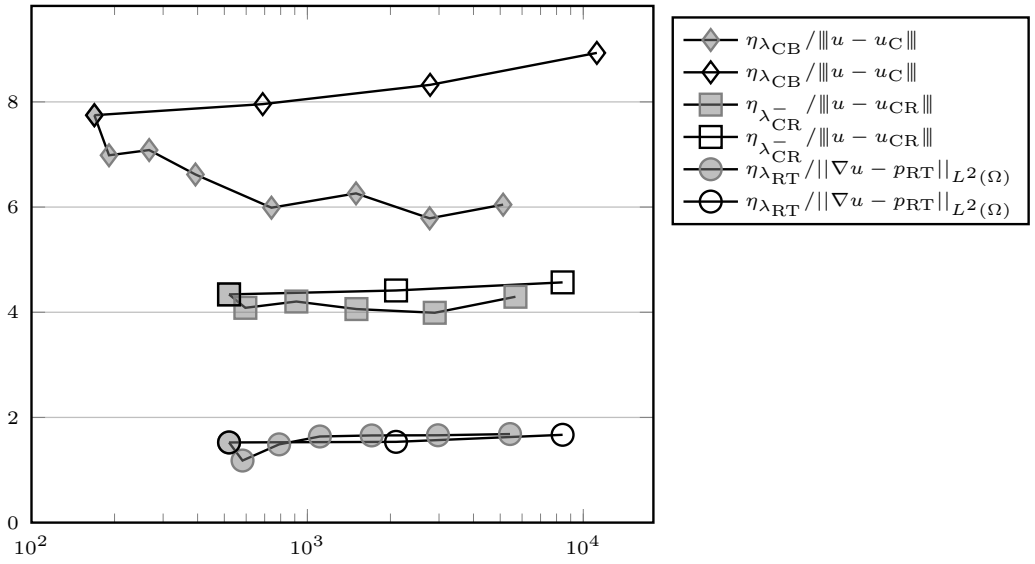

Figure 6.31.: Efficiency indices for the error of the primal variable in the energy norm for CFEM with $\mu = \lambda_{\mathrm{CB}}$, NCFEM, and MFEM for the experiment from Subsection 6.1.4 for adaptive (grey) and uniform (white) mesh-refinement.

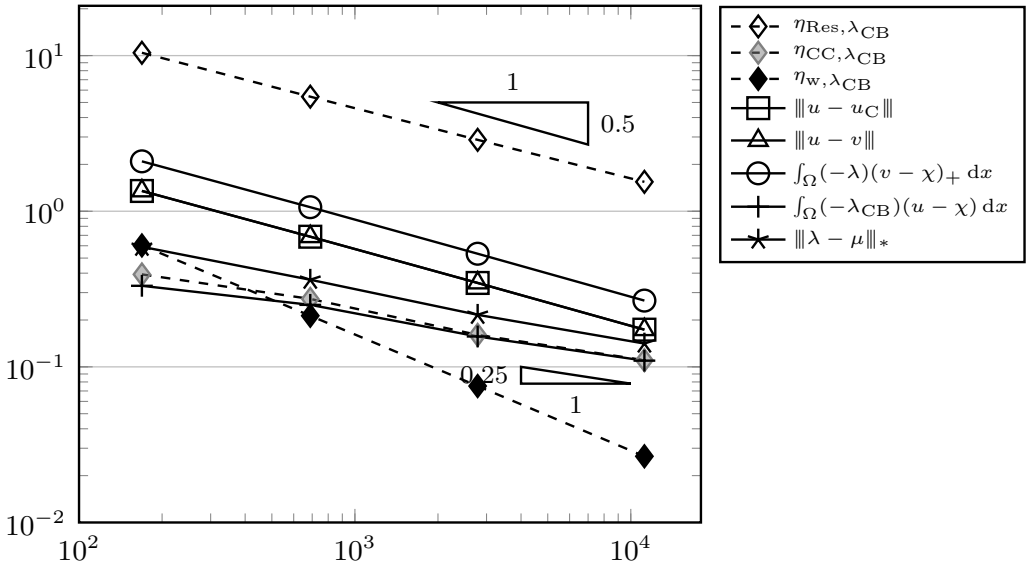

Figure 6.32.: Comparison of different error and estimator components for CFEM, with $\mu = \lambda_{\mathrm{CB}}$, for the experiment from Subsection 6.1.4 for uniform mesh-refinement.

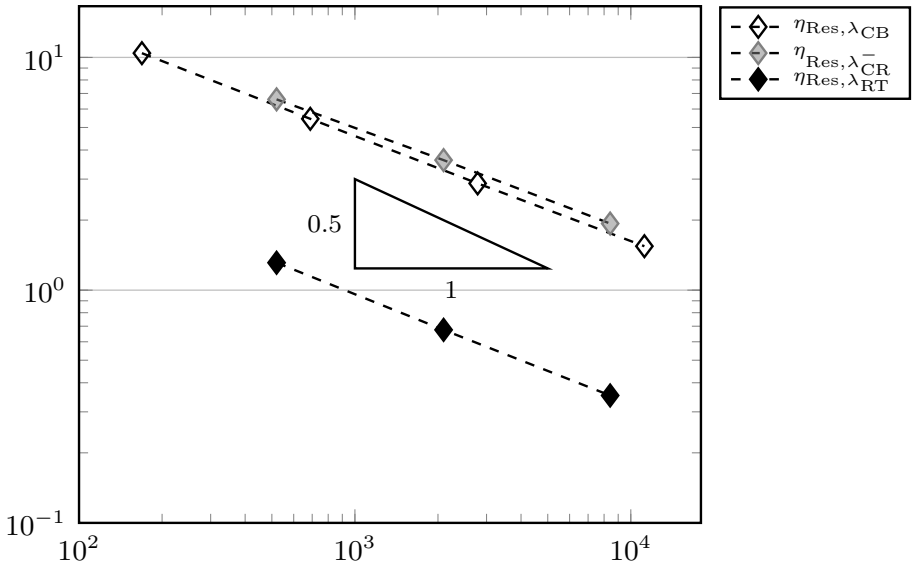

Figure 6.33.: Residual component of the estimator for CFEM with $\mu = \lambda_{\mathrm{CB}}$, NCFEM, and MFEM for the experiment from Subsection 6.1.4 for uniform mesh-refinement.

6.1.5. Non-affine smooth obstacle on square domain

This benchmark example from Gräser and Kornhuber (2009) considers the square domain $\Omega := (-1,1)^2$, the obstacle $\chi(x,y) = -(x^2-1)(y^2-1)$, and the right-hand side $f = -\Delta\chi$.

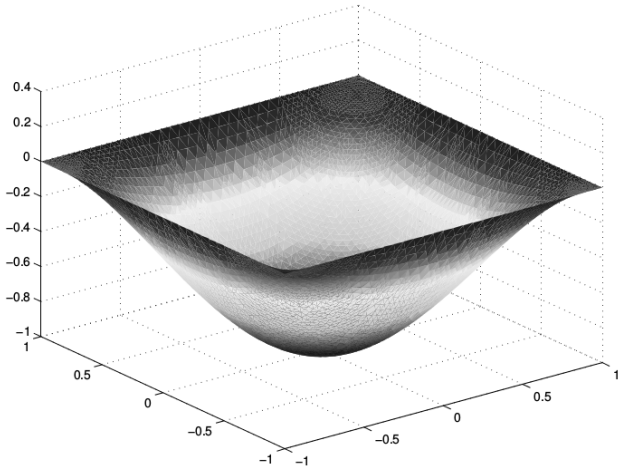

Figure 6.34.: Solution after 10 levels of adaptive refinement for NCFEM for the experiment from Subsection 6.1.5.

The exact solution displayed in Figure 6.34 reads

$$u \equiv \chi.$$

Figure 6.35 shows that both the total error and error estimator converge with a convergence rate of -0.5 with respect to the number of degrees of freedom on uniformly and adaptively refined meshes. This leads to efficiency indices between 1.2 for the mixed MFEM and 4.5 for the conforming CFEM (cf. Figure 6.36) with respect to the total error. As in the previous examples, this behaviour is explained by the dominant estimator term $\eta_{\mathrm{Res},\mu}$ (cf. Figure 6.37) for CFEM (NCFEM, and MFEM show the same behaviour and the results are undisplayed) and the good approximation to this term for the mixed MFEM in Figure 6.38. These results suggest that the results of Corollaries 3.30, 3.41, and 3.50 also hold true for more general situations where $\chi \notin P_1(\Omega)$. Figure 6.39 displays the error of the primal variable in the energy norm and the error estimator (adapted for NCFEM and MFEM) for the three finite element methods. All these terms converge with the optimal convergence rate of -0.5 with respect to the number of degrees of freedom. Figure 6.40 shows that this leads to efficiency indices between 2.8 for MFEM and 6.5 for the conforming CFEM.

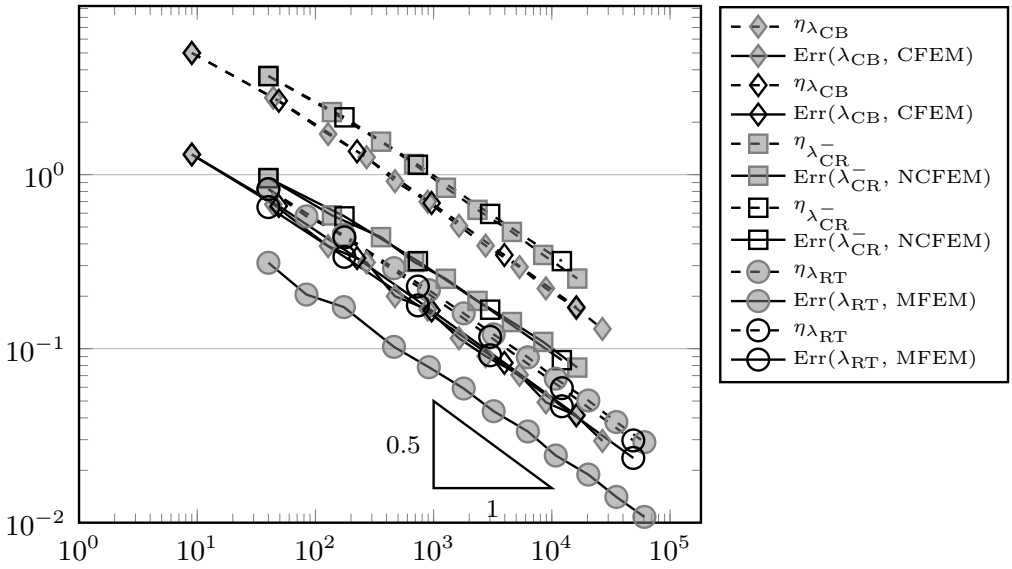

Figure 6.35.: Total error and error estimators for CFEM with $\mu = \lambda_{\mathrm{CB}}$, NCFEM, and MFEM for the experiment from Subsection 6.1.5 for adaptive (grey) and uniform (white) mesh-refinement.

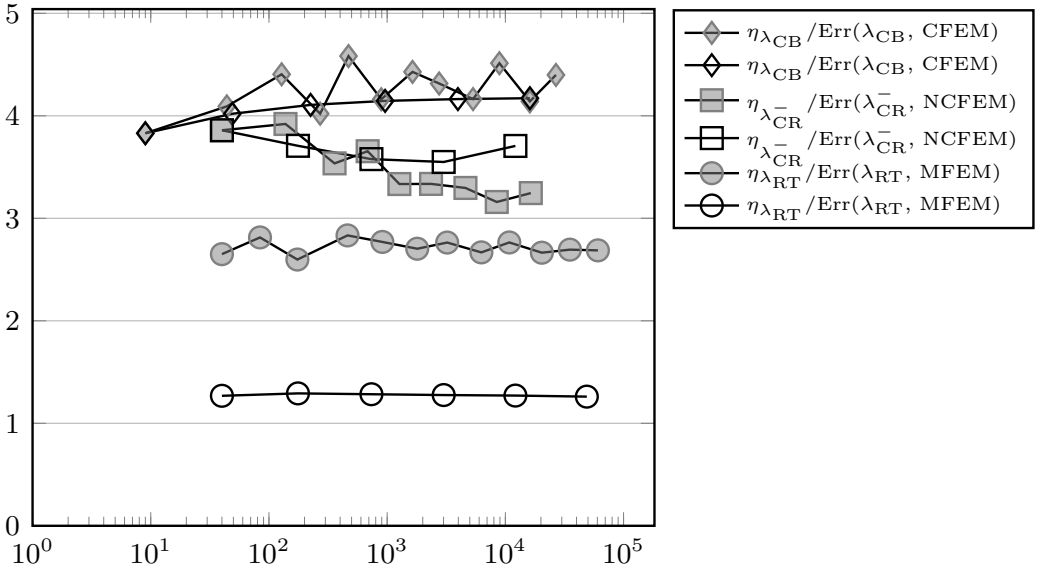

Figure 6.36.: Efficiency indices for the total error for CFEM with $\mu = \lambda_{\mathrm{CB}}$, NCFEM, and MFEM for the experiment from Subsection 6.1.5 for adaptive (grey) and uniform (white) mesh-refinement.

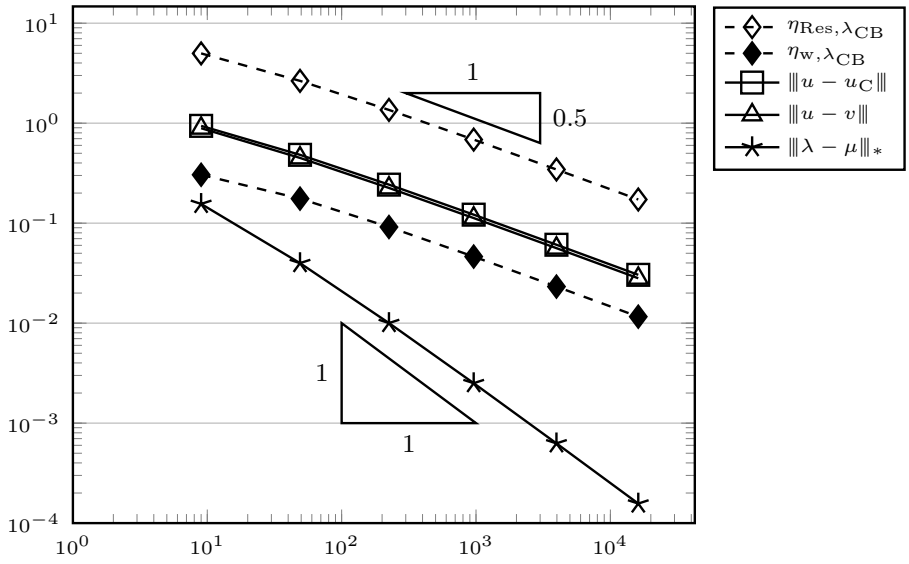

Figure 6.37.: Comparison of different error and estimator components for CFEM, with $\mu = \lambda_{\mathrm{CB}}$, for the experiment from Subsection 6.1.5 for uniform mesh-refinement.

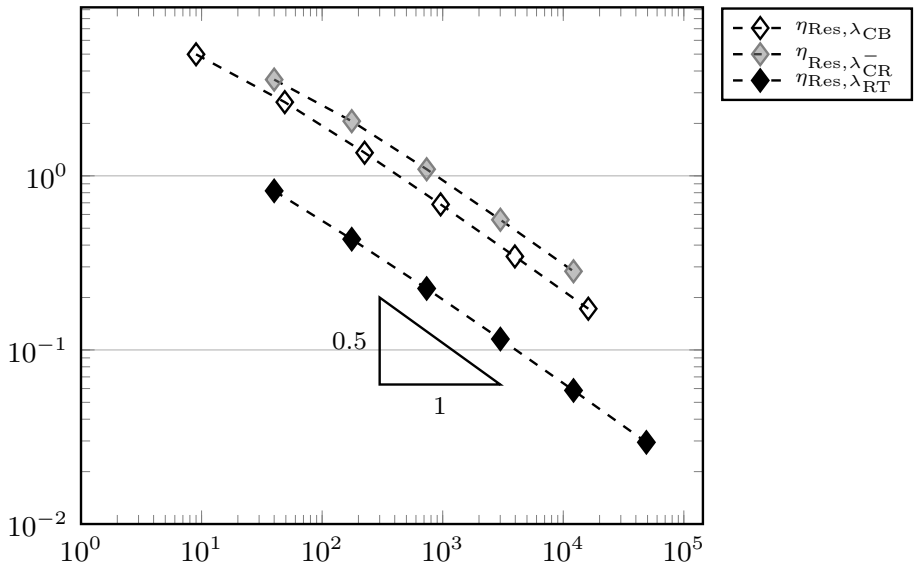

Figure 6.38.: Residual component of the estimator for CFEM with $\mu = \lambda_{\mathrm{CB}}$, NCFEM, and MFEM for the experiment from Subsection 6.1.5 for uniform mesh-refinement.

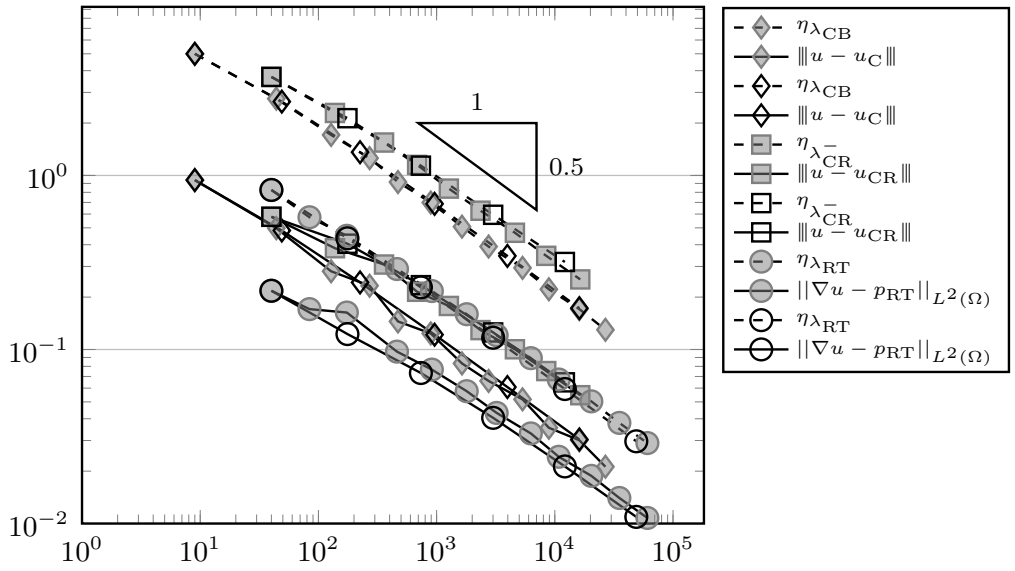

Figure 6.39.: Error of the primal variable in the energy norm and error estimators for CFEM with $\mu = \lambda_{\mathrm{CB}}$, NCFEM, and MFEM for the experiment from Subsection 6.1.5 for adaptive (grey) and uniform (white) mesh-refinement.

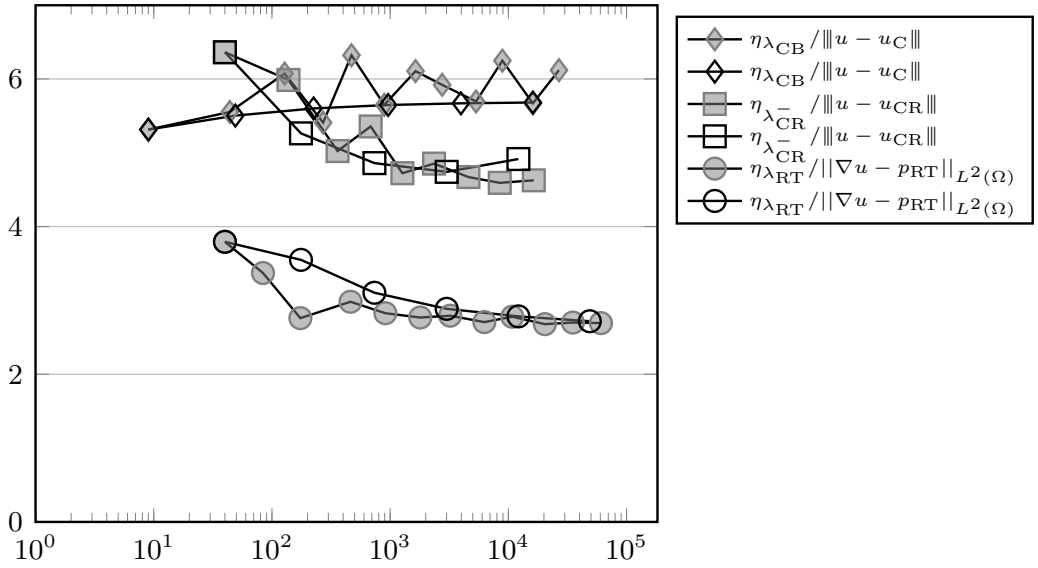

Figure 6.40.: Efficiency indices for the error of the primal variable in the energy norm for CFEM with $\mu = \lambda_{\mathrm{CB}}$, NCFEM, and MFEM for the experiment from Subsection 6.1.5 for adaptive (grey) and uniform (white) mesh-refinement.

6.2. Signorini problem

This section presents four different numerical benchmark examples for Signorini's problem, discretized with the conforming Courant FEM, the non-conforming Crouzeix-Raviart FEM, and the mixed Raviart-Thomas FEM. For a given triangulation $\mathcal{T}$, recall the discrete Lagrange multiplier λ_{C} from (4.21) on Page 70, λ_{CR} from (4.28) on Page 81, and λ_{RT} from (4.39) on Page 91. For each finite element method, recall the approximation $v \in \mathcal{A}$ to the exact solution $u \in K$ and the residual

$$\mathrm{Res}(\varphi) = \int_\Omega f\varphi \,\mathrm{d}x - \int_{\Gamma_C} \mu\varphi \,\mathrm{d}s - a(v,\varphi) \quad \text{for all } \varphi \in H^1_D(\Omega)$$

where μ abbreviates any of the above discrete Lagrange multipliers. The estimator splits into three components

$$\mathrm{Est}^2 = \|\!|\mathrm{Res}|\!\|_*^2 + \int_{\Gamma_C} (-\mu)(v-\chi)_+ \,\mathrm{d}s + \|\!|\min\{0, v-\chi\}|\!\|^2.$$

The terms $\eta^2_{\mathrm{CC},\mu} := \int_{\Gamma_C}(-\mu)(v-\chi)_+ \,\mathrm{d}s$ and $\eta_{\mathrm{w},\mu} := \|\!|\min\{0,v-\chi\}|\!\|^2$ are computable element wise and satisfy

$$\eta^2_{\mathrm{CC},\mu} = \sum_{T\in\mathcal{T}} \eta^2_{\mathrm{CC},\mu}(T) \quad \text{and} \quad \eta^2_{\mathrm{w},\mu} = \sum_{T\in\mathcal{T}} \eta^2_{\mathrm{w},\mu}(T).$$

To find a computable bound for $\|\!|\mathrm{Res}|\!\|_*^2$, recall Remarks 4.15 and 3.20, and let $z_{\mathrm{C}} \in S^1_0(\mathcal{T})$ denote the Riesz-representation of $\mathrm{Res}|_{S^1_0(\mathcal{T})}$ for $\mu = \lambda_{\mathrm{C}}$ and let $z_2 \in S^2_0(\mathcal{T})$ denote the Riesz representation of $\mathrm{Res}|_{S^2_0(\mathcal{T})}$ for $\mu = \lambda_{\mathrm{CR}}$. Let $w_D \in H^1(\Omega)$ from Theorem 2.28 on Page 18 be the function which corrects the boundary conditions in accordance to the finite element method. For $T \in \mathcal{T}$, this leads to the following computable element-wise upper bounds of $\|\!|\mathrm{Res}|\!\|_*^2 \le \sum_{T\in\mathcal{T}} \eta^2_{\mathrm{Res},\mu} = \eta^2_{\mathrm{Res},\mu}(T)$ (cf. for example Braess (2007)) for

$$\begin{aligned}
\eta^2_{\mathrm{Res},\lambda_{\mathrm{C}}}(T) &:= ||h_T f||^2_{L^2(T)} + \sum_{E\in\mathcal{E}(T)} |E| \,|||[\nabla(u_{\mathrm{C}} + z_{\mathrm{C}})\cdot\nu_E + \lambda_{\mathrm{C}}|_E]_E||^2_{L^2(E)} \\
&\quad + \|\!|w_D|\!\|_T + \|\!|z_{\mathrm{C}}|\!\|_T^2, \\
\eta^2_{\mathrm{Res},\lambda_{\mathrm{CR}}}(T) &:= ||h_T f||^2_{L^2(T)} + \sum_{E\in\mathcal{E}(T)} |E| \,|||[\nabla I_{\mathrm{C}}(v+z_2)\cdot\nu_E + \lambda_{\mathrm{CR}}|_E]_E||^2_{L^2(E)} \\
&\quad + \|\!|(1-I_{\mathrm{C}})v|\!\|_T + \|\!|w_D|\!\|_T + \|\!|z_2|\!\|_T, \\
\eta^2_{\mathrm{Res},\lambda_{\mathrm{RT}}}(T) &:= \mathrm{osc}^2(f,\mathcal{T}) + \mathrm{osc}_{1/2}(g,\mathcal{E}) + ||p_{\mathrm{RT}} - \nabla v||^2_{L^2(\Omega)}.
\end{aligned}$$

To clarify the notation of the legends, let $\eta^2_\mu = \eta^2_{\mathrm{Res},\mu} + \eta^2_{\mathrm{CC},\mu} + \eta^2_{\mathrm{w},\mu}$ for any of the three discrete Lagrange multipliers above denote the error estimator and let $\mathrm{Err}(\mu, \mathrm{FEM})$ denote the total error for a given discrete Lagrange multiplier and FEM=CFEM, NCFEM, or MFEM.

6.2.1. Constant obstacle on square domain

The first experiment from Hild and Nicaise (2005) concerns the constant obstacle $\chi \equiv 0$ on the square domain $\Omega := (0,1)^2$. The contact boundary is the interval $\Gamma_C :=$

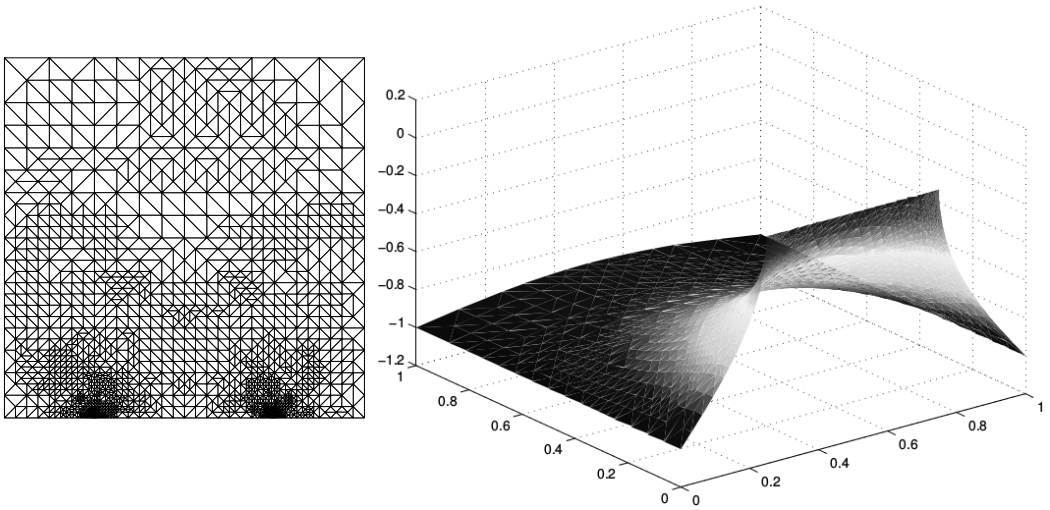

Figure 6.41.: Triangulation (left) and solution (right) after 10 levels of adaptive mesh-refinement for NCFEM for the experiment from Subsection 6.2.1

$[0.25, 0.75] \times \{0\}$, the Dirichlet boundary Γ_D is given by the intervals $\{0\} \times (0, 1)$ and $\{1\} \times (0, 1)$. The remaining parts of the boundary describe the Neumann boundary Γ_N. The unknown exact solution u is subject to the Dirichlet data $u_D \equiv -1$, the homogeneous Neumann data $g \equiv 0$, and the right-hand side $f \equiv 0$. The solution is unknown and has to be approximated as described on Page 110. Figure 6.41 right depicts the approximated solution, and suggests that the contact interval is the entire contact boundary Γ_C. The triangulation displayed in Figure 6.41 left shows that the adaptive algorithm leads to local refinement at the boundary of the contact zone. Figure 6.42 displays the total error and the estimators for the three finite element methods, both on adaptive and uniform meshes. Hild and Nicaise (2005) show that the exact solution satisfies $u \in H^s(\Omega)$ for all $s < 3/2$. This reduced regularity is reflected in the reduced convergence rate for uniform mesh-refinement (cf. Figure 6.42). Adaptive mesh refinement captures the optimal convergence rate of -0.5 with respect to the number of degrees of freedom (cf. Figure 6.42). The efficiency indices with respect to the total error in Figure 6.43 lie at 0.8 for the mixed finite element method, at 1.4 for the non-conforming method, and at 3.5 for the conforming finite element method. Recall that Theorem 4.14 implies that the efficiency indices lie between $1/\sqrt{30}$ and $\sqrt{2}$ if the residual $\|\mathrm{Res}\|_*$ can be evaluated exactly. Figure 6.44 shows the convergence of the error of the primal variable in the energy norm and of the estimator Est (for the non-conforming and mixed FEM, the additional term $\|u_{\mathrm{CR}} - v\|_{\mathrm{NC}}$, respectively $\|\tilde{u}_{\mathrm{CR}} - v\|_{\mathrm{NC}}$ are added to Est). On uniform meshes these error and estimator terms converge with a convergence rate of -0.25 with respect to the number of degrees of freedom, whereas on uniform meshes, they converge with the optimal convergence rate of -0.5 with respect to the number

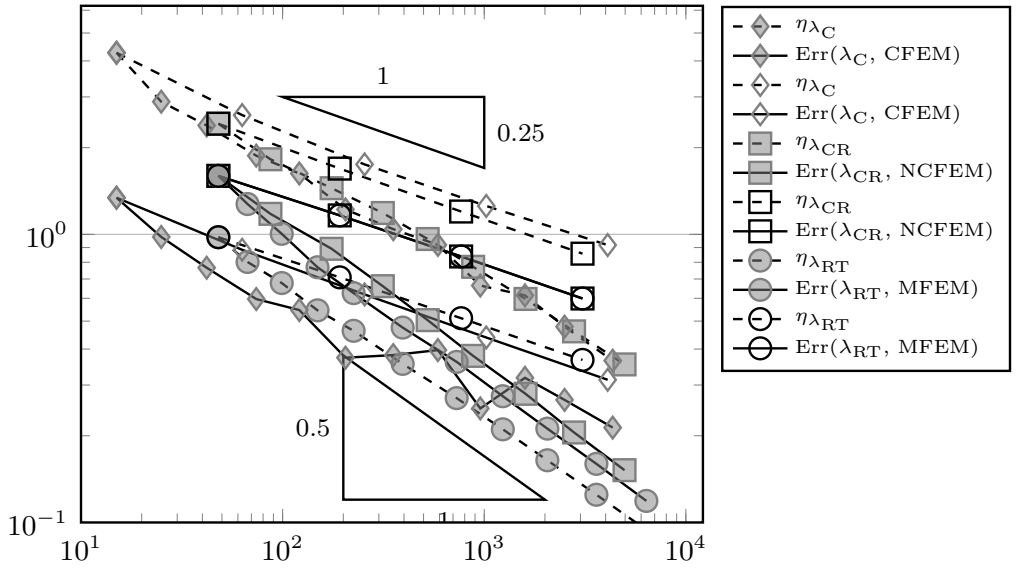

Figure 6.42.: Total error and error estimators for CFEM, NCFEM, and MFEM for the experiment from Subsection 6.2.1 for adaptive (grey) and uniform (white) mesh-refinement.

of degrees of freedom. Figure 6.45 depicts the efficiency indices with respect to the error of the primal variable in the energy norm, which lie at 2 for the mixed FEM on adaptive and uniform meshes, at 3 for the non-conforming FEM on uniform meshes and at 5 on adaptive meshes, at 5 for the conforming FEM on uniform meshes and 7 on adaptive meshes. The numerical experiments suggests, that the Lagrange multiplier satisfies $\lambda = 0$ and hence the estimator term $\int_{\Gamma_C}(-\mu)(v-\chi)_+ \,\mathrm{d}s$ does not contribute to Est and the error terms $\int_{\Gamma_C}(-\mu)(u-\chi)\,\mathrm{d}s$ and $\int_{\Gamma_C}(-\lambda)(v-\chi)_+\,\mathrm{d}s$ do not contribute to the error. The same behaviour is observed in Hild and Nicaise (2005). This means that only $\eta_{\mathrm{Res},\mu}$ contributes to Est. Figure 6.46 shows that this estimator terms converges with a convergence rate of -0.25 with respect to the number of degrees of freedom for all three methods and is lowest for the mixed FEM, which explains the lower efficiency indices for this method in Figures 6.43 and 6.45.

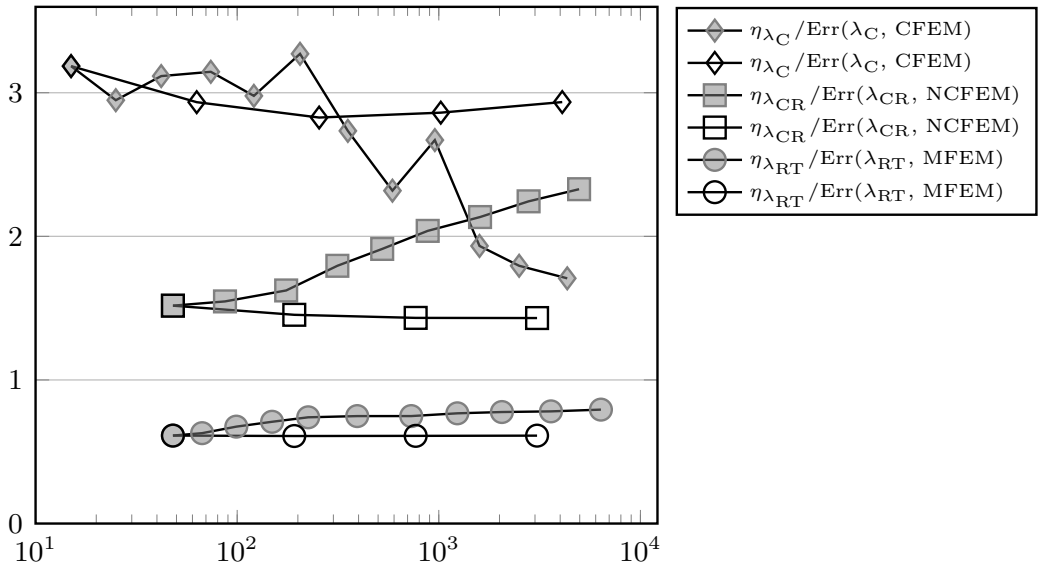

Figure 6.43.: Efficiency indices for the total error for CFEM, NCFEM, and MFEM for the experiment from Subsection 6.2.1 for adaptive (grey) and uniform (white) mesh-refinement.

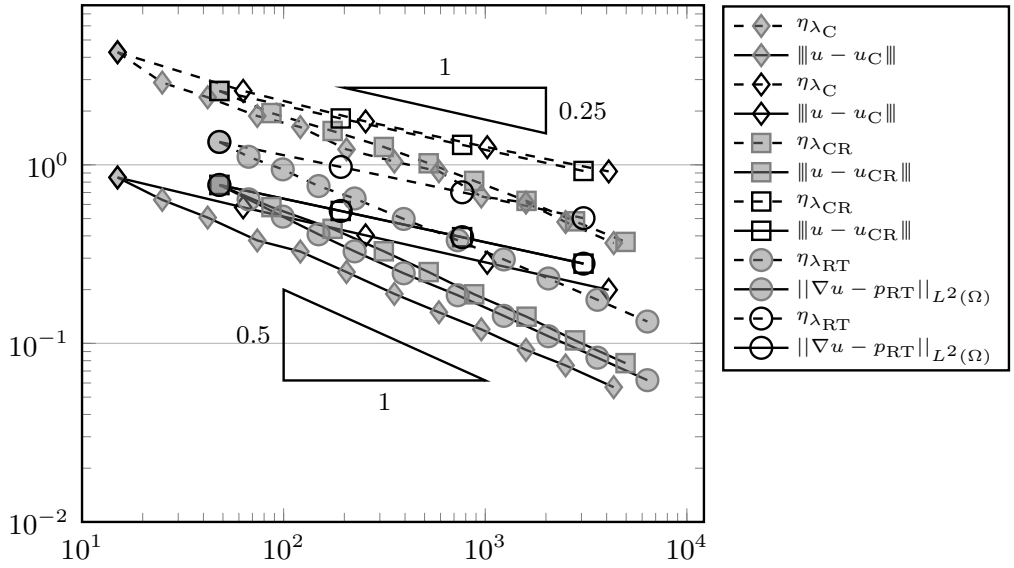

Figure 6.44.: Error of the primal variable in the energy norm and error estimators for CFEM, NCFEM, and MFEM for the experiment from Subsection 6.2.1 for adaptive (grey) and uniform (white) mesh-refinement.

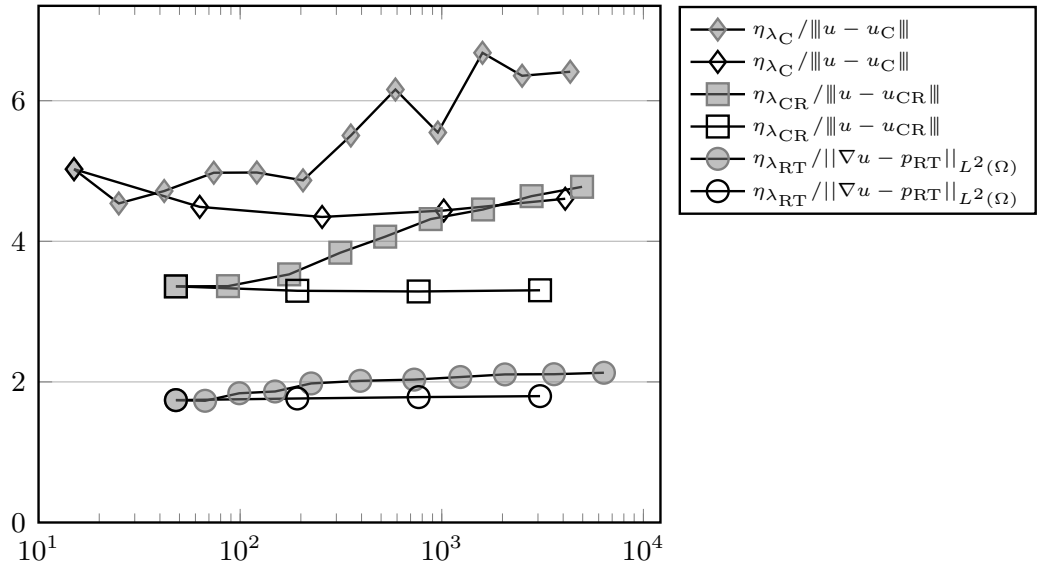

Figure 6.45.: Efficiency indices for the error of the primal variable in the energy norm for CFEM, NCFEM, and MFEM for the experiment from Subsection 6.2.1 for adaptive (grey) and uniform (white) mesh-refinement.

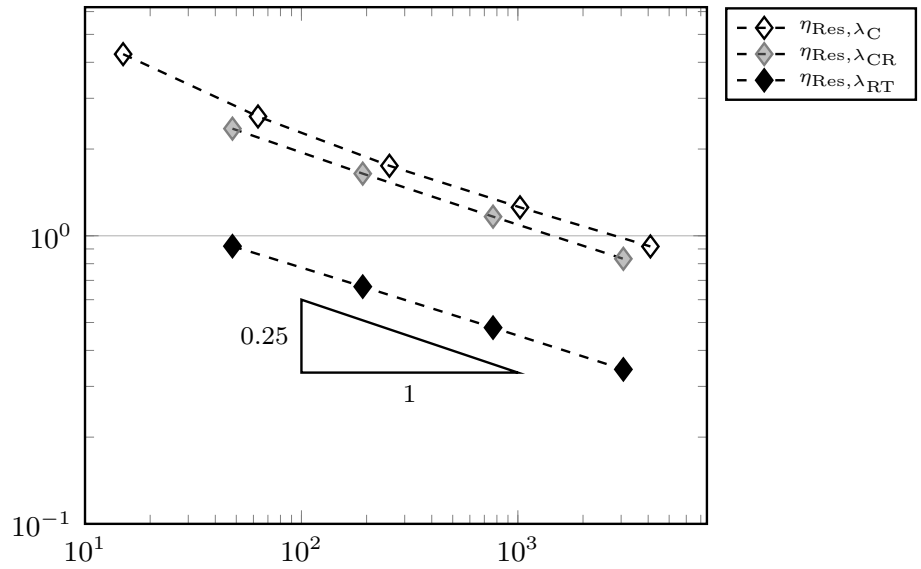

Figure 6.46.: Residual component of the estimator for CFEM, NCFEM, and MFEM for the experiment of Subsection 6.2.1 for uniform mesh-refinement.

6.2.2. Quadratic obstacle on square domain

This example is similar to the problem in Schröder (2009) but with slightly modified boundary conditions to ensure that this problem satisfies the assumptions on the obstacle χ, i.e., $\chi = u_D$ along Γ_D. The problem is formulated on the square domain $\Omega := (-1,1)^2$, with the contact boundary $\Gamma_C := [-1,1] \times \{-1\}$, the Dirichlet boundary $\Gamma_D := [-1,1] \times \{1\}$, and the Neumann boundary $\Gamma_N := \{-1,1\} \times (-1,1)$. The problem concerns the right-hand side $f \equiv -1$, the homogeneous Dirichlet boundary conditions $u_D \equiv 0$, the homogeneous Neumann conditions $g \equiv 0$, and the obstacle $\chi(x,y) := -x^2$.

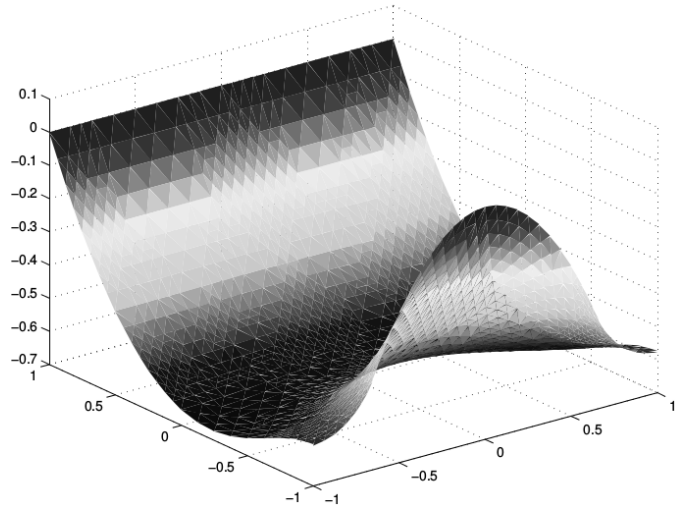

Figure 6.47.: Solution after 10 levels of adaptive mesh-refinement for NCFEM for the experiment from Subsection 6.2.2.

The exact solution for this problem is unknown, and does not satisfies $u \in H^2(\Omega)$ (cf. Theorem 4.3). It is approximated as described on Page 110. An approximation is depicted in Figure 6.47. Since $u \notin H^2(\Omega)$, the Lagrange multiplier λ is not an L^2 function. The data satisfy the assumptions for Theorem 4.14 but not those of the realizations of Theorem C in Section 4.3–4.5. Figure 6.48 depicts the convergence of the total error Err and the error estimator η_μ for CFEM, NCFEM, and MFEM. The considered errors and estimators display the expected convergence rate of -0.5 with respect to the number of degrees of freedom, both for uniform and adaptive meshes. This leads to efficiency indices in Figure 6.49 between 0.9 for the mixed FEM on adaptive and uniform meshes, between 3 and 4 for the non-conforming FEM on adaptive and uniform meshes, and between 1 and 4 for the conforming FEM on adaptive and uniform meshes. Recall that Theorem 4.14 implies that the efficiency indices lie between $1/\sqrt{30}$ and $\sqrt{2}$ if the term $\|\mathrm{Res}\|_*$ is evaluated exactly. Figure 6.50 displays the convergence of the error of the primal variable in the

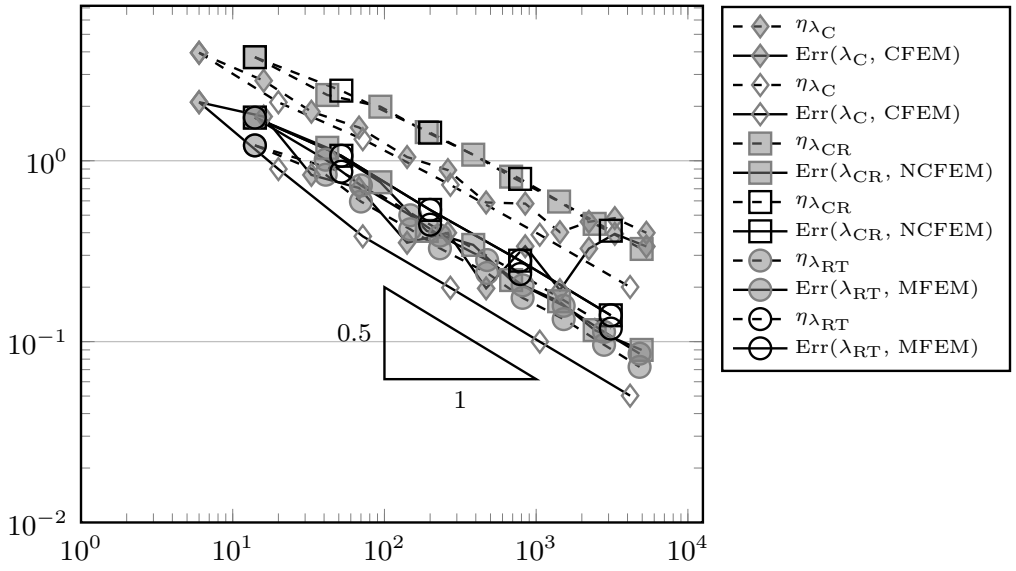

Figure 6.48.: Total error and error estimators for CFEM, NCFEM, and MFEM for the experiment from Subsection 6.2.2 for adaptive (grey) and uniform (white) mesh-refinement.

energy norm and the guaranteed upper bounds (with the respective modification for NCFEM and MFEM). Both the error and the estimators converge with the expected convergence rate of -0.5 with respect to the number of degrees of freedom, which leads to the efficiency indices of 1.9 for MFEM on adaptive and uniform meshes, of 5.9 for CFEM and NCFEM on uniform meshes, 6.2 for NCFEM on adaptive meshes, and rather unbounded efficiency indices for CFEM on adaptive meshes in Figure 6.51. Figures and 6.53 shows, that both $\eta_{\mathrm{Res},\lambda_C}$ and $\|\lambda - \lambda_C\|_*$ converge with a reduced convergence rate, whereas $\|u - u_C\|$ converges with a convergence rate of -0.5 with respect to the number of degrees of freedom. Since the error term $\|\lambda - \lambda_C\|_*$ is not considered in Figure 6.51, this explains the unbounded efficiency indices displayed therein. This does not contradict the results in Chapter 4 since Theorem 4.20 shows that the discrete Lagrange multiplier λ_C is not efficient if $\lambda \notin L^2(\Gamma_C)$. Figures 6.52 and 6.53 show that the error estimator is dominated by $\eta_{\mathrm{Res},\mu}$ for all three methods, and that the error terms $\int_{\Gamma_C}(-\mu)(u-\chi)\,\mathrm{d}s$, and $\Lambda((v-\chi)_+)$ are of higher order. Figure 6.54 displays the convergence of the estimator term $\eta_{\mathrm{Res},\mu}$ for the three finite element methods on uniform meshes. In all three cases it converges with a convergence rate of -0.5 and has the smallest values for the mixed FEM, which explains the lower efficiency indices for this method in Figures 6.49 and 6.51.

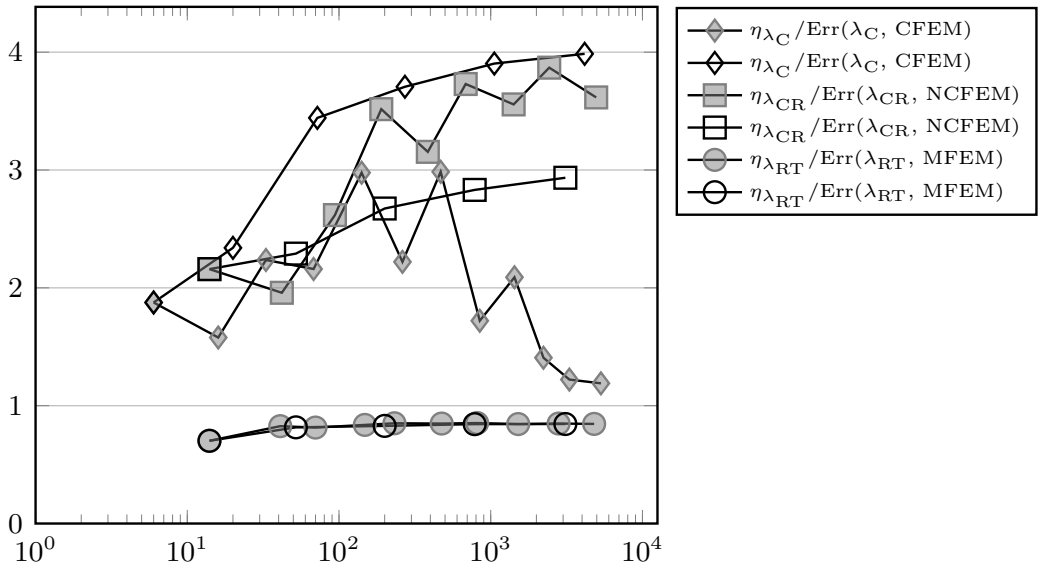

Figure 6.49.: Efficiency indices for the total error for CFEM, NCFEM, and MFEM for the experiment from Subsection 6.2.2 for adaptive (grey) and uniform (white) mesh-refinement.

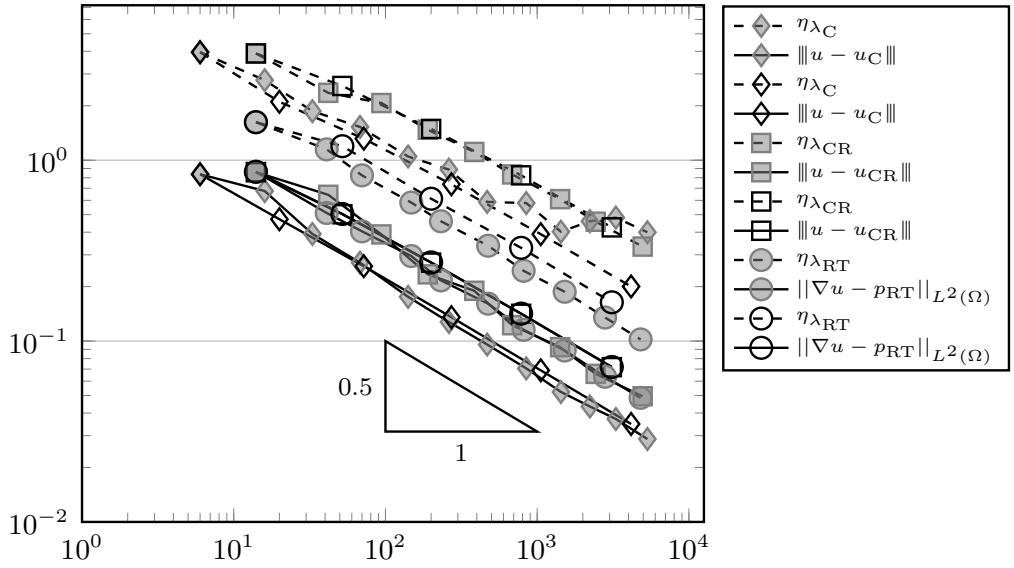

Figure 6.50.: Error of the primal variable in the energy norm and error estimators for CFEM, NCFEM, and MFEM for the experiment from Subsection 6.2.2 for adaptive (grey) and uniform (white) mesh-refinement.

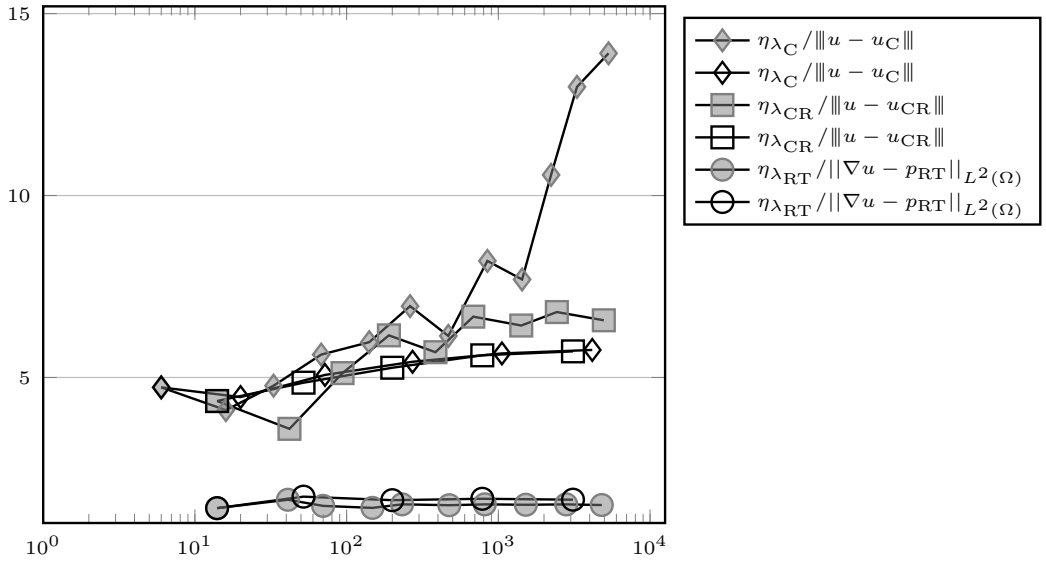

Figure 6.51.: Efficiency indices for the error of the primal variable in the energy norm for CFEM, NCFEM, and MFEM for the experiment from Subsection 6.2.2 for adaptive (grey) and uniform (white) mesh-refinement.

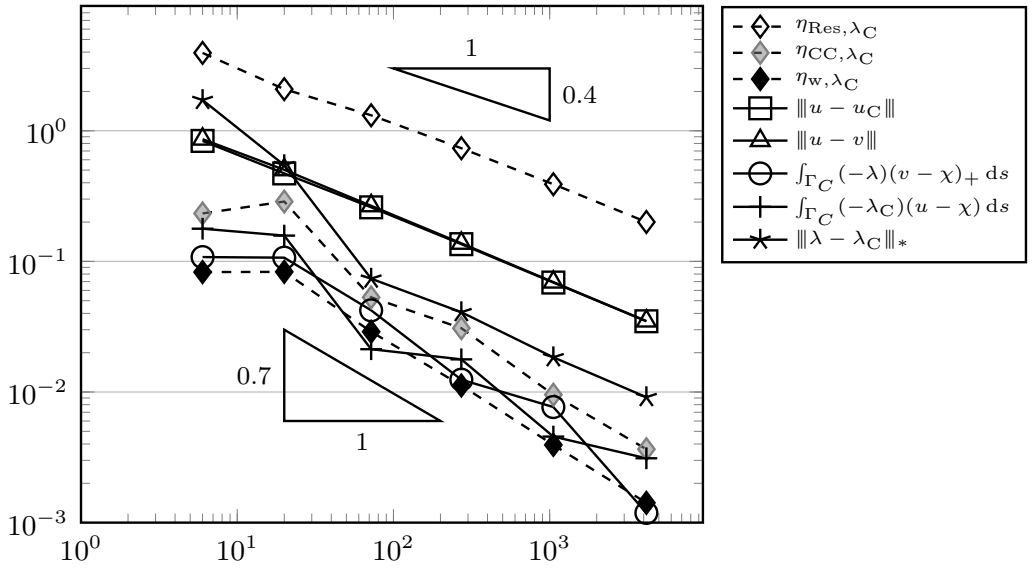

Figure 6.52.: Comparison of different error and estimator components for CFEM for the experiment from Subsection 6.2.2 for uniform mesh-refinement.

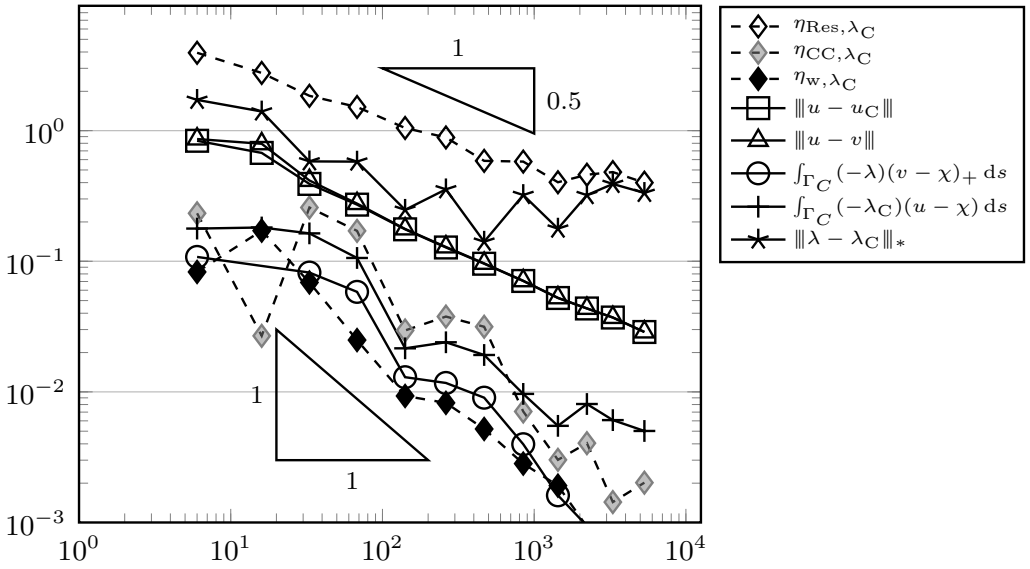

Figure 6.53.: Comparison of different error and estimator components for CFEM for the experiment from Subsection 6.2.2 for adaptive mesh-refinement.

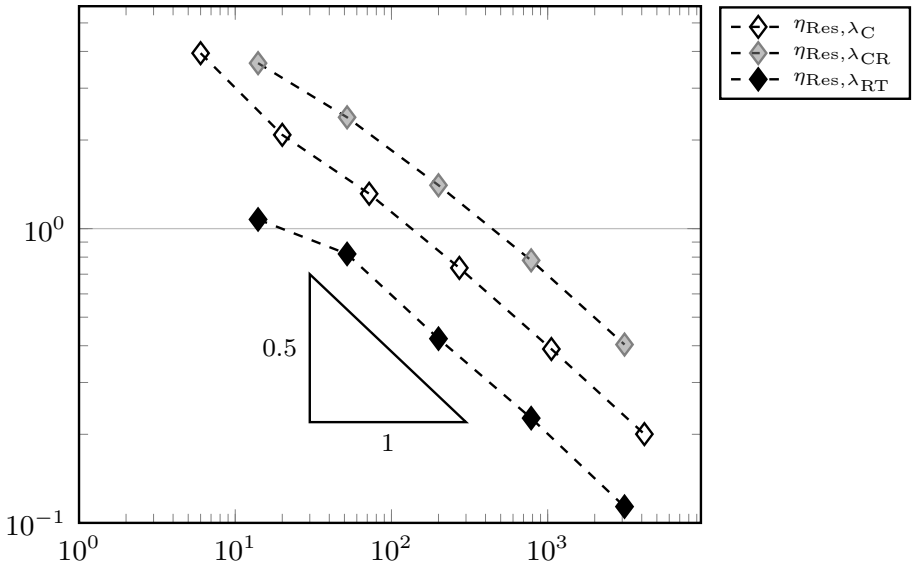

Figure 6.54.: Residual component of the estimator for CFEM, NCFEM, and MFEM for the experiment from Subsection 6.2.2 for uniform mesh-refinement.

6.2.3. Triangular domain

This numerical experiment is taken from Hild and Nicaise (2005). It concerns the triangular domain $\Omega := \operatorname{conv}\{(0,0),(1,0),(1/2,1/2)\}$. The Dirichlet boundary satisfies $\Gamma_D := \operatorname{conv}\{(1,0),(1/2,1/2)\}$, the contact boundary is given by $\Gamma_C := \operatorname{conv}\{(0,0),(1,0)\}$, and the Neumann boundary is $\Gamma_N := \partial\Omega \setminus (\Gamma_D \cup \Gamma_C)$. The obstacle χ satisfies $\chi \equiv 0$, the Dirichlet boundary condition is given by $u_D \equiv 0.05$, and the right-hand side is $f \equiv 1$. The exact solution is unknown and is approximated as described on Page 110. In this example, the Dirichlet boundary condition does not satisfy $u_D = \chi$ along Γ_D and hence the theoretical results from Sections 4.3–4.5 are not valid, but it will be explored whether they hold experimentally. Figure 6.55 depicts the total errors and error estimators on uniform and adaptive meshes. All converge with a convergence rate of -0.5 with respect to the number of degrees of freedom. This leads to efficiency indices at 1 for MFEM and 5 for the conforming and non-conforming method both on uniform and adaptive meshes. Although the assumptions in Theorem 4.24, 4.38, and 4.49 are not valid, Figure 6.57 depicts the convergence rate of the error of the primal variables in the energy norm and the estimators (with the appropriate modifications for NCFEM and MFEM). These errors converge with the expected convergence rate of -0.5 with respect to the number of degrees of freedom and lead to efficiency indices of 2 for MFEM and between 7 and 9 for CFEM and NCFEM on uniform and adaptive meshes (cf. Figure 6.58). This reveals experimentally that the results of Theorems 4.24, 4.38, and 4.49 hold true also for this case. The numerical experiments show that the estimator term $\int_{\Gamma_C}(-\mu)(v-\chi)_+ \,\mathrm{d}s$ vanishes and since $\partial^2 u_D/\partial s^2 \equiv 0$ only $\eta_{\mathrm{Res},\mu}$ contributes to Est. The error terms $\int_{\Gamma_C}(-\mu)(u-\chi)\,\mathrm{d}s$ and $\int_{\Gamma_C}(-\lambda)(v-\chi)_+\,\mathrm{d}s$ vanish. Figure 6.59 depicts the convergence of the estimator term $\eta_{\mathrm{Res},\mu}$ for CFEM, NCFEM, and MFEM on uniform meshes. All converge with the expected convergence rate of -0.5 with respect to the number of degrees of freedom. The term for the mixed FEM is lowest, which explains the smaller efficiency indices for this method in Figure 6.56 and 6.58.

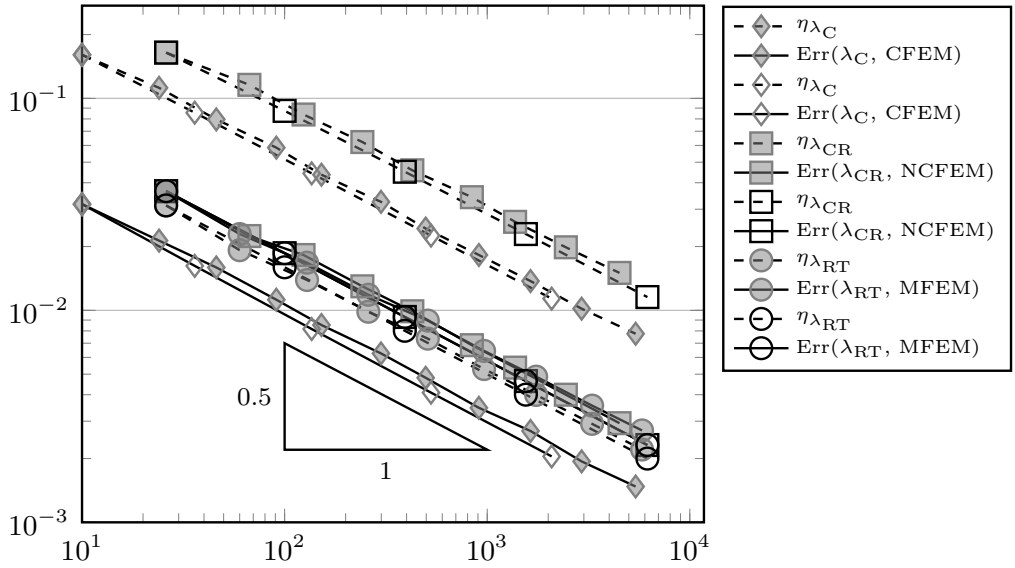

Figure 6.55.: Total error and error estimators for CFEM, NCFEM, and MFEM for the experiment from Subsection 6.2.3 for adaptive (grey) and uniform (white) mesh-refinement.

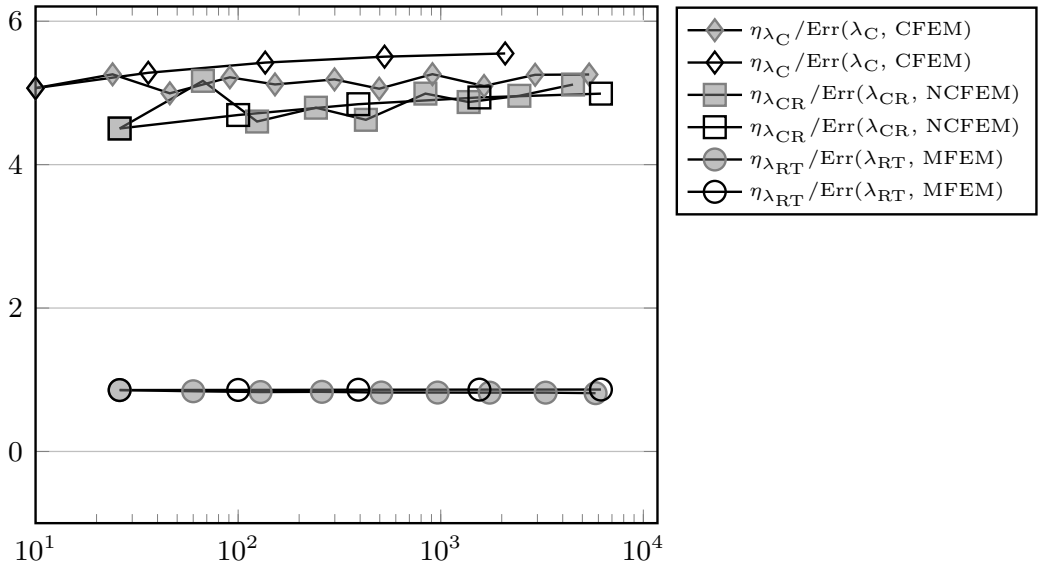

Figure 6.56.: Efficiency indices for the total error for CFEM, NCFEM, and MFEM for the experiment from Subsection 6.2.3 for adaptive (grey) and uniform (white) mesh-refinement.

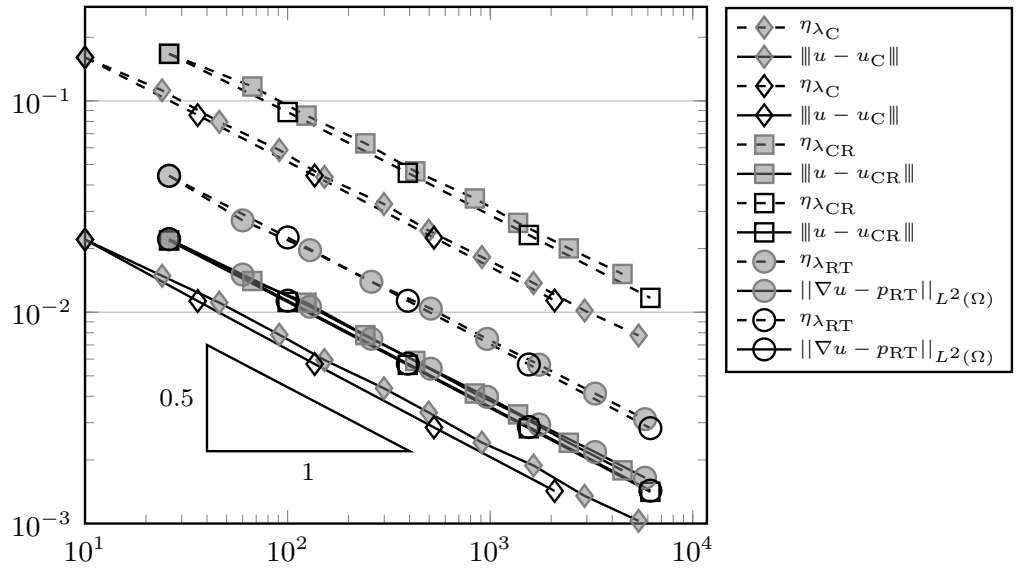

Figure 6.57.: Error of the primal variable in the energy norm and error estimators for CFEM, NCFEM, and MFEM for the experiment from Subsection 6.2.3 for adaptive (grey) and uniform (white) mesh-refinement.

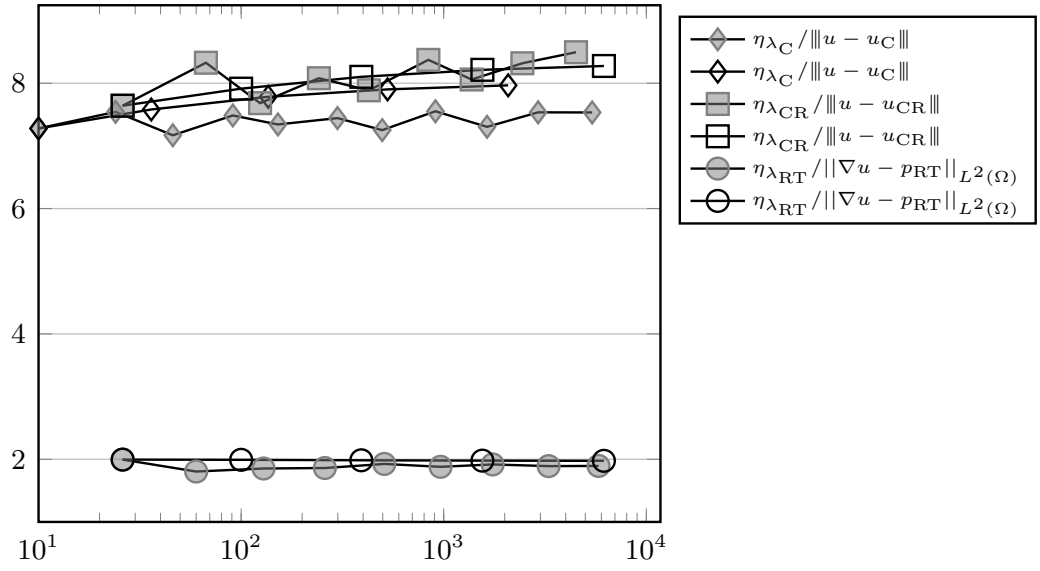

Figure 6.58.: Efficiency indices for the error of the primal variable in the energy norm for CFEM, NCFEM, and MFEM for the experiment from Subsection 6.2.3 for adaptive (grey) and uniform (white) mesh-refinement.

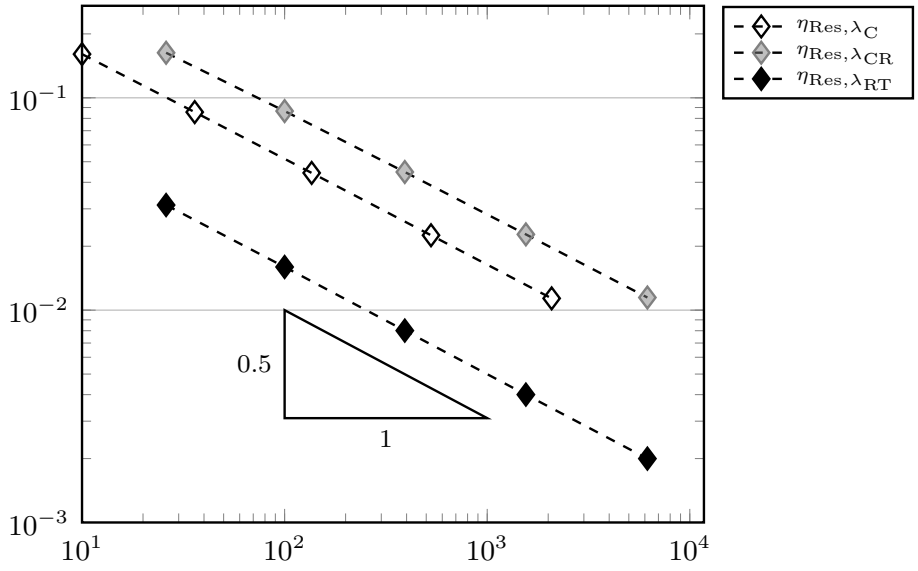

Figure 6.59.: Residual component of the estimator for CFEM, NCFEM, and MFEM for the experiment of Subsection 6.2.3 for uniform mesh-refinement.

6.2.4. 3/4 circle

This numerical benchmark examples also presents an exceptions from the theoretical results in Section 4.3–4.5. It is taken from Hild and Nicaise (2005) and concerns the three quarter circle $\Omega := B_1(0) \setminus ((0,1) \times (0,-1))$. The contact boundary is given by $\Gamma_C := [0,1) \times 0$, the Neumann boundary by $\Gamma_N := \{0\} \times (0,-1)$, and the Dirichlet boundary satisfies $\Gamma_D := \partial\Omega \setminus (\Gamma_C \cup \Gamma_N)$. The problem concerns the obstacle $\chi \equiv 0$, the Dirichlet boundary condition $u_D(r,\varphi) = \cos(2\varphi/3)$, the homogeneous Neumann conditions $g \equiv 0$, and the force term $f \equiv 0$.

The exact solution, depicted in Figure 6.60 right, reads

$$u(r,\varphi) := r^{2/3} \cos(2\varphi/3).$$

The domain includes a re-entrant corner and hence the solution is of reduced regularity. Figure 6.60 left shows that Algorithm 2 refines the area of the re-entrant corner. Figure 6.61 presents the convergence of the total error Err for the conforming, the non-conforming, and the mixed FEM and the corresponding error estimators on uniform and adaptive meshes. Since the solution u does not satisfy $u \in H^2(\Omega)$, the errors and estimators display a reduced order or convergence ($-.33$ with respect to the number of degrees of freedom) on uniform meshes. The corresponding adaptive algorithms improve this convergence rate to the optimal order of -0.5 with respect to the number of degrees of freedom (cf. Figure 6.61). Figure 6.62 shows that the methods display the expected efficiency, with efficiency below 1 (around 0.9) for MFEM on uniform and adaptive meshes, between 2 and 3 for NCFEM on adaptive and uniform meshes, and between 3 and 4 for CFEM on adaptive and uniform meshes. Efficiency indices below 1 are possible, since the factor 30 in Theorem 4.14

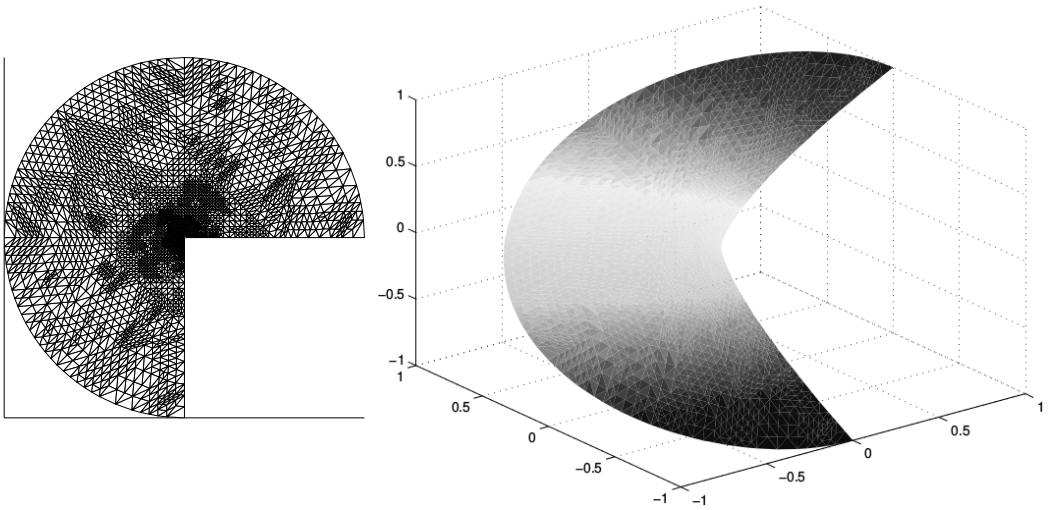

Figure 6.60.: Triangulation (left) and solution (right) after 10 levels of adaptive mesh-refinement for CFEM for the experiment from Subsection 6.2.4.

is not included in the numerical experiments. Figure 6.63 shows the convergence of the error in the primal variables in the energy norm and the corresponding estimator Est (with the necessary modifications for NCFEM and MFEM). On adaptive meshes, the error and estimator for all methods converge with a convergence rate of -0.5 with respect to the number of degrees of freedom and with -0.33 on uniform meshes. This leads to efficiency indices at around 2.5 for MFEM, between 4 and 5.5 for NCFEM and between 5.5 and 7 for CFEM on uniform and adaptive meshes. Since the exact solution satisfies $\partial u/\partial \nu = 0$ along Γ_C the Lagrange multiplier satisfies $\lambda = 0$. This is mimicked by the finite element methods and hence the estimator only includes $\eta_{\mathrm{Res},\mu}$ for all considered methods. Figure 6.65 depicts the convergence of this estimator term for the three methods on uniform meshes and shows, that it is lowest for the mixed FEM which explains the smaller efficiency indices.

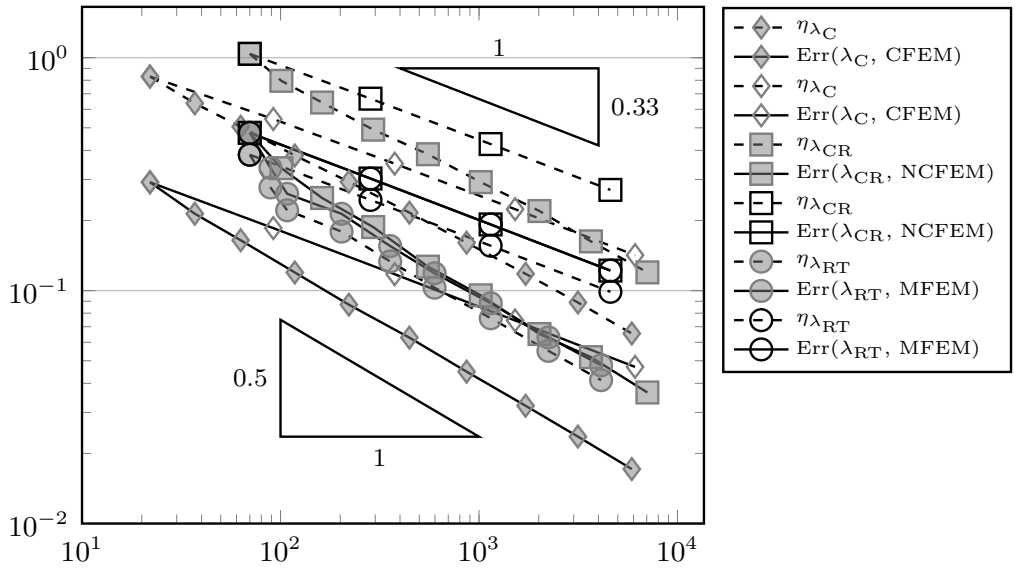

Figure 6.61.: Total error and error estimators for CFEM, NCFEM, and MFEM for the experiment from Subsection 6.2.4 for adaptive (grey) and uniform (white) mesh-refinement.

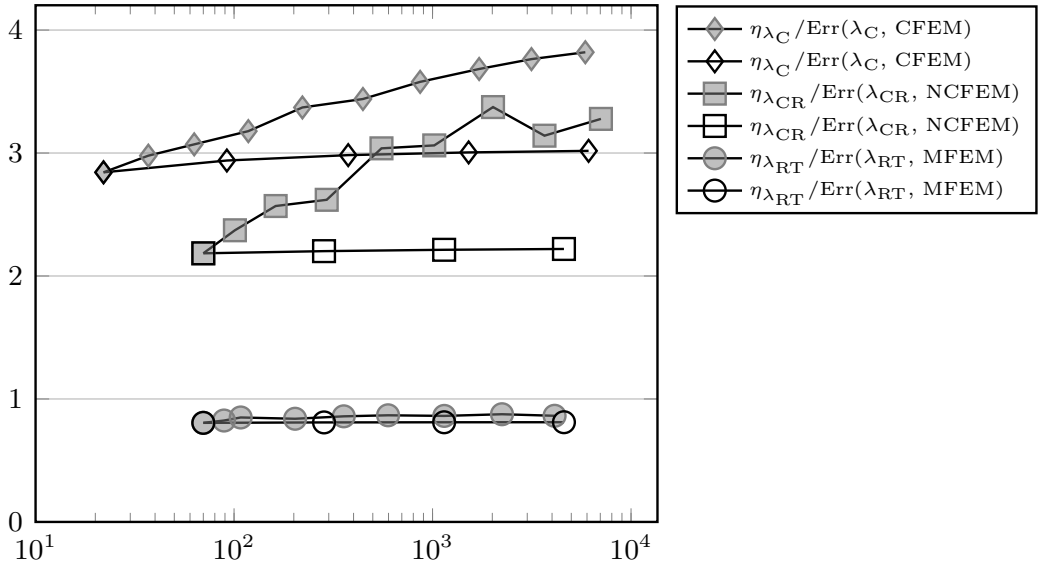

Figure 6.62.: Efficiency indices for the total error for CFEM, NCFEM, and MFEM for the experiment from Subsection 6.2.4 for adaptive (grey) and uniform (white) mesh-refinement.

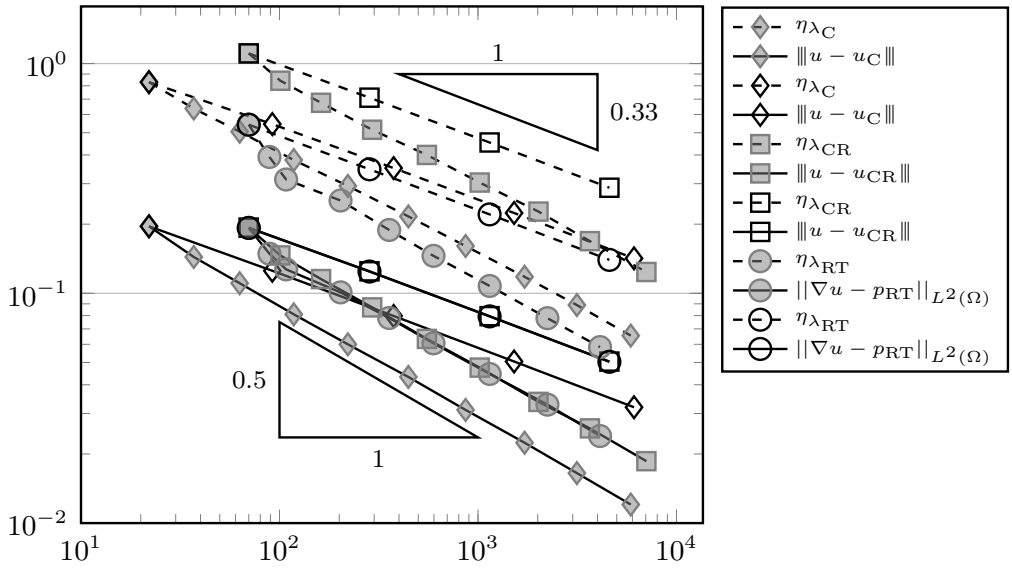

Figure 6.63.: Error of the primal variable in the energy norm and error estimators for CFEM, NCFEM, and MFEM for the experiment from Subsection 6.2.4 for adaptive (grey) and uniform (white) mesh-refinement.

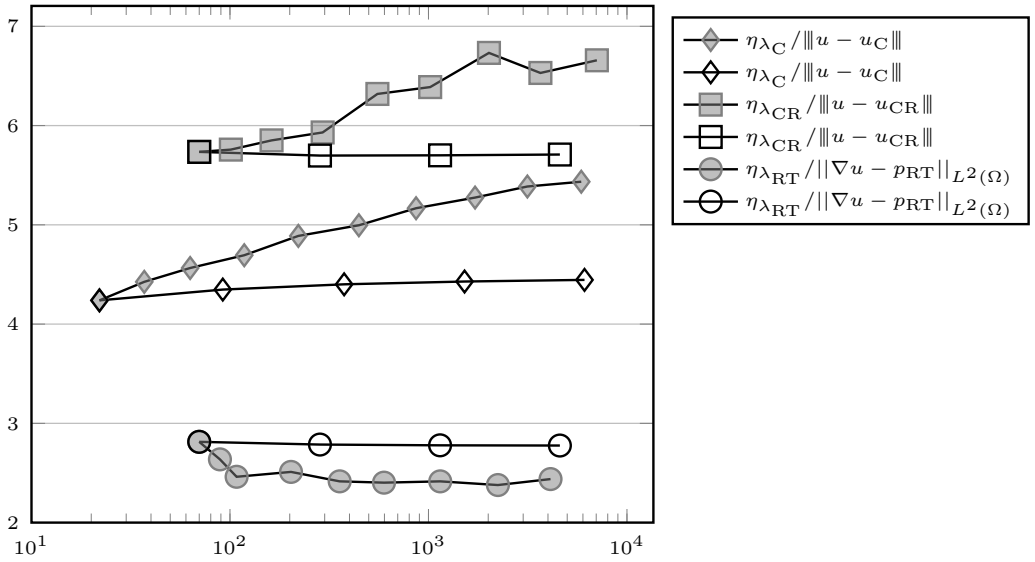

Figure 6.64.: Efficiency indices for the error of the primal variable in the energy norm for CFEM, NCFEM, and MFEM for the experiment from Subsection 6.2.4 for adaptive (grey) and uniform (white) mesh-refinement.

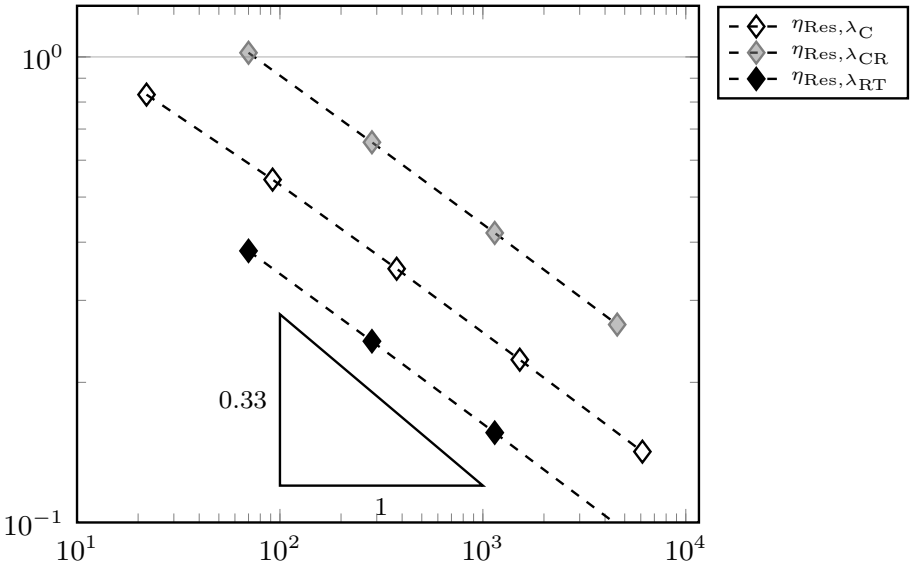

Figure 6.65.: Residual component of the estimator for CFEM, NCFEM, and MFEM for the experiment from Subsection 6.2.4 for uniform mesh-refinement.

6.3. Bingham flow problem

This section presents four different numerical benchmark examples for the Bingham flow problem problem, discretized with the conforming Courant FEM and the non-conforming Crouzeix-Raviart FEM. For a given triangulation $\mathcal{T}$, recall the discrete Lagrange multiplier λ_{C} from the solution to (5.11)–(5.12) on Page 102, λ_{CR} from the solution to (5.18)– (5.19) on Page 106, and $\lambda_{\mathrm{CR}}^{\mathrm{mod}}$ which results from the modification described in Algorithm 1 on Page 108. For each finite element method, recall the approximation $v \in \mathcal{A}$ to the exact solution $u \in H_0^1(\Omega)$ and the residual

$$\mathrm{Res}(\varphi) = \int_\Omega f\varphi \,\mathrm{d}x - \int_\Omega \mu \cdot \nabla\varphi \,\mathrm{d}x - a(v,\varphi) \quad \text{for all } \varphi \in H_D^1(\Omega)$$

where μ abbreviates any of the above discrete Lagrange multipliers. The estimator splits into two components

$$\mathrm{Est}^2 = \|\!|\mathrm{Res}|\!\|_*^2 + (j(v) - g\int_\Omega \mu \cdot \nabla v \,\mathrm{d}x).$$

The term $\eta_{j,\mu}^2 := j(v) - g\int_\Omega \mu \cdot \nabla v \,\mathrm{d}x$ is computable element wise and satisfies

$$\eta_{j,\mu}^2 = \sum_{T\in\mathcal{T}} \eta_{j,\mu}^2(T).$$

The estimates for the residual in (5.13) on Page 103 and (5.20) on Page 106 lead to the computable element-wise bounds for $\|\!|\mathrm{Res}|\!\|_*^2 \leq \eta_{\mathrm{Res},\mu}^2 = \sum_{T\in\mathcal{T}} \eta_{\mathrm{Res},\mu}^2(T)$ with

$$\eta_{\mathrm{Res},\lambda_{\mathrm{C}}}^2(T) := ||h_T f||_{L^2(T)}^2 + \sum_{E\in\mathcal{E}(T)} |E| \, ||[(\nabla u_{\mathrm{C}} + \lambda_{\mathrm{C}}) \cdot \nu_E + \lambda_{\mathrm{C}}|_E]_E||_{L^2(E)}^2,$$

$$\eta^2_{\mathrm{Res},\lambda_{\mathrm{CR}}}(T) := (1/48 + 1/j^2_{1,1})||h_T f||^2_{L^2(T)} + \|\!|u_{\mathrm{CR}} - v|\!\|_T,$$
$$\eta^2_{\mathrm{Res},\lambda^{\mathrm{mod}}_{\mathrm{CR}}}(T) := \eta^2_{\mathrm{Res},\lambda_{\mathrm{CR}}} + ||\lambda_{\mathrm{CR}} - \lambda^{\mathrm{mod}}_{\mathrm{CR}}||_{L^2(T)}.$$

Then it holds

$$\eta^2_{\mathrm{Res},\mu} = \sum_{T\in\mathcal{T}} \eta^2_{\mathrm{Res},\mu}(T).$$

To clarify the notation of the legends, let $\eta^2_\mu = \eta^2_{\mathrm{Res},\mu} + \eta^2_{j,\mu}$ denote the estimator for any of the three discrete Lagrange multipliers above and let $\mathrm{Err}(\mu, \mathrm{FEM})$ denote the total error for a given discrete Lagrange multiplier and FEM= CFEM or NCFEM.

6.3.1. Circular domain

The first experiment is well known and can be found in Glowinski (2008). For a circular domain with radius R, a constant force term $f = C$, and some given yield stress g, the exact solution is known and given by $u = 0$ if $g \geq CR/2$ and otherwise by

$$u(x) = C(R^2 - r^2)/4 + g(R - r) \qquad \text{if } 2g/C \leq r \leq R,$$
$$u(x) = C(R - 2g/C)^2/4 \qquad \text{if } 0 \leq r \leq 2g/C$$

The present example concerns the domain $\Omega := B_1(0)$, the force term $f = 10$, and the yield stress $g = 2$.

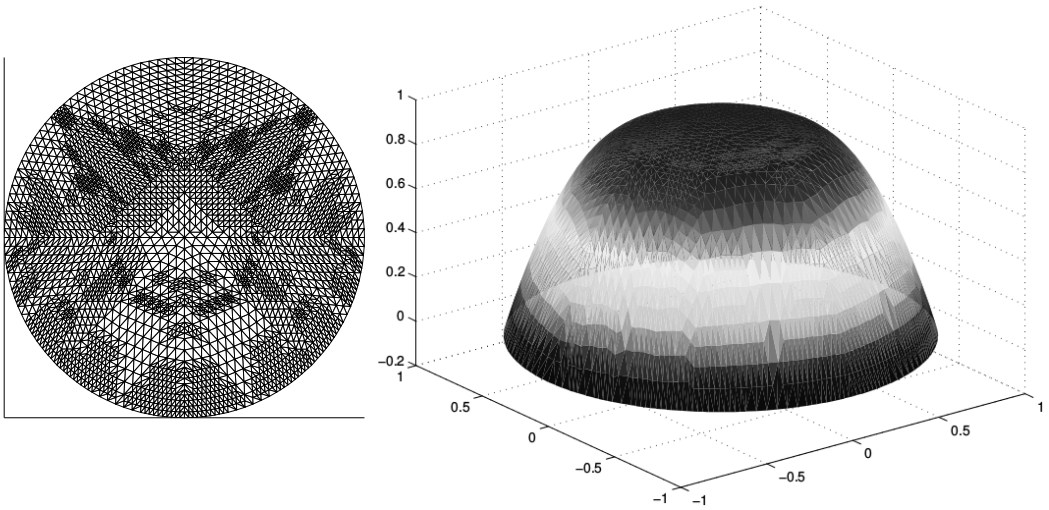

Figure 6.66.: Triangulation (left) and solution after 12 levels of adaptive refinement (right) for NCFEM for the experiment from Subsection 6.3.1.

Figure 6.66 depicts the solution (right) and the output of Algorithm 2 (left) after 12 levels of refinement. Figure 6.67 shows the convergence of the total error Err and the error estimator Est for the conforming and the non-conforming FEM (with an unmodified discrete Lagrange multiplier λ_{CR}) on adaptive and uniform meshes.

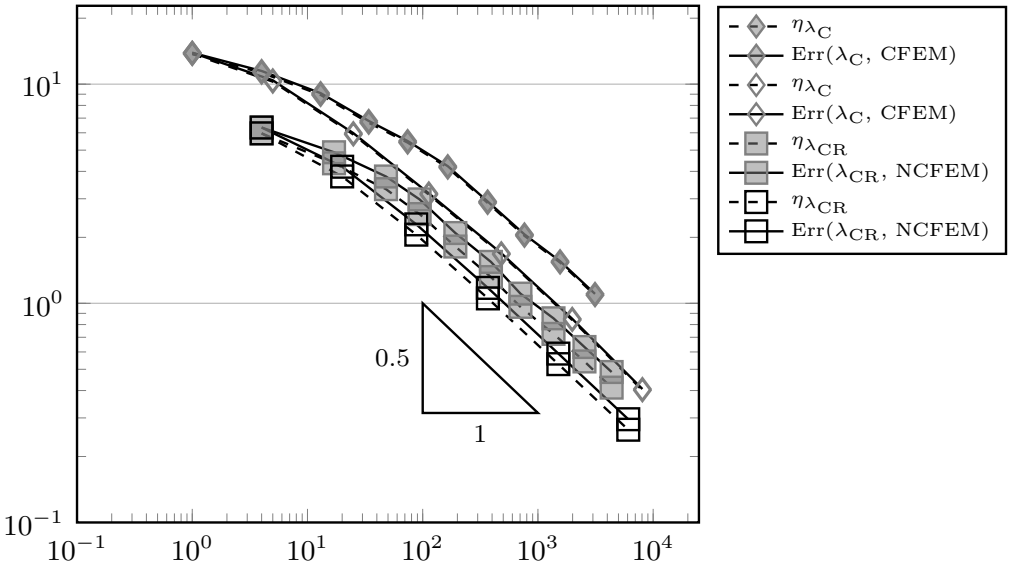

Figure 6.67.: Total error and error estimators for CFEM and NCFEM for the experiment from Subsection 6.3.1 for adaptive (grey) and uniform (white) mesh-refinement.

Both methods converge with a convergence rate of -0.5, although Glowinski (2008, Ch. 2, Thm. 6.7) shows only converge of $h\sqrt{\log(1/h)}$ with respect to the mesh-size. The efficiency indices in Figure 6.68 lie at 0.85 for the non-conforming FEM on adaptive meshes, at 0.9 for the non-conforming FEM on uniform meshes and at 0.99 for the conforming FEM both on adaptive and uniform meshes. Recall that efficiency indices below one are possible (cf. Theorem 5.12). In Figure 6.69 only the error of the primal variable in the energy norm is concerned and again both the error and the error estimator (with the necessary modification for NCFEM) exhibit a convergence rate of -0.5 with respect to the number of degrees of freedom. Since only the error of the primal variable in the energy norm is considered, this leads to efficiency indices around 3 for the non-conforming FEM, and between 8 and 10 for the conforming FEM on uniform and adaptive meshes in Figure 6.70. Figure 6.71 depicts the convergence of the different error and estimator components for the non-conforming NCFEM on uniform meshes and reveals, that the estimator is dominated by the residual term $\eta_{\mathrm{Res},\lambda_{\mathrm{CR}}}$. The dominance of this estimator term and the lower values of it for the non-conforming NCFEM in Figure 6.72 (which shows the convergence of $\eta_{\mathrm{Res},\mu}$ with respect to the number of degrees of freedom) explain the lower efficiency indices for this method. Figure 6.73 compares the estimator Est and the total error Err for the modified discrete Lagrange multiplier and the original discrete Lagrange multiplier. All terms converge with the same convergence rate of -0.5 with respect to the number of degrees of freedom and there is no visible difference.

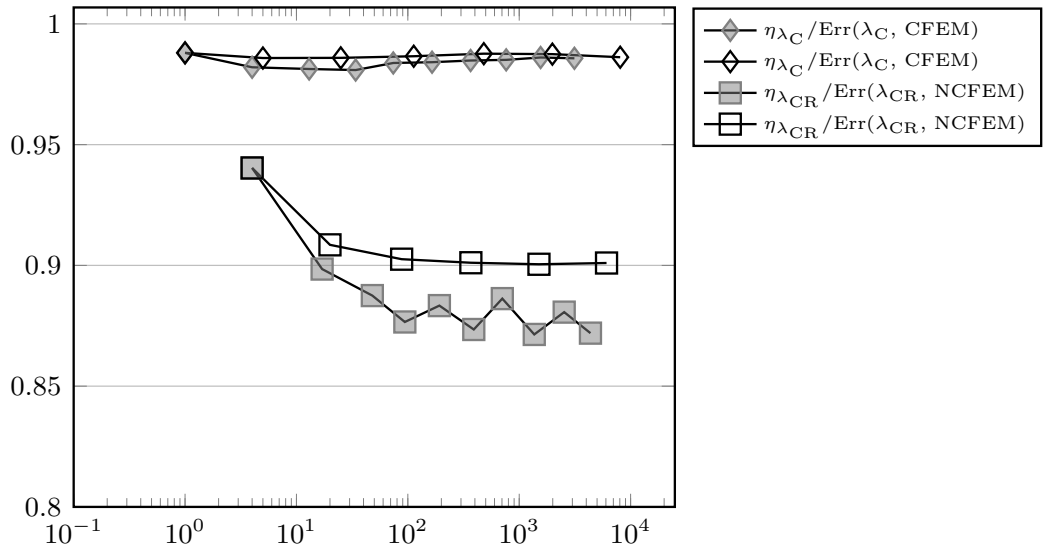

Figure 6.68.: Efficiency indices for the total error for CFEM and NCFEM for the experiment from Subsection 6.3.1 for adaptive (grey) and uniform (white) mesh-refinement.

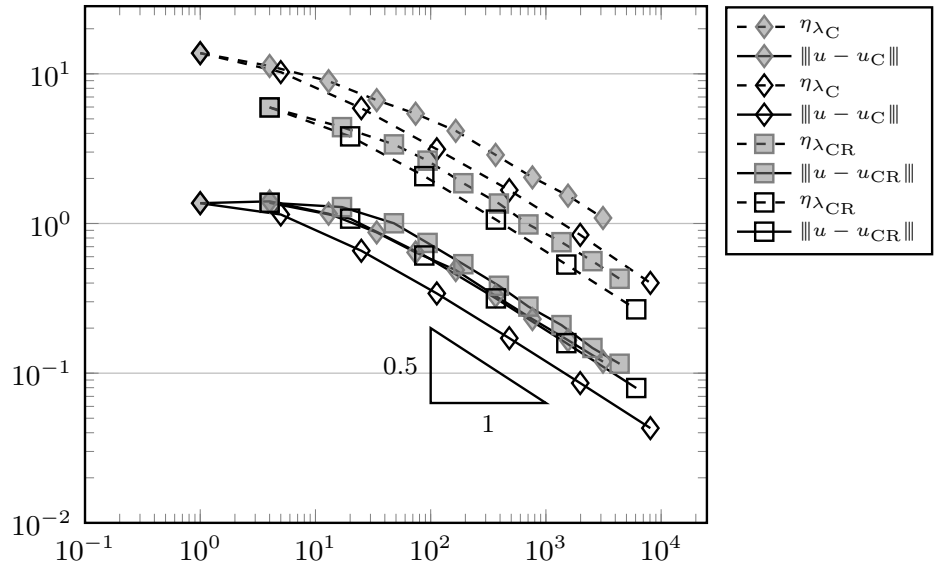

Figure 6.69.: Error of the primal variable in the energy norm and error estimators for CFEM and NCFEM for the experiment from Subsection 6.3.1 for adaptive (grey) and uniform (white) mesh-refinement.

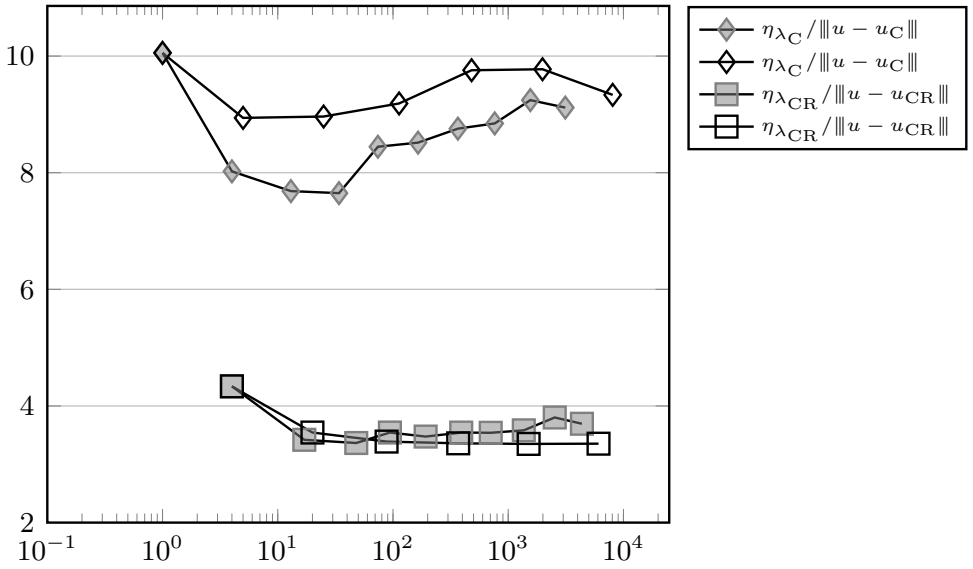

Figure 6.70.: Efficiency indices for the error of the primal variable in the energy norm for CFEM and NCFEM for the experiment from Subsection 6.3.1 for adaptive (grey) and uniform (white) mesh-refinement.

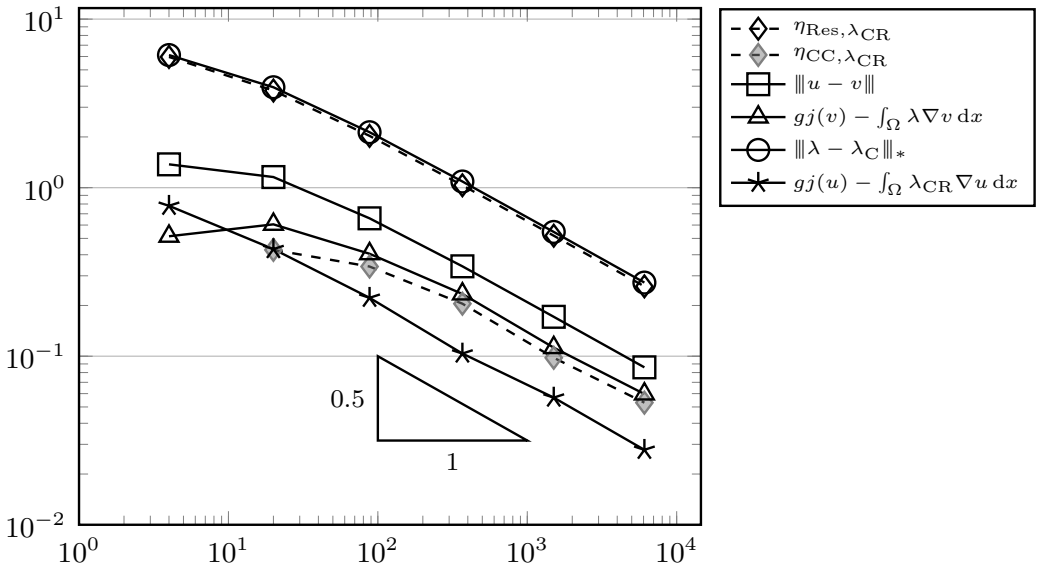

Figure 6.71.: Comparison of different error and estimator components for NCFEM for the experiment from Subsection 6.3.1 for uniform mesh-refinement.

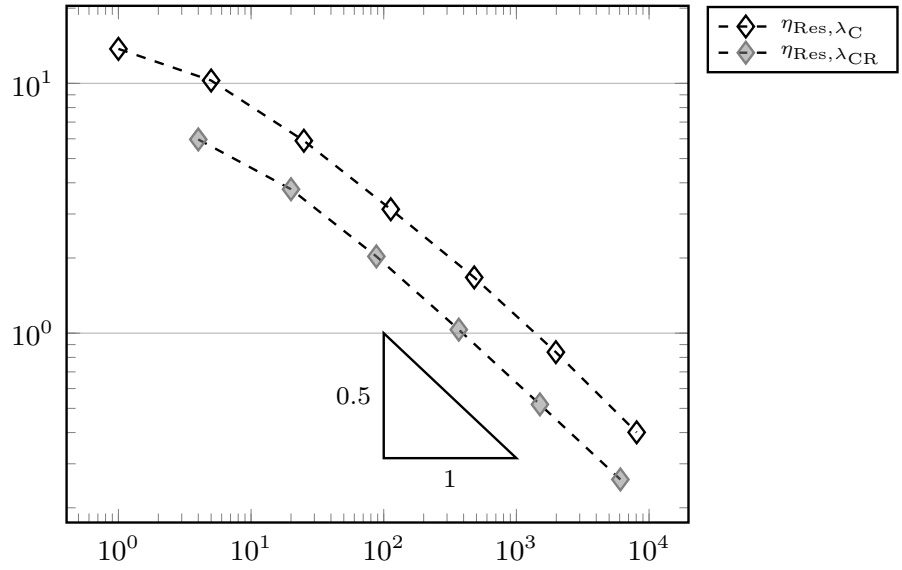

Figure 6.72.: Residual component of the estimator for CFEM and NCFEM for the experiment from Subsection 6.3.1 for uniform mesh-refinement.

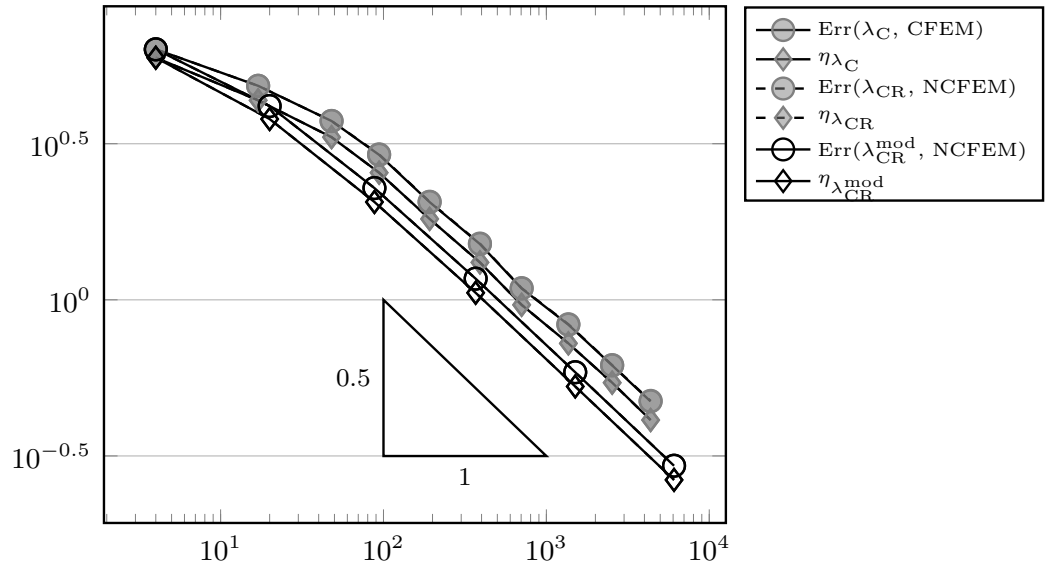

Figure 6.73.: Total error and estimator for CFEM, NCFEM, and NCFEM with modified Lagrange multiplier for the experiment from Subsection 6.3.1 for adaptive mesh-refinement.

6.3.2. Square with circular hole

This experiment considers a square domain with a circular hole at the centre inspired by Roquet and Saramito (2003), $\Omega := (-3,3) \times (-3,3) \setminus B_1(0)$. The right-hand side is given by $f = 10$ and the yield stress is chosen to be $g = 2$.

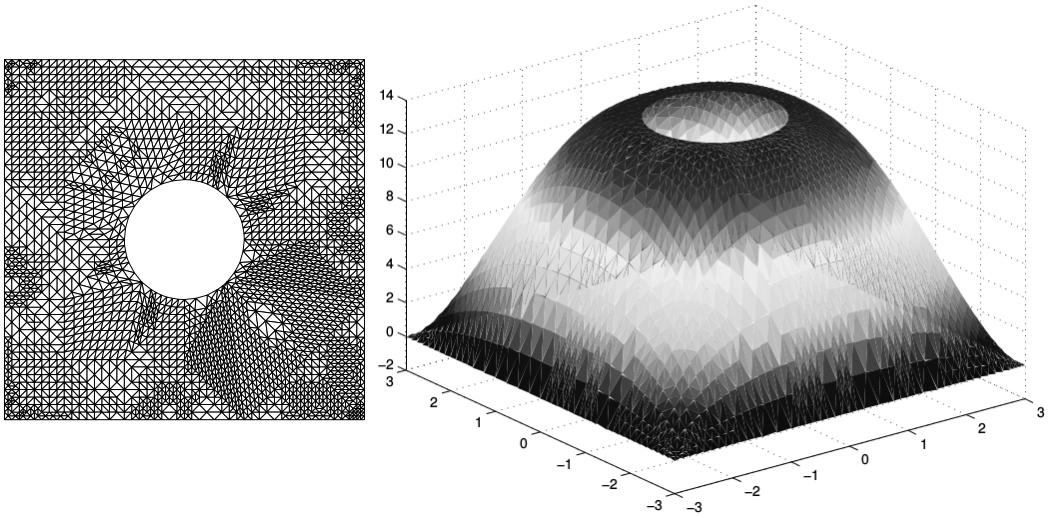

Figure 6.74.: Triangulation (left) and solution after 10 levels of adaptive refinement (right) for NCFEM for the experiment from Subsection 6.3.2.

The exact solution u is unknown and is approximated as described on Page 110. An approximation with NCFEM is depicted in Figure 6.74 right. Since the circle can only be approximated by polygons, the novel boundary nodes, that form after a refinement are projected onto a smaller circle. The approximation of the circle becomes smoother after each refinement. The output of the adaptive Algorithm 2 is displayed in Figure 6.74 left. Figure 6.75 depicts the convergence of the total error and the error estimator Est for uniform and adaptive mesh-refinement. All presented terms converge with a convergence rate of -0.5 with respect to the number of degrees of freedom. This leads to efficiency indices in Figure 6.76 between 1.9 for the non-conforming FEM and 6 for the conforming FEM, both on adaptive and uniform meshes. The convergence of the error of the primal variables in the energy norm and the corresponding estimator (with the modification for NCFEM) in Figure 6.77 shows a convergence rate of -0.5 with respect to the number of degrees of freedom and leads to efficiency indices of 2.4 for NCFEM and 7 for CFEM on uniform and adaptive meshes. Figure 6.79 depicts the different error and estimator components for the non-conforming FEM on uniform meshes. All terms except the error term $gj(v) - \int_\Omega \lambda \nabla v \, \mathrm{d}x$ converge with a convergence rate of -0.5 with respect to the number of degrees of freedom. The term $j(v) - g \int_\Omega \lambda \nabla v \, \mathrm{d}x$ has a lower convergence rate. Similar results are observed for CFEM and are undisplayed. If this is not a pre-asymptotic effect, a lower convergence rate should become visible in

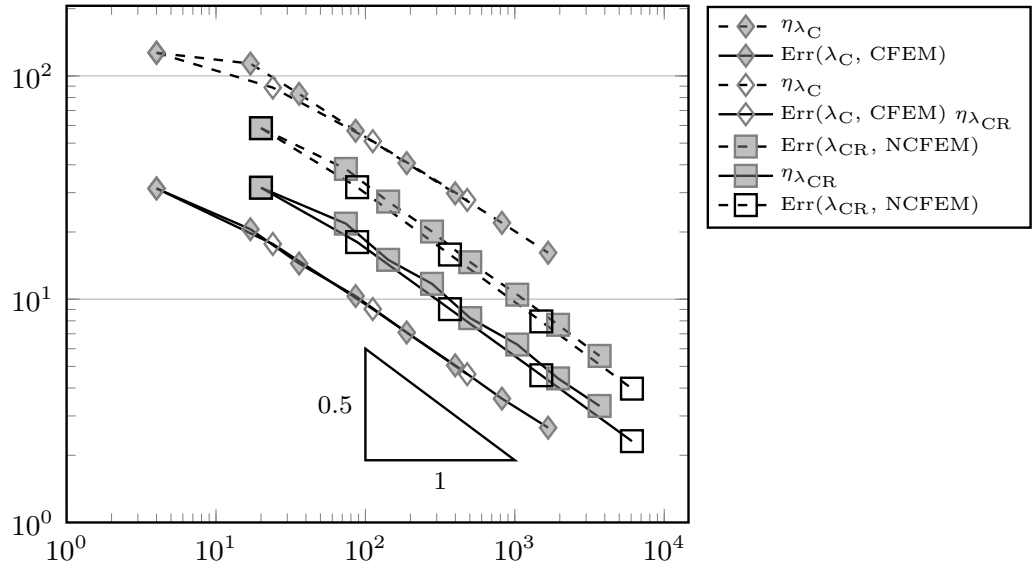

Figure 6.75.: Total error and error estimators for CFEM and NCFEM for the experiment from Subsection 6.3.2 for adaptive (grey) and uniform (white) mesh-refinement.

the total error after some time, but since the error is dominated by the term $\|\!|u-v|\!\|$ it is not visible in Figure 6.75 for the number of refinements performed in the experiment. As in the previous example, the estimator is dominated by the residual term and the lower values of this term for the non-conforming finite element method in Figure 6.80 explain the lower efficiency indices for this method. Figure 6.81 compares the convergence of the total error and the estimator for NCFEM with the original discrete Lagrange multiplier and the modification of Subsection 5.4.4. The Figure shows, that there is no real visible difference and hence there is numerical evidence that both Lagrange multipliers are efficient.

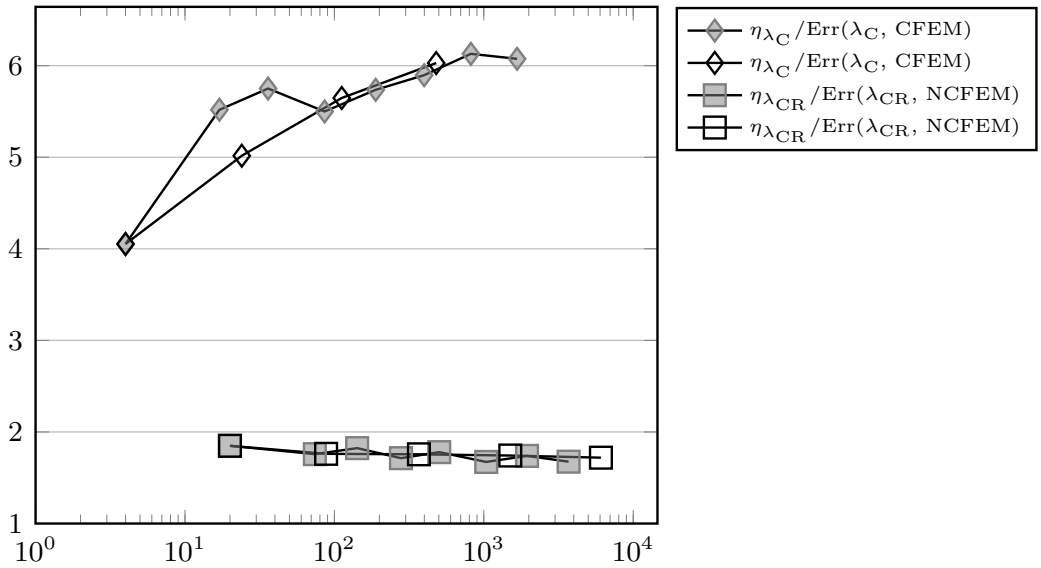

Figure 6.76.: Efficiency indices for the total error for CFEM and NCFEM for the experiment from Subsection 6.3.2 for adaptive (grey) and uniform (white) mesh-refinement.

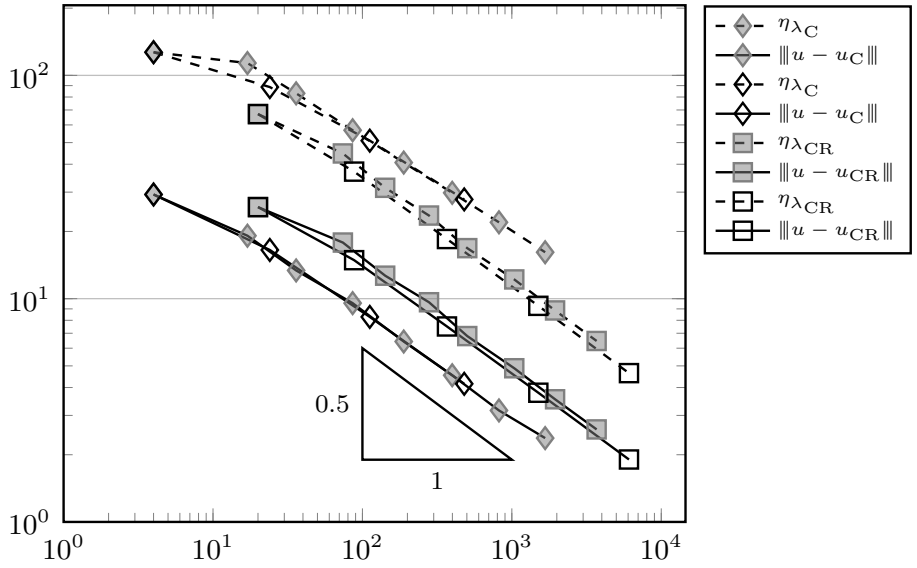

Figure 6.77.: Error of the primal variable in the energy norm and error estimators for CFEM and NCFEM for the experiment from Subsection 6.3.2 for adaptive (grey) and uniform (white) mesh-refinement.

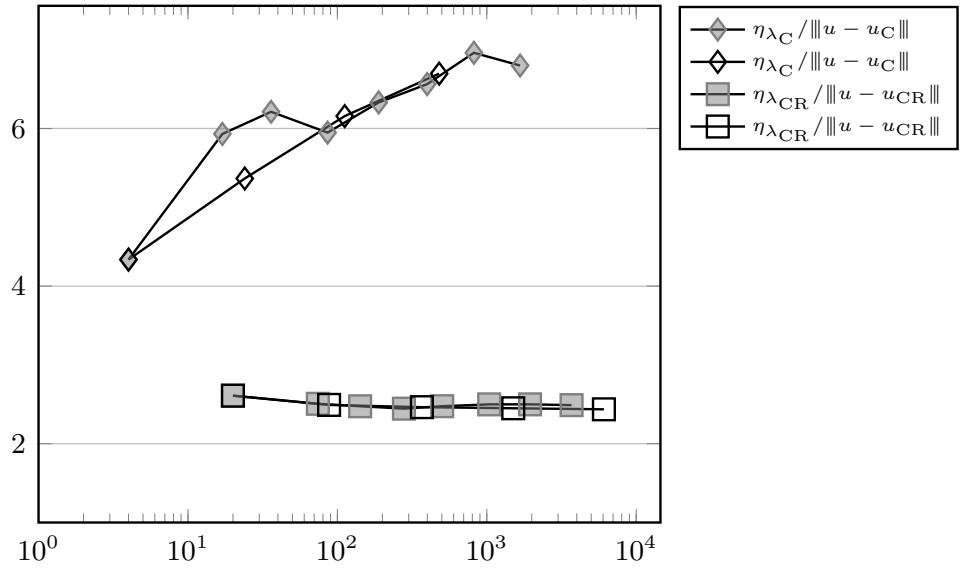

Figure 6.78.: Efficiency indices for the error of the primal variable in the energy norm for CFEM and NCFEM for the experiment from Subsection 6.3.2 for adaptive (grey) and uniform (white) mesh-refinement.

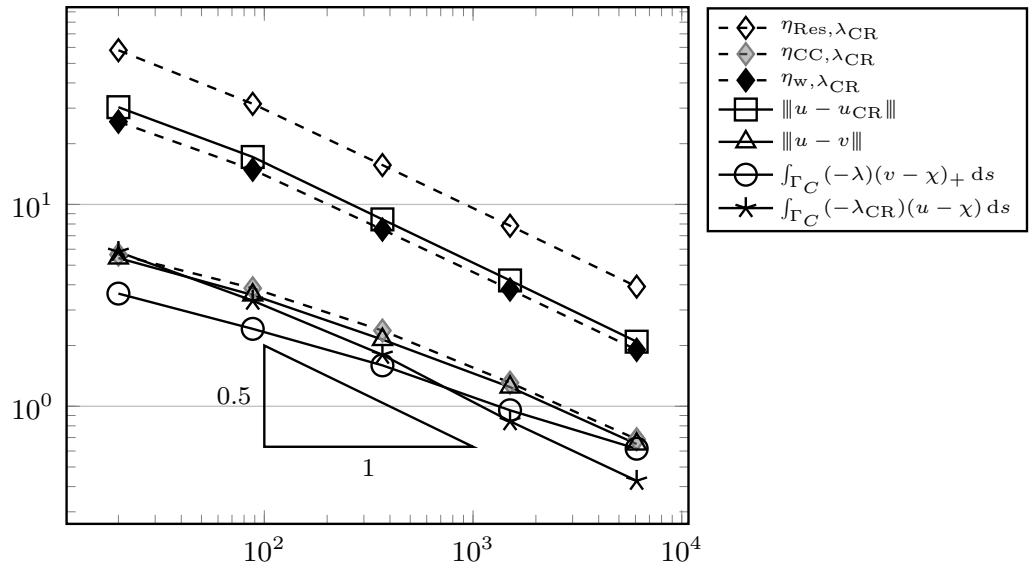

Figure 6.79.: Comparison of different error and estimator components for NCFEM for the experiment from Subsection 6.3.2 for uniform mesh-refinement.

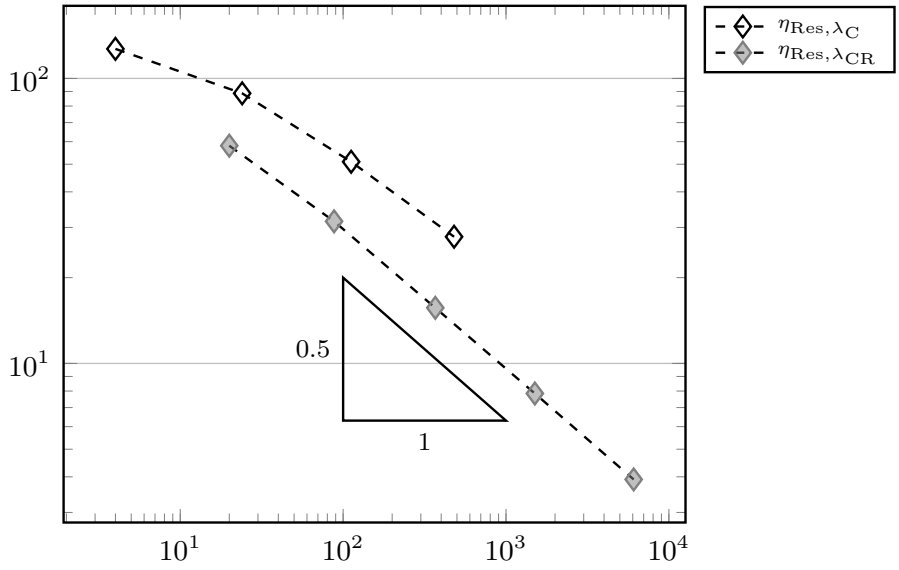

Figure 6.80.: Residual component of the estimator for CFEM and NCFEM for the experiment from Subsection 6.3.2 for uniform mesh-refinement.

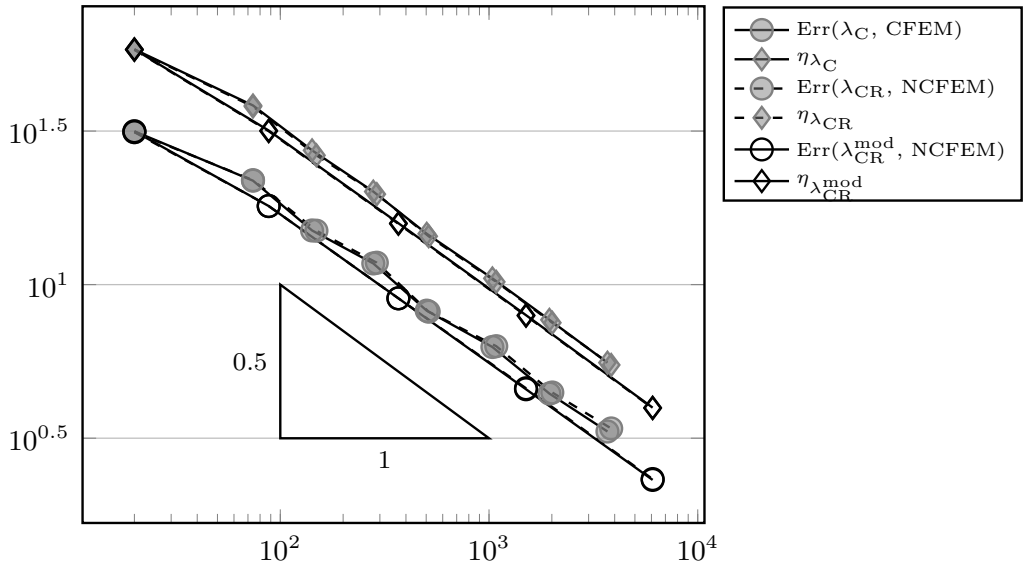

Figure 6.81.: Total error and estimator for CFEM, NCFEM, and NCFEM with modified Lagrange multiplier for the experiment from Subsection 6.3.2 for adaptive mesh-refinement.

6.3.3. Square

The following example concerns the square domain $\Omega := (0,2) \times (0,2)$ and the right-hand side $f = 10$. The yield stress is chosen as $g = 2$. A similar experiment can be found in Carstensen et al. (2015b).

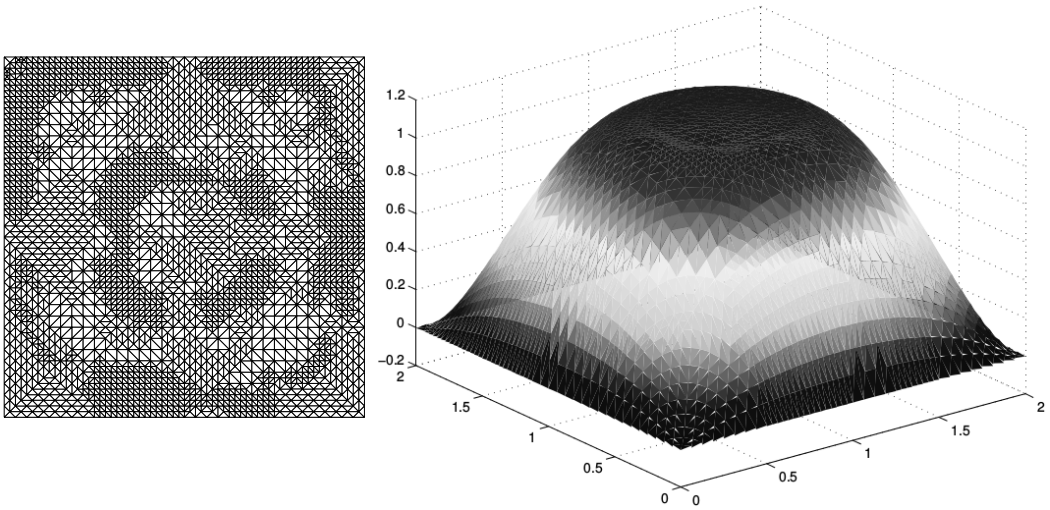

Figure 6.82.: Triangulation (left) and solution after 11 levels of adaptive refinement (right) for NCFEM for the experiment from Subsection 6.3.3.

The exact solution is unknown and is approximated as described on Page 110. The approximated solution is depicted in Figure 6.82 right. On the left, the output of Algorithm 2 for NCFEM after 11 levels of refinement is displayed. Figure 6.83 presents the convergence of the total error and the estimator on uniform and adaptive meshes for the conforming and non-conforming finite element method. All terms converge with a convergence rate of -0.5 with respect to the number of degrees of freedom. This leads to the efficiency indices between 1.9 for NCFEM and 7 for CFEM on uniform and adaptive meshes in Figure 6.84. The convergence of the estimator (with the modifications for NCFEM) and the error of the primal variable in the energy norm with respect to the number of degrees of freedom in Figure 6.85 shows the same convergence behaviour and exhibits a convergence rate of -0.5 with respect to the number of degrees of freedom. The resulting efficiency indices lie between 4 for NCFEM and 10 for CFEM on adaptive and uniform meshes. The error and estimator terms for NCFEM in Figure 6.87 of the non-conforming method on uniform meshes, reveal the same convergence rate of -0.5 with respect to the number of degrees of freedom in all components, and display, that the residual term $\eta_{\mathrm{Res},\mu}$ dominates the error. Similar results hold true for CFEM and are undisplayed. This and the results presented in Figure 6.88, where this residual term is displayed for the two methods on uniform meshes, explain the lower efficiency indices for NCFEM. As in the previous two experiments, Figure 6.89 ascertains, that

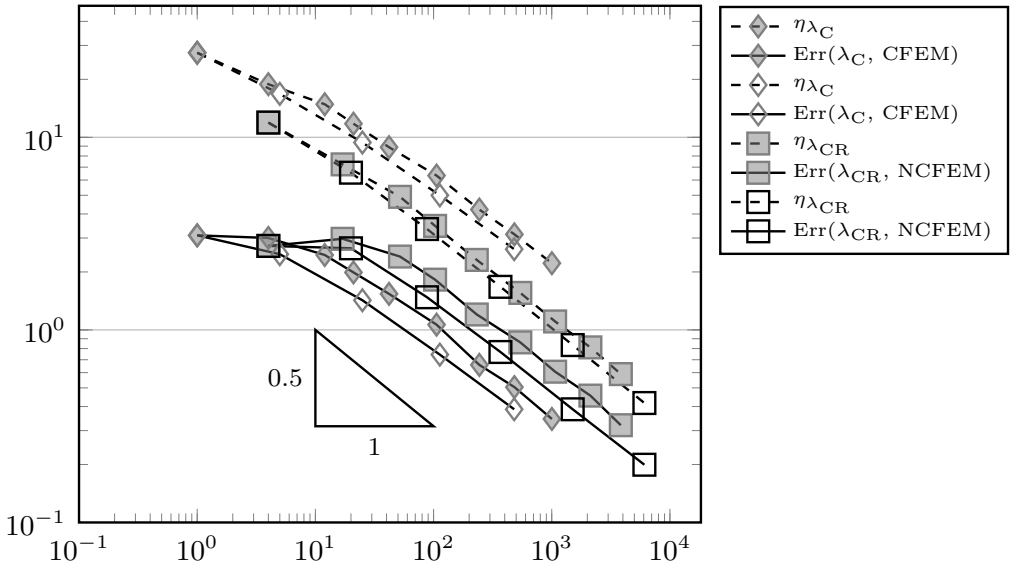

Figure 6.83.: Total error and error estimators for CFEM and NCFEM for the experiment from Subsection 6.3.3 for adaptive (grey) and uniform (white) mesh-refinement.

the discrete Lagrange multiplier and its modification from Subsection 5.4.4 are both efficient and the total error and estimator Est converge with the same convergence rate of -0.5 with respect to the number of degrees of freedom.

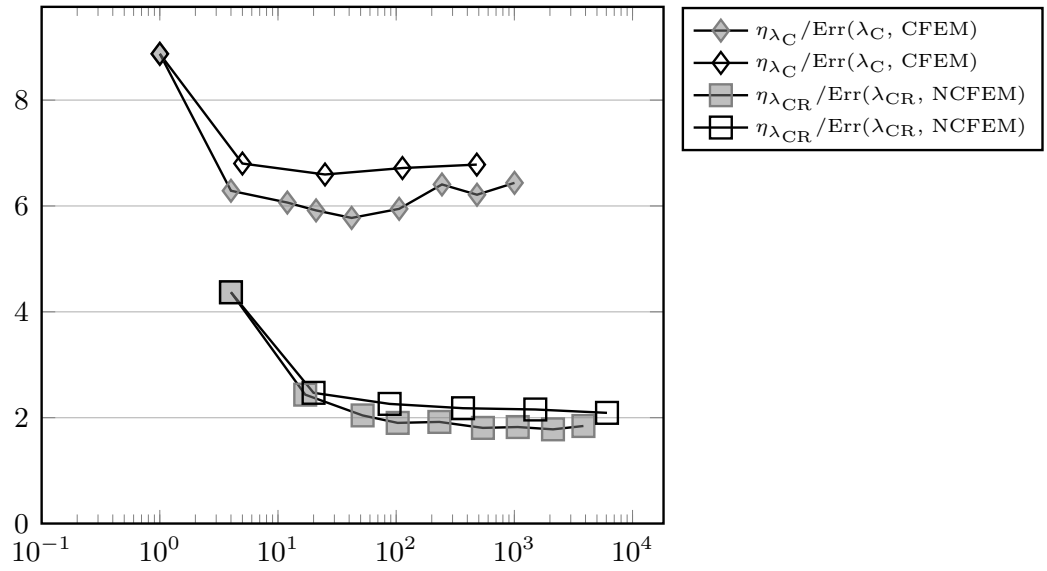

Figure 6.84.: Efficiency indices for the total error for CFEM and NCFEM for the experiment from Subsection 6.3.3 for adaptive (grey) and uniform (white) mesh-refinement.

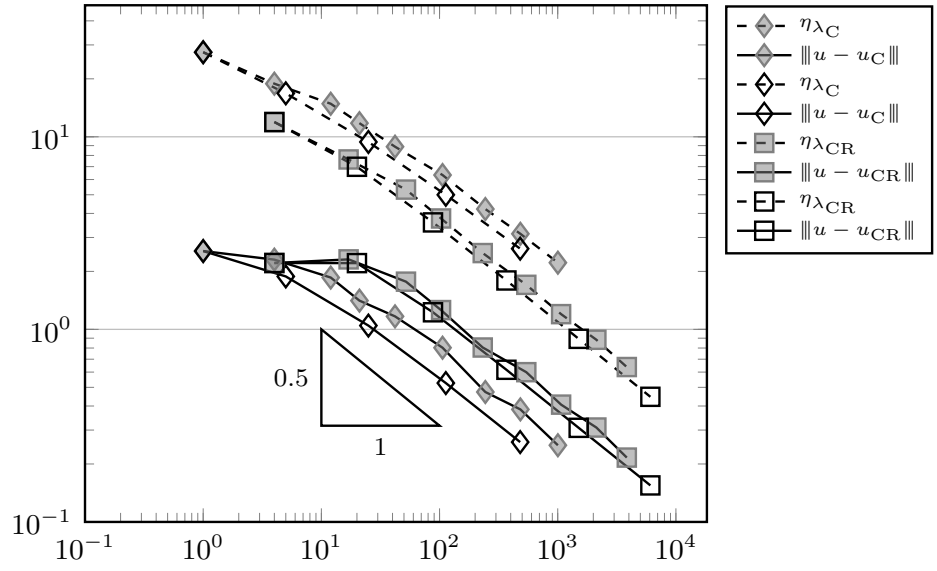

Figure 6.85.: Error of the primal variable in the energy norm and error estimators for CFEM and NCFEM for the experiment from Subsection 6.3.3 for adaptive (grey) and uniform (white) mesh-refinement.

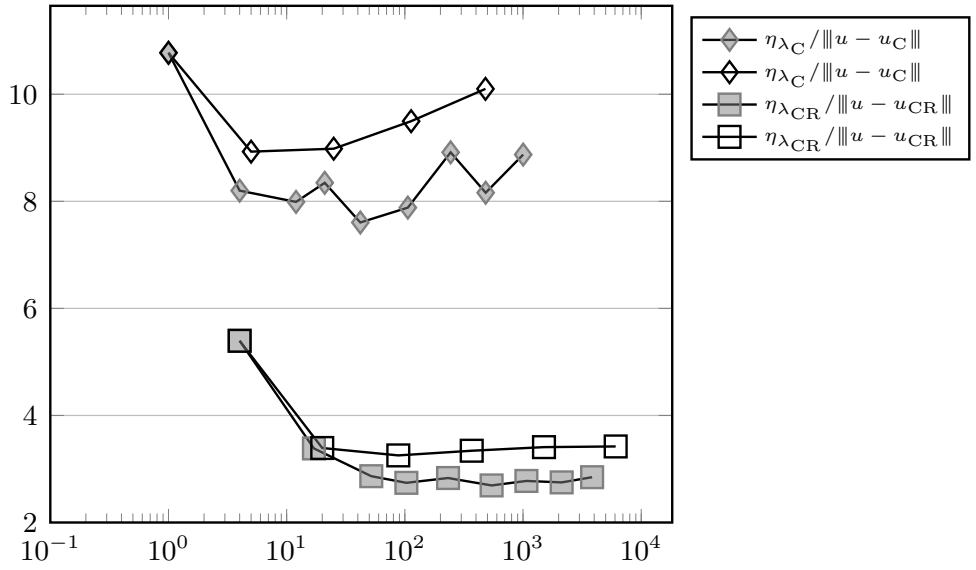

Figure 6.86.: Efficiency indices for the error of the primal variable in the energy norm for CFEM and NCFEM for the experiment from Subsection 6.3.3 for adaptive (grey) and uniform (white) mesh-refinement.

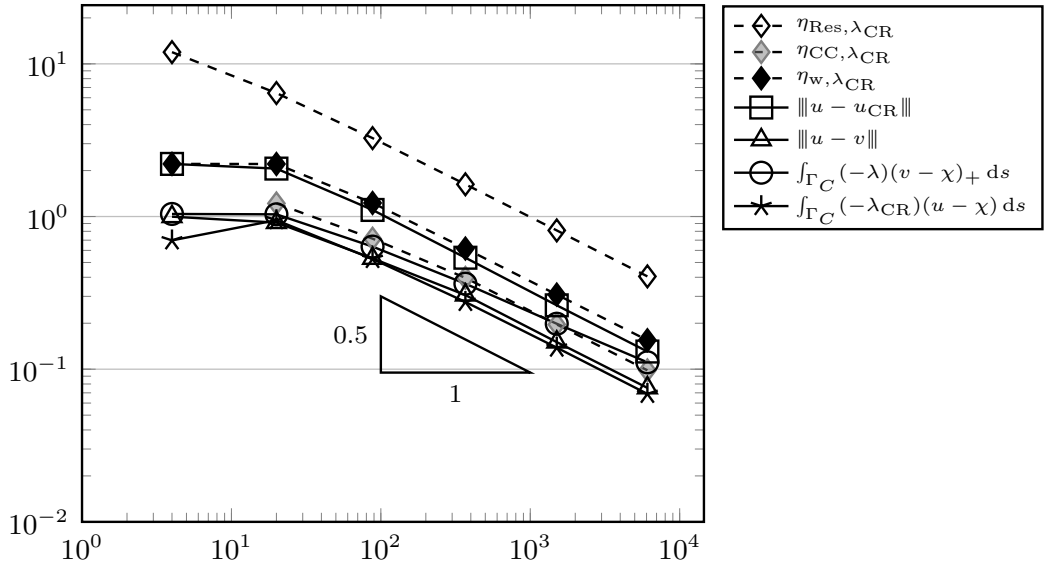

Figure 6.87.: Comparison of different error and estimator components for NCFEM for the experiment from Subsection 6.3.3 for uniform mesh-refinement.

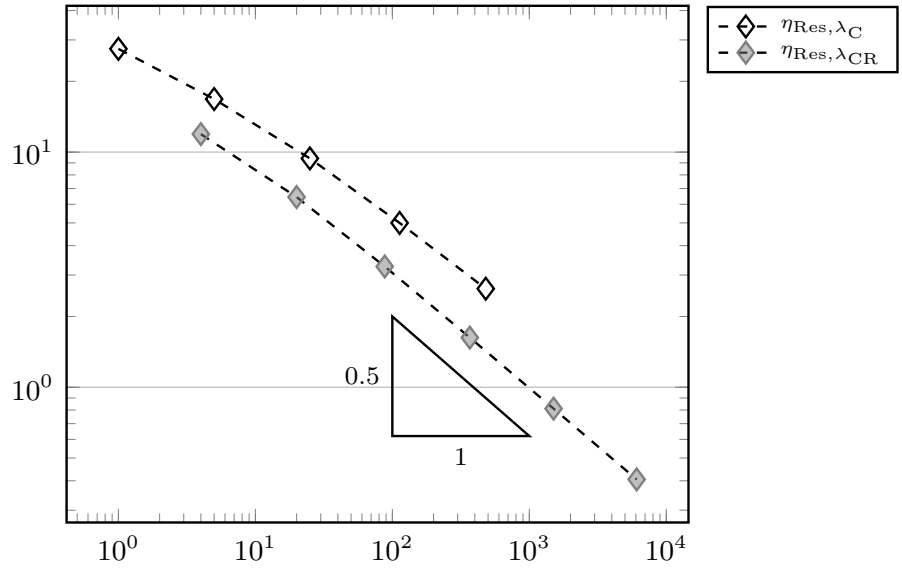

Figure 6.88.: Residual component of the estimator for CFEM and NCFEM for the experiment from Subsection 6.3.3 for uniform mesh-refinement.

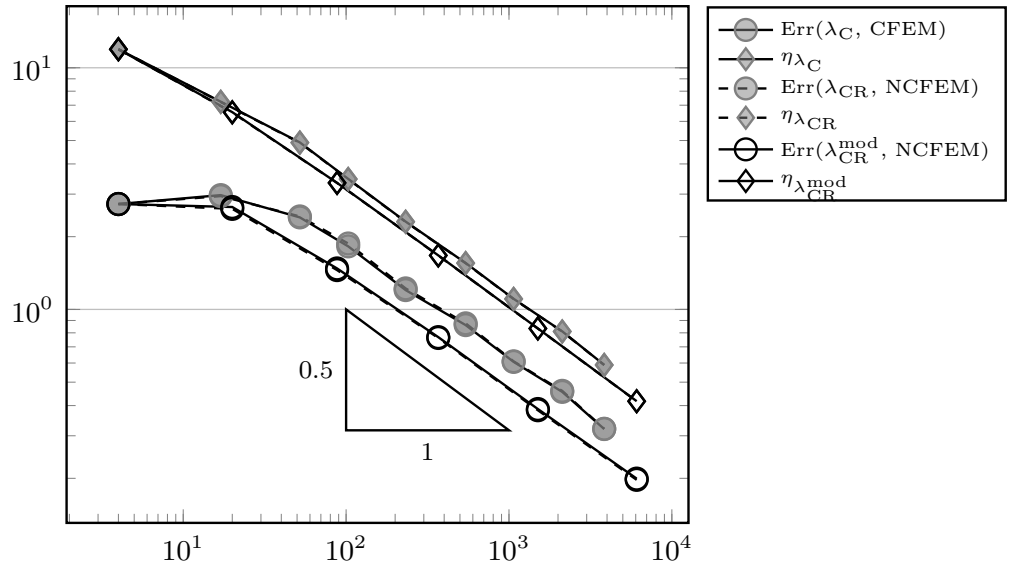

Figure 6.89.: Total error and estimator for CFEM, NCFEM, and NCFEM with modified Lagrangemultiplier for the experiment from Subsection 6.3.3.

6.3.4. Lshape

This example concerns the L-shaped domain $\Omega := (-2,2)\times(-2,2)\setminus((0,2)\times(0,-2))$ and the right-hand side $f = 10$. The yield stress is chosen as $g = 2$. A similar experiment can be found in Carstensen et al. (2015b).

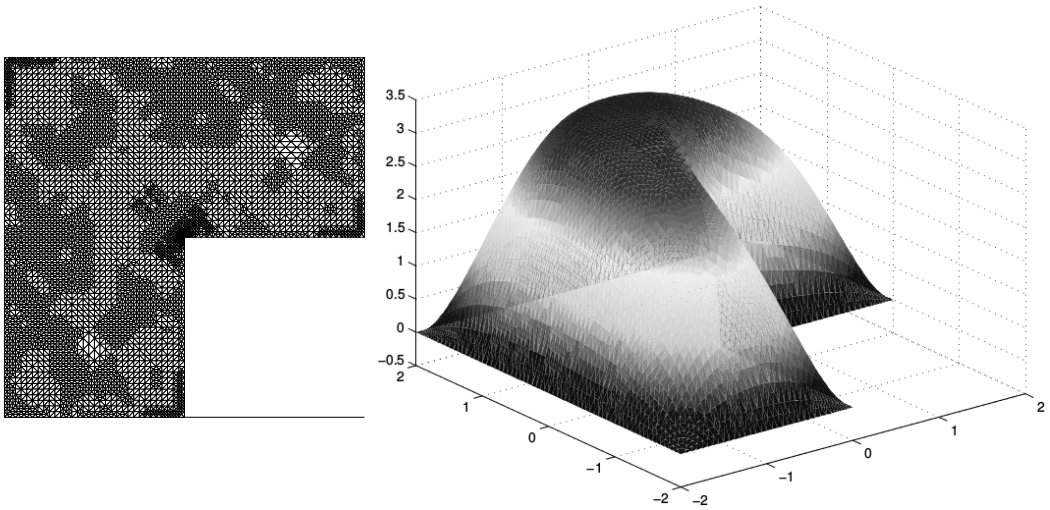

Figure 6.90.: Triangulation (left) and solution after 13 levels of adaptive refinement (right) for NCFEM for the experiment from Subsection 6.3.4.

The exact solution u is unknown and is approximated as described on Page 110. The domain exhibits a typical corner singularity because of the re-entrant corner. Figure 6.90 displays the solution on the right and the output of Algorithm 2 after 13 levels of refinement (for NCFEM) on the left. The re-entrant corner leads to a reduced convergence rate for uniform mesh-refinement and the recovered optimal rate for adaptive mesh-refinement. This behaviour can be seen in Figure 6.91 which displays the estimator Est and the total error Err on uniform and adaptive meshes for CFEM and NCFEM and in Figure 6.93, which depicts the adapted estimator and the error of the primal variable in the energy norm for CFEM and NCFEM on uniform and adaptive meshes. On uniform meshes the convergence rate is -0.4 with respect to the number of degrees of freedom, and it is -0.5 on adaptive meshes. This leads to the efficiency indices with respect to the total error in Figure 6.92 which lie between 1.9 for NCFEM and 6 for CFEM on adaptive and uniform meshes. The efficiency indices with respect to the error of the primal variable in the energy norm are depicted in Figure 6.94 and lie between 2.2 for NCFEM and 7 for CFEM on adaptive and uniform meshes. Figure 6.95 depicts the error and estimator components for NCFEM on uniform meshes and displays a convergence rate of -0.4 with respect to the number of degrees of freedom. The dominating estimator term is $\eta_{\mathrm{Res},\lambda_{\mathrm{CR}}}$. Similar results are observed for CFEM and are undisplayed. Figure 6.96 shows the convergence of this estimator term for both methods on uniform meshes.

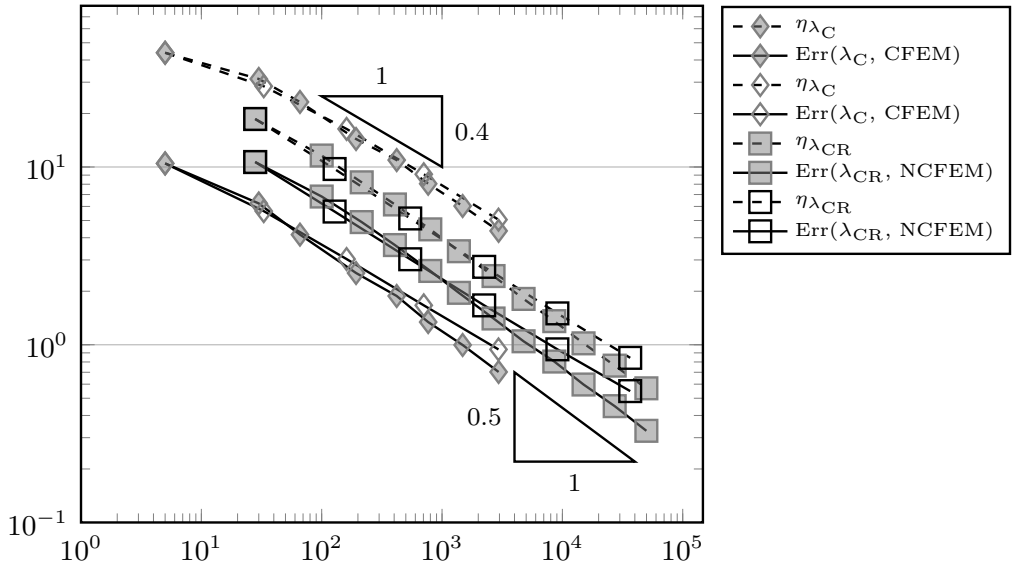

Figure 6.91.: Total error and error estimators for CFEM and NCFEM for the experiment from Subsection 6.3.4 for adaptive (grey) and uniform (white) mesh-refinement.

The value for $\eta_{\mathrm{Res},\lambda_{\mathrm{CR}}}$ is smaller than $\eta_{\mathrm{Res},\lambda_{\mathrm{C}}}$ and hence explains the lower efficiency indices for the non-conforming method. The results displayed in Figure 6.97 reveal, that both non-conforming Lagrange multipliers, the one that results from the discrete problem and the modified one (cf. Subsection 5.4.4) lead to the same values and hence there is numerical evidence that both Lagrange multipliers are efficient although there is no theoretical result.

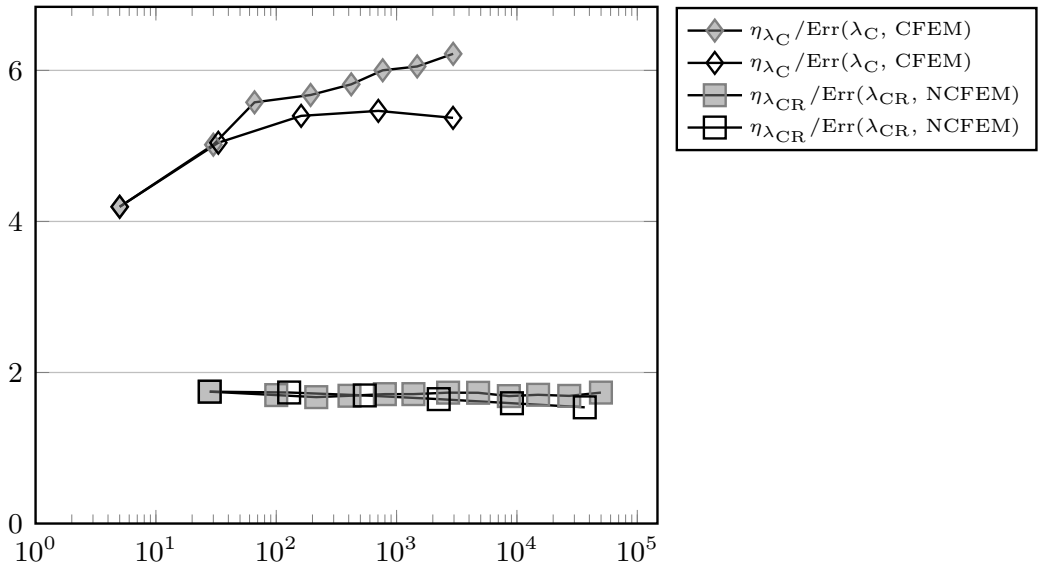

Figure 6.92.: Efficiency indices for the total error for CFEM and NCFEM for the experiment from Subsection 6.3.4 for adaptive (grey) and uniform (white) mesh-refinement.

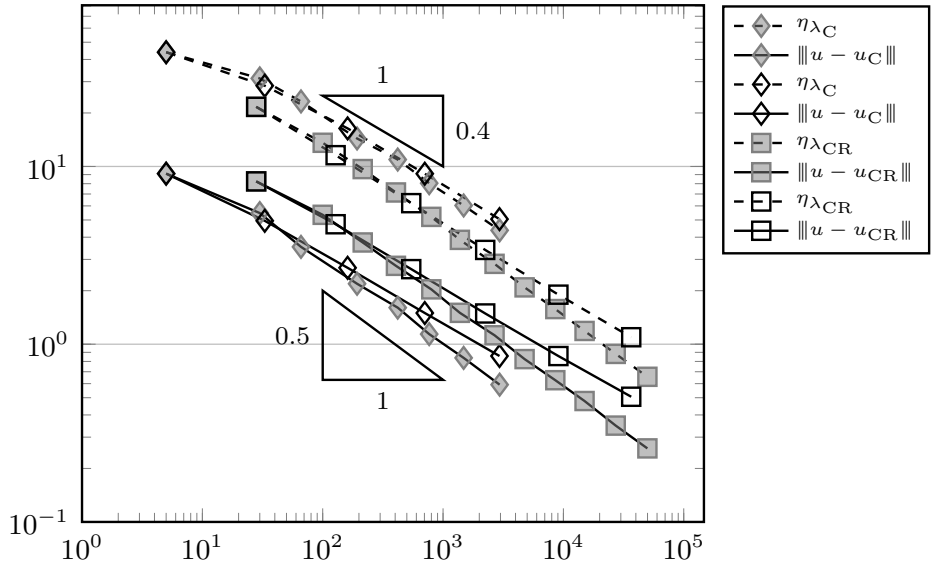

Figure 6.93.: Error of the primal variable in the energy norm and error estimators for CFEM and NCFEM for the experiment from Subsection 6.3.4 for adaptive (grey) and uniform (white) mesh-refinement.

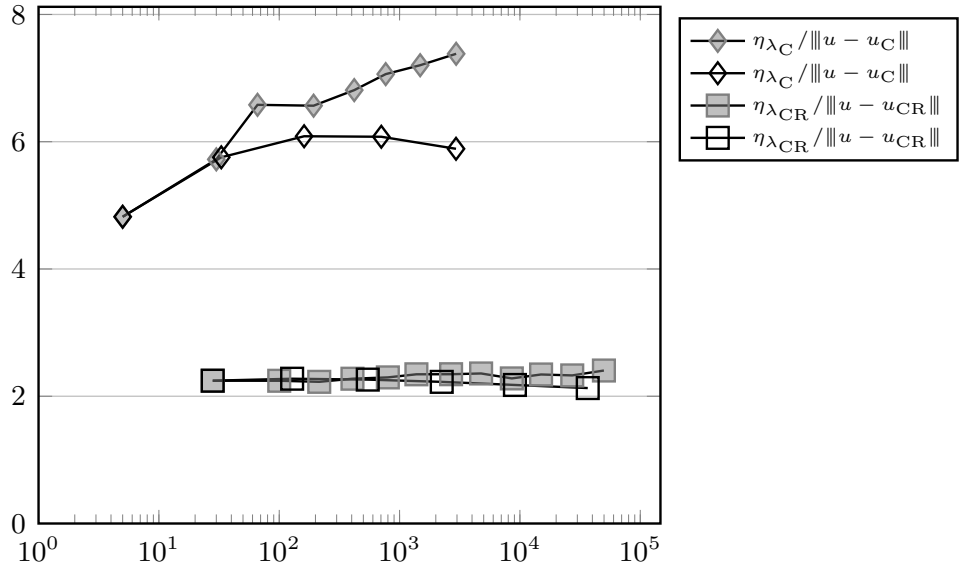

Figure 6.94.: Efficiency indices for the error of the primal variable in the energy norm for CFEM and NCFEM for the experiment from Subsection 6.3.4 for adaptive (grey) and uniform (white) mesh-refinement.

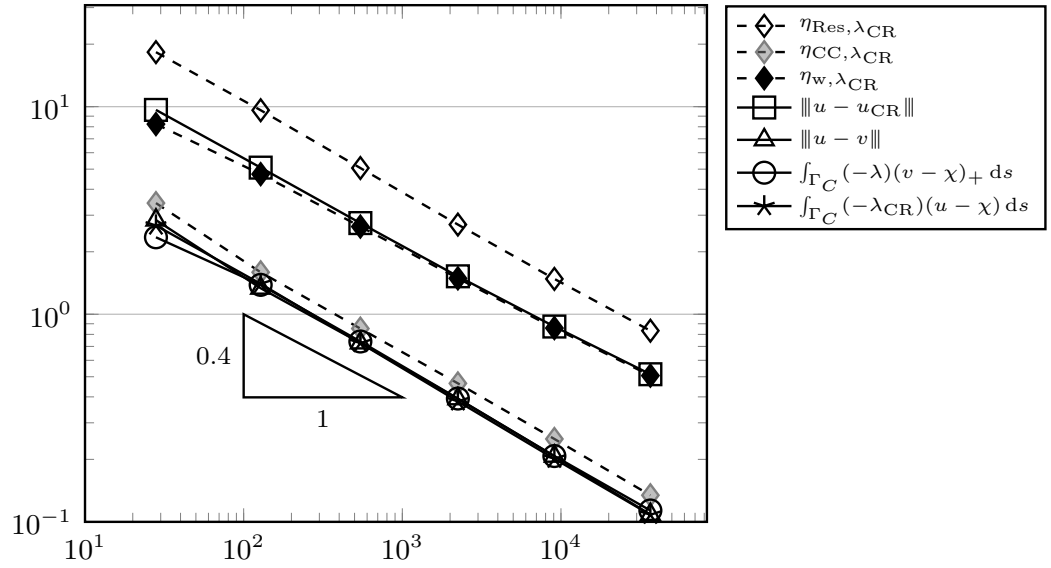

Figure 6.95.: Comparison of different error and estimator components for NCFEM for the experiment from Subsection 6.3.4 for uniform mesh-refinement.

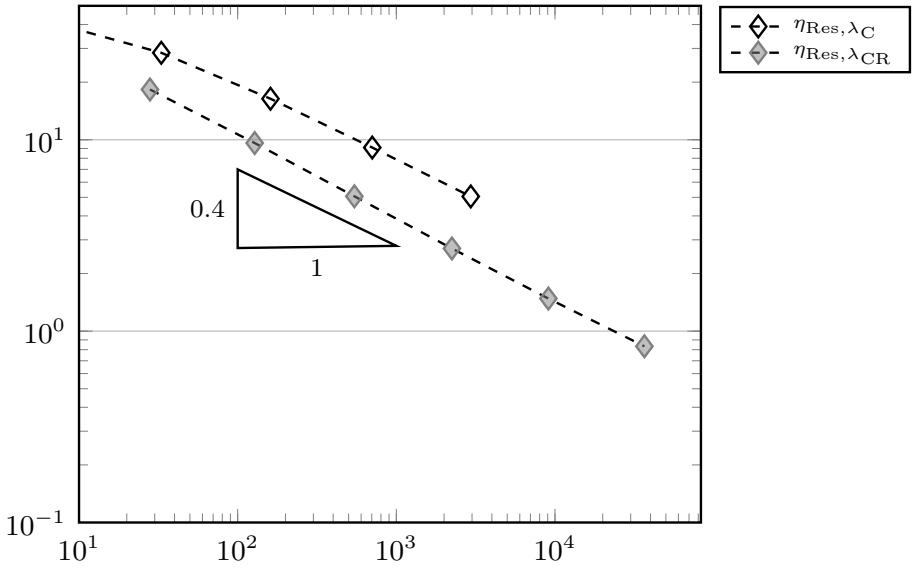

Figure 6.96.: Residual component of the estimator for CFEM and NCFEM for the experiment from Subsection 6.3.4 for uniform mesh-refinement.

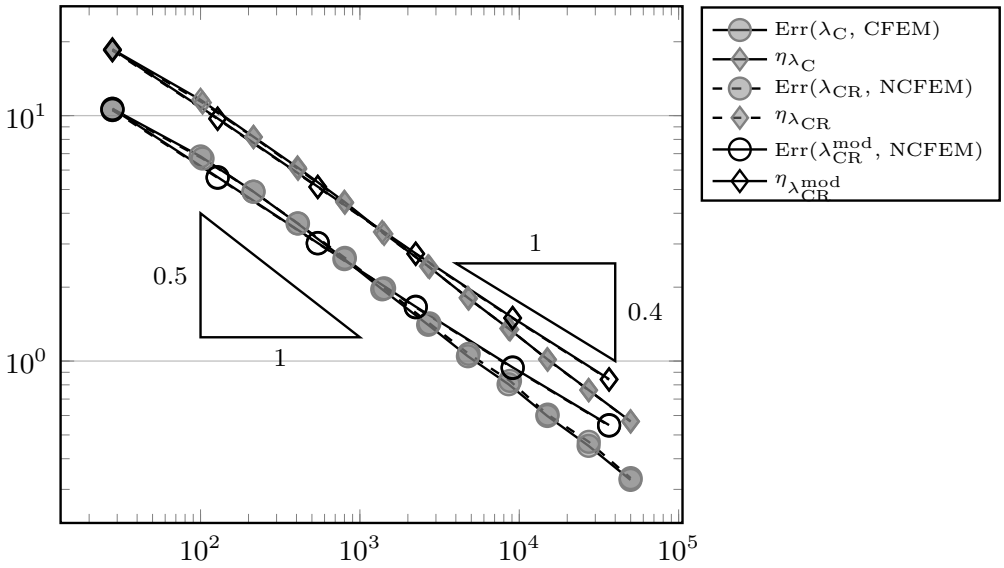

Figure 6.97.: Total error and estimator for CFEM, NCFEM, and NCFEM with modified Lagrange multiplier for the experiment from Subsection 6.3.4 for adaptive mesh-refinement.

6.4. Conclusion

The numerical experiments confirm the results of the realizations of Theorem A for the obstacle problem, Signorini's problem, and the Bingham flow problem in Theorems 3.18, 4.14, and 5.12. For the obstacle problem and Signorini's problem, the numerical experiments lead to an overestimation of the total error by a maximal factor of $5\sqrt{60}$ for CFEM and NCFEM and a maximal factor of $3\sqrt{60}$ for MFEM. For the Bingham flow problem, the maximal overestimation factor is $7\sqrt{33}$ for CFEM and $2\sqrt{33}$ for NCFEM. All experiments show, that the residual term dominates the estimator. For the conforming and non-conforming FEM, this term has to be approximated and estimated itself. Improvements of the overestimation factors are expected if more efficient residual based error estimators, which are for example collected in Carstensen and Merdon (2010) for the lowest order conforming method and in Carstensen and Merdon (2013a) for the Crouzeix-Raviart FEM, are employed. The numerical experiments show, that the realizations of Theorem B in Chapters 3–5 exploit the existence of an L^2 representation of the exact Lagrange multiplier. In the case of Experiment 6.1.3, the exact Lagrange multiplier has no such L^2 representation and the results of Corollaries 3.30 and 3.41 are not valid, which can also be seen numerically in Figure 6.23. The numerical experiments reveal, that the mixed Raviart-Thomas finite element method avoids such behaviour. The numerical examples (cf. the example in Subsection 6.1.5) show that the realization of Theorem C in Chapters 3–4 are also valid in more general settings and the assumption $\chi \in P_1(\Omega)$ resp $\chi \in P_1(\Gamma_C)$ might be avoidable.

Bibliography

M. Ainsworth. A posteriori error estimation for lowest order Raviart-Thomas mixed finite elements. *SIAM J. Sci. Comput*, 30(1):189–204, 2007.

M. Ainsworth and J. T. Oden. *A posteriori error estimation in finite element analysis*. Pure and Applied Mathematics (New York). Wiley-Interscience [John Wiley & Sons], New York, 2000.

C. Baiocchi, F. Gastaldi, and F. Tomarelli. Some existence results on noncoercive variational inequalities. *Ann. Scuola Norm. Sup. Pisa Cl. Sci. (4)*, 13(4):617–659, 1986.

L. Banz and A. Schröder. Biorthogonal basis functions in *hp*-adaptive FEM for elliptic obstacle problems. *Comput. Math. Appl.*, 70(8):1721–1742, 2015.

S. Bartels and C. Carstensen. Averaging techniques yield reliable a posteriori finite element error control for obstacle problems. *Numer. Math*, 99(2):225–249, 2004.

S. Bartels, C. Carstensen, and G. Dolzmann. Inhomogeneous Dirichlet conditions in a priori and a posteriori finite element error analysis. *Numer. Math.*, 99(1): 1–24, 2004.

V. Bostan and W. Han. A posteriori error analysis for finite element solutions of a frictional contact problem. *Comput. Methods Appl. Mech. Engrg.*, 195(9-12): 1252–1274, 2006.

V. Bostan, W. Han, and B. D. Reddy. A posteriori error estimation and adaptive solution of elliptic variational inequalities of the second kind. *Appl. Numer. Math.*, 52(1):13–38, 2005.

D. Braess. A posteriori error estimators for obstacle problems—another look. *Numer. Math.*, 101(3):415–421, 2005.

D. Braess. *Finite elements: Theory, fast solvers, and applications in solid mechanics*. Cambridge University Press, 2007.

D. Braess. An a posteriori error estimate and a comparison theorem for the nonconforming P_1 element. *Calcolo*, 46(2):149–155, 2009.

D. Braess, C. Carstensen, and R. Hoppe. Convergence analysis of a conforming adaptive finite element method for an obstacle problem. *Numer. Math.*, 107(3): 455–471, 2007.

D. Braess, R. Hoppe, and J. Schöberl. A posteriori estimators for obstacle problems by the hypercircle method. *Computing and Visualization in Science*, 11(4-6): 351–362, 2008.

S. Brenner and L. Scott. *The mathematical theory of finite element methods*. Springer, 2008.

H. Brézis. Monotonicity methods in Hilbert spaces and some applications to nonlinear partial differential equations. In *Contributions to nonlinear functional analysis (Proc. Sympos., Math. Res. Center, Univ. Wisconsin, Madison, Wis., 1971)*, pages 101–156. Academic Press, New York, 1971.

H. Brézis. Problèmes unilatéraux. *J. Math. Pures Appl. (9)*, 51:1–168, 1972.

F. Brezzi, W. W. Hager, and P.-A. Raviart. Error estimates for the finite element solution of variational inequalities. *Numer. Math.*, 28(4):431–443, 1977.

F. Brezzi, W. Hager, and P. Raviart. Error estimates for the finite element solution of variational inequalities, part ii. Mixed methods. *Numer. Math.*, 31:1–16, 1978.

M. Bürg and A. Schröder. A posteriori error control of *hp*-finite elements for variational inequalities of the first and second kind. *Comput. Math. Appl.*, 70(12): 2783–2802, 2015.

C. Carstensen. Quasi-interpolation and a posteriori error analysis in finite element methods. *M2AN*, 33(6):1187–1202, 1999.

C. Carstensen and D. Gallistl. Guaranteed lower eigenvalue bounds for the biharmonic equation. *Numer. Math.*, 126:33–51, 2014.

C. Carstensen and K. Köhler. Efficient discrete Lagrange multipliers in three first-order finite element discretizations for the a posteriori error control in an obstacle problem. 2016a. submitted to SIAM J. Numer. Anal.

C. Carstensen and K. Köhler. Non-conforming FEM for the obstacle problem. *IMA J. Numer. Anal.*, 2016b. published online.

C. Carstensen and C. Merdon. Estimator competition for Poisson problems. *J. Comput. Math.*, 28(3):309–330, 2010.

C. Carstensen and C. Merdon. Computational survey on a posteriori error estimators for nonconforming finite element methods for the Poisson problem. *J. Comput. Appl. Math.*, 249:74–94, 2013a.

C. Carstensen and C. Merdon. A posteriori error estimator competition for conforming obstacle problems. *Numer. Methods Partial Differential Equations*, 29 (2):667–692, 2013b.

C. Carstensen and R. Verfürth. Edge residuals dominate a posteriori error estimates for low order finite element methods. *SIAM J. Numer. Anal.*, 36(5):1571–1587, 1999.

C. Carstensen, S. Bartels, and R. Klose. An experimental survey of a posteriori Courant finite element error control for the Poisson equation. *Advances in Computational Mathematics*, 15(1-4):79–106, 2001.

C. Carstensen, R. Klose, and A. Orlando. Reliable and efficient equilibrated a posteriori finite element error control in elastoplasticity and elastoviscoplasticity with hardening. *Comput. Methods Appl. Mech. Engrg.*, 195(19-22):2574–2598, 2006.

C. Carstensen, M. Eigel, R. Hoppe, and C. Löbhard. A review of unified a posteriori finite element error control. *Numer. Math. Theory Methods Appl.*, 5(4):509–558, 2012a.

C. Carstensen, J. Gedicke, and D. Rim. Explicit error estimates for Courant, Crouzeix-Raviart, and Raviart-Thomas finite element methods. *J. Comput. Math.*, 30(4):337–353, 2012b.

C. Carstensen, D. Peterseim, and M. Schedensack. Comparison results of finite element methods for the Poisson model problem. *SIAM J. Numer. Anal.*, 50(6): 2803–2823, 2012c.

C. Carstensen, D. Gallistl, and M. Schedensack. Adaptive nonconforming Crouzeix-Raviart FEM for eigenvalue problems. *Math. Comp.*, 84:1061?1087, 2015a.

C. Carstensen, B. Reddy, and M. Schedensack. A natural nonconforming FEM for the Bingham flow problem is quasi-optimal. *Numer. Math.*, pages 37–66, 2015b.

C. Carstensen et al. Afem software package and documentation. Humboldt-Universität zu Berlin, unpublished, 2009.

R. Courant. Variational methods for the solution of problems of equilibrium and vibrations. *Bull. Amer. Math. Soc.*, 49:1–23, 1943.

M. Crouzeix and P.-A. Raviart. Conforming and nonconforming finite element methods for solving the stationary Stokes equations. I. *Rev. Française Automat. Informat. Recherche Opérationnelle Sér. Rouge*, 7(R-3):33–75, 1973.

A. Dond, T. Gudi, and N. Nataraj. A nonconforming finite element approximation for optimal control of an obstacle problem. *in preparation*, 2016.

L. C. Evans. *Partial differential equations*, volume 19 of *Graduate Studies in Mathematics*. American Mathematical Society, Providence, RI, second edition, 2010.

R. Falk. Error estimates for the approximation of a class of variational inequalities. *Mathematics of Computation*, 28(128):963–971, 1974.

R. S. Falk and B. Mercier. Error estimates for elasto-plastic problems. *RAIRO Anal. Numér.*, 11(2):135–144, 219, 1977.

A. Gaevskaya, M. Hintermüller, R. H. W. Hoppe, and C. Löbhard. Adaptive finite elements for optimally controlled elliptic variational inequalities of obstacle type. In *Optimization with PDE constraints*, volume 101 of *Lect. Notes Comput. Sci. Eng.*, pages 95–150. Springer, Cham, 2014.

G. N. Gatica and M. Maischak. A posteriori error estimates for the mixed finite element method with Lagrange multipliers. *Numer. Methods Partial Differential Equations*, 21(3):421–450, 2005.

V. Girault and P.-A. Raviart. Finite element methods for Navier-Stokes equations. 5:x+374, 1986. Theory and algorithms.

R. Glowinski. *Numerical methods for nonlinear variational problems*. Scientific Computation. Springer-Verlag, Berlin, 2008. Reprint of the 1984 original.

R. Glowinski, J.-L. Lions, and R. Trémolières. *Numerical analysis of variational inequalities*, volume 8 of *Studies in Mathematics and its Applications*. North-Holland Publishing Co., Amsterdam-New York, 1981. Translated from the French.

C. Gräser and R. Kornhuber. Multigrid methods for obstacle problems. *J. Comput. Math.*, 27(1):1–44, 2009.

P. Hild and S. Nicaise. A posteriori error estimations of residual type for Signorini's problem. *Numer. Math.*, 101(3):523–549, 2005.

D. Kinderlehrer and G. Stampacchia. *An introduction to variational inequalities and their applications*. Harcourt Brace Jovanovich, 1980.

R. Laugesen and B. Siudeja. Minimizing Neumann fundamental tones of triangles: An optimal Poincaré inequality. *J. Differential Equations*, 249(1):118–135, 2010.

J.-L. Lions and G. Stampacchia. Variational inequalities. *Comm. Pure Appl. Math.*, 20:493–519, 1967.

L. Marini. An inexpensive method for the evaluation of the solution of the lowest order Raviart-Thomas mixed method. *SIAM J. Numer. Anal.*, 22, 1985.

P. Mosolov and V. Miasnikov. On stagnant flow regions of a viscous-plastic medium in pipes. *Journal of Applied Mathematics and Mechanics*, 30(4):841–854, 1966.

R. Nochetto, K. Siebert, and A. Veeser. Pointwise a posteriori error control for elliptic obstacle problems. *Numer. Math.*, 95(1):163–195, 2003.

R. Nochetto, K. Siebert, and A. Veeser. Fully localized a posteriori error estimators and barrier sets for contact problems. *SIAM J. Numer. Anal.*, 42(5):2118–2135, 2005.

L. Payne and H. Weinberger. An optimal Poincaré inequality for convex domains. *Arch. Rational Mech. Anal.*, 5:286–292 (1960), 1960.

P.-A. Raviart and J. M. Thomas. A mixed finite element method for 2nd order elliptic problems. In *Mathematical aspects of finite element methods (Proc. Conf., Consiglio Naz. delle Ricerche (C.N.R.), Rome, 1975)*, pages 292–315. Lecture Notes in Math., Vol. 606. Springer, Berlin, 1977.

S. I. Repin. Functional a posteriori estimates for elliptic variational inequalities. *Zap. Nauchn. Sem. S.-Peterburg. Otdel. Mat. Inst. Steklov. (POMI)*, 348(Kraevye Zadachi Matematicheskoi Fiziki i Smezhnye Voprosy Teorii Funktsii. 38):147–164, 305, 2007.

S. I. Repin. *A posteriori estimates for partial differential equations*, volume 4. de Gruyter, 2008.

J. Rodrigues. *Obstacle Problems in mathematical Physics*. Elsevier, 1987.

N. Roquet and P. Saramito. An adaptive finite element method for Bingham fluid flows around a cylinder. *Comput. Methods Appl. Mech. Engrg.*, 192(31-32):3317–3341, 2003.

A. Schröder. Error control in *h*- and *hp*-adaptive FEM for Signorini's problem. *J. Numer. Math.*, 17(4):299–318, 2009.

A. Schröder. A posteriori error estimates of higher-order finite elements for frictional contact problems. *Comput. Methods Appl. Mech. Engrg.*, 249/252:151–157, 2012.

W. Spann. On the boundary element method for the Signorini problem of the Laplacian. *Numerische Mathematik*, 65(1):337–356, 1993.

The MathWorks. Matlab version 7.14.0.739 (R2012a). Natick, Massachusetts, United States, 2012.

A. Veeser. Efficient and reliable a posteriori error estimators for elliptic obstacle problems. *SIAM J. Numer. Anal.*, 39(1), 2001.

R. Verfürth. *A Review of a posteriori error estimation and adaptive mesh-refinement techniques*. Wiley-Teubner, 1996.

R. Verfürth. *A posteriori error estimation techniques for finite element methods*. Numerical Mathematics and Scientific Computation. Oxford University Press, Oxford, 2013.

F. Wang and W. Han. Another view for a posteriori error estimates for variational inequalities of the second kind. *Appl. Numer. Math.*, 72:225–233, 2013.

L. Wang. On the error estimate of nonconforming finite element approximation to the obstacle problem. *J. Comput. Math.*, 21(4):481–490, 2003.

B. Wohlmuth. Variationally consistent discretization schemes and numerical algorithms for contact problems. *Acta Numer.*, 20:569–734, 2011.

A. Table of notation

Elementary notation

$\bullet$	identity mapping
$\emptyset$	empty set
$A \cup B$, $\cup\mathcal{B}$	union of two sets A and B or of the sets B, $B \in \mathcal{B}$
$A \cap B$	intersection of two sets A and B
$A \subseteq B$, $A \subset B$	A subset of of B, A is a real subset B
$A \setminus B$	$= \{a \in A \mid a \notin B\}$
$\mathbb{N}$	positive integers, $\mathbb{N} = \{1, 2, 3, ...\}$
$\mathbb{N}_0$	positive integers and zero, $\mathbb{N}_0 = \{0\} \cup \mathbb{N}$
$\mathbb{R}$	field of real numbers
$\mathbb{R}^{m\times n}$	space of $m \times n$ matrices with real coefficients
$x \cdot y$	Euclidean scalar product $x \cdot y = \sum_{j=1}^{n} x_j y_j$
$\lvert x\rvert$	absolute value of $x \in \mathbb{R}$, Euclidean length of $x \in \mathbb{R}^n$
(a, b), $[a, b]$	open resp. closed interval
$\mathrm{dist}(x, y)$	Euclidean distance of $x, y \in \mathbb{R}$
$\mathrm{diam}(A)$	$= \sup_{x,y\in A} \lvert x - y\rvert$, diameter of a set $A \subseteq \mathbb{R}^n$
$\mathrm{conv}\{x_1, ..., x_n\}$	convex hull of $x_1, ..., x_n \in \mathbb{R}^n$
$\overline{\omega}$	closure of the set $\omega \subseteq \mathbb{R}^n$ with respect to the Euclidean norm
$\mathrm{int}(\omega)$	interior of the set $\omega \subseteq \mathbb{R}^n$ with respect to the Euclidean norm
$\partial\omega$	boundary of the set $\omega \subset \mathbb{R}^n$ with respect to the Euclidean norm
$\delta_{j,k}$	Kronecker delta, $= 1$ if $j = k$ and zero otherwise
$\mathrm{meas}(\omega)$	n dimensional Lebesgue measure of $\omega \subset \mathbb{R}^n$
$\mathrm{meas}_{n-1}(\omega)$	$n - 1$ dimensional Hausdorff measure of $\gamma \subseteq \partial\omega$
supp	support of a function
$v\lvert_\omega$	restriction of v to ω
sgn	sign function

Differential operators

D, D^2	first resp. second partial derivatives
∇	gradient

div	divergence
Curl	Curl operator,Curl $v = (-\partial v/\partial y, \partial v/\partial x)$,=
$\partial f/\partial \rho$	directional derivative

Lebesgue and Sobolev spaces

X^*	topological dual of a normed space X
$\int_\omega \bullet \,\mathrm{d}x$, $\int_\gamma \bullet \,\mathrm{d}s$	n-dimensional Lebesgue integral over $\omega \subset \mathbb{R}^n$, resp. $n-1$-dimensional Lebesgue integral over $\gamma \subset \mathbb{R}^{n-1}$
$⨍_\omega \bullet \,\mathrm{d}x$, $⨍_\gamma \bullet \,\mathrm{d}s$	$\lvert\omega\rvert^{-1} \int_\omega \bullet \,\mathrm{d}x$ resp. $\lvert\gamma\rvert^{-1} \int_\gamma \bullet \,\mathrm{d}s$
$L^2(\omega; X)$, $L^2(\omega)$	square integrable function with values in X resp. $\mathbb{R}$, measure clear from context
$H^k(\omega; X)$, $H^k(\omega)$	Sobolev space of k time weakly differentiable L^2 functions with values in X resp. $\mathbb{R}$
$H^k_\gamma(\omega; X)$, $H^k_\gamma(\omega)$	closure of $C^\infty_\gamma(\omega, X)$, resp$C^\infty_0(\omega)$ with respect to $\lvert\lvert\bullet\rvert\rvert_{H^k(\omega)}$ for $\gamma \subseteq \partial\omega$ with $\mathrm{meas}_{n-1}(\gamma > 0)$
$H^{-k}(\omega; X)$, $H^{-k}(\omega)$	dual of $H^k_0(\omega; X)$ resp. $H^k_0(\omega)$
$H^{-k}_\gamma(\omega; X)$, $H^{-k}_\gamma(\omega)$	dual of $H^k_\gamma(\omega; X)$ resp. $H^k_\gamma(\omega)$ for $\gamma \subseteq \partial\omega$ with $\mathrm{meas}_{n-1}(\gamma > 0)$
$\lvert\lvert\bullet\rvert\rvert_{L^2(\omega)}$	L^2 norm over $\omega \subset \mathbb{R}^n$
$\lVert\!\lVert \bullet \rVert\!\rVert$	$= \lvert\lvert\nabla\bullet\rvert\rvert_{L^2(\omega)}$ energy (semi norm)

Triangulation

$\mathcal{T}$	set of triangles
$\mathcal{N}$, $\mathcal{N}(\omega)$	set of nodes, resp. interior nodes
$\mathcal{E}$, $\mathcal{E}(\omega)$	set of edges, resp. interior edges
$\mathcal{T}(z)$	$= \{T \in \mathcal{T} \mid z \in \mathcal{N}(T)\}$
$\mathcal{T}(E)$	$= \{T \in \mathcal{T} \mid E \in \mathcal{E}(T)\}$
ω_z	$= \cup_{T\in\mathcal{T}(z)} T$
ω_E	$= \cup_{T\in\mathcal{T}(E)} T$
Ω_T	$= \cup\{K \in \mathcal{T} \mid \mathcal{N}(K) \cap \mathcal{N}(T) \neq \emptyset\}$
Ω_E	$= \cup\{T \in \mathcal{T} \mid \mathcal{N}(T) \cap \mathcal{N}(\omega_E) \neq \emptyset\}$
h_T	$= \mathrm{diam}(T)$ for triangle T
h_E	$= \lvert E\rvert$ for edge E
$P_k(\mathcal{T}; X)$, $P_k(\mathcal{T})$	piecewise polynomials with total degree $\leq k$ with values in X resp. $\mathbb{R}$
$[\bullet]_E$, $\langle\bullet\rangle_E$	jump, average across an edge E
$\lVert\!\lVert \bullet \rVert\!\rVert_{\mathrm{NC}}$	$= \sum_{T\in\mathcal{T}} \lvert\lvert\nabla\bullet\rvert\rvert_{L^2(T)}$
Π_0, Π_0^γ	projection onto $P_0(\mathcal{T})$, resp. $P_0(\mathcal{E}(\gamma))$

B. Implementation

This appendix gives an overview of the Matlab implementation of the numerical experiments from Sections 6.1, 6.2, and 6.3. The code is based on the Matlab software package AFEM (Carstensen et al, 2009) maintained at the Humboldt-Universität and runs with Matlab version 7.14.0.739 (R2012a) (The MathWorks, 2012).

B.1. Structure of the implementation

Solvers for variational inequalities

The following programs compute the discrete solutions to (3.2) for the conforming Courant FEM, the non-conforming Crouzeix-Raviart FEM, and the mixed Raviart-Thomas FEM.

```
function [x,ndof,A,b] = solveObstacleC(c4n,n4e,n4sDb,n4sNb,f,g,chi,u4Db,...
    degree_f,degree_g,degree_chi,degree_ud)

function [x,nrDof,A,b] = solveObstacleCR(c4n,n4e,n4sDb,n4sNb,f,g,chi,u4Db,...
    degree_f,degree_g,degree_chi,degree_ud)

function [x_p,x_u,x_l,nrDoF,A,b,A_loc,sig4e,Iters,fmean] =...
    solveObstacleRT(f,~,chi,u4Db,c4n,n4e,n4sDb,~,deg)
```

The following programs compute the discrete solutions to (4.2) for the conforming Courant FEM, the non-conforming Crouzeix-Raviart FEM, and the mixed Raviart-Thomas FEM.

```
function [x,ndof,A,b] = solveSignoriniC(c4n,n4e,n4sDb,n4sNb,n4sCb,f,g,chi,...
    u4Db,degree_f,degree_g,degree_chi,degree_ud)

function [x,nrDof,A,b] = solveSignoriniCR(c4n,n4e,n4sDb,n4sNb,n4sCb,f,g,...
```

The following programs compute the discrete solutions to (5.2) for the conforming Courant FEM, and the non-conforming Crouzeix-Raviart FEM.

```
function [ucr,gradInt,lambda0,nrDof,iters]=solveBinghamUzawaCR(c4n,n4e,...
    n4sDb,n4sNb,f,ys,g,u4Db,rho,eps,lambda0)

function [ucr,gradInt,lambda0,nrDof,iters]=solveBinghamUzawaCR(c4n,n4e,...
```

Estimators

The error estimators for the obstacle problem for the conforming Courant FEM, the non-conforming Crouzeix-Raviart FEM, and the mixed Raviart-Thomas FEM are implemented in

```
function [lambda4n,eta4e,etaRes,etaCC,etaW]...
    = estimateObstacleBC(c4n,n4e,n4sDb,n4sNb,f,g,chi,grad4chi,u4Db,...
    u4Db_DT2,xc,b,A,degree_f,degree_ud)

function [lambda4n,eta4e,etaRes,etaCC,etaW]...
    = estimateObstacleCM(c4n,n4e,n4sDb,n4sNb,f,g,chi,grad4chi,u4Db,...
    u4Db_DT2,xc,b,A,degree_f,degree_ud)

function [lambda4n,eta4e,etaRes,etaCC,etaW]...
    = estimateObstacleVeeser1(c4n,n4e,n4sDb,n4sNb,f,g,chi,grad4chi,u4Db,...
    u4Db_DT2,xc,b,A,degree_f,degree_ud)

function [lambda4n,eta4e,etaRes,etaComplementary,etaWd]...
    = estimateObstacleVeeser2(c4n,n4e,n4sDb,n4sNb,f,g,chi,grad4chi,u4Db,...
    u4Db_DT2,xc,b,A,degree_f,degree_ud)

function [lambda4s,LcrTemp,c4nInt, n4eInt,z2,v4n,eta4e, etaRes, etaCC,...
    etaW,etaUcrV] = estimateObstacleCR(c4n,n4e,n4sDb,n4sNb,f,g,chi,...
    grad4chi,u4Db,u4Db_DT2,xcr,b,A,degree_f,degree_ud)

function [lambda4e,v4n,eta4e, etaRes, etaCC, etaW,etaPrtV,uM4e]...
    = estimateObstacleRT(c4n,n4e,n4sDb,n4sNb,f,g,chi,grad4chi,u4Db,...
    u4Db_DT2,xp,sig4e,degree_f,degree_ud)
```

The error estimators for the simplified Signorini problem for the conforming Courant FEM, the non-conforming Crouzeix-Raviart FEM, and the mixed Raviart-Thomas FEM are implemented in

```
function [lambda4n,eta4e,etaRes,etaCC,etaW]= ...
    estimateSignoriniC(c4n,n4e,n4sDb,n4sNb,n4sCb,f,g,chi,u4Db,u4Db_DT2,...
    xc,b,A,degree_f,degree_ud)

function [v4n,lambda4s,eta4e,etaRes,etaCC,etaW,etaUcrV]=...
    estimateSignoriniCR(c4n,n4e,n4sDb,n4sNb,n4sCb,f,g,chi,u4Db,u4Db_DT2,...
    xcr,b,A,degree_f,degree_ud,problem)

function [v4n,lambda4s,eta4e,etaRes,etaCC,etaW,etaPrtV]=...
    estimateSignoriniRT(c4n,n4e,n4sDb,n4sNb,n4sCb,f,g,chi,u4Db,u4Db_DT2,...
    xcrt,degree_f,degree_ud,problem)
```

The error estimators for the Bingham flow problem for the conforming Courant FEM and the non-conforming Crouzeix-Raviart FEM are implemented in

```
function eta4e=estimateBinghamC(c4n,n4e,n4sDb,n4sNb,f,g,ys,xc,lambdaC)

function [eta4e,etaCCMu,etaRes,lambdaCR,etaUcrV,v4n]=...
    estimateBinghamCR(c4n,n4e,n4sDb,f, ys,xcr,gradXcr,lcr,u4Db,modLcr)
```

Computation of errors

The error terms for the obstacle problem with a known exact solution for the conforming Courant FEM, the non-conforming Crouzeix-Raviart FEM, and the mixed Raviart-Thomas FEM are computed in

```
function [errUV,errUVW,errCCMu,errCCLambda,errLambdaMu]...
    =errorObstacleC(c4n,n4e,n4sDb,n4sNb,xc,lambda4n,chi,u4Db,u4Db_DT2,f,...
    grad4chi,gradUExact,UExact,LaplaceUExact,degree_f,degree_chi,degree_u)

function [errUV,errUVW,errCCMu,errCCLambda,errLambdaMu,errUcrU]...
```

```
    =errorObstacleCR(c4n,n4e,n4sDb,xcr,v4n,z2,lambda4s,LcrTemp,c4nInt,...
    n4eInt,chi,u4Db_DT2,f,grad4chi,gradUExact,UExact,LaplaceUExact,...
    degree_f, degree_chi,degree_u)

function [errUV,errUVW,errCCMu,errCCLambda,errLambdaMu,errUPrt]...
    =errorObstacleRT(c4n,n4e,n4sDb,n4sNb,xp,sig4e,v4n,lambda4e,chi,u4Db...
    ,u4Db_DT2,f,grad4chi,gradUExact,UExact,LaplaceUExact,degree_f,...
    degree_chi,degree_u)
```

The error terms for the obstacle problem with an unknown exact solution for the conforming Courant FEM, the non-conforming Crouzeix-Raviart FEM, and the mixed Raviart-Thomas FEM are computed in

```
function [errUV,errUVW,errCCMu,errCCLambda,errLambdaMu]=...
    errorExUnknownObstacleC(c4n,n4e,n4sDb,n4sNb, xc, lambda4n, chi,g,...
    u4Db,u4Db_DT2,f,gradChi, degree_g,degree_f, degree_chi, degree_ud)

function [errUV,errUVW,errCCMu,errCCLambda,errLambdaMu,errUcrU]=...
    errorExUnknownObstacleCR(c4n,n4e,n4sDb,n4sNb,xcr,v4n, lambda4s, chi,...
    g,u4Db,u4Db_DT2,f,gradChi, degree_g,degree_f,degree_chi,degree_ud)

function [errUV,errUVW,errCCMu,errCCLambda,errLambdaMu,errUPrt]=...
    errorExUnknownObstacleRT(c4n,n4e,n4sDb,n4sNb,uM4e,v4n,lambda4e,chi,...
    g, u4Db,u4Db_DT2,f,gradChi,degree_f, degree_chi,degree_g,degree_ud)
```

The error terms for the simplified Signorini problem with a known exact solution for the conforming Courant FEM, the non-conforming Crouzeix-Raviart FEM, and the mixed Raviart-Thomas FEM are computed in

```
function [errUV,errUVW,errCCMu,errCCLambda,errLambdaMu]...
    =errorSignoriniC(c4n,n4e,n4sDb,n4sNb,n4sCb,xc,lambda4n,chi,g,u4Db,...
    u4Db_DT2,f,gradUExact,UExact,degree_chi,degree_u)

function [errUV,errUVW,errCCMu,errCCLambda,errLambdaMu,errUcrU]...
    =errorSignoriniCR(c4n,n4e,n4sDb,n4sNb,n4sCb,xcr,v4n,lambda4s,chi,g,...
    u4Db,u4Db_DT2,f,gradUExact,UExact, degree_chi,degree_u)

function [errUV,errUVW,errCCMu,errCCLambda,errLambdaMu,errPrtU]...
    =errorSignoriniRT(c4n,n4e,n4sDb,n4sNb,n4sCb,xcrt,v4n,lambda4s,chi,...
    g,u4Db,u4Db_DT2,f,gradUExact,UExact,degree_f, degree_chi,degree_u)
```

The error terms for the simplified Signorini problem with an unknown exact solution for the conforming Courant FEM, the non-conforming Crouzeix-Raviart FEM, and the mixed Raviart-Thomas FEM are computed in

```
function [errUV,errUVW,errCCMu,errCCLambda,errLambdaMu]=...
    errorExUnknownSignoriniC(c4n,n4e,n4sDb,n4sNb,n4sCb, xc,lambda4n,chi,...
    g,u4Db,u4Db_DT2,f, degree_f, degree_chi, degree_ud)

function [errUV,errUVW,errCCMu,errCCLambda,errLambdaMu,errUcrU]=...
    errorExUnknownSignoriniCR(c4n,n4e,n4sDb,n4sNb,n4sCb,xcr,v4n,lambda4s,...
    chi,g,u4Db,u4Db_DT2, f,degree_g,degree_chi, degree_f,degree_ud)

function [errUV,errUVW,errCCMu,errCCLambda,errLambdaMu,errPrtU]=...
    errorExUnknownSignoriniRT(c4n,n4e,n4sDb,n4sNb,n4sCb,xcrt,v4n,lambda4s,...
    chi,g,u4Db,u4Db_DT2, f,degree_g,degree_chi, degree_f,degree_ud)
```

The error terms for the Bingham flow problem with a known exact solution for the conforming Courant FEM and the non-conforming Crouzeix-Raviart FEM are computed in

```
function [errUV errLambdaMu errCCLambda errCCMu]=...
    errorBinghamC(c4n,n4e,f,ys,xc,LambdaC,gradUExact,degree_u,...
    degree_f,etaRes)

function [errUV errLambdaMu errCCLambda errCCMu,errUcrU]=...
    errorBinghamCR(c4n,n4e,f,ys,xcr,LambdaCR,gradUExact,...
    degree_u,degree_f,etaRes,v4n)
```

The error terms for the Bingham flow problem with an unknown exact solution for the conforming Courant FEM and the non-conforming Crouzeix-Raviart FEM are computed in

```
function [errUV errLambdaMu errCCLambda errCCMu]=...
    errorExUnknownBinghamC(c4n,n4e,n4sDb,n4sNb,xc,lambda4e,g,u4Db,f,...
    ys,rho,epsilon)

function [errUV errLambdaMu errCCLambda errCCMu,errUcrU]...
    =errorExUnknownBinghamCR(c4n,n4e,n4sDb,n4sNb,xcr,lambda4e,g,u4Db,...
    f,ys,rho,epsilon,v4n)
```

AFEM loop

The adaptive algorithms for the obstacle problem, the simplified Signorini problem, and the Bingham Problem are given in

```
ObstacleProblemC(problem,minNrDoF,refine,theta,multiplier,path2folder,
    foldername)

ObstacleProblemCR(problem,minNrDoF,refine,theta,path2folder,foldername)

ObstacleProblemRT(problem,minNrDoF,refine,theta,path2folder,foldername)

SignoriniProblemC(problem, minNrDoF,refine, theta, path2folder,foldername)

SignoriniProblemCR(problem, minNrDoF,refine, theta, path2folder,foldername)

SignoriniProblemRT(problem, minNrDoF,refine, theta, path2folder,foldername)

BinghamProblemC(problem,minNrDoF,refine, theta, ys,path2folder,foldername,
    LagrangeAdaptive)

BinghamProblemCR(problem,minNrDoF,refine, theta, ys,path2folder,foldername,
    LagrangeAdaptive,lcrMod)
```

Further functions

The conforming companion $J2v_{\mathrm{CR}}$, for $v_{\mathrm{CR}} \in \mathrm{CR}_0^1(\mathcal{T})$ is computed in

```
function [v4n]=v_J2(c4n,c4n_fine,DbNodes,u4Db4s,DbSides,...
    nodeval4e,x,n4e,u4Db)
```

Extra refine routines for circular domains are given in

```
function [c4nNew,n4eNew,n4sDbNew,n4sNbNew,n4sCbNew] = ...
    refineRGBContact(c4n,n4e,n4sDb,n4sNb,n4sCb,n4sMarked)

function [c4n,n4e,n4sDb,n4sNb,n4sCb,parents4e,prolong,childnr]...
       = refineUniformRedC(c4n,n4e,n4sDb,n4sNb,n4sCb)
```

All methods rely on the computation of discrete Riesz representation of the residuals, which employ the solve of a Poisson problem in

```
function [x,nrDof,A,b] = ...
    solveCRPoissonDataVector(f,g,u4Db,c4n,n4e,n4sDb,n4sNb)

function [x,nrDof,A,b] = ...
    solveP1PoissonMu(c4n,n4e,n4sDb,n4sNb,f,mu,g,u4Db,degree_f)

function [x,ndof,A,b] = solveP2PoissonMu(c4n,n4e,n4sDb,f, mu,u4Db,typeMy)

function [x,ndof,A,b] = ...
    solveP2PoissonSignoriniMu(c4n,n4e,n4sDb,n4sNb,n4sCb,f,g,mu,u4Db,type)

function [x,ndof,A,b] = solveP2PoissonVChiP(c4n,n4e,n4sDb,n4sCb,v,chi)

function [x,ndof,A,b] = solveP2PoissonW(c4n,n4e,n4sCb,v,chi,type)
```

B.2. Reproduction of numerical experiments

The numerical experiments in Subsection 6.1, 6.2, and 6.3 can be reproduced by running `TestExperiment.m`. (For the different experiments the input parameters have to be adapted).

B.3. Content of the software archive

```
afem ..... files taken from AFEM (Carstensen et al, 2009)
    closure.m            computeN4s.m          estimateP1EtaSides.m
    computeArea4e.m      computeNormal4e.m     integrate.m
    computeArea4n.m      computeNormal4s.m     markBulk.m
    computeE4n.m         computeS4e.m          P0NormalJump.m
    computeE4s.m         computeS4n.m          refineRGB.m
    computeLength4s.m    computeTangent4s.m    refineRGBwithParent.m
    computeMid4e.m       error4eCREnergy.m     refineUnformRed.m
    computeMid4s.m       error4eP1Energy
Common ..... *.m files used for all three methods
    matMul.m (C. Merdon)      rowaddr.m (C. Merdon)
    P0NormalJumpLambdaC.m     vJ2.m
    P0NormalJumpLambdaNC.m
Data ..... *.m files which contain the Data for each problem
Error ..... *.m files to compute errors
    DbError.m (C. Merdon)         errorExUnknownSignoriniCR.m
    errorBingham.C                errorExUnknownSignoriniRT.m
    errorBinghamCR.m              errorObstacleC.m
    errorExUnknownBinghamC.m      errorObstacleCR.m
    errorExUnknownBinghamCR.m     errorObstacleRT.m
    errorExUnknownObstacleC.m     errorP2.m
    errorExUnknownObstacleCR.m    errorSignoriniC.m
    errorExUnknownObstacleRT.m    errorSignoriniCR.m
    errorExUnknownSignoriniC.m    errorSignoriniRT.m
Estimate ..... *.m files to compute estimators
```

```
    AinsworthPostProcessing.m (C. Merdon)   estimteObstacleVeeser1.m
    estimateBinghamC.m                      estimteObstacleVeeser2.m
    estimateBinghamCR.m                     estimateP1EtaSidesMy.m
    estimteObstacleBC.m                     estimateSignoriniC.m
    estimteObstacleCM.m                     estimateSignoriniCR.m
    estimteObstacleCR.m                     estimateSignoriniRT.m
    estimteObstacleRT.m                     lcrMinus.m
Experiments ..... Folder to save numerical experiments
MainFiles ..... Folder contains AFEM loops
    BinghamProblemC.m     ObstacleProblemRT.m
    BinghamProblemCR.m    SignroniProblemC.m
    ObstacleProblemC.m    SignoriniProblemCR.m
    ObstacleProblemCR.m   SignroniProblemRT.m
Refine ..... *.m files for refinement of triangulation
    CuspTriangulation.m              refineRGBContact.m
    markZeroOnly.m                   refineUniformRedC.m
    RefineCircle.m (M. Schedensack)
Solve ..... *.m files to solve variational inequalities
    solveBinghamUzawaC.m    solveObstacleRT.m (N. Graß)
    solveBinghamUzawaCR.m   solveSignoriniC.m
    solveObstacleC.m        solveSignoriniCR.m
    solveObstacleCR.m       solveSignoriniRT.m
SolvePoisson ..... *.m files to solve Poisson problems
    solveCRPoissonDataVector.m (N. Graß)   solveP2PoissonSignoriniMu.m
    solveP1PoissonMu.m                     solveP2PoissonVChiP.m
    solveP2PoissonMu.m                     solveP2PoissonW.m
TestExperiment.m ..... Test Environment
```

C. Data medium containing the software

The online version of this document contains the software as an embedded zip-file. Please use an appropriate pdf viewer to extract the file, such as KDE Okular or Adobe Reader. In contrast to the thesis' text, the code is provided under the terms of the GNU General Public Licence as published by the Free Software Foundation, either version 3 of the Licence, or (at your option) any later version. Refer to the file LICENSE.txt in the software archive for more information.

List of Figures

Selbstständigkeitserklärung

Hiermit erkläre ich, dass ich die vorliegende Dissertation selbstständig und nur unter Verwendung der angegebenen Literatur und Hilfsmittel angefertigt habe.

Berlin, den 18. April 2016 Karoline Köhler